

ЕҢБЕК ҚЫЗЫЛ ТУ ОРДЕНДІ
«Ә. Б. БЕКТҰРОВ АТЫНДАҒЫ
ХИМИЯ ҒЫЛЫМДАРЫ ИНСТИТУТЫ»
АКЦИОНЕРЛІК ҚОҒАМЫ

ҚАЗАҚСТАННЫҢ ХИМИЯ ЖУРНАЛЫ

ХИМИЧЕСКИЙ ЖУРНАЛ КАЗАХСТАНА

CHEMICAL JOURNAL of KAZAKHSTAN

АКЦИОНЕРНОЕ ОБЩЕСТВО
ОРДЕНА ТРУДОВОГО КРАСНОГО ЗНАМЕНИ
«ИНСТИТУТ ХИМИЧЕСКИХ НАУК
им. А. Б. БЕКТУРОВА»

2 (62)

АПРЕЛЬ – ИЮНЬ 2018 г.
ИЗДАЕТСЯ С ОКТЯБРЯ 2003 ГОДА
ВЫХОДИТ 4 РАЗА В ГОД

АЛМАТЫ
2018



Основатель и главный редактор
академик НАН РК

Е. Е. ЕРГОЖИН

лауреат Государственной премии в области науки и техники,
заслуженный деятель науки,
заслуженный изобретатель Республики Казахстан,
доктор химических наук, профессор,
генеральный директор
АО «Институт химических наук
им. А. Б. Бектурова»

Основатель и главный редактор
академик НАН РК
Е. Е. ЕРГОЖИН

Редакционная коллегия:
У.Ж.Джусипбеков,
член-корреспондент НАН РК, заместитель главного редактора,
Б.Н.Абсадыков,
член-корреспондент НАН РК, заместитель главного редактора

Члены редколлегии:
Вице-президент Российской академии наук, академик РАН **А.Р.Хохлов**, академик РАН **М.П.Егоров**, академик НАН Беларуси **В.С.Солдатов**, член-корреспондент РАН **Е.Ф.Панарин**, академик НАН РК **М.Ж.Журинов**, академик НАН РК **И.К.Бейсембетов**, академик НАН РК **К.Д.Пралиев**, академик АН Республики Таджикистан **Д.Х.Халиков**, академик АН Республики Узбекистан **М.А.Аскарров**, академик АН Республики Узбекистан **С.Ш.Рашидова**, член-корреспондент НАН Азербайджана **Э.Б.Зейналов**, Professor University de la Rochelle **Brahim Elouadi**, Research Director, Institute of Drug Discovery, Hebrew University, Jerusalem, Israel, professor **V.M. Dembitsky**, Director of Dicle University Graduate School of Natural and Applied Sciences, Turkey, professor **Н. Temel**, доктор химических наук, профессор **Б.С.Закиров**, доктор химических наук, профессор **Г.А.Мун**, доктор химических наук, профессор **К.Б.Ержанов**, доктор технических наук, профессор **Д.С.Бержанов**, доктор химических наук, профессор **Б.Т.Утелбаев**, доктор технических наук, профессор **С.У.Усманов**

Ответственный секретарь
доктор PhD **А.Е.Малмакова**

«Химический журнал Казахстана» зарегистрирован Министерством культуры, информации и общественного согласия Республики Казахстан (свидетельство о постановке на учет средств массовой информации № 3995-Ж от 25 июня 2003 г.), Международным центром ISSN в Париже (регистрационный номер ISSN 1813-1107 от 6 августа 2005 г.) и включен в Перечень изданий для публикации основных результатов научной деятельности, рекомендованный Комитетом по контролю в сфере образования и науки МОН РК (приказ № 532 от 15 марта 2013 г.).

Адрес редакции:
050010, Республика Казахстан, г. Алматы, ул. Ш. Уалиханова, 106,
АО «Институт химических наук им. А. Б. Бектурова».
Fax: 8-727-291-24-64. E-mail: ics_rk@mail.ru

© АО «Институт химических наук
им. А. Б. Бектурова», 2018

Подписной индекс 75241 в Каталоге газет и журналов АО «Казпочта» или в дополнении к нему.

SPRINGER NATURE

CERTIFICATE

THIS CERTIFIES THAT

Ergozhin Edil

Has successfully completed the official
SPRINGER NATURE TRAINING

How to use
How to publish

IRINA ALEXANDROVA

Licensing manager

Kazakhstan, Kyrgyzstan, Tajikistan, Uzbekistan, Turkmenistan



March 27, 2018







ҚАЗАҚСТАН РЕСПУБЛИКАСЫНЫҢ
БІЛІМ ЖӘНЕ ҒЫЛЫМ МИНИСТРАЛІГІ
Манаш Қозыбаев атындағы
Солтүстік Қазақстан мемлекеттік
университеті



МИНИСТЕРСТВО ОБРАЗОВАНИЯ
И НАУКИ РЕСПУБЛИКИ КАЗАХСТАН
Северо-Казахстанский
государственный университет
им. Манаша Козыбаева



АЛҒЫС ХАТ БЛАГОДАРНОСТЬ



Уважаемый **Едил Ергожаевич!**

Выражаем Вам нашу искреннюю благодарность за книги, переданные в дар. Эти издания имеют для нас особое значение, поскольку направление «Химия и химические технологии» является приоритетным в развитии нашего вуза. Книги займут достойное место в фондах библиотеки Северо-Казахстанского государственного университета им. М. Козыбаева.

Издания будут актуальны в учебном и научно-исследовательском процессах. Надеемся на сохранение сложившихся дружеских отношений и формирование более тесного взаимодействия в рамках совместных проектов в области развития химической науки.

Ректор



С. Омирбаев

Петропавл қ., 2018 ж.



Информационное сообщение

24 мая 2018 года в АО "Институт химических наук им. А.Б.Бектурова" состоялся семинар "Использование прав на объекты промышленной собственности и коммерциализация результатов интеллектуальной деятельности (РИД)".

На семинаре обсуждались такие вопросы, как лицензионные договора и коммерческое использование РИД в современных экономических условиях. Первый вопрос подробно осветил Федурин Владимир Петрович, главный эксперт управления патентных исследований по изобретениям, а второй – Курмангали Булат Серикович, президент Ассоциации владельцев интеллектуальной собственности.

В.П.Федурин и Б.С.Курмангали в своих сообщениях привели много конкретных примеров из многолетней практической работы и ответили на вопросы сотрудников АО "Институт химических наук им. А.Б.Бектурова", а также представителей АО "Институт металлургии и обогащения" и АО "Институт органического катализа и электрохимии им. Д.В.Сокольского".

Данный семинар не первый в рамках сотрудничества Института химических наук и Учебного центра Алматинского филиала Института интеллектуальной собственности. На протяжении многих лет Институт химических наук и филиал НИИС поддерживают деловые связи, направленные на повышение квалификации научных сотрудников в области интеллектуальной собственности.

*N. A. BEKTENOV¹, E. E. ERGOZHIN¹, S. B. RYSPAeva¹,
K. A. SADYKOV¹, I. S. MOLDAGALYEVA², A. A. MARATOVA²*

¹JSC Institut of Chemical Sciences named after A.B. Bekturov, Almaty, Republic of Kazakhstan,

²Kazakh-British Technical University, Almaty, Republic of Kazakhstan.

E-mail: bekten_1954@mail.ru

ECOLOGY OF OIL AND OIL SORBENTS

Abstract. The article contains materials on oil-sorbents and their application. Methods of liquidation of spills and accidents of oil and oil products on soil and water surface are shown.

Keywords: oil, sorbents, ecology, chemical composition, water, soil, peat, cellulose

1.1. Oil, its composition and properties. The chemical nature and composition of petroleum, petroleum fractions and residues predetermines the entire complex of their physicochemical properties and the colloid-dispersed structure of petroleum systems.

According to the theory of oil formation as a result of long transformations of organic residues, the main part of the oil is made up of hydrocarbons of different structures. However, the oil that coming out to the surface carries with it associated gas, water and mechanical particles of sand, rock, etc. The number of these components for different oilfields is different. These components are insoluble, oleophobic and form a disperse system that undergoes separation. But even after the separation of insoluble components, according to the chemical nature of the oil itself, it is not a molecular solution, or a Newtonian fluid. The presence of heteroatom compounds in the oil, as well as high-molecular compounds, most of which contain sulfur, nitrogen, oxygen and metals, impart oil, oil fractions and residues to the specific properties inherent to colloidal and disperse systems. Depending on the particle size of the dispersed phase, such systems can be either ultraheterogeneous (particle size from 1 to 100 nm) or coarsely dispersed (particle size > 10 nm).

The hydrocarbons and other compounds contained in the oil in one degree or another interact with each other. Physical intermolecular interactions are determined both by the nature and structure of the compounds, and by external conditions [1-3].

1.1.2. Element composition. Oil is a mixture of a very large number of chemical compounds based on hydrocarbons formed from the initial organic matter as a result of prolonged interaction with the environment under the influence of many factors.

Oil is an oily liquid, the complete chemical composition of which is virtually impossible to determine with modern instrumental methods.

The main chemical elements that make up the oil are carbon, hydrogen, sulfur, nitrogen and oxygen. Carbon and hydrogen are contained in various oils in

the amount of 82-87% and 11-14%, respectively. They are an integral part of all chemical compounds of oil. Among minerals (excluding petroleum gas), oil has the highest calorific value, since it contains the greatest amount of hydrogen. In connection with this, the combustible properties of oil are usually characterized by the ratio of the quantities of hydrogen and carbon (H: C) in%. Sulfur is a part of heteroatomic compounds. The sulfur content of oil is divided into three classes: in low sulfuric oils, it is up to 0.5%, in sulphurous oils - from 0.51 to 2,0% and in high sulfur - from 2.01%. Nitrogen and oxygen in oil-up to 1,8 and 3,0%, respectively. In oil ash, about 6 metals are found, of which the most common are V, Ni, Te, Zn, Cu, Mg, Al [4, 5].

1.1.3. Group chemical and fractional composition. The composition of oil includes the following groups of compounds: hydrocarbons, heteroatom compounds, resins and asphaltenes. Hydrocarbons of natural oils are represented by three groups-alkanes, cycloalkanes and arenes. The heteroatomic compounds include sulfur-, nitrogen-, oxygen- and metal-containing compounds. Resins and asphaltenes are not a characteristic group of chemical compounds. Heteroatomic compounds are chemical compounds based on hydrocarbons of any group containing one or more different atoms of chemical elements of sulfur, nitrogen, oxygen, chlorine and metals. Heteroatomic oil compounds have a significant impact on the level of environmental pollution. Oil and petroleum products are a complex mixture of hydrocarbons and non-hydrocarbon compounds. Parts are called fractions. The main fractions released from oil at the industrial plant are the following: petrol, kerosene, diesel and the remainder of oil distillation - fuel oil [6].

1.2. Sources of oil pollution and the impact of oil production, transportation and refining on the environment. Among the numerous harmful substances of anthropogenic origin that enter the environment (air, water, soil, vegetation, etc.), one of the first places belong to petroleum products. The work of vehicles and oil refineries and petrochemical industry, gaseous emissions and sewage of industrial enterprises, numerous oil and oil products spills as a result of accidents of pipelines and oil tankers (tankers), accidents and fires at oil storage facilities and oil refineries lead to pollution of air, water and soil with significant amounts of crude oil and products of its processing and create a serious threat to the environment [7].

Anthropogenic pollution of the biosphere, caused by human economic activity, has a negative impact on the state of water, soil, atmospheric air, renewable natural resources.

Oil and its products are one of the most common ecotoxicants. Technogenic pollution appears at all levels - from local to global and poses a serious threat. Oil pollution differs from other anthropogenic influences in that it gives not a constant, but a "volley" load on the environment, causing its rapid response. By the nature of the occurrence of pollution are divided into natural and anthropogenic (figure 1). The main mass of pollution of the World Ocean (about 95%) are sources of anthropogenic origin [8].

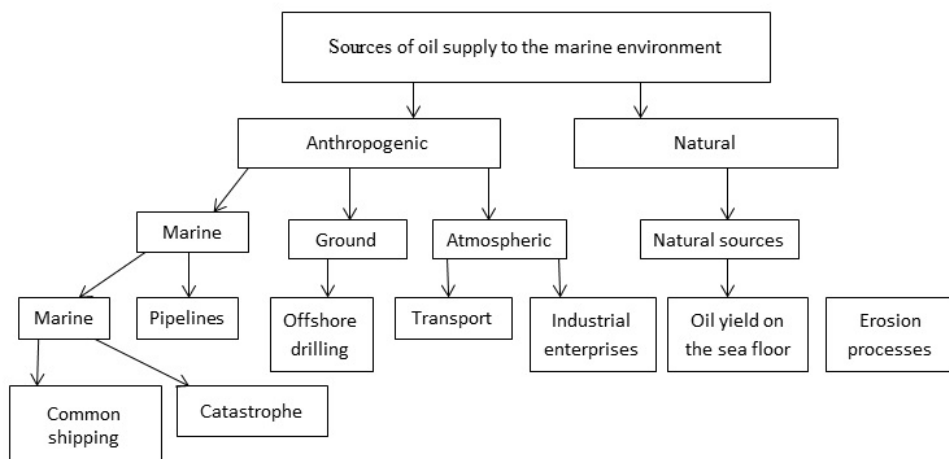


Figure 1 – Sources of pollution

Toxication is very resistant and extends over long distances. Pollution occurs during the extraction, transportation and refining of oil.

The main natural sources of oil pollution of the marine environment are the release of oil at the seabed, and less significant sources are erosion processes. To the most important anthropogenic sources of oil pollution includes:

- marine - marine transport, warships, vessels for various purposes, pipelines, installations and devices used in the development of seabed and subsoil resources;
- ground - rivers, lakes and other water systems, where pollutants enter with groundwater, and also as a result of wastewater discharge from various coastal objects;
- atmospheric - various industrial enterprises, vehicles and other objects from where emissions of hydrocarbon compounds to the atmosphere can occur [9].

There are several groups of sources of pollution of the World Ocean, the classification of which is shown in figure 1.

Oil and gas deposits are in most cases located at a considerable distance from oil and gas refineries. Due to the high fire and explosion hazard during the transportation of oil, and especially natural gas, there are increased requirements for ensuring high integrity, reliability, and fire safety of vehicles.

One of the most economical and technically modern modes of transport oil and gas is the sea and river oil-loading fleet. In the 1970s and 1980s, large-tonnage tankers were put into operation with a carrying capacity of 100-250 thousand tons and giant supertankers - up to 750 thousand tons. A fleet of gas tankers for ocean and sea transport was also created.

On land, oil and gas transportation through pipelines is the most economical. The share of pumping oil and gas through pipelines in our country reaches 85%.

For transportation of oil to areas remote from pipeline magistrates, railroad transport with special oil tankers [10] are used. When transporting is conducted by these methods above, unforeseen accidents and spills on ground and water occur.

1.2.1. Water. The ingress of oil and its components into the environment (air, water and soil) causes a change in the physical, chemical and biological properties and characteristics of the natural habitat, disrupts the course of natural biochemical processes. In the process of the transformation of oil hydrocarbons, even more toxic compounds can be formed than the original ones, which have carcinogenic and mutagenic properties and are resistant to microbiological cleavage.

Any of the classes of petroleum products can become a harmful impurity that pollutes the water. In small concentrations, oil contamination can affect the taste and smell of water, and with large concentrations, they form giant oil spills and cause environmental disasters. The last one occurs during oil spills (for example, in the case of tanker accidents at sea or in oil pipeline breaks) or when large quantities of oil or petrochemical waste streams enter surface and ground water.

Contamination of the world's oceans with oil and oil products is the most vivid example of global anthropogenic impact. Currently in the World Ocean there is practically no such area where oil contamination would not be felt. Background levels of petroleum hydrocarbons in the marine environment vary within very wide limits: 10-5-10 mg/l in water and 10-1-104 mg/kg in bottom sediments, depending on many natural and technogenic factors. Maximum concentrations tend to coastal and inland sea waters, zones of intensive navigation and other economic activities, as well as to areas of hydrocarbons escape from deposits on the shelf.

The problem of oil products pollution is very acute in the Northern Caspian, as a systematic accumulation of a large mass of oil spots is observed in its water area due to imperfect systems and equipment of the oil production complex, as well as an increase in the volumes of crude oil and oil products transportation by tankers. Significant amounts of oil fall into the sea in the event of a ship accident, especially oil-loading [11].

1.2.2. Soil. Sources of soil pollution with petroleum products are the same as in the case of water and air. The main ones are oil and oil products spills, wastewater and emissions from oil refineries and petrochemical enterprises, as well as harmful waste from chemical enterprises that accumulate in landfills.

In soils, Oil and Petroleum products are in the following forms:

- in a porous medium - in a vaporous and liquid easy-moving state, in a free or dissolved aqueous or water-emulsion phase;
- in a porous medium and cracks - in a free motionless state, playing the role of viscous or solid cement between particles and aggregates of the soil, in a sorbed state associated with particles of rock or soil, including humus constituents of soils;
- in the surface layer of soil or soil in the form of a dense organomineral mass;

Both free and inactive sedimentary forms of oil products release volatile fractions to the atmosphere, and soluble compounds into water. This process does not completely stop with time, since the microbiological processes of hydrocarbon transformation lead in part to the formation of volatile and water-soluble products of their metabolism [12].

1.2.3. Analysis of petroleum products in water. Qualitative and quantitative determination of the composition of contaminant since wage is necessary not only for the selection of the technology for their purification, but also for compliance with the norms for discharging treated sewage into water bodies.

It should be recalled that existing standards for the maximum allowable concentration of petroleum products in water in reservoirs are set at 0.1 mg/l for multi-sulfuroil, 0.3 mg/l for other types of oil, 0.1 mg/l for gasoline, tractor (GOST 1843-52) 0.01 ml/l, lighting (GOST 24753-68) 0.05 mg/l, sulfated with 0.1 mg/l. The limiting indicator of the harmfulness of all oil products is organoleptic.

Due to the fact that oil and petroleum products are an extremely complex mixture of substances - low- and high-molecular, limiting, unsaturated, aliphatic, naphthenic, aromatic hydrocarbons, oxygen-, sulfur- and nitrogen-containing compounds, asphaltenes and other compounds - In the analysis of waters, "oil products" are considered to be the sum of nonpolar and low-polar hydrocarbons - aliphatic, alicyclic, aromatic, which make up the bulk of oil and are soluble in hexane. Accordingly, methods for determining petroleum products in wastewater should include the concentration and recovery of petroleum products, the separation of the hydrocarbon part from foreign matter and the quantitative analysis of the released substances.

There is a significant amount of specialized literature on sampling methods and analytical methods for determining petroleum products in water. Also there are presented the most widely used methods used in the USSR and abroad mainly for routine analysis.

In our country, depending on the equipment of sanitary laboratories for the determination of petroleum products in effluents, the gravimetric method, IR and UV spectrophotometric, and also gas chromatographic, are used, which, as noted in [13], "give the same exact results if all conditions are met correctly and (GC-MS), the method of high-performance gas chromatography (HPLC), etc. (see / 16, 19-21 (and references therefrom). Nevertheless, when choosing the method for the quantitative determination of petroleum products in waste water, the main requirements are sensitivity and the possibility of wide application in practice. To determine the level of MPC, gravimetric, spectrophotometric (in the IR and UV regions of the spectrum), luminescent and gas chromatographic methods are used. Gas chromatography methods are useful for determining the qualitative and quantitative composition of petroleum products, but their sensitivity largely depends on the type of instrument. When determining the total content, which is stipulated by hygienic standards, gravimetric and optical methods are more convenient, having sufficient sensitivity and expressiveness, the most universal

method of infrared spectroscopy, taking into account aliphatic and naphthenic hydrocarbons, the content of which in oil reaches 70-90 % [13, 14].

1.3. Elimination methods of spills and accidents of oil and oil products on soil and water surfaces. Methods of removing oil products from the water surface and soil, which are divided into four large groups:

- mechanical methods, carried out with the help of various constructions and devices for collecting oil;
- physicochemical methods based on the use of physical and chemical phenomena;
- biological methods, carried out with the help of microbiological cultures;
- photochemical, passing under the influence of sunlight and catalysts [15].

For the elimination of the consequences of a spill of oil and oil products, mainly mechanical and sorption methods are used. However, when the thickness of the oil layer is less than 1-2 mm, and also with a small depth of the reservoir, the use of mechanical methods becomes impossible. In such conditions, special oil absorbing materials are most effective. The qualitative removal of oil contamination does not occur without the use of various kinds of sorbents [16].

Currently, the most acute problem is the removal of spilled petroleum products from the water surface. The simplest methods to combat the contamination of the water surface by petroleum products include the way that the spill is localized with the help of booms. The designs and methods of implementing the oil spill (containment) can be very diverse.

1.4. Classification of petroleum sorbents. Classification of oil sorbents [17, 18] by raw materials, table 1; by dispersion, table 2.

Table 1 – Classification of petroleum sorbents by raw materials

Inorganic sorbents		Organic sorbents			
Natural materials	Synthetic materials	Caustobioliths	Natural raw materials vegetable and animal origin and wastes of their processing	Organo-mineral	Synthetic
Disperse silica	Perlite	Coal	Cereal husks	Slates	Polypropylene
Zeolites	Expanded clay	Graphite	Moss, foliage	Sapropel	Polyurethane
Layered silicates	SilicaGel	Peat	Bark, sawdust	Oilsludge	Teflon

Table 2 – Classification of oil sorbents by dispersion

Dispersed		Molded			
Finely dispersed	Large-dispersed	Fibrous	Pressed	Combined	
Powders	Crumbs Granule Flakes	Woven and non-woven roll materials	Plates	Sorbent booms Pillows Mats with a shell of permeable material	

1.4.1. Inorganic sorbents. 1.4.1.1. Carbon sorbents. The history of the use of sorbents is associated with microporous carbon materials - active coals.

Active coals are porous solids, the voids of which are interconnected so that their structure resembles the structure of the wood. Depending on the formation conditions, all active carbons have a mono- or polydisperse system. They consist of many randomly arranged microcrystals of graphite formed as a result of a combination of carbon atoms when the carbon-containing raw material is heated. The dimensions of these crystals are 1.8–2.6 nm in diameter and 0.7–1 nm in height.

The ability of charcoal to decolorize solutions is known from the XV century, but only in 1785. T.E. Lovitz took advantage of this property for practical purposes - sorption purification of liquids.

At present, granular and powdered coals, as well as carbon fibers, are used for the sorption of aqueous solutions.

Granulated active carbons have a particle size of 0.07–7 mm. Depending on the size of the pores, they can be successfully used to extract contaminants from the water with a different size of molecules, coarse dispersed impurities and mixtures of polydisperse composition (domestic sewage).

Carbon sorbents with a particle size of 0.07–0.12 mm are classified as powdered active carbons. The main advantages of active coals include their low cost and good sorption kinetics, and a considerable area of the outer surface [19].

Currently, the main directions of the use of carbon sorbents are related to technological processes of adsorption purification, separation, isolation and concentration in gas and liquid media. The role of carbon sorbents in the solution of environmental problems is constantly growing: purification of drinking water, oil effluents, exhaust gases of industrial and energy enterprises.

Porous carbon materials were first obtained predominantly by thermal treatment of wood, then by coal. Now they are produced almost from all types of carbon-containing raw materials: wood and cellulose, stone and brown coals, peat, oil and coal pitches, synthetic polymeric materials, liquid and gaseous hydrocarbons, various organic waste. The modern world production of porous carbon materials (PCM) approximates to one million tons per year. Carbon sorbents are used in various forms: in the form of a powder with a particle size of up to 0.8 mm, granules of a larger size, blocks of various shapes and sizes, films, fibers of tissues. The most common ones are powdery sorbents, which are easy to obtain from crushed raw materials. Porous carbon materials are formed as a result of topochemical reactions during pyrolysis (heating in the absence of air oxygen) of fossil coals, peat, wood, cellulose, carbides. At present, about 36% of carbon sorbents are produced from wood, of coals - 28, of brown coals - 14, of peat - 10, of coconut shells - about 10% [20].

The use of graphite as an oil sorbent is very relevant and has a practical future. Penograft is a well-studied material used in industry and engineering.

It is obtained by very rapid heating (thermal shock) of interstitial compounds in graphite (CSG) of various nature. In mass production, interstitial compounds

are used with sulfuric and nitric acids, which are obtained by chemical or electrochemical oxidation of natural graphite powder. After the thermal shock, a product consisting of worm-like carbon particles is formed, the so-called peculiar "black snow". The results of the studies show that the total sorption capacity of STRP and UWRM, depending on the viscosity and on the time of sorption, is 50-60 g of oil per gram of sorbent, then as for commercial sorbents, this value ranges from 3 to 20 g/g [21].

1.4.1.2. Non-carbon sorbents. There is a method for producing a composite cryogel absorbent based on polyvinyl alcohol containing dispersed filler - iron-containing precipitate, isolated at the water intake of Akademgorodok (Tomsk). The sorption properties of the cryogelabsorbant with respect to oil and phenol in the purification of water are investigated. It has been established that cryogel-sorbent possesses the highest phenol-and oil-absorbing capacity on the basis of iron-containing precipitate heat-treated at 250 °C. The degree of water purification in single-stage treatment was 89.5 and 93.5% for oil and phenol, respectively [22].

1.4.1.3. Other natural materials and sorbents on their basis. In connection with the increase in pollution of water basins, the urgency of creating highly efficient sorbents for the removal of oil products (oil and its derivatives) from their surfaces during pollution increases. These sorbents (oil sorbents) must be sufficiently oil-intensive (hydrocarbons absorbability is not less than their own weight), hydrophobic with respect to water and hydrophilic with respect to petroleum products, such as Sorbohole, etc. There are many varieties of oil sorbents from highly porous vegetable materials (peat, sawdust), mineral and artificial origin. These oil adsorbents do not sink, but float on the surface for a long time after absorbing oil products. At the same time, it is recognized that in most situations (fire-danger, excitement, proximity of the coast, lack of special means of collection), it would be advisable to have sorbents drowning after absorbing oil. In this regard, diatomites are natural powder-like nanostructured materials-siliceous rocks consisting of microscopic shells of plankton, 1-5 microns in size with a wall thickness of 50-100 nm of amorphous silicon oxide aggregated in soto-like structures are perspective. Specific high pore volume causes a low specific gravity of dry diatomite - $Picu = 0.4-0.6 \text{ g/cm}^3$.

Natural diatomite is equally hydrophilic to both water and hydrocarbons, which does not allow its use in collecting petroleum products from water and wet surfaces. The authors worked out several methods for hydrophobizing diatomite by creating hydrophobic films on the particles with a thickness of about 5-10 nm (estimated evaluation) and obtaining from it an oil sorbent called "Diasorb". The first is to apply a hydrophobizing layer from the vapor of the "high boiling" hydrocarbon to a cold diatomite powder, mixed in a steam-air stream. Hydrophobization of diatomite is achieved by condensation on it of the order of (3-5)% (weight) hydrophobes. Even loose agglomerates of particles with a size of up to 5 mm are hydrophobic. The second method consists in impregnating diatomite (1-2) with a solution of a high-boiling hydrocarbon in a low-boiling hydrocarbon,

followed by evaporation of the low-boiling solvent. The advantage of the first method is the relative cheapness for industrial implementation. The second is the possibility of organizing an efficient (due to the microsize of particles) process of demulsification of oil emulsions with the organization of closed component cycling [23].

1.4.2. Cellulose-containing sorbents. Lignine. Lignin (from latin "*lignum*" a tree, wood) - the natural polymer which is a part of almost all land plants. Content of lignin in wood of coniferous and deciduous breeds, respectively, is 23–38 and 14–25% on weight. Lignin is located in cellular walls and intercellular space of plants and fastens cellulose fibers. Lignin – amorphous substance from light-cream till dark brown color with a molecular weight from 1 to 150 thousand, with a density of 1250–1450 kg/m³.

From vegetable fabrics lignin can be emitted in many ways, for example hydrolysis in the presence of mineral acids (chamois). Hydrolytic lignin has the following elementary structure, masses. %:

Carbon – 63,5–65;
Hydrogen – 5,4–5,9;
Oxygen – 29,1–30,1.

In industrial scale lignin is received in the course of cellulose and hydrolytic timber-chemical production. The lignins emitted in various ways distinguish on structure and properties as from a product in a native form (protolignin), and from each other.

Lignin – irregular polymer. His branched macromolecules are constructed mainly of the remains of the replaced phenol alcohols:

I – 3-methoxyhydroxycoric, or coniferyl;
II – 3,5-dimethoxy-4-hydroxycinnamic, or synapic;
III – n-hydroxycinnamic, or p-coumaric.

Lignin of wood of coniferous breeds includes, generally the remains of alcohol I, deciduous breeds - I and II alcohols, grassy plants and some tree species (aspen) - alcohol III.

Large-tonnage waste of bark of a larch can be bricketed without use of the binding and increased temperatures. The coal-raw received from briquettes has the sufficient mechanical durability and other properties allowing to use it in various productions, replacing the charcoal produced from birch stem wood. Sorption properties of the received active coals on iodine and methylene blue are at the level of 67-75% and 265 mg/g respectively that above requirements of the standard, BAU-A and OU-A shown to active coals of industrial brands [24].

Lignin easily is exposed to chlorination, nitridation and oxidation, when processing by acids - to hydrolysis. Development of new types of sorbents is based on these properties of lignin. Hydrolytic lignin absorbs 1,5 kg of oil on sorbent kg. The oil capacity of lignin can be increased by processing of the hydrolyzed lignin by solution of the caustic soda or ammoniac water.

1.4.3. Sorbents based on peat. Destruction of oil in the soil is a difficult physical and chemical and biochemical process which orientation and speed

depend on a complex of direct and indirect factors. The climate, properties and the modes of soils, seasonal activity of microflora, humidity, concentration and fractional composition of oil in the soil concern them. The leading role at recultivation is played by biological factors. One of important conditions of biological clarification of the soil from oil is degree of functional activity of soil microflora.

Industrial territories of cold regions are characterized by high extent of oil pollution against the background of extremely adverse soil climatic conditions.

Recently much attention is paid to development of ways of biological recultivation of the petropolluted soils which cornerstone activation of processes of microbiological destruction of oil in the soil is. One of perspective solutions of removal of oil from a surface of the water is use of the sorption and biosorption technologies providing use of the special petroabsorbing materials. The peat processing products used for mitigation of consequences of oil pollution must meet the following requirements: high operational characteristics, rather simple technology of receiving and existence of necessary raw material resources, low cost, biospheric compatibility, i.e. application and utilization of the fulfilled materials shouldn't lead to repeated environmental pollution. There searches conducted by us have shown that sufficiently peat has universality of the properties meeting the above-mentioned requirements. Peat owing to the structure and existence of hydrocarbon-oxidizing microflora (HOM) can serve both as a sorbent of oil hydrocarbons, and their destructor. HOM number in peat by 4-5 times exceeds a similar indicator for soils. Besides, microorganisms of peat aren't antagonists of soil microorganisms.

Peat, owing to the structure and to existence of hydrocarbon-oxidizing microflora (HOM), can serve both as a sorbent of oil hydrocarbons, and their destructor. Sorption capacity of peat in relation to oil depends on extent of decomposition and for riding peat is 8-10, for low-lying – 2-4 g of oil/1 of air and dry peat.

For receiving a peat sorbent, it is recommended to use the riding peat of moss group of low extent of decomposition (5-10%) having the high porosity which was more developed by cellular structure and, respectively, higher sorption ability in relation to oil hydrocarbons. For giving to a sorbent of hydrophobic properties it is modified by, for example, drying at 100-120 °C.

The peat sorbent prepared from riding peat possesses the following characteristics: sorption capacity in relation to oil - 8-10 g of oil/g of a sorbent; saturation time sorbent oil up to the extreme size - 5-10 min.; selectivity in relation to oil in system oil - water - 90-95%; the preservation of oil in volume of a sorbent excluding her spontaneous drain isn't limited on time; buoyancy - more than 30 days.

Utilization of a sorbent is possible in road construction and at production of fuel briquettes [25].

1.4.4. Sorbents based on raw materials of vegetable origin. One of perspective decisions in the field of purification of the petropolluted waters is use of technologies with use as the sorption materials (SM) of vegetable waste. The

efficiency of the last is defined, mainly, by their capacity in relation to NP, water repellency degree, buoyancy after sorption and a possibility of a desorption of oil product, regeneration or utilization of a sorbent [26].

By production of sorbents for absorption of oil and oil products as raw materials it is possible to use both pod of buckwheat and sunflower, and a peel of oats and rice, both a cane chaff, and a black shell of walnut, etc.

The petroabsorbing ability of vegetable waste is the main criterion which should be considered by production of this or that type of a sorbent as the oil capacity of the made sorbent on a straight line depends on initial oil capacity of pure raw materials.

Due to the above as SM were studied the following waste of agriculture: wheat peel (WP), barley (BY) and linen fire (LF). Interest in the called materials is connected with a lot of tonnage and an available source of raw materials in the Republic of Tatarstan. For determination of oil capacity of sorbents at a temperature of 200 of C the oil samples got in NGDU “Elkhovneft” of JSC “Tatneft” were used.

Original lyphysicomechanical properties of waste were defined.

The oil capacity of the called sorption materials in static conditions was defined. The obtained data are presented in table 2. It is noted that within fifteen minutes of engagement the oil capacity of WP reaches 4,12 g/g, and BY - 5,95 g/g. The oil capacity in the dynamic conditions determined by transmission of a certain amount of oil through a layer of a sorbent, weighing 1 g, placed in a glass column for WP and BY, didn't exceed the 5th g/g, for linen fires - 9,44 g/g. In static conditions, the greatest values of oil capacity are received when using linen fires. Existence in its structure of large amounts of cellulose (38-40%) while for other SM, no more than 23% and lignin (23-24%) are caused, most likely, by high value of required parameter in comparison with other studied waste [27].

Use of all these materials which are potential local raw materials for production of sorbents allows to combine elimination of waste of agricultural production with nature protection activity.

The petroabsorbing ability of vegetable waste is the main criterion which should be considered by production of this or that type of a sorbent as the oil capacity of the made sorbent on a straight line depends on initial oil capacity of pure raw materials.

The petroabsorbing ability of vegetable raw materials, including rice peel (after special processing) is from 6 to 10 kg.

One more of the major factors characterizing quality of sorbents is absorption of water by them.

Absorbing moisture in a varying degree vegetable sorbents increase the weight therefore their buoyancy and also oil capacity as the part of pore space is occupied by a water phase worsens.

The Kyzylorda region is widely known for the developed rice growing which in turn is also a source of annual large-tonnage withdrawal – the rice peel polluting the environment.

Because a rice peel being silicone polymer of a phytogenesis, doesn't burn and doesn't decay and owing to availability and low cost, it is an irreplaceable source for receiving the biocompass necessary for biodegradation of oil products.

For receiving this compost we have in vitro made experiments according to influence of a rice peel as filler of the polluted soil therefore have come to a conclusion that a rice peel creating airspace in the soil, promotes intensive oxidation of oil products oxygen of air and their degradation and also experiments on destruction of cellulose and lignin structure of a peel by means of soil aerobic and anaerobic microorganisms were made.

For definition of a possibility of purification of the petropolluted waters and soils by means of the rice peel (RP) we have studied her sorption characteristics in dynamic conditions:

- the oil desorption degree characterizing return of oil to a production cycle and a possibility of his repeated use;
- oil capacity;
- moisture absorption;
- buoyancy.

It is known that the sorption capacity of the studied materials depends on viscosity of oil: if oil easy, low-viscous (for example, the viscosity is equal 3,27sst at 20 °C), the full sorption capacity of RP is equal 4,09, if oil – heavy, high-viscosity (for example, the viscosity is equal to 186,5 sst), the full sorption capacity of RP is equal to 8,82.

By a mechanical extraction depending on type of oil and properties of a sorbent it is possible to return from 60 to 95% of collected oil in a production cycle: RP gives from 61,12 to 65,34% of oil. Regeneration is economically inexpedient in the chemical ways since expense of large volume of reagents is required, there is also a problem a further processing of the formed waste. In this plan thermal processing of sorbents with the residual content of oil is of interest.

When determining a possibility of sewage treatment from oil and oil products of a research have shown that the efficiency of cleaning is depending on the speed of transmission of the purified solution through a motionless layer of adsorbent and from concentration of oil in the purified water.

The table 3 – Efficiency of Purification of Waters from oil products depending on the speed of transmission and concentration of oil

Type of a sorbent	Extent of purification of waters (%) of oil products at speeds			Extent of purification of waters (%) depending on concentration of oil		
	6 ml/min	15 ml/min	32 ml/min	1,4 mg/l	27,6 mg/l	60 mg/l
Sorbenton the basis of RP	99,4	99,3	97,7	0,04	0,2	0,8

Being a product of processing of waste of vegetable raw materials, on extent of cleaning the sorbent based on RP provides high extent of purification of waters of oil products. It should be noted one more advantage also: the sorbent contains small amount of impurity, has high content of carbon therefore it is close on the

structure to active coals, and the branched structure of dioxide of silicon gives him durability and thermal stability [28].

1.4.5. Synthetic sorbents. Synthetic organic sorbents, thanks to the availability and production commercially, find more and more broad application for collecting the poured oil. Besides, they often are production wastes. The open and cellular structure and high oleophilicity of these materials provide efficiency of their use as petroabsorbers. Application for these purposes of expanded polystyrene, polypropylene, phenol formaldehyde and carboamid of ormaldehyde pitch, a rubber crumb, materials based on polyurethane foam, etc. is well known [29].

In recent years one of the most developing directions of a research is development and use the foamed polymeric of the sorbents microcontainers capable at any weather conditions to make collecting oil and oil products from a surface of the water. At the same time quiet, strict requirements are imposed to foamed polymeric sorbents today: high speed of sorption and sorption capacity on oil and oil products, long buoyancy, water repellency, ability to repeated regeneration, simplicity of technology of collecting sorbents from a water surface and ecologically safe utilization of the fulfilled sorbents. An integrated approach to the solution of this problem the foamed polymeric of sorbents at emergency oil spills opens very perspective opportunities of use. There searches conducted for a row of years in this direction, as a matter of fact, allow us to look a little differently at a problem of development and selection the foamed polymeric of sorbents considering not only their sorption capacity, but also the macrostructure, volume weight (seeming to density), the chemical composition of a polymeric basis, type of oil product, flood scale, etc.

Also, the rubber crumb is applied as a sorbent. Data are provided in table 4.

Table 4 – The Main technical characteristics of an oil sorbent on the basis of rubber powder

Indicators	Value
Bulkweight	350–400 kg/m ³
Oilcapacity, kg/kg	4–4,4
Time of full saturation, min.	5–10
Moisturecapacity	10±1%
Buoyancy	Morethan 96 h.
Utilization	Extraction, as a component in the rubber-bituminous and asphalt concrete mixes

As sorbents use of rubbers in view of variety of their chemical and structural structure and also their physical and chemical properties find more and more wide circulation. As sorbents use rubbers with polar groups, for example nitrilacrylic, methacrylic acids and rubbers without polar groups.

The representative of rubbers without polar groups is butadiene styrene rubber. Received as withdrawal from production of rubber products, material

based on this rubber represents a rubber crumb with sizes of 0,5–3 mm. His absorbing ability grows with reduction of the size of a crumb and with increase in time of contact with film oil. Results of researches of these indicators are given in figure 2.

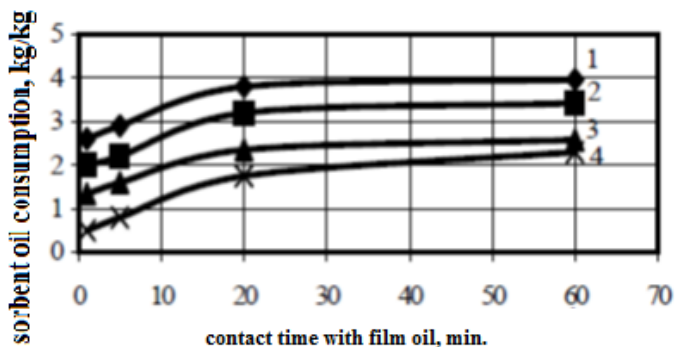


Figure 2 – Dependence of oil capacity of butadienestyrene rubber on time of contact with film oil on a water surface for the size of fractions:
1 – 0,5–1 mm; 2 – 1–2 mm; 3 – 2–3 mm; 4 – 3–5 mm

This sorbent can be reused after an extraction. Fractions of a rubber crumb from 0,63 to 2,5 mm in size have the greatest absorbing ability. Application of a shallow crumb, namely less than 0,63 mm, leads to formation of gel weight that considerably complicates her collecting from a reservoir surface. Besides, the fine crumb has very small weight, and even at small wind at sieving bears her that also complicates her use. In view of the above-mentioned reasons the recommended fraction of the rubber crumb used as a sorbent is fraction from 0,63 to 1,5 mm. As a result of oil sorption the sorbent is agglomerated in large agglomerates up to several kilograms which remain on a surface of the water at any her state within several days and easily gather mechanically, without leaving marks even in the form of thin oil films. Rubber powder after collecting oil can be used as filler for a paving. In world practice a significant amount of a rubber crumb is applied in the mixes used at construction of paving (bituminous rubber BITREK mix). The share of mass of rubber powder in bituminous and rubber knitting in paving can make up to 10%. At the same time physic-mechanical characteristics of all covering (the increased crack resistance and the module of elasticity, increases by 20+30% frost resistance coefficient) significantly improve that affects positively a resource (service life of a covering of roads increases by 1,5+2 times).

In all actions connected with removal of pollution from waters of different function it is necessary to proceed from the main principle: not to do to an ecosystem bigger harm, than that which is already put at pollution. One of the main problems of sorption purification of waters is the problem of further utilization of the fulfilled sorbents. The important moment is the solution of the questions connected with utilization of the fulfilled polymeric sorbents after repeated

sorption. In our opinion one of effective methods of their utilization is burning in the furnace at rather high temperature over 1273 To at which to zero formation of toxic products during thermal decomposition of a polymeric sorbent practically comes down. Based on the above it is possible to come to conclusion about what in relation to conditions of emergency situations, the received results of researches have not only scientific, but also important applied value. It is established that one of the main advantages the foamed polymeric sorbents their high sorption capacity on oil products, buoyancy and ability to repeated regeneration is. Becomes obvious that the choice of sorbents for cleaning of a surface of the water of oil and oil products must be comprehensively reasonable at which has to be considered not only their sorption capacity, but also oil product type, scale of an emergency flood, thickness of an oil layer on a surface of the water, a macrostructure and morphological features of a sorbent. The same sorbent can't be "panacea from all troubles", i.e. at the same time to be effective for sorption of various types of oil products. Probably time to speak about a set of polymeric sorbents and selective approach to their use has come for a long time. So, for example, it is established that for cleaning of a surface of the water of oil and fuel oil it is necessary to use sorbents based on foam polyolefins with a volume weight of 80-170 kg/m³, and for cleaning of diesel fuel sorbents with a volume weight of 500-600 kg/m³. And, not only foam polyolefins, but also other polymeric materials and their mixes, in relation to these or those conditions, can become highly effective supersorbents for collecting oil and oil products [30-32].

The research was carried out according to the scientific and technical program No. BR05234667 within the framework of program-targeted financing CS MES RK.

REFERENCES

- [1] Sorption method of liquidation of emergency oil spills and petroleum products: Proc. allowance / Samoilov N.A., Khlestkin R.N., Shemetov A.V., Shammazov A.A. M.: Chemistry, 2001. 190 p.
- [2] Series of reports IPIECA 5th volume. Dispersers and their role in the elimination of oil spills. 2nd edition. 2001. 105 p.
- [3] William L. Leffler Petroleum Refining. Publishing: Olimp-Business, 2009. 224 p.
- [4] Akhmetov S.A. Technology of deep oil and gas processing: Textbook for high schools. Ufa: Guillem, 2002. 672 p.
- [5] Boyko E.V. Chemistry of oil and fuels: a manual. Ulyanovsk: UISTU, 2007. 60 p.
- [6] Akhmetov S.A., etc. Technology and equipment for oil and gas processing. St. Petersburg: Nedra, 2006. 868 p.
- [7] Revell P., Revelle C. The environment of our habitat. Pollution of water and air. Trans. with English. M.: Mir, 1995. 296 p.
- [8] Beskid P.P., Duryagin E.G. Pollution of the marine environment by oil and oil products // Operation of maritime transport. 2010. N 4(62).
- [9] Kamenshikov F.A., Bogomolny E.I. Oil sorbents. Moscow-Izhevsk: SRC "Regular and chaotic dynamics", 2005. 268 p.
- [10] Primary oil refining / Ed. Glogolova O.F., Kapustina V.M. M.: Kolos, 2006. 400 p.

- [11] Serikov T.P., Karabalin U.S. Theoretical and practical bases of ecologization of oil operations in marine conditions: Monograph. Almaty: Evero, 2009. 176 p.
- [12] Rodin A.A. Environmental analyzes for oil spills and oil products. St. Petersburg: Anatalia, 2000. 250 p.
- [13] Kuzubova L.M., Morozov S.V. Purification of oily wastewater. Novosibirsk, 1992. 72 p.
- [14] Drugov Yu.S. Environmental analysis for oil spills and oil products. Practical guidance. M.: BINOM. Laboratory of Knowledge, 2007. 270 pp.
- [15] Kamenshikov F.A., Bogomolny E.I. Removal of oil products from the water surface and soil. M. – Izhevsk: SRC "Regular and chaotic dynamics", 2006. – 528 p.
- [16] Temirkhanov B.A., Sulygova Z.Kh. New carbon materials for oil spill response // Fundamental research. 2012. Vol. 2, N 6. P. 471.
- [17] Arena V.Zh., Gridin O.M. The problem of oil spills and the role of sorbents in solving it // Oil, gas and business. 2000. N 5. P. 27-30.
- [18] Arena V.Zh., Gridin O.M., Yanshin A.L. Oil pollution: how to solve the problem // Ecology and industry of Russia. 1999. N 9. P. 33-36.
- [19] Kamenshikov F.A., Bogomolny E.I. Oil sorbents. Moscow-Izhevsk: SRC "Regular and chaotic dynamics", 2005. 268 p.
- [20] Kuznetsov B.N. Synthesis and application of carbon sorbents // Sorokovsky educational journal. 1999. N 12. P. 29-34.
- [21] Temirkhanov B.A., Sulygova Z.Kh., Salamov A.H., Nal'gieva A.M. New carbon materials for oil spill response // Fundamental research. 2012. N 6 (part 2). P. 471-475.
- [22] Sirotkina E.E., Pogadaeva N.I., Fufayeva M.S. Cryogel sorbent based on polyvinyl alcohol and iron-containing sediment for the removal of oil and phenol from water // Izvestia Tomsk Polytechnic University. 2010. Vol. 317, N 3. P. 49-53.
- [23] Aleksandrov K.A., Latynin K.V., Evstyukhin I.A. Water-absorbent oil sorbents based on natural nanostructured materials-diamites // Moscow Engineering Physics Institute (State University) International Scientific and Technical Center. Moscow.
- [24] Simkin Yu.Ya., Besedina I.N., Epifantseva N.S. Processing of bark of larch on carbon sorbents // Modern high technology. 2007. N 3. P. 46-46.
- [25] Burmistrova T.I., Alekseeva T.P., Stakhina L.D., Seredina V.P. Research of properties of peat for the decision of ecological problems // Chemistry of vegetative raw materials. 2009. N 3. P. 157-160.
- [26] Khlestkin R.N., Samoilo N.A. On the Elimination of Spills Using Plant Waste // Oil Industry. 2000. N 7. P. 84-85.
- [27] Stepanova S.V., Kondalenko O.A., Trushkov S.M., Domozhirov V.A. Liquidation of oil spills by the sorption method with the use of new materials // Bulletin of Kazan Technological University. 2011. P. 159-160.
- [28] Zholbaeva G.A. Development of technology for the use of rice husk as an oil sorbent // Vestnik Kyzylorda State University. Kazakhstan. 2011. <http://conf.dalrybvtuz.ru/>
- [29] Magerramov A.M., Azizov A.A., Alosmanov R.M., Kerimova E.C., Buniyat-zade I.A. Removal of thin oil films from the water surface // The Young Scientist. 2011. Vol. I, N 7(30). P. 65.
- [30] Kahramanli Yu.N. Sorbents on the basis of foam polyolefins for the sorption of oil and oil products from the water surface during emergency spills // Oil and gas business. Scientific and technical journal. 2010. Vol. 8, N 1. P. 80.
- [31] Tarasova T.F., Chapalda D.I., Abdrakhimov Yu.R. Application of rubber crumbs as an oil sorbent in emergency oil spills // Ufa State Petroleum Technical University. Bulletin of the OSU. 2007. N 4. P. 150.
- [32] Strepetov I.V., Muscovite E.V. The use of sorbents on the basis of waste polymeric materials for the treatment of waste water from oil pollution. 2006. <http://vestnik.vgasu.ru/attachments/strepetov.pdf>

Резюме

*Н. А. Бектенов, Е. Е. Ергожин, С. Б. Рыспаева,
К. А. Садыков, И. С. Молдагалиева, А. А. Маратова*

ЭКОЛОГИЯ НЕФТИ И НЕФТЕСОРБЕНТЫ

Изложены материалы о нефтесорбентах и их применении. Показаны методы ликвидации разливов и аварий нефти и нефтепродуктов на почве и водной поверхности.

Ключевые слова: нефть, сорбенты, экология, химический состав, вода, почва, торф, целлюлоза.

Резюме

*Н. А. Бектенов, Е. Е. Ергожин, С. Б. Рыспаева,
К. А. Садыков, И. С. Молдагалиева, А. А. Маратова*

МҰНАЙ ЖӘНЕ МҰНАЙ СОРБЕНТТЕРІ ЭКОЛОГИЯСЫ

Мақалада мұнай сорбенттері және оларды қолдану туралы материалдар берілген. Топырақ және су бетіндегі мұнай мен мұнай өнімдерінің төгілуін және авариясын жою әдістері көрсетілген.

Түйін сөздер: мұнай, сорбенттер, экология, химиялық құрамы, су, топырақ, шымтезек, целлюлоза.

I. N. ANUARBEKOVA, N. O. AKIMBAYEVA, S. A. VIZER, K. B. YERZHANOV

JSC "Institute of Chemical Sciences named after A. B. Bekturov's",
Almaty, Republic of Kazakhstan.
E-mail: Indikosha_1987@mail.ru

SELECTIVE MONOALKYLATION AND DITHIOCARBONYLATION OF ETHYLENEDIAMINE

Abstract. Selective monoalkylation and one-pot monoalkylation-dithiocarbonylation reactions of ethylenediamine were carried out in good and high yields (60-78%). The structures of the obtaining products – N-alkylethane-1,2-diamines and sodium 2-(alkylamino)ethyl dithiocarbamates were confirmed by IR, ^1H NMR and ^{13}C spectra.

Key words: ethylenediamine, alkylation, alkyl bromide, dithiocarbonylation, sodium 2-(alkylamino)ethylcarbamodithioates.

Introduction. Before we in [1, 2] have got excellent results with sodium N-(3-phenylprop-2-yn-1-yl)-N-butyldithiocarbamate (AN-16) as rooting accelerator on cuttings of blackcurrant, exceeding over 10 % results obtained with the help of a known rooting agent - indolylacetic acid (IAA) [3]. At the same time, its working concentration was as 10 times lower as than the working concentration of IAA. This compound proved highly effective in stimulating the laying of generative buds of fruit trees, which makes it promising for use in innovative technologies for producing fast-growing seedlings [4], and it is also of practical interest in the cultivation of wild medicinal plants, for example, *Serratula coronata*, increasing threefold the germination of seeds [5].

In this regard, the search of highly effective plant growth regulators among the new sodium dithiocarbamates of alkylated diamines can be fruitful.

EXPERIMENTAL PART

The spectra of NMR were recorded on a JNN-ECA 400 spectrometer from Jeol (Japan). The working frequency of the spectrometer is 400 MHz on the ^1H and 100 MHz on ^{13}C nuclear cores, respectively. The survey was carried out at room temperature in a solvent of DMSO. Chemical shifts are measured relative to signals of residual protons or carbon atoms of a deuterated solvent.

The melting points of the obtained substances were determined on a Boetius heating table. The IR spectra are recorded on a Nicolet 5700 spectrometer in KBr tablets. The course of the reaction and the purity of the products were monitored by thin-layer chromatography on plates of "Silufol UV-254", eluent - benzene: ethanol, 1:3 with the appearance of spots of substances with iodine vapor.

N-butylethane-1,2-diamine 1. A 3-necked flask equipped with a mechanical stirrer, reflux condenser and dropping funnel was charged with 5 ml (0.075 mol) of ethylenediamine, 20 ml of ethanol and 7.3 g (0.074 mol) of acetate potassium

were added. At a temperature of 50 °C 7.9 ml (0.075 mol) of freshly distilled butyl bromide in 10 ml of ethanol was added dropwise over a period of 30 minutes. The reaction was monitored by thin layer chromatography. After a two-day stirring, TLC showed the completion of the reaction to the disappearance of the octyl bromide and ethylenediamine spots. After removal of the precipitate and ethanol, an oily substance was obtained. As a result, 5.7 g (a yield 66%) of N-butylethane-1,2-diamine **1** was obtained.

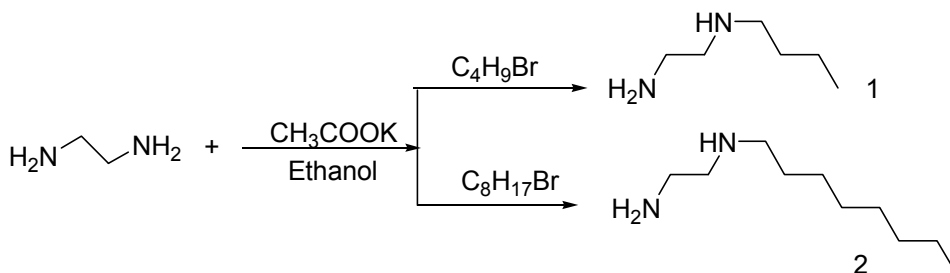
N-octylethane-1,2-diamine 2. A 3-necked flask equipped with a mechanical stirrer, reflux condenser and dropping funnel was charged with 5 ml (0.075 mol) of ethylenediamine, solute in 20 ml of ethanol and 7.3 g (0.074 mol) of potassium acetate. At a temperature of 50 °C, 16 ml (0.09 mole) of freshly distilled octyl bromide solute in 20 ml of ethanol was added dropwise to the reaction flask over a period of 30 minutes. The reaction was monitored by thin layer chromatography. After a two-day stirring, TLC showed the completion of the reaction to the disappearance of the octyl bromide and ethylenediamine spots. After removal of the precipitate and ethanol, an oily substance was obtained. As a result, 10.1 g of N-octylethane-1,2-diamine **2** was obtained in a yield of 78%.

Sodium 2-(heptylamino)ethyl-dithiocarbamate 3. 10 ml (0.15 mol) of ethylenediamine solute in 20 ml of ethanol were introduced into a three-necked flask equipped with a mechanical stirrer, reflux condenser and dropping funnel. 12 ml (0.076 mole) of heptyl bromide was added dropwise to the reaction flask within 30 minutes. At a temperature of 50-60 °C the reaction mixture was stirred for 4 hours. The reaction was monitored by thin layer chromatography (silufol, eluent benzene: alcohol, 1:3). After the disappearance of the spots of heptyl bromide and ethylenediamine, the reaction temperature was lowered to -5 °C. 3.27 g (0.082 mol) of sodium hydroxide dissolved in water and 4.9 ml (0.079 mol) of carbon disulphide were introduced into the flask. After completion of the reaction, the mass was filtered off, ethanol was removed. The combined crystalline mass was washed with acetonitrile. As a result, 23 g of the sodium 2-(heptylamino)ethyl-dithiocarbamate **3**, mp 120-122 °C was obtained in a yield of 60%.

Sodium 2-(octylamino)ethyl-dithiocarbamate 4. 10 ml (0.15 mol) of ethylenediamine solute in 20 ml of ethanol were introduced into a three-necked flask equipped with a mechanical stirrer, reflux condenser and dropping funnel. 13 ml (0.075 mole) octyl bromide was added dropwise to the reaction flask within 30 minutes. At a temperature of 50-60 °C, the reaction mixture was stirred for 4 hours. The reaction was monitored by thin layer chromatography. After the disappearance of the octyl bromide and ethylenediamine stains, the reaction temperature was lowered to -5 °C. 2.99 g (0.074 mol) of sodium hydroxide dissolved in water and 5.1 ml (0.08 mol) of carbon disulphide were introduced into the flask. After completion of the reaction, the crystalline mass was filtered off, ethanol was removed. The combined crystalline mass was washed with acetonitrile. As a result, 12.75 g (63% yield) of the sodium 2-(octylamino)ethyl-dithiocarbamate, mp 133 °C were obtained.

RESULTS AND DISCUSSION

In order to synthesize the new hetero-organic compounds and study their chemical, physico-chemical and biological properties, in particular physiological and surface activity, we carried out the selective monoalkylation of ethylenediamine by the method we used earlier for the N-alkylation of monoethanolamine [6]. Alkylation of ethylenediamine was carried out with alkyl bromide in an ethanol medium at the presence of potassium acetate on equimolar ratio of the reagents at the reaction temperature about 50-55 °C. After the usual procedure of isolation the product, N-butylethane-1,2-diamine **1** was obtained in an individual form by yield of 66% and N-octylethane-1,2-diamine **2** by yield of 78%.



The structures of the synthesized compounds were proved by the methods of IR, ¹H NMR and ¹³C spectroscopy (the spectra of the synthesized N-octylethane-1,2-diamine **2** are shown in figures 1–5).

In the IR spectra of amines **1** and **2**, absorption bands at 3479 cm⁻¹, 3412 cm⁻¹ and 1671 cm⁻¹, characteristic for the NH₂ group, are observed. In the regions 2955 cm⁻¹, 2887 and 2935 cm⁻¹, intensive bands of stretching vibrations of C-H bonds characteristic for saturated hydrocarbon substituents are observed.

In the PMR spectrum of N-butyl ethane-1,2-diamine **1**, there is a broadened singlet of CH₃ protons at 0.98 ppm, proton's signals of (CH₂)₃-methylene groups appear in the range of 1.0-2.65 ppm. Protons of NH-CH₂ groups of the ethylene bridge resonate at 3.4-3.5 ppm. as a multiplet, NH-protons of amine groups are resonated at 3.0-3.10 ppm. In the PMR spectrum of N-octylethane-1,2-diamine **2**, (Figure 1), the signal of the terminal methyl group (H-12) appears as a weakly ordered triplet at 0.82 ppm. Resonance signals of methylene (H-6 - H-11) groups of the octyl fragment are observed as a highly intense broad singlet at 1.22 ppm. The protons of NCH₂ group (H-5) under the influence of the neighboring nitrogen heteroatom resonate at a region of 2.46 ppm. The protons of the CH₂-groups of the ethylene bridge give signals at a frequency of 1.56 and 2.88 ppm. The highest-frequency signal (3.19 ppm) belongs to the protons of the amino groups.

Figures 2 and 3 show the COSY spectrum and COSY correlations for N-octyl ethane-1,2-diamine **2**, which indicate groups of protons interacting with each other. These data confirm the assignment of signals of the PMR spectrum and the structure of N-octylethane-1,2-diamine **2**.

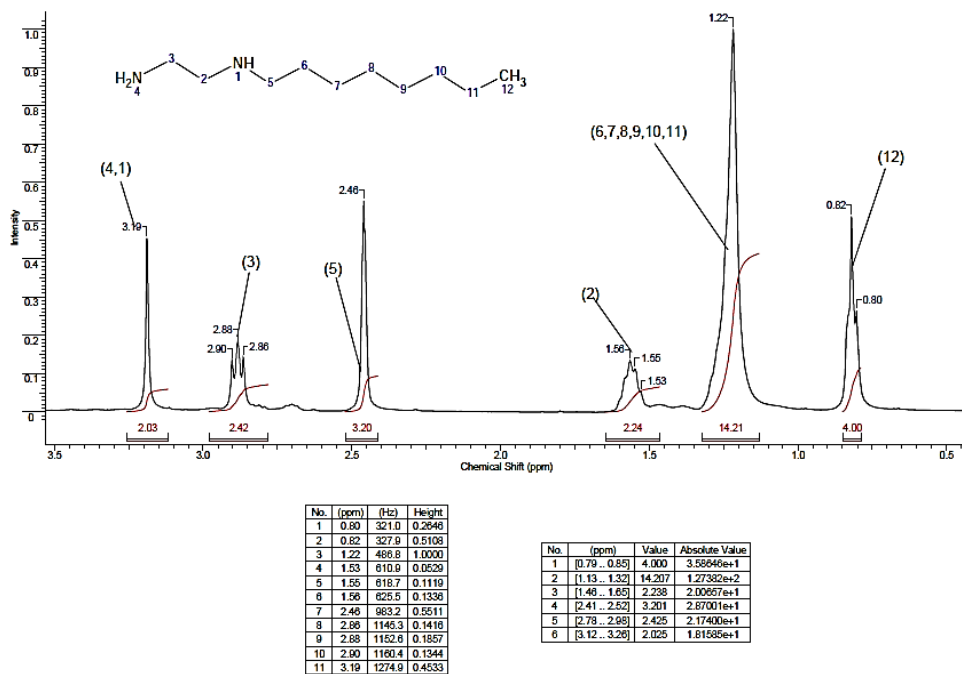


Figure 1 – PMR spectrum of N-octylethane-1,2-diamine 2

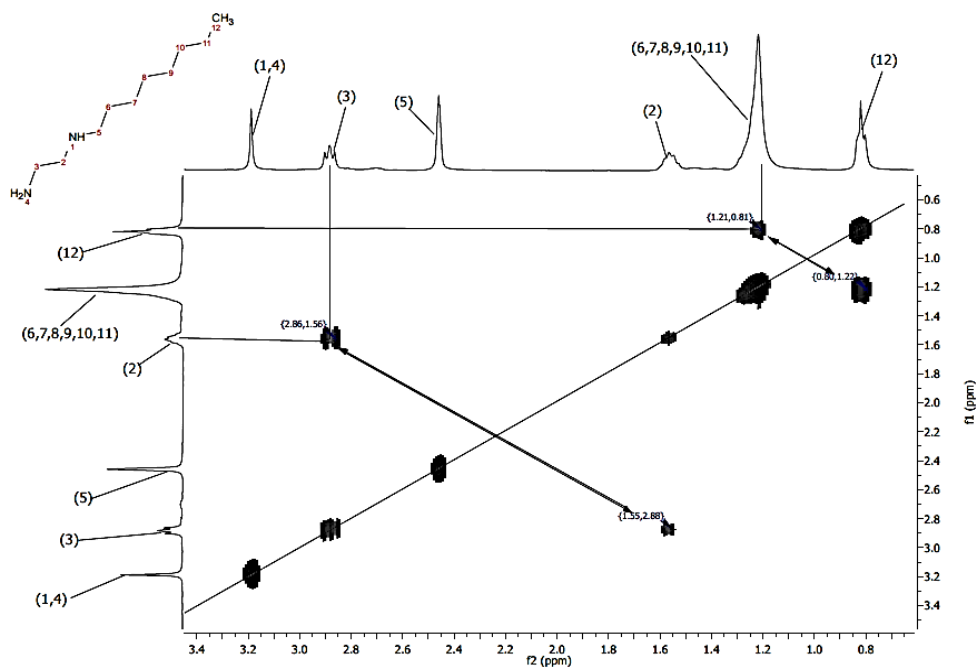


Figure 2 – COSY spectrum of N-octylethane-1,2-diamine 2

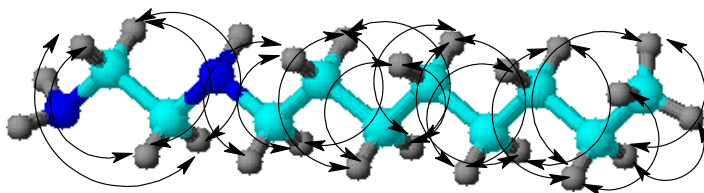


Figure 3 – COSY Correlations for N-octylethane-1,2-diamine 2

In the carbon spectrum of N-octylethane-1,2-diamine 2 shown in figure 4, the signal of the terminal methyl group of the octyl fragment is observed at 14.46 ppm. The signals of the carbon atoms of C-6 – C-11 methylene groups in the range from 22.58 to 31.67 ppm are observed. Signal of the N-CH₂ group of the octyl substituent is manifested at 40.72 ppm. Signals at 43.37 and 47.63 ppm. can be attributed to the carbon atoms of the ethylene chain C-2 and C-3, respectively.

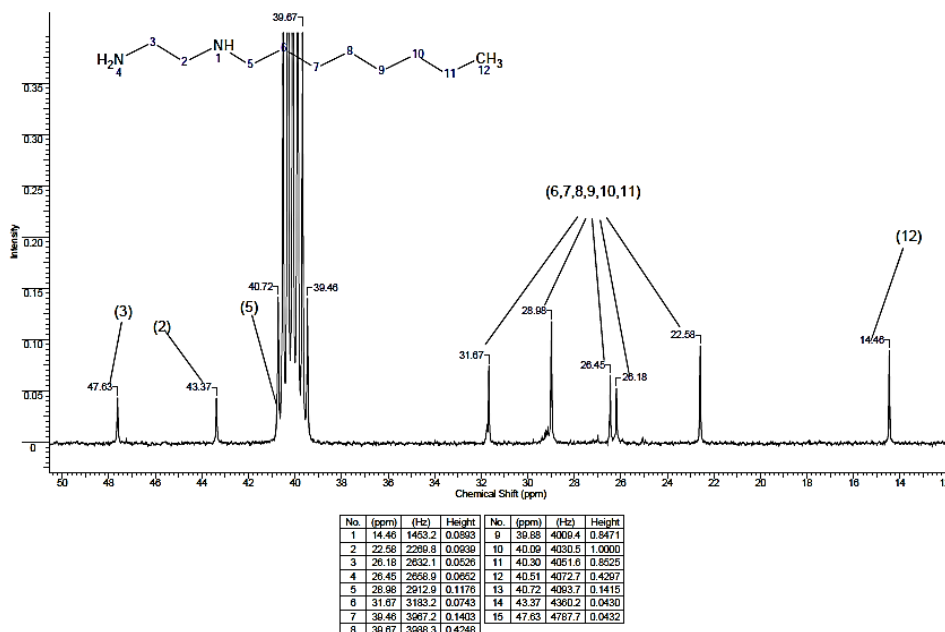


Figure 4 – NMR ¹³C spectrum of N-octylethane-1,2-diamine 2

The NMR ¹³C spectrum of N-butylethane-1,2-diamine 1 also shows a signal at 14.0 ppm corresponding to the carbon atom of the terminal CH₃ group, signals at 25.1; 32.0 and 42.2 ppm. are referred to the carbon atoms of the butyl group, the signals at 49.3 and 54.4 ppm. can be attributed to the carbon atoms of the group NH₂-CH₂-CH₂-NH.

Figures 5 and 6 show the HMQC spectrum and HMQC correlations for N-octylethane-1,2-diamine 2, indicating which carbon atoms interact with certain

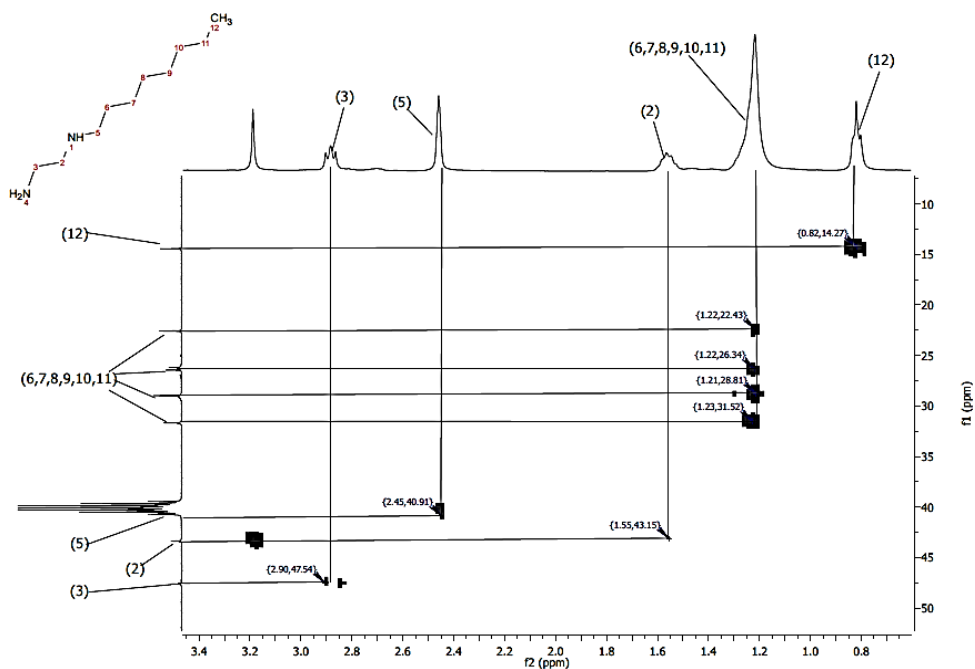


Figure 5 – HMQC spectrum of N-octylethane-1,2-diamine 2

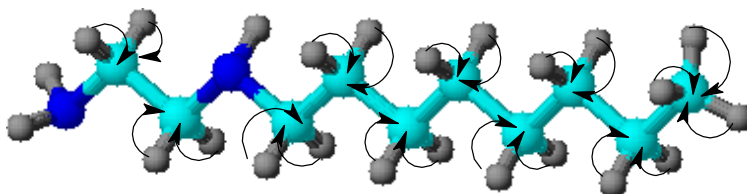
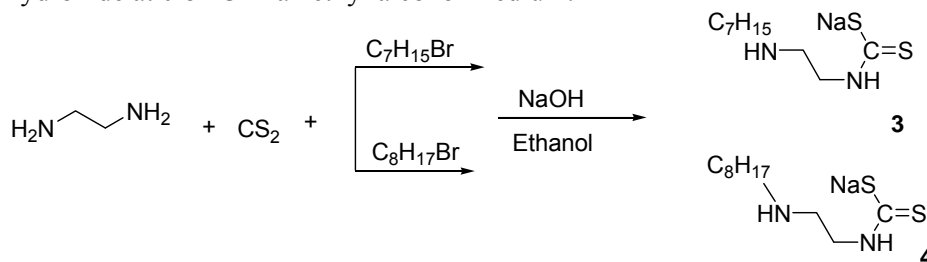


Figure 6 – Correlation of the HMQC compound of N-octylethane-1,2-diamine 2

proton groups. These data confirm the assignment of the signals from NMR ^{13}C and PMR spectra and the structure of N-octylethane-1,2-diamine 2.

The sodium dithiocarbamates 3 and 4 were obtained by successive interaction of equimolar amounts of ethylenediamine with alkyl bromide at the temperature 50-60 °C and then with carbon disulphide in the presence of sodium hydroxide at 0-5 °C in an ethyl alcohol medium.



Dithiocarbamates **3**, **4** settled out of the reaction solution as white crystalline substances with R_f 0.26 and R_f 0.29 (silufol, benzene: alcohol, 1:3), which after reaction finishing are filtered off and washed with acetonitrile. The yields of the sodium salts of 2-(heptylamino)ethyl-dithiocarbamate **3** and 2-(octylamino)ethyl-dithiocarbamate **4** are 60% and 63%, melting points 120-122 °C and 133 °C, respectively.

In the IR spectra of synthesized new dithiocarbamates **3**, **4**, there are absorption bands of C=S bond stretching vibrations in the region of 1420-1460 cm^{-1} and C-S bond in the region of 638-735 cm^{-1} . Absorption bands in the region of 3300-3500 cm^{-1} characteristic for NH groups are also observed. In the region of 2887-2935 cm^{-1} intense bands of stretching vibrations of C-H bonds characteristic for saturated hydrocarbon substituents are observed.

Compounds **3** and **4** are characterized by PMR spectroscopy. A broaden singlet of CH_3 protons is observed in the spectrum at 0.96 - 0.98 ppm. The protons of the $(\text{CH}_2)_n$ -methylene groups in the region of 1.1-2.6 ppm in the form of multiplets are observed. The protons of the NCH_2 group are resonated in the region of 3.60-3.80 ppm as the multiplets. The protons of the amine group are resonated in the region of 3.0-3.30 ppm.

In the PMR spectrum of the sodium 2-(octylamino) ethyl-dithiocarbamate **4**, a singlet of CH_3 -group protons is observed at 0.96. Protons $(\text{CH}_2)_n$ -methylene groups in the region and 1.1-2.6 ppm in the form of multiplets are observed. The protons of NH-CH_2 groups at 3.73 and 3.60 ppm. in the form of multiplets are resonated, the NH protons of the amine and amide groups are resonated at 3.0 and 3.20 ppm.

Conclusion. Thus, as a result of our studies, the conditions for the selective monoalkylation of ethylenediamine have been experimentally established. For the first time, a one-pot synthesis of sodium 2-(alkylamino)ethyl-dithiocarbamates was carried out. The structure of synthesized compounds is confirmed by physicochemical methods of investigation.

The research was carried out according to the scientific and technical program No. BR05234667 within the framework of program-targeted financing CS MES RK.

REFERENCES

- [1] Vizer S.A., Akimbayeva N.O., Yerzhanov K.B. Regulatory rosta rasteniy, sozdannyye v laboratorii khimii fiziologicheskii aktivnykh soyedineniy Instituta khimicheskikh nauk im. A.B. Bek-turova // Khim. zh. Kaz. 2016. N 4. P. 10-45.
- [2] Yerzhanov K.B., Vizer S.A., Sycheva Ye.S. Sozdaniye innovatsionnykh regulyatorov rosta rasteniy shirokogo spektra deystviya. Almaty, 2017. 158 p.
- [3] Pat. 22965 RK. MPK8 A01N 39/02, C07C 49/172. N-(3-fenilprop-2-in-1-il)-N-butilditiokarbamat natriya, obladayushchiy korneobrazuyushchey aktivnost'yu / Yerzhanov K.B., Akimbayeva N.O., Saurbayeva B.S., Yermagambetov R.R., Oleychenko S.N., Kampitova G.A.; zayavl. 28.10.2009; opubl. 15.03.2012, Byul. N 3. 3 p.
- [4] Ya znayu – sadu tsvest' // Zhurnal Zhaylau. Tematicheskoye prilozheniye k zhurnalu AgroAlem. 2009. N 3(3). P. 2-4.
- [5] Innov. pat. 25744 RK. MPK8 C08M 39/18. Regulyator rosta semyan dikorastushchikh lekarstvennykh rasteniy / Yerzhanov K.B., Akimbayeva N.O., Anuarbekova I.N., Sultanova Z.K., Sotnikova V.V.; zayavl. 30.05.2011; opubl. 15.05.2012, Byul. № 5.

[6] Anuarbekova I.N., Akimbayeva N.O., Kurmankulov N.B. Sintez N(alkil)-N-monoetanolaninonov na osnove pervichnogo amina // «Innovatsionnyye tekhnologii i issledovaniya, napravlennyye na razvitiye zelenoy energetiki i glubokuyu pererabotku produktcii» sb. materialov mezhd. shkola-seminara. Ust'-Kamenogorsk, 2013. P. 64.

Резюме

И. Н. Әнуарбекова, Н. О. Әкімбаева, С. А. Визер, Қ. Б. Ержанов

ЭТИЛЕНДИАМИНДІ СЕЛЕКТИВТІ N-МОНОАЛКИЛДЕУ ЖӘНЕ ДИТИОКАРБОНИЛДЕУ

Этилендиминді бромды алкилдермен этанолды ортада ацетат калий қатысында реагенттердің эквимольді қатынасында 50-55 °С температурада моноалкилдеу нәтижесінде 66% шығыммен N-бутилэтан-1,2-диамин және 78% шығыммен N-октилэтан-1,2-диамин синтезделінді. Әрекеттесудің жалғасы ретінде бір реакциялық колбада эквимольді мөлшерде этиленаминнің алкил броммен 50-60 °С температурада және содан кейін күкіртті көміртеппен натрий гидроксиді қатысында 0-5 °С температурада этил спирті ортасында натрий дитиокарбаматтары алынды. 2-(гептиламино)этилдитиокарбаматтың және 2-(октиламино)этилдитиокарбаматтың шығымдары 60 және 63%, сәйкесінше балку температуралары 120-122 °С және 133 °С тең. N-алкилэтан-1,2-диаминдер және натрий 2-(алкиламино)этилдитиокарбаматтарының құрылысы ИК, ЯМР ¹H және ¹³C-спектрлерінің көмегімен дәлелденді. N-октилэтан-1,2-диаминнің COSY және HMQC спектрлері, корреляциясы келтірілген.

Түйін сөздер: этилендиамин, алкилдеу, бромды алкилдер, дитиокарбонилдеу, натрий 2-(алкиламино)этилкарбамодитиоаты.

Резюме

И. Н. Ануарбекова, Н. О. Акимбаева, С. А. Визер, Қ. Б. Ержанов

СЕЛЕКТИВНОЕ МОНОАЛКИЛИРОВАНИЕ И ДИТИОКАРБОНИЛИРОВАНИЕ ЭТИЛЕНДИАМИНА

Путем селективного моноалкилирования этилендиамин бромистыми алкилами в этанольной среде в присутствии ацетата калия при эквимольном соотношении реагентов и температуре реакции 50-55 °С синтезированы N-бутилэтан-1,2-диамин с выходом 66% и N-октилэтан-1,2-диамин с выходом 78%. Последовательным взаимодействием в одной реакционной колбе эквимольных количеств этилендиамин с алкилбромидом при температуре 50-60 °С и затем с сероуглеродом в присутствии гидроксида натрия при температуре 0-5 °С в среде этилового спирта получены соответствующие дитиокарбаматы натрия. Выходы натриевых солей 2-(гептиламино)этилдитиокарбамата и 2-(октиламино)этилдитиокарбамата составляют 60 и 63%, температуры плавления 120-122 и 133 °С соответственно. Строение N-алкилэтан-1,2-диаминов и 2-(алкиламино)этилдитиокарбаматов натрия подтверждено данными ИК-, ЯМР ¹H- и ¹³C-спектров. Приведены COSY и HMQC спектры и соответствующие корреляции N-октилэтан-1,2-диамин.

Ключевые слова: этилендиамин, алкилирование, бромистые алкилы, дитиокарбонилирование, натрий 2-(алкиламино)этилкарбамодитиоаты.

B. S. TEMIRGAZIEV^{1,3}, T. M. SEILKHANOV^{2*}, S. TYANAKH^{1,3},
A. M. KOZHANOVA¹, O. T. SEILKHANOV², YE. V. MINAYEVA³,
L. K. SAL'KEEVA³, B. I. TULEUOV¹, S. M. ADEKENOV¹

¹JSC International Research and Production Holding "Phytochemistry",
Karaganda, Republic of Kazakhstan,

²Kokshetau State University named after Sh. Ualikhanov, Kokshetau, Republic of Kazakhstan,

³Karaganda State University named after E.A. Buketov, Karaganda, Republic of Kazakhstan

OBTAINING AND INVESTIGATION OF SUPRAMOLECULAR INCLUSION COMPLEX OF 2-DEOXY-20-HYDROXYECDYSONE WITH γ -CYCLODEXTRINE BY NMR SPECTROSCOPY METHOD

Abstract. For the first time, 2-deoxy-20-hydroxyecdysone (2-deoxyecdysterone) has been isolated from the above-ground part of *Silene fruticulosa* (Pall.) Schischk (*Caryophyllaceae* Juss. family). The formation of complex of phytoecdysteroids with γ -cyclodextrin has been studied with the help of NMR spectroscopy. Due to changing the chemical shifts of the substrate and receptor protons, it has been revealed that 2-deoxy-20-hydroxyecdysone interacts with γ -cyclodextrin to form a supramolecular inclusion complex of the stoichiometric composition of 1:1 with the entry of the fragment A of the substrate molecule into the inner cavity of the receptor.

Keywords: *Silene fruticulosa* (Pall.) Schischk, 2-deoxy-20-hydroxyecdysone, cyclodextrin, inclusion complexes, NMR spectroscopy.

Introduction. At the present stage of development of supramolecular chemistry, the most promising and intensively developing direction is the preparation and investigation of inclusion complexes of steroid compounds with cyclodextrins (CDs) [1-3]. The increased interest in CDs is due to their cyclic structure and the ability to form supramolecular host-guest inclusion complexes (receptor-substrate) due to the internal hydrophobic cavity. The supramolecular inclusion complexes of CDs with biologically active compounds make it possible to increase the solubility of the latter in water, reduce toxicity, allow liquid substances to be converted into solid substances, increase the stability of the substances to oxidation and hydrolysis [4-6]. Therefore, the preparation of inclusion complexes of phytoecdysteroids of ecdysterone and 2-desoxyecdysone that are promising synthons for regioselective modifications with CDs are in great demand [7-10].

Selection as a substrate of supramolecular self-assembly of 2-deoxy-20-hydroxyecdysone (3 β , 14 α , 20R, 22R, 25-pentahydroxy-5 β (H)-cholest-7-en-6-one, 2-deoxyecdysterone) **1** is due to the wide range of biological activity of the latter. Compound **1** in small doses exhibits hormonal activity for insects in *in vivo* tests [11] and was previously first isolated from the *Jacustalandei* crayfish [12] and the *Blechnum minus* fern [13]. The compound **1** was also isolated from the Kazakh plant *Silene fruticulosa* (Pall.) Schischkhar vested in flowering phase [14,15].

EXPERIMENTAL PART

The reversed-phase high-performance liquid chromatography method was carried out on a HEWLETT PAKKARD Agilent 1100 Series instrument, an analytical column 4.6×150 mm, Zorbax SB-C_18; mobile phase: 10% isopropyl alcohol, UV detection at a length of 254 nm, a column temperature of 20° , a flow rate of the eluent of 0.75 ml/min, and a sample volume of 20 μ l.

^1H and ^{13}C NMR spectra were recorded on the JeolJNM-ECA 400 spectrometers (399.78 and 100.53 MHz on ^1H and ^{13}C nuclei, respectively) in a solution of DMSO- d_6 and BrukerAvance DRX-500 (500 and 125 MHz on ^1H and ^{13}C nuclei, respectively) for solutions in CDCl_3 . Chemical shifts are measured relative to the residual signals of protons or carbon atoms DMSO- d_6 and CDCl_3 . The mass spectra were obtained on an LCQ Fleet mass spectrometer (ThermoElectron Corporation, USA) under the conditions of chemical ionization at atmospheric pressure. Positive ion spectra were analyzed using the Xcalibur program. TLC was performed on Kieselgel 60 F254 chromatographic plates. Column chromatography was carried out on Kieselgel 60 (VWR, Art. 7734)silica gel.

γ -CD was used by Fluka's production facilities with a purity of 99%.

The melting point of the inclusion complex was determined on a Boetius instrument. The course of the reaction and the purity of the obtained compounds were monitored by thin-layer chromatography on Sorbfil plates in the ethanol-chloroform system (2:8). The plates were developed with a mixture of H_2SO_4 :vanillin.

Isolation of the ecdysteroid-containing fraction of *Silene fruticulosa* (Pall.) Schischk. Airborne aerial parts of *Silene fruticulosa* (Pall.) Schischk sem. of *Caryophyllaceae* Juss. family (6 kg, collected on August 20, 2015 during the flowering phase in the Karaganda region of the Ulytau district of the Republic of Kazakhstan) was extracted four times with 70% aqueous ethanol by heating in a water bath. The resulting ethanol extract was treated with a 2:1 mixture of petroleum ether and ethyl acetate to remove non-polar components, the remaining water soluble portion was extracted with isobutanol. Isobutanol extracts were combined, and then isobutanol was distilled off to dryness in vacuo. There was obtained the sum of ecdysteroids with concomitant substances in the form of a thick green syrupy mass in the amount of 504 g.

Chromatographic separation of the ecdysteroid-containing fraction. The extract (16.3 g) was dissolved in a mixture of chloroform-methanol (150 ml, 1:1) in an ultrasonic bath. The resulting solution with a small suspension of insoluble substance was mixed with silica gel and the solvent was evaporated. The residue was applied to a silica gel column, eluting with a chloroform-methanol (50: 1 \rightarrow 1: 1) mixture. The eluate from the column in 30 ml portions was collected in separate tubes (the first 19 tubes were discarded as substance-free), which were pooled into 8 fractions based on TLC analysis.

Acetylation of F-5 fraction. A solution of the F-5 oil (235 mg) and DMAP (9.4 mg) in pyridine (5 ml) and Ac_2O (2.5 ml) was held at $40\text{--}45^\circ\text{C}$ for 5 hours.

The solvent was then evaporated in vacuum; the residue was applied to a SiO₂-containing column. Elution was carried out with a mixture of CHCl₃-MeOH (100: 1 → 30: 1). 123.14 mg of (22R)-2β,22-diacetoxy-5β-cholest-7-en-6-one-14α,25-diol was obtained as an oil. ¹H NMR (500 MHz, CDCl₃, δ, ppm, J/Hz): 0.66 (3H, s, CH₃-18), 0.93 (3H, d, J=6.7, CH₃-21), 0.97 (3H (2H, s, CH₃-19), 1.21 (3H, s, CH₃-26), 1.23 (3H, s, CH₃-27), 2.04 (3H, s, CH₃-COO-2), 2.05 (3H, s, CH₃-OCO-20), 2.35 (1H, dd, J = 12.6, 3.9, H-5), 3.09 (1H, m, H-9), 4.87 (1H, d, J=10.1, H-22), 5.05 (1H, br. s, H-3), 5.84 (1H, d, J=1.9, H-7). ¹³C NMR (125 MHz, CDCl₃, δ, ppm): 13.39, 15.69, 20.50, 21.36, 21.91, 23.94, 25.36, 25.43, 28.93, 29.48, 29.89, 30.78, 31.90, 36.38, 39.01, 40.34, 47.31, 51.64, 67.66, 70.72, 77.20, 84.70, 121.28, 164.44, 170.46, 170.98, 203.01. MS (APCI⁺) *m/z* (%): 532.8 ([M]⁺, 15), 515.1 ([M-H₂O+H]⁺, 100), 497.2 ([M-2H₂O+H]⁺, 46), 473.3 ([M-AcOH+H]⁺, 64), 455.6 ([M-H₂O-AcOH+H]⁺, 95).

Acetylation of F-7 fraction. A solution of the F-7oil (240 mg) and DMAP (9.4 mg) in pyridine (5 ml) and Ac₂O (2.5 ml) was held at 40-45°C for 5 hours. The solvent was then evaporated in vacuum; the residue was applied to a SiO₂-containing column. Elution was carried out with a mixture of CHCl₃-MeOH (100: 1 → 30: 1). 31.2 mg of (22R)-2β,22-diacetoxy-5β-cholest-7-en-6-one-14α,20,25-triol was obtained. ¹H NMR (500 MHz, CDCl₃, δ, ppm, J/Hz): 0.86 (3H, s, 3H, CH₃-18), 0.98 (3H, s, CH₃-19), 1.21 (3H, s, CH₃-26), 1.23 (3H, s, CH₃-27), 1.27 (3H, s, CH₃-21), 2.06 (3H, s, CH₃-COO-2), 2.12 (3H, s, CH₃-COO-20), 2.32-2.43 (1H, m, H-5), 3.11 (1H, s, H-9), 4.80 - 4.90 (1H, m, H-22), 5.08 (1H, br. s, H-3), 5.86 (1H, d, J=2.1, H-7). ¹³C NMR (125 MHz, CDCl₃, δ, ppm): 17.46, 20.53, 21.14, 21.38, 23.92, 24.75, 25.35, 28.87, 29.12, 29.68, 30.01, 31.27, 31.72, 36.42, 40.24, 47.69, 49.49, 51.70, 67.59, 70.60, 77.21, 79.54, 84.87, 121.56, 164.32, 170.46, 172.48, 202.87. MS (APCI⁺) *m/z* (%): 549.1 ([M+H]⁺, 41), 531.6 ([M-H₂O+H]⁺, 100), 513.1 ([M-2H₂O+H]⁺, 36), 471.4 ([M-H₂O-AcOH+H]⁺, 8), 453.4 ([M-2H₂O-AcOH+H]⁺, 26).

Preparation of compound 1 from diacetate. 40 mg of potassium bicarbonate in 3 ml of water was added to a solution of 31.2 mg of diacetate in 4 ml of methanol and left at 40°C for one hour. The reaction mixture was diluted with water, neutralized with acetic acid and extracted with ether. The ether was distilled off; the residue was chromatographed on a thin layer of silica gel in chloroform-methanol (9:1). 12 mg of **1** with m.p. 250-252°C (from acetone-hexane) was obtained. The yield is 38.4%.

The inclusion complex 1 with γ-CD was obtained by the interaction of equimolecular quantities of solutions of **1** and γ-CD. 0.032 g (0.025 mmol) of γ-CD dissolved in 4 ml of distilled water was added to 0.022 g (0.025 mmol) of **1** dissolved in 3 ml of absolute ethanol. The solution was stirred with a magnetic stirrer at 50°C for 8 hours. The precipitate formed was filtered off, washed with ethanol and dried in a vacuum oven at 40°C. The inclusion complex of **1**-γ-CD was obtained as a white powder, melting with decomposition at 350°C.

RESULTS AND DISCUSSION

At the obtaining **1** in the first stage the yield of extractives extracted by 70% aqueous ethyl alcohol was studied, and then, the reverse-phase high-performance liquid chromatography method was used to analyze the extract of the aerial part for the content of phytoecdysteroids.

Before it was revealed that the above-ground parts of *Silene fruticulosa* (Pall.) Schischk contain ecdysterone as the main ecdysteroid (content 2.4 g/kg of dry weight), as well as 2-deoxyecdysone (0.45 g/kg) and **1** (0.11 g/kg) as minor representatives of this class of polyhydroxysteroids [14].

For the preparative isolation of the above-mentioned compounds, the air dried plant was subjected to extraction with aqueous ethyl alcohol and the resulting extract was then purified from non-polar components by washing with a mixture of petroleum ether and ethyl acetate. Purification from water-soluble impurities was carried out by the extraction of ecdysteroid fraction dissolved in water with isobutanol. The resulting ecdysteroid mixture was applied to a silica gel column, eluting with a step gradient of chloroform with ethanol. The eluate from the column was combined into 8 fractions based on the TLC analysis. ¹H NMR and mass spectra were recorded for all F-1-F-8 fractions, on the basis of which the F-1-F-4 and F-6 fractions were excluded from further consideration as steroid-free. Fraction F-8 contained an individual compound 20-hydroxyecdysone, the structure of which was identified by the NMR spectroscopy method.

Further work with F-5 and F-7 fractions suggested their additional purification, but repeated chromatography on silica gel using other solvents did not yield the desired results. The solution of the problem was the acetylation of F-5 and F-7 fractions, followed by the isolation of 2-deoxyecdysone and **1** acetates, respectively, identified by NMR and mass spectrometry. Deacetylation of the resulting compounds was carried out with potassium bicarbonate according to the procedure [16].

It is known that the sizes, shape and geometric complementarity of the interacting components play an important role in supramolecular chemistry, therefore, γ -CD was chosen as the most suitable for obtaining the inclusion complex **1**, the most suitable according to the above-mentioned criteria. [17] Currently, NMR spectroscopy is one of the most informative research methods of structure and intermolecular interactions in inclusion complexes of steroid compounds [3, 18]; therefore this method of investigation was chosen for the study of the supramolecule **1** with γ -CD.

The supramolecular inclusion complex **1** with γ -CD was obtained by the interaction of equimolecular amounts of the substrate with the receptor in an alcoholic solution upon heating.

DMSO-d₆ proved to be the most suitable solvent for NMR spectroscopic studies of inclusion complexes **1** with γ -CD; therefore, NMR spectra of **1** and its complexes with γ -CD were obtained in this solvent. Previously, NMR spectra of **1** were identified in deuterated pyridine and methanol [13], so the results of the

Chemical shifts of ^1H and ^{13}C NMR of **1** and γ -CD in the free state (δ_0) and in the inclusion complex (δ)

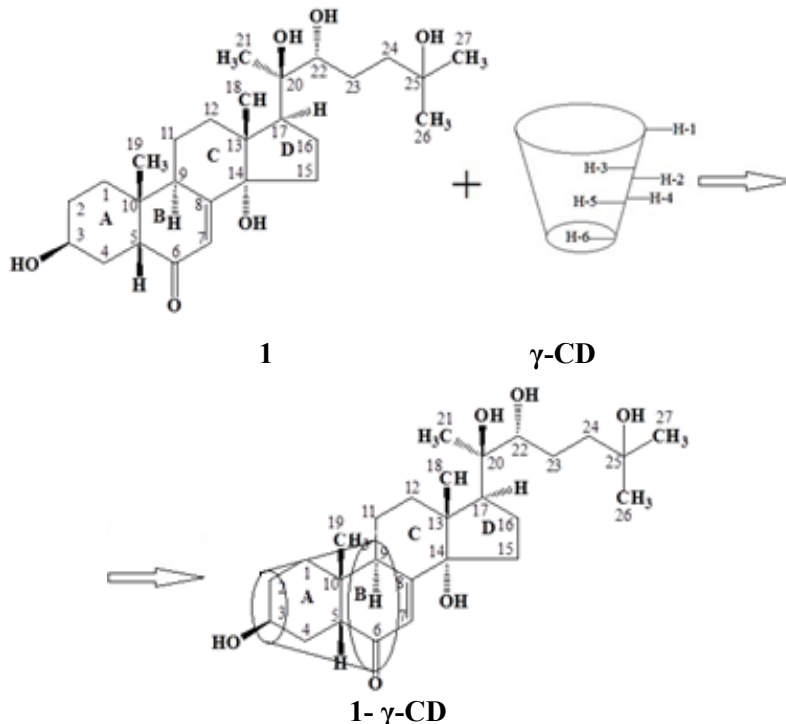
C Atom	CH_x Group	$\delta_0(^{13}\text{C})$, ppm	$\delta(^1\text{H})$, ppm	$\delta(^1\text{H})$, ppm	$\Delta\delta(^1\text{H})=\delta(^1\text{H})-\delta_0(^1\text{H})$, ppm
1					
1	$-\text{CH}_2-$	28.56			
2	$-\text{CH}_2-$	28.56			
3	$>\text{CH}-\text{OH}$	63.15			
4	$-\text{CH}_2-$	29.51			
5	$>\text{CH}-$	51.40			
6	$>\text{C}=\text{O}$	210.97	–	–	–
7	$-\underline{\text{C}}\text{H}=\text{C}<$	120.85	5.58 s	5.57 s	-0.01
8	$>\underline{\text{C}}=\text{C}<$	166.19	–	–	–
9	$>\text{CH}-$	36.10	3.06 m	3.04 m	-0.02
10	$>\text{C}<$	36.56	–	–	–
11	$-\text{CH}_2-$	21.49			
12	$-\text{CH}_2-$	31.30			
13	$>\text{C}<$	48.56	–	–	–
14	$>\text{C}<$	83.63	–	–	–
15	$-\text{CH}_2-$	32.56			
16	$-\text{CH}_2-$	21.49			
17	$>\text{CH}-$	49.21	2.22 m	2.21 m	-0.01
18	$-\text{CH}_3$	17.68	0.71 s	0.70 s	-0.01
19	$-\text{CH}_3$	24.05	0.80 s	0.79 s	-0.01
20	$>\text{C}<(\text{OH})$	76.19			
21	$-\text{CH}_3$	22.11	1.03 s	1.02 s	-0.01
22	$>\text{CH}-$	76.68			
23	$-\text{CH}_2-$	26.60			
24	$-\text{CH}_2-$	41.92			
25	$>\text{C}<$	69.21	–	–	–
26	$-\text{CH}_3$	30.55	1.00 s	0.99 s	-0.01
27	$-\text{CH}_3$	30.55	1.00 s	0.99 s	-0.01
γ -CD					
1	$>\text{CH}-$		4.83	4.83	0
2	$>\text{CH}-$		3.30	3.27	-0.03
3	$>\text{CH}-$		3.37	3.33	-0.04
4	$>\text{CH}-$		3.32	3.29	-0.03
5	$>\text{CH}-$		3.41	3.33	-0.04
6	$-\text{CH}_2-$		3.58	3.56	-0.02

previous work were used in determining NMR chemical shifts of ^1H and ^{13}C atoms of **1** (table) in DMSO-d_6 . Since a change in the solvent during NMR studies leads to a change in the chemical shift of the ^1H and ^{13}C atoms, two-dimensional NMR spectroscopy of HMQC (^1H - ^{13}C) correlation through one bond and COSY (^1H - ^1H) NMR correlations through three bonds was used to identify the signals.

The superposition of proton NMR spectra of **1** does not allow identifying all the hydrogen atoms in the solvent chosen by us. Singlet signals of five CH_3 -groups are manifested in the strong-field region at 0.72-1.03 ppm of the proton NMR spectrum. The resonance of the signals of the CH_2 groups of the molecule is found in the area of 1.20-2.00 ppm. The multiplet signal at 2.22 ppm can be attributed to the proton of the methine group H-17, another methionine proton H-9 resonates at 3.06 ppm. Proton of the H-7 fragment $-\text{CH} = \text{C}$ -resonates at 5.58 ppm.

In the HMQC (^1H - ^{13}C) NMR spectra of **1** certain protons correlate with the corresponding nuclei of carbon atoms. Cross peaks corresponding to spin-spin proton interactions through three bonds are observed in the two-dimensional COSY (^1H - ^1H) NMR spectra.

Thus, the obtained one- and two-dimensional NMR spectra allowed identifying all carbon atoms and detectable protons of the molecule **1**, potential substrate or guest when obtaining inclusion complexes with γ -CD.



The proposed scheme for the formation of a supramolecular inclusion complex **1** with γ -CD

Investigation of the structure of supramolecular complexes by the method of ^1H and ^{13}C NMR spectroscopy is based on the determination of the difference in the values of chemical shifts of certain signals in the spectra of substrate **1** and the γ -CD receptor in the free state and in the complex that arises as a result of intermolecular interaction. Thus, in terms of the values of the chemical shifts of the internal or external protons of the CDs, it is possible to reveal the formation of, respectively, internal or external complexes. The change in the chemical shifts of ^1H and ^{13}C in the substrate spectra makes it possible to determine the direction of occurrence of the latter in the cavity of the CD [19, 20].

Signals of protons belonging to substrate molecules are observed (table) in ^1H NMR spectra of inclusion complexes with γ -CD. There were no significant changes in chemical shifts of the identified protons **1** after complexation with γ -CD. In the inclusion complexes **1** with γ -CD, the greatest change was observed in the chemical shifts of protons H-3 and H-5 of the inner cyclodextrin cavity (table, figure).

This indicates the entry of the steroid molecule into the internal cavity of host molecules with the formation of a supramolecular inclusion complex.

Conclusion. A comparison of the values of the integrated intensities of the signals of protons **1** and γ -CD in the composition of the inclusion complex showed the formation of supramolecules of the composition of one guest molecule per molecule of the host.

The imposition of proton NMR spectra in free states and in the inclusion complex did not completely allow identifying the structure of the supramolecules with γ -CD. A slight change in the chemical shifts of the protons of the methyl groups H-26, 27, 21 and 18 allows one to make the assumption that the inclusion of the molecule **1** in the cyclodextrin cavity occurs as the entry of the guest molecule fragment A into the interior cavity of the host molecule.

REFERENCES

- [1] Rinaldi L., Binello A., Stolle A., Curini M., Cravotto G. Efficient mechano-chemical complexation of various steroid compounds with α -, β - and γ -cyclodextrin // *Steroids*. 2015. Vol. 98. P. 58-62.
- [2] Moon J.-Y., HJung H.-J., Moon M.Y., Chung B.C., Choi M.H. Inclusion complex-based solid-phase extraction of steroidal compounds with entrapped β -cyclodextrin polymer // *Steroids*. 2008. Vol. 73. P. 1090-1097.
- [3] Forgo P., Vincze I., Kover K.E. Inclusion complexes of ketosteroids with β -cyclodextrin // *Steroids*. 2003. Vol. 68. P. 321-327.
- [4] Yanga R., Chena J.-B., Dai X.-Y., Huang R., Xiao C.-F., Gao Zh.-Y., Yang B., Yang L.-J., Yan S.-J., Zhang H.-B., Qing Ch., Lin J. Inclusion complex of GA-13315 with cyclodextrins: Preparation, characterization, inclusion mode and properties // *Carbohydr. Polym.* 2012. Vol. 89, Iss. 1. P. 89-97.
- [5] Yuan Ch., Jin Zh., Xu X. Inclusion complex of astaxanthin with hydroxypropyl- β -cyclodextrin: UV, FTIR, ^1H NMR and molecular modeling studies // *Carbohydr. Polym.* 2012. Vol. 89, Iss. 2. P. 492-496

[6] Dandawate P.R., Vyas A., Ahmad A., Banerjee S., Deshpande J., Swamy K.V., Jamar A., Dumhe-Klaire A.K., Padhye S., Sarkar F.H. Inclusion Complex of Novel Curcumin Analogue CDF and β -Cyclodextrin (1:2) and Its Enhanced In Vivo Anticancer Activity Against Pancreatic Cancer // *Pharm. Res.* 2012. Vol. 29, Iss. 7. P. 1775-1786.

[7] Tuleuov B.I., Seilkhanov T.M., Nurkenov O.A., Temirgazyev B.S., Kudabayeva P.K., Kuatbayev O.U., Adekenov S.M. Complexes of 20-hydroxyecdysone with α -, β - and γ -cyclodextrins // *Proc. Natl. Acad. Sci. Belarus, Chem. Ser.* 2016. N 3. P. 85-87.

[8] Temirgazyev B.S., Salkeyeva L.K., Agitayeva G.S., Kozhanova A.M., Tuleuov B.I., Adekenov S.M. Regioselective synthesis of new phosphorus and nitrogen-2-deoxyecdysone-based derivatives // *Proc. Natl. Acad. Sci. Belarus, Chem. Ser.* 2016. N 3. P. 114.

[9] Kudabayeva P.K., Temirgazyev B.S., Kazbekova A.T., Atanbaev A.Sh., Habdolda G., Tuleuov B.I., Adekenov S.M. The study of antioxidant activity of ecdysterone inclusion complexes with α -, β - and γ -cyclodextrins // 12th International Symposium on the Chemistry of Natural Compounds. Tashkent, 2017. P. 253.

[10] Kudabayeva P.K., Temirgazyev B.S., Kazbekova A.T., Atanbaev A.Sh., Habdolda G., Tuleuov B.I., Adekenov S.M. Issledovanie antioksidantnoy aktivnosti kompleksov vkluycheniya ekdisteronov α -, β - i γ -tsiklodekstrinami // *Razrabotka, issledovanie i marketing novoy farmatsevticheskoy produktsii.* Izhevsk: Print, 2017. P. 139-142.

[11] Akhrem A.A., Kovganko N.V. Ekdisteroidy: Khimiya i biologicheskaya aktivnost'. Minsk: Naukaitekhnika, 1989. 327 p.

[12] Galbraith M.N., Horn D.H.S., Middleton E.J., Hackney R.I. Structure of deoxycrustecdysone, a second crustacean moulting hormone // *Chem. Commun.* 1968. Iss. 2. P. 83-85.

[13] Chong Y.K., Galbraith M.N., Horn D.H.S. Isolation of deoxycrustecdysone, deoxyecdysone, and α -ecdysone from the fern *Blechnum minus* // *Chem. Commun.* 1970. Iss. 18. P. 1217-1218.

[14] Adekenov S.M., Al'magambetov A.M., Gulyakevich O.V., Zhabinskiy V.N., Kozhanova A.M., Tuleuov B.I., Tuleuova B.K., Habdolda G., Khripach V.A. Sostav i sodержanie ekdisteroidov v rasteniyakh *Silene fruticulosa* (Pall.) Schischk // *Izv. NAN Belarusi. Ser. khim.* 2014. N 1. P. 64-67.

[15] Kumatbaev O.U., Tuleuov B.I., Khripach V.A., Adekenov S.M. Khimicheskoe izuchenie nadzemnoy chasti *Silene fruticulosa* (Pall.) Schischk // *Farmatsevticheskiy byulleten'.* 2015. N 3-4. P. 126-130.

[16] Zatsny I.L., Gorovits M.B., Abubakirov N.K. Fitoekdizony. Vitikosteron E iz *Serratulasogdianai* ego chastichnyysintez // *Khimiya prirod. soedineniy.* 1973. N 2. P. 175-178.

[17] Gimp G., Gehrig-Burger K. Probes for studying cholesterol binding and cell biology // *Steroids.* 2011. Vol. 76. P. 216-231.

[18] Jover A., Budal R.M., Al-Soufi W., Mejjide F., Tato J.V., Yunes R.A. Spectra and structure of complexes formed by sodium fusidate and potassium helvolate with β - and γ -cyclodextrin // *Steroids.* 2003. Vol. 68. P. 55-64.

[19] Nowakowski M., Ejchart A. Complex formation of fenchone with α -cyclodextrin: NMR titrations // *J. Incl. Phenom. Macrocycl. Chem.* 2014. Vol. 79, Iss. 3. P. 337-342.

[20] Maheshwari A., Sharma M., Sharma D. Complexation of sodium picosulphate with beta cyclodextrin: NMR spectroscopic study in solution // *J. Incl. Phenom. Macrocycl. Chem.* 2013. Vol. 77, Iss. 1-4. P. 337-342.

Резюме

Б. С. Темірғазиев, Т. М. Сейілханов, С. Тянах, А. М. Қожанова,
О. Т. Сейілханов, Е. В. Минаева, Л. К. Салкеева, Б. И. Төлеуов, С. М. Әдекенов

2-ДЕЗОКСИ-20-ГИДРОКСИЭКДИЗОННЫҢ γ -ЦИКЛОДЕКСТРИНМЕН СУПРАМОЛЕКУЛАЛЫҚ ҚОСУ КОМПЛЕКСІН АЛУ ЖӘНЕ ЯМР-СПЕКТРОСКОПИЯЛЫҚ ӘДІСПЕН ЗЕРТТЕУ

Бұташық сылдыршөптің (*Silene fruticulosa* (Pall.) Schischk, *Caryophyllaceae*Juss.) жер үсті бөлігінен алғаш рет 2-дезоксидизон бөлініп алынды. ЯМР-спектроскопия әдісі арқылы фитостероидтың γ -циклодекстринмен комплекс түзілуі зерттелінді. Субстрат пен рецептордың протондарының химиялық жылжуларының өзгерістері бойынша, 2-дезоксидизон γ -циклодекстринмен 1:1 стехиометриялық құрамдағы супрамолекулалық комплекс түзіп, рецептор молекуласының қуысына субстрат молекуласы А фрагментімен енетіні анықталды.

Түйін сөздер: бұташық сылдыршөп (*Silene fruticulosa* (Pall.) Schischk, *Caryophyllaceae* Juss.), 2-дезоксидизон, циклодекстрин, қосу комплекстері, ЯМР-спектроскопия.

Резюме

Б. С. Темірғазиев, Т. М. Сейілханов, С. Тянах, А. М. Қожанова,
О. Т. Сейілханов, Е. В. Минаева, Л. К. Салькеева, Б. И. Тулеуов, С. М. Адекенов

ПОЛУЧЕНИЕ И ИССЛЕДОВАНИЕ СУПРАМОЛЕКУЛЯРНОГО КОМПЛЕКСА ВКЛЮЧЕНИЯ 2-ДЕЗОКСИ-20-ГИДРОКСИЭКДИЗОНА С γ -ЦИКЛОДЕКСТРИНОМ МЕТОДОМ СПЕКТРОСКОПИИ ЯМР

Из надземной части смолевки кустарничковой (*Silene fruticulosa* (Pall.) Schischk, семейства *Caryophyllaceae*Juss.) впервые выделен 2-дезоксидизон (2-дезоксидистерон). Методом ЯМР-спектроскопии изучено комплексобразование фитостероида с γ -циклодекстрином. По изменению химических сдвигов протонов субстрата и рецептора установлено, что 2-дезоксидизон взаимодействует с γ -циклодекстрином с образованием супрамолекуларного комплекса включения стехиометрического состава 1:1 с вхождением фрагмента А молекулы субстрата во внутреннюю полость рецептора.

Ключевые слова: смолёвка кустарничковая (*Silene fruticulosa* (Pall.)Schischk), 2-дезоксидизон, циклодекстрин, комплексы включения, спектроскопия ЯМР.

F. R. YERMAKHANOVA¹, S. USMANOV², G. T. OMAROVA²

¹ Eurasian National University named after L. N. Gumilyov, Astana, Republic of Kazakhstan,
²JSC “Institute of Chemical Sciences named after A. Bekturov”, Almaty, Republic of Kazakhstan.
 E-mail: farym@mail.ru

PHYSICAL AND CHEMICAL PROPERTIES OF THE PRODUCTION TECHNOLOGY OF INDIVIDUAL UREA-FORMALDEHYDE COMPOUNDS AND MULTIFUNCTIONAL COMPOUNDS ON THE BASIS OF THOSE COMPOUNDS AND ZINC ACETATE

Abstract. Optimum parameters of drying process of the thin layers of low-molecular urea-formaldehyde compounds - monomethylolurea, dimethylolurea and methylene di-carene, as well as multifunctional compounds on the base of those compounds and zinc acetate, were determined. The input parameters were: pH 6.5-7.4, temperature 70-95 °C and drying process time 2-40 minutes. Output parameters: the content of methylol, methylene formaldehyde, free urea.

The optimum drying parameters were: pH of solutions 6.5-7.0, temperature 70-90 °C, drying time of solutions 2-10 min. The data of the conducted studies allow us to recommend a spray dryer for the production of solid urea-formaldehyde compounds, as well as multifunctional compounds based on them and zinc acetate.

Key words: urea-formaldehyde compounds, drying process, phase composition changes, polycondensation process, spray dryer.

Introduction. For the physical and chemical justification of the technology for obtaining low-molecular urea-formaldehyde compounds (UFC) – monomethylol ureas, dimethylol urea and methylene-diuria, as well as multifunctional compounds based on them and zinc acetate, studies were conducted in order to determine the change in their phase composition as a function of pH, temperature, duration drying process in thin layers.

To carry out the experiment, model saturated solutions of UFC (table 1) were prepared and their composition is defined by the conditions of their synthesis [1-3].

Table 1 – Composition of model solutions of individual UFC

Compound	Composition, mass. %			
	UFC	formaldehyde	Urea	Water
H ₂ NCONHCH ₂ OH	40,0	0	0	60,0
	38,0	0,67	1,33	60,0
HOCH ₂ NHCONHCH ₂ OH	40,0	0	0	60,0
	34,0	3,0	3,0	60,0
H ₂ NCONHCH ₂ NHCONH ₂	30,0	0	0	70,0

EXPERIMENTAL PART

Experiment methodology. Model solutions of UFC were applied in a thin layer on a surface having a temperature of 70, 90 and 95 °C, and the products were dried for 2, 5, 10, 15, 20, 25, 30 minutes.

At the first stage of the study, experiments on drying solutions of UFC in thin layers were carried out at pH 6.5-7.4, in the temperature range 70-95 °C for a constant time equal to two minutes.

RESULTS AND DISCUSSION

It is established (table 2) that in the case of using a solution of monomethylolurea that does not contain free urea and unreacted formaldehyde having a pH of 6.5, with thin-layer UFC drying in the temperature range 70-95 °C, it is

Table 2 – Composition of drying product obtaining from monomethylolurea solution

Composition of drying product of monomethylolurea, mass %	Experiment conditions		Composition of product, mass %		
	pH	temperature, °C	Monomethylolurea	Condensation product	Free urea
Monomethylolurea – 40,0 Formaldehyde – 0 Urea – 0 Water – 60,0	6,5	70	86,0	12,0	2,0
		90	76,0	22,2	1,8
		95	72,0	26,8	1,2
	6,8	70	100	0	0
		90	98,2	1,8	0
		95	92,5	7,5	0
	7,0	70	100	0	0
		90	100	0	0
		95	98,4	1,6	0
	7,4	70	100	0	0
		90	100	0	0
		95	99,2	0,8	0
Monomethylolurea – 38,0 Formaldehyde – 0,67 Urea – 1,33 Water – 60,0	6,5	70	97,2	1,1	1,7
		90	95,0	3,8	1,2
		95	89,1	10,2	0,7
	6,8	70	97,5	0	2,5
		90	69,4	2,1	1,5
		95	91,2	7,8	1,0
	7,0	70	96,62	2,5	3,38
		90	96,62	2,5	3,38
		95	95,3	3,0	1,7
	7,4	70	92,62	0	7,38
		90	92,65	0	7,35
		95	92,7	6,0	1,3

impossible to obtain a stable product due to the polycondensation reaction of monomethylolurea with the formation, according to paper chromatography analysis, of monomethylolmethylene compounds of urea.

When the pH of the monomethylolurea solution is increased to 6.8, the product of stable composition can only be obtained at a temperature of 70 °C, increasing the temperature to 90 °C promotes the formation of condensation products, as well as formation and release of free urea.

When the pH of the monomethylolurea solution is 7.0-7.5, the product does not undergo polycondensation in the drying temperature range from 70 to 90 °C, and with rising the temperature to 95 °C, observed a slight formation of condensation products about 0.8-1.6%. In case of using a solution of monomethylolurea containing 0.67% formaldehyde and 1.33% urea at pH 6.5 at the temperature range from 70 to 90 °C, the polycondensation process takes place forming monomethylolmethylene derivatives of urea. An increase in pH to 6.8 makes it possible to obtain a stable product only at 70 °C. At a solution pH value about 7.0-7.4 and temperature range from 70 to 90 °C, condensation don't occur and obtained product contains 96.62% monomethylolurea and 3.38% urea. However, increase the drying temperature to 95 °C promotes formation of the condensation products. In this case, the products contain less urea, which is defined by its interaction with formaldehyde and methylol derivatives of urea [4, 5]. Thus, the optimum condition for obtaining a stable monomethylolurea of stable composition by drying in thin layers are : aeration process about 2 minutes with a minimum content of condensation products; pH of solution 6.8-7.4 and temperature range from 70 to 90 °C.

At the next stage of the experiment, carried out determination the change in the phase composition of the products depending on the drying time (interval 2-30 minutes) in the model solutions of monomethylolurea. At the same time, the constant factors of the drying process were the temperature 75 °C and the pH of

Table 3 – Characteristics of monomethylolurea in relation to the time of heat treatment

Composition of drying product of monomethylolurea, mass %	Duration drying process, minute	Drying temperature, °C	Composition of the product, mass %		
			monomethylolurea	Condensation product	Free urea
Monomethylolurea – 40 Formaldehyde – 0 Urea – 0 Water – 60,0	2	75	100	0	0
	5		100	0	0
	10		100	0	0
	20		99,5	0,5	0
	30		91,2	6,7	2,1
Monomethylolurea – 38 Formaldehyde – 0,67 Urea – 1,33 Water – 60,0	2	75	96,62	0	3,38
	5		96,62	0	3,38
	10		96,62	0	3,38
	20		96,62	Traces negligible	3,37

the solution 7.0. From the data obtained (table 3) it follow that at the temperature 75 °C in a neutral medium, a product of stable composition can be obtained with a drying time about 2-10 minutes. When the heat treatment time is increased to 20-30 minutes, takes place formation of condensation products up to 0.5-6.7% in the system.

Experimental data on the change in the phase composition of the drying products of dimethylolurea solutions in thin layers, depending on pH 6.5-7.4 and temperature 70-95 °C are presented in table 4.

Table 4 – Composition of the drying product of dimethylolurea solution

Composition of drying product of monomethylolurea, mass %	Experiment conditions		Composition of the product, mass %		
	pH	temperature, °C	Dime-thylolurea	Condensation product	Free urea
Monomethylolurea – 40 Formaldehyde – 0 Urea – 0 Water – 60,0	6,5	70	82	15,8	2,2
		90	73	21,9	5,1
		95	65	26,3	8,7
	6,8	70	100	0	0
		90	83	13,7	3,3
		95	75	19,8	5,2
	7,0	70	100	0	0
		90	100	0	0
		95	95,4	3,0	1,6
	7,4	70	100	0	0
		90	100	0	0
		95	96,5	2,7	0,8
Dimethylolurea 34 Formaldehyde – 3,0 Urea – 0 Water – 60,0	6,5	70	85,2	2,6	12,2
		90	70,3	13,6	16,1
		95	65,2	15,5	19,3
	6,8	70	91,9	0	8,1
		90	79,1	9,4	11,5
		95	75,0	11,7	13,3
	7,0	70	91,9	0	8,1
		90	91,9	0	8,1
		95	85,0	4,2	10,8
	7,4	70	91,9	0	8,1
		90	91,9	0	8,1
		95	85,9	3,7	10,4

The drying time of the products was constant - 2 minutes. Drying process for model solutions of dimethylolurea with a pH of 6.5 at the temperature range from 70 to 95 °C does not make it possible to obtain a stable product. The amount of condensation product is 15.8-26.3%. In this case, 2.2-8.7% of free urea is formed. According to the paper chromatography analysis, dimethylolmethylene and methylene compounds of urea are formed in the product. With an increase the pH of the solution to 6.8, the product of stable composition can be obtained only at the temperature about 70 °C. At pH 7.0-7.4 in the temperature range from 70 to 90 °C there is no condensation of dimethylolurea. An increase the temperature to 95 °C leads to the formation of a 2.7-3.0% condensation product in the system; thus forming free urea in an amount about 0.8-1.6%.

Using a solution of dimethylolurea containing free urea and unreacted formaldehyde, when drying the salt, such patterns of the composition of the products are observed depending on the pH and temperature of the process (table 4), as in the case of a solution of dimethylolurea that does not contain impurities.

However, in this case, the formaldehyde presence in the solution of dimethylolurea is dried out during the drying process of the product into the gas phase and must be disposed. When the pH of the solutions is 7.0-7.4, condensation of the product is excluded in the temperature range of 70-90 °C.

Increasing the temperature to 95 °C promotes the formation about 3.7-4.2% condensation product in the system.

The results of the studies to determine the change in the composition of the products during the drying process of solutions of dimethylolurea in the range of 2-30 minutes at a constant temperature of 75 °C and pH 7.0 showed (table 5) that the composition of the product is stable in the drying time of 2-10 minutes, 10-30 minutes condensation of dimethylolurea takes place with the formation of urea in dimethylolmethylene compounds (7.1-18.0%).

Table 5 – Composition of the drying product of dimethylolurea as a function of the time of heat treatment

Dimethylolurea pulp composition, mass %	Duration of drying process, minutes	Drying temperature, °C	Composition of the product, mass %		
			Monomethylolurea	Condensation product	Free urea
Monomethylolurea – 40 Formaldehyde – 0 Urea – 0 Water – 60,0	2	75	100	0	0
	5		100	0	0
	10		100	0	0
	20		98,5	1,5	0
	30		88,3	7,1	4,6
Dimethylolurea 34 Formaldehyde – 3,0 Urea – 0 Water – 60,0	2	75	91,9	0	9,1
	5		91,9	0	9,1
	10		91,9	0	9,1
	20		88,9	2,0	9,1
	30		77,0	18,0	5,0

The studies carried out to determine the change in the composition of the products of drying of methylenedimourea pulp in thin layers in the temperature range 70-95 °C, the pH of solutions of 6.5-7.4 and the process time of 2-30 minutes have shown the possibility of obtaining a solid product of stable composition that is not condensed.

Thus, optimal conditions for the preparation of solid individual low-molecular-weight UFC - monomethylol-, dimethylolurea, methylene-diureas of stable composition were determined: the pH of UFC solutions was 6.8-7.4, the temperature was 70-90 °C, the drying time of UFC solutions in thin layers was 2-10 minutes. For drying solutions of UFC to obtain solid products, a spray dryer is recommended.

For the justification of the technology of preparation of multifunctional action compounds, based on low molecular weight UFC and zinc acetate, studies have also been carried out to change the composition of the preparations depending on the temperature, pH and drying time in thin layers of saturated solutions of double salts.

To carry out the research, solutions of 20% concentration of polyfunctional action preparations - double compounds based on monomethylol-, dimethylol ureas and 20% pulps based on methylene-diureas were used. The experiments were carried out as follows. Model solutions of double UFC compounds with zinc acetate were deposited in a thin layer on the surface at a temperature of 70, 90, 95 °C and the products were dried for 2-30 minutes.

In the first stage of the experiment drying of solutions of double compounds in thin layers was carried out in the temperature range 70-95 °C, pH of solutions 5.5-7.0 for a constant time equal to 2 minutes.

The results of studies of products based on monomethylol- and dimethylol ureas are presented in tables 6 and 7. When drying solutions of a double compound based on monomethylol urea and zinc acetate (Table 6) at pH 5.5-6.0 in the temperature range 70-95 °C, stable product, the amount of methylol formaldehyde was 65-92%, and methylene 8-35%.

At the pH value 6.5-7.0 of solutions at the temperature range from 70 to 90 °C there is no hydrolysis of the double compound and the formation of condensation products, as indicated by a 100% content in the final product of methylol formaldehyde. Increasing the drying temperature to 95 °C promotes the polycondensation of monomethylolurea in the composition of the double salt. This is evidenced by a decrease in the amount of methylol formaldehyde to 90-92% and the formation of 8.0-10.0% methylene formaldehyde in the product.

Thus, during the drying process 2 minute of a solution of a double compound based on monomethylolurea and zinc acetate at the temperature range from 70 to 90 °C and pH 6.5-7.0, hydrolysis of the product and condensation of monomethylolurea does not occur. Conditions obtaining a preparation of multifunctional action of stable composition.

Table 6 – Content of methylol and methylene formaldehyde in the product of drying of a double compound based on monomethylolurea and zinc acetate

Experiment conditions		Fragment forms of formaldehyde in the product,% mass	
pH	temperature, °C	methylol	Methylene
5,5	70	86	14
	90	72	28
	95	65	35
6,0	70	92	8
	90	86	14
	95	76	24
6,5	70	100	0
	90	100	0
	95	90	10
7,0	70	100	0
	90	100	0
	95	92	8

The next stage of the experiment, the composition of the products, depending on the drying time of model solutions of a double compound based on monomethylolurea and zinc acetate in the time interval from 2 to 40 minutes, at isothermic condition (75 °C) and pH 7.0 were determined.

Table 7 – Containing the methylol and methylene forms of formaldehyde in the product after drying of a double compound based on dimethylolurea and zinc acetate

Experiment conditions		Fragment forms of formaldehyde in the product,% mass	
pH	temperature, °C	methylol	Methylene
5,5	70	81	19
	90	69	31
	95	62	38
6,0	70	86	14
	90	82	18
	95	73	27
6,5	70	100	0
	90	100	0
	95	83	17
7,0	70	100	0
	90	100	0
	95	86	14

It was found that at a drying temperature of solutions which prepared at 75 °C and pH 7.0, a product of stable composition can be obtained during the drying time from 2 to 10 minutes. Increasing the time of heat treatment of solution of the double compound to 20-30 minutes leads to the condensation of monome-thylolurea to 5.8% of the total formaldehyde content. During the drying time from 40 minute, the amount of condensation product of the latter was 10.8%.

Table 7 presents the obtained data on the change in the composition of the drying products of solutions of a double compound based on dimethylolurea and zinc acetate depending on pH and temperature. The drying time of the products was conducted during 2 minutes.

From the data obtained, it follows that the patterns of variation in the composition of the double compound by methylol and methylene formaldehyde are similar to those for a double compound based on monomethylol urea and zinc acetate. However, the amount of formed methylene formaldehyde in the product is greater. This indicates a less stable product at high temperatures of 90-95 °C.

Conclusion. The optimal conditions of drying process to preparation products of stable composition based on dimethylol urea and zinc acetate are pH 6.5-7.0, temperature 70-90 °C. The studies carried out to determine the change in the composition of the products during the drying process of the solutions of the preparation for 2-40 minutes at a constant temperature 75 °C and pH of solution 7.0. It show that during the drying time from 2 to 10 minutes at temperature 75 °C, the products are stable and do not undergo hydrolysis and polycondensation in the future. Drying the samples for 20-40 minutes lead to formation of of methylene formaldehyde in the products about 7.0-12.0%.

Studies on drying solutions of a double compound based on dimethylenourea and zinc acetate in thin layers the temperature range from 70 to 90 °C, pH solutions 5.5-7.0 and drying time about 2 to 20 minutes have shown the possibility of obtaining a product of stable composition which does not undergo to polycondensation.

Thus, the optimal conditions for the preparation of solid compounds based on monomethylol-, dimethylol- and methylenedimourenes of stable composition at pH solutions about 6.5 to 7.0, the temperature from 70 to 90 °C, drying time of solutions of double compounds based on UFC 2-10 minutes have been determined. These studies allow the recommendation for spray drying and drying of solutions of compounds based on UFC and zinc acetate to obtain solid products.

The research was carried out according to the scientific and technical program No. BR05234667 within the framework of program-targeted financing CS MES RK.

REFERENCES

[1] Usmanov S., Ugaj D.P., Ermahanova F.R. Razrabotka tehnologii stimulyatorov rosta rastenij na osnove nizkomolekuljarnyh mochevino-formal'degidnyh soedinenij i acetatov dvuh-valentnyh metallov. Soobshhenie 1. Politerma rastvorimosti sistemy $H_2NCONHCH_2OH-Zn(CH_3COO)_2 \cdot H_2O$ / Deponir. v VINITI 1991 g., № 1218-V91., Tashkent.

[2] Usmanov S., Ermahanova F.R., Bogdanov A.V., Rudnik O.D. Sistema dimetilolmochevina – acetat cinka- voda / Deponir. v Uz NIINTI 1992 g., № 153-A92., Tashkent.

[3] Usmanov S., Ermahanova F.R., Bogdanov A.V., Rudnik O.D. Sistema metilendimochevina – acetat cinka – voda pri 25°S / Deponir. v Uz NIINTI 1992 g., № 154-A92.

[4] Usmanov S., Ermahanova F.R., Bogdanov A.V., Isakov H., Rudnik O.D. Issledovanie tehnologii nizkomolekuljarnyh mochevino-formal'degidnyh soedinenij v raspylitel'noj sushilke / Deponir. v Uz NIINTI 1992 g., № 148-A92., Tashkent.

[5] Usmanov S., Ermahanova F.R., Bogdanov A.V., Bandurina O. Fiziko-himicheskie osnovy tehnologii nizkomolekuljarnyh mochevino-formal'degidnyh soedinenij i stimulyatorov rosta rastenij // Tezisy dokladov Mezhdunarodnoj nauchno-prakticheskoy konferencii «Nauka i tehnologija – 93», Shymkent, Kazahstan, 1993. Shymkent, 2015. P. 467.

Резюме

Ф. Р. Ермаханова, С. Усманов, Г. Т. Омарова

ЖЕКЕ МОЧЕВИНО-ФОРМАЛЬДЕГИДТІК ҚОСЫЛЫСТАР МЕН ОЛАРДЫҢ НЕГІЗІНДЕ МЫРЫШ АЦЕТАТЫМЕН ПОЛИФУНКЦИОНАЛДЫ ӘРЕКЕТТІ ПРЕПАРАТТАР АЛУДЫҢ ФИЗИКА-ХИМИЯЛЫҚ ТЕХНОЛОГИЯ НЕГІЗДЕРІ

Төменмолекулалы мочевино-формальдегидті қосылыстар – монометилломочевина диметилломочевина және метилендимочевинаның, сонымен қатар олардың негізінде мырыш ацетатымен полифункционалды әрекетті препараттарды жұқа кабатта кептірудің оңтайлы параметрлері анықталды. Кіріс параметрлері: рН 6,5–7,4, температурасы 70–95 °С кептіру ұзақтығы 2–40 мин. Шығыс параметрлері: метилолды, метиленді формальдегидтер мазмұны, еркін мочевино.

Кептірудің оңтайлы параметрлеріне жатады: рН-6,5–7,0 ерітінділер, температура 70–90 °С, кептіру ұзақтығы 2–10 минут. Жүргізілген зерттеулер деректері қатты мочевиноформальдегидті қосылыстар, сонымен қатар олардың негізінде мырыш ацетатымен полифункционалды әрекетті препараттар алу үшін бүркеуші кептіргішті ұсынуға мүмкіндік береді.

Түйін сөздер: мочевино-формальдегидті қосылыстар, кептіру, фазалық құрам өзгерістері, поликонденсация, бүркеуші кептіргіш.

Резюме

Ф. Р. Ермаханова, С. Усманов, Г. Т. Омарова

ФИЗИКО-ХИМИЧЕСКИЕ ОСНОВЫ ТЕХНОЛОГИИ ПОЛУЧЕНИЯ ИНДИВИДУАЛЬНЫХ МОЧЕВИНО-ФОРМАЛЬДЕГИДНЫХ СОЕДИНЕНИЙ, ПРЕПАРАТОВ ПОЛИФУНКЦИОНАЛЬНОГО ДЕЙСТВИЯ НА ИХ ОСНОВЕ И АЦЕТАТА ЦИНКА

Определены оптимальные параметры сушки в тонких слоях низкомолекулярных мочевино-формальдегидных соединений – монометилломочевины, диметилломочевины и метилендимочевины, а также препаратов полифункционального действия на их основе и ацетата цинка. Входными параметрами были: рН 6,5–7,4, температура 70–95 °С и продолжительность сушки 2–40 мин. Выходные параметры: содержание метилолового, метилолового формальдегида, свободной мочевины.

Оптимальными параметрами сушки явились: рН растворов 6,5–7,0, температура 70–90°С, продолжительность сушки растворов 2–10 мин. Данные проведенных исследований позволяют рекомендовать распылительную сушилку для получения твердых мочевино-формальдегидных соединений, а также препаратов полифункционального действия на их основе и ацетата цинка.

Ключевые слова: мочевино-формальдегидные соединения, процесс сушки, изменения фазового состава, процесс поликонденсации, распылительная сушилка.

ZH. K. KAIRBEKOV, I. M. JELDYBAYEVA, YE. T. YERMOLDINA

SSE Research Institute of New Chemical Technologies and Materials,
RSE Al-Farabi Kazakh National University, Almaty, Republic of Kazakhstan.
E-mail: us.niinhtm@mail.ru

APPLICATION NATURAL ORE MATERIALS AS CATALYSTS AT HYDROGENATION OF KENDERLYK COAL

Abstract. This work discusses the effect of bauxites as catalysts of hydrogenation of the coal from Kenderlyk deposit. According obtained results output of liquid and gaseous products increased with the increase of iron content in the catalyst was established. Also, dependent output of liquid products on the temperature at the various catalyst mass have been studied. It was shown the increase of the catalyst mass due to increase of liquid products by 50% in comparison without catalyst.

Key words: coal, Kenderlyk, catalyst, bauxite.

Introduction. The concept of coal hydrogenation catalyst has indefinite, often conditional meaning, since this process involves many chemical reactions (destruction of coal multi-structure, activation of molecular hydrogen, its interaction with coal substance, etc.) and the compounds and mixtures used as a catalyst which undergo irreversible changes. The objective of development of active catalysts is complicated by small level of knowledge in molecular and supramolecular structure of coal, causes of high reactive power when heating, and the nature of transformation of coal substances [1, 2].

It is commonly supposed that the coal hydrogenation catalysts comprise compounds that promote the increase of level of transformation of coal into liquid products soluble in benzene. Such compounds include oxides, sulfides of metals with mixed valence (Mo, W, Co, Ni, Fe, etc.), natural formations, production wastes and their compounds [3-5].

Recently, there are ongoing studies of possibility to apply the wastes of metallurgical industry and natural ore materials as catalysts of coal liquefaction. In some cases, for activation of ore catalytic systems are used sulfur and sulfur compounds or various natural additives containing nickel, cobalt and molybdenum. The economic feasibility of the use of such catalytic systems resides in their low cost, availability, avoidance of catalyst extraction from hydrogenation mud [6].

The variety of combinations of micro- and macro-components in natural ore materials, changes of their content and structure at the stage of enrichment and preliminary processing for production assume availability of wide range of catalytic properties both of interim products and mill tailings [7].

EXPERIMENT

As an object of hydrogenation study it was decided to select the coal from Kenderlyk deposit with the following physical and chemical properties: $W^a - 8,0 \%$; $A^d - 15,2 \%$; $V^{daf} - 38,2 \%$; $C^{daf} - 65,2 \%$; $H^{daf} - 3,9 \%$; $N^{daf} - 1,7 \%$; $Q^{daf} - 7244 \text{ kcal/mol}$.

The testing of catalytic properties for coal hydrogenation involved Turgai bauxite with different iron content and red mud (wastes from processing of bauxite ore from Pavlodar Aluminum Plant). The testing was performed at flow unit with the chamber of 100 cm^3 .

RESULTS AND DISCUSSION

The results of testing of Turgai bauxite and red mud for hydrogenation of Kenderlyk coal are shown in table 1. As is seen from the table, the most active catalyst is Turgai bauxite – 094 and red mud. The catalytic activity of the tested catalysts was evaluated against output of liquid products (OLP). In coal hydrogenation without a catalyst OLP was 38.1% from coal amount upon distillation of the generated mass after the test within the temperature range from 80 to 320 °C without use of vacuum. At the same time the main amount of the liquid product (LP) (50-60 %wt) comprise high-boiling fraction (250-320 °C).

According to the obtained extreme values (figure1), an output of valuable liquid and gaseous products is increasing with the increase of ore content in the catalyst.

An optimal way that may be considered is the use of bauxite 094, which application leads to production of 53.1 % of liquid products and 45.5 % of gas from mud with the loss of 3.2 %.

As is seen from figure 1, OLP has linear dependence on the ore content in the catalyst ($R^2=0.765$). Therefore, further testing was performed on bauxite 094 catalyst.

Table 1 – Effect of catalyst nature on output of liquid products from hydrogenation of Kenderlyk coal

Catalyst	Chemical composition	Content of Fe in catalyst, %	OLP, %	Sludge, %	Losses, %
Without catalyst		–	38,1	53,9	8,0
Bauxite 706	$\text{Fe}_2\text{O}_3 - \text{SiO}_2 - \text{Al}_2\text{O}_3 - \text{TiO}_2$	1,55	42,0	50,8	7,2
Bauxite 710	$\text{Fe}_2\text{O}_3 - \text{SiO}_2 - \text{Al}_2\text{O}_3$	10,29	44,0	49,3	6,7
Bauxite 916	$\text{Fe}_2\text{O}_3 - \text{SiO}_2 - \text{Al}_2\text{O}_3$	11,55	46,5	47,7	5,8
Bauxite 704	$\text{Fe}_2\text{O}_3 - \text{SiO}_2 - \text{Al}_2\text{O}_3$	14,40	47,6	54,6	2,8
Bauxite 094	$\text{Fe}_2\text{O}_3 - \text{SiO}_2 - \text{Al}_2\text{O}_3$	16,59	51,3	45,5	3,2
Bauxite 110	$\text{Fe}_2\text{O}_3 - \text{SiO}_2 - \text{Al}_2\text{O}_3 - \text{TiO}_2$	16,94	49,2	44,3	6,5
Red mud	$\text{Fe}_2\text{O}_3 - \text{SiO}_2 - \text{Al}_2\text{O}_3 - \text{TiO}_2 - \text{MnO}_2$	28,40	49,6	45,7	6,3

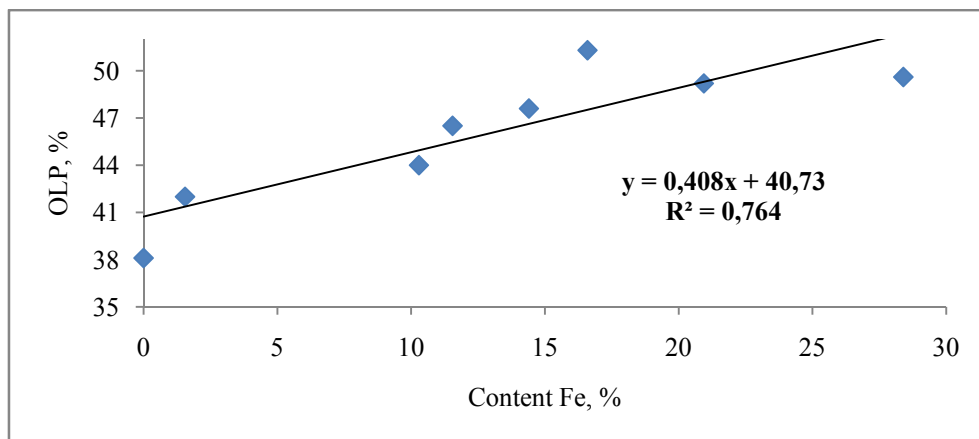


Figure 1 – Dependence of output of liquid products (OLP) on Fe content in the catalyst

An output of LP within wide range of temperatures (from 350 to 440 °C) upon contacting with bauxite 094 is 31.7 to 51.3% (table 2). At the same time, LP output is increasing at the range temperature from 350 to 420 °C, and above the 420 °C, the output decrease (figure 2) This, presumably, happens due to the fact that at >420 °C the side processes are identified, particularly, generation of gas and semi-coke. An output of light fraction is also symbatically increasing (3.1 % to 8.0 %) with the increase of temperature from 350 to 420 °C with further decrease.

Therefore, an optimal temperature of hydrogenation reaction for Kenderly coal is the temperature within 400-420 °C, at which further tests have been performed.

A positive effect on transformation of coal in hydrogenation under low pressure provides the amount of catalyst (table 3). With the increase of the catalyst amount from 0.34 to 0.67 g an output of liquid products is increasing more than twice and further increase of the catalyst amount to 1.68 g does not affect liquid products output. Based on the data of table 3 we produced diagrams

Table 2 – Effect of temperature on output of liquid products from hydrogenation of coal (m_{coal}=10 g, m_{PU}=20 g, m_{kt}=0,67, τ=30 min., Kt- bauxite 094)

T, °C	P _{max} , MPa	V _{gazs} , l	OLP, %				Sludge, %	Losses, %
			to 180 °C	180-250 °C	250-320 °C	Σ φр		
350	1,1	1,8	2,4	3,1	26,2	31,7	64,8	3,5
385	2,1	3,8	4,6	5,2	31,5	41,3	55,1	3,6
400	2,6	4,6	4,4	5,0	36,9	46,3	51,0	2,7
420	3,8	4,0	14,4	9,0	27,9	51,3	45,5	3,2
440	4,4	9,0	10,2	7,8	22,5	40,5	54,4	5,1

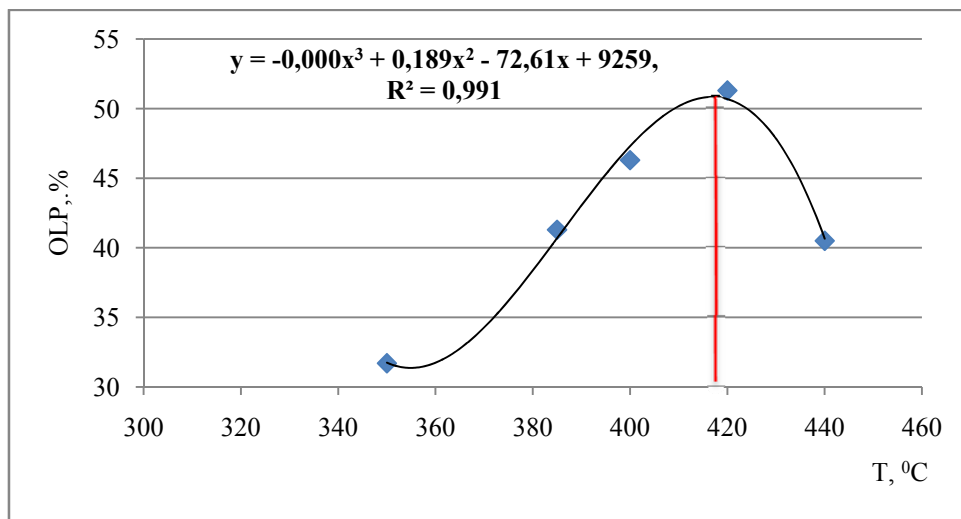


Figure 2- Dependence of output of liquid products on process temperature.

Table 3 – Effect of catalyst amount (bauxite-094) on output of LP from hydrogenation ($m_{\text{coal}}=10$ g, $m_{\text{PU}}=20$ g, $T=420$ °C, $\tau=30$ min)

Mass of catalyst, g	P_{max} , MPa	V_{gaz} , l	OLP, %				Sludge, %	Losses, %
			to 180 °C	180-250 °C	250-320 °C	Σ fraction		
–	2,8	3,1	5,7	6,5	14,5	26,7	67,2	6,1
0,34	2,0	4,2	6,2	7,3	14,8	28,3	66,9	4,8
0,67	3,8	5,0	14,4	9,0	27,9	51,3	45,5	3,2
1,0	3,9	5,1	11,7	11,2	14,7	37,6	58,2	4,2
1,34	4,2	6,0	15,6	8,1	23,6	47,3	45,4	7,3

of dependence of catalyst amount (figure 3) and pressure (figure 4) on the output of liquid products.

Conclusion. Thus, based on the obtained results there could be made a conclusion on sufficiently high activity of Turgai bauxite 094 in hydrogenation of coal from Kenderlyk deposit, where its activity depends on of iron content in the catalyst. It was demonstrated that with increase of catalyst mass to 0.67 g an output of liquid products is increasing almost by 50% in comparison with the process without a catalyst.

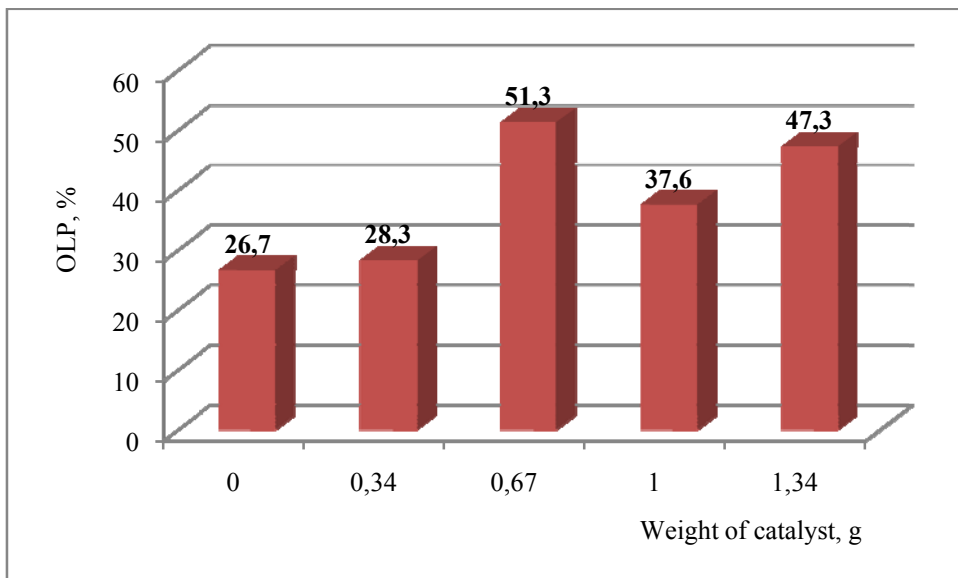


Figure 3 – Dependence of output of liquid products on catalyst amount

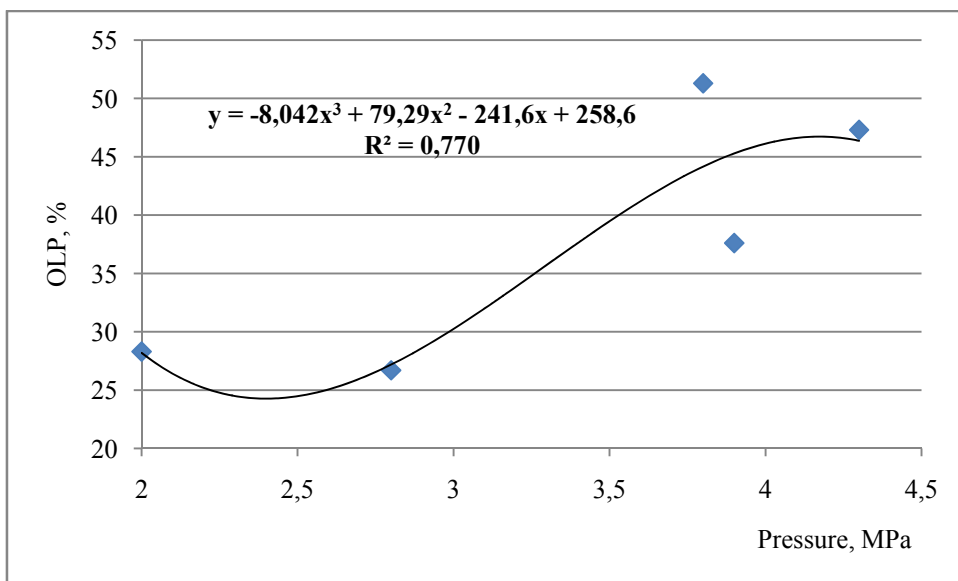


Figure 4 – Dependence of output of liquid products on process pressure

REFERERENS

- [1] Golovin G.S., Maloletnev A.S. Catalog-reference book "Complex processing of coals and increasing the efficiency of their use". Moscow: STC "Track", 2007. 292 p., 28 ill.
- [2] Gyulmaliev A.M., Golovin G.S., Gladun T.G. Theoretical foundations of coal chemistry. Moscow: Izd-vo MGGU, 2003. 556 p.
- [3] Kairbekov J.K., Yemelyanova V.S., Zhubanov K.A., Myttykbayeva Zh.K., Bayzhomartov B.B. Theory and practice of coal processing: Monograph. Almaty: Publishing house "Bylim", 2013. 496 p.
- [4] Kairbekov J.K., Toktamysov M.T., Zhalgasuly N., Yeshova Zh.T. Complex processing of brown coals of Central Kazakhstan: monograph. Almaty: Kazakh university, 2014. 278 p.
- [5] Kairbekov J.K., Zhalgasuly N., Aubakirov E. New technologies of mining and processing of minerals: Monograph. Almaty: Kazakh university, 2014. 224 p.
- [6] Kairbekov J.K. Processing of solid fossil fuels: Book. Almaty: Printing house «BTS print», 2014. 260 p.
- [7] Rusanova N.D. Uglekhimiya. Moscow: Science, 2003. 316 p. ISBN 5-02-033064-7.

Резюме

Ж. К. Каирбеков, И. М. Джелдыбаева, Э. Т. Ермолдина

КЕНДЕРЛІК КЕН ОРНЫ КӨМІРІН ГИДРОГЕНДЕУ ҮРДІСІНЕ
КАТАЛИЗАТОР РЕТІНДЕ ТАБИҒИ КЕНДІ МАТЕРИАЛДАРДЫ ҚОЛДАНУ

Берілген жұмыста «Кендерлік» кен орны көмірін гидрогендеу үрдісіне катализатор ретінде бокситтердің әсері қарастырылған. Алынған тәжірибелік деректерге сәйкес, бағалы сұйық және газ тәрізді өнімдердің шығымы катализатордың құрамындағы темірдің жоғарылауымен арта түседі. Сондай-ақ сұйық өнімдердің температурасы мен катализатор массасына тәуелділігі зерттелінді. Катализатор массасының ұлғаюымен сұйық өнімдердің шығуын катализаторсыз өндеуге қарағанда 50%-ға арттыру байқалады.

Түйін сөздер: көмір, Кендерлік, катализатор, боксит.

Резюме

Ж. К. Каирбеков, И. М. Джелдыбаева, Э. Т. Ермолдина

ПРИМЕНЕНИЕ ПРИРОДНЫХ РУДНЫХ МАТЕРИАЛОВ В КАЧЕСТВЕ
КАТАЛИЗАТОРОВ ГИДРОГЕНИЗАЦИИ КЕНДЕРЛЫКСКОГО УГЛЯ

Рассмотрено влияние бокситов в качестве катализаторов гидрогенизации угля месторождения «Кендерлык». Согласно полученным экспериментальным данным, установлено, что выход ценных жидких и газообразных продуктов повышается с увеличением содержания железа в катализаторе. Также была исследована зависимость выхода жидких продуктов от температуры и от массы катализатора. Показано, что с увеличением массы катализатора наблюдается увеличение выхода жидких продуктов на 50 % по сравнению с осуществлением процесса без катализатора.

Ключевые слова: уголь, Кендерлык, катализатор, боксит.

F. R. YERMAKHANOVA¹, S. USMANOV², G. T. OMAROVA²

¹Eurasian National University named after L. N. Gumilyov, Astana, Republic of Kazakhstan,
²JSC “Institute of Chemical Sciences named after A. Bekturov”, Almaty, Republic of Kazakhstan.
E-mail: farym@mail.ru

STUDY OF THE TECHNOLOGY FOR THE PRODUCTION OF INDIVIDUAL UREA-FORMALDEHYDE COMPOUNDS OF MULTIFUNCTIONAL ACTION ON THE BASIS OF UFC AND ZINC ACETATE IN SPRAY DRYER

Abstract. This article presents studies of the process of obtaining low-molecular urea-formaldehyde compounds, drugs of multifunctional action on the basis of low-molecular urea-formaldehyde compounds and zinc acetate in a spray dryer. Optimum technological parameters of their production are determined. The temperature of the heat carrier is 250-30 °C, the temperature in the reaction zone is 70-90 °C, the moisture content of the obtained products is 1-4%.

Key words: urea formaldehyde compounds, zinc acetate, drugs of multifunctional action, drying process, phase composition changes, polycondensation process, spray.

Introduction. Urea-formaldehyde compounds and fertilizers based on them are obtained in a drying drum, a drum-granulator-dryer, under fluidized bed conditions [1-3]. Obtaining of these fertilizers in the form of a powder for low-tonnage chemistry would become great practical tool for the field of chemistry and industrial chemistry.

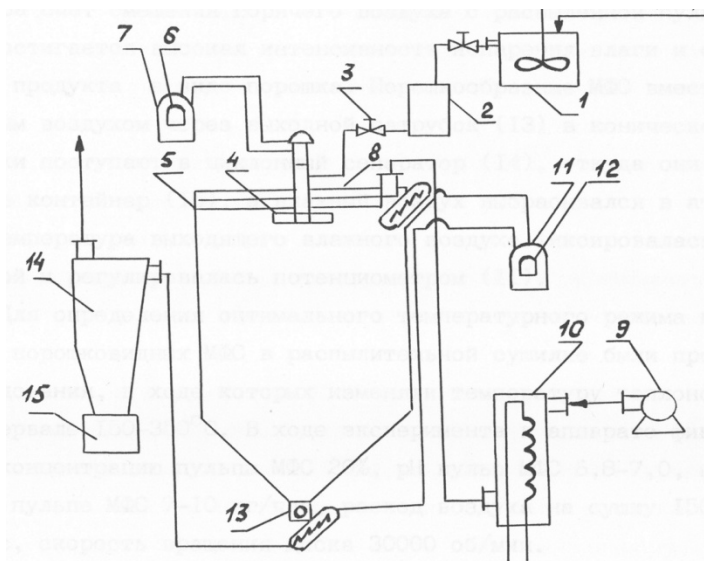
The task of the search was study the process of obtaining low-molecular urea-formaldehyde compounds (UFC) – monomethylolurea, dimethylolurea, methylene-diurea and multifunctional action compounds such as a zinc acetate in powder form.

EXPERIMENT

A pilot plant the main unit of which is a spray dryer is represented in figure. The pulps of UFC and drugs of multifunctional action based on them and zinc acetate were obtained in a tank heated reactor with a stirrer (1), where water, UFC and zinc acetate were supplied based on the calculation of 20% pulp. By feeding the heating steam into the jacket of the reactor, the pulp temperature was maintained at 40-45 °C, at which the pulp was well mobile.

As drugs of multifunctional action based on UFC and zinc acetate, double compounds obtained on the basis of monomethylolurea and zinc acetate, dimethylolurea and zinc acetate obtained at molar ratios of 1: 1, as well as methylene-diurea of 4 molecules and 1 molecule of zinc acetate were used.

Further pulps from the tank (1) was fed to the pressure vessel (2), from where it was dosed to the central disk of the spray dryer (5) by the means of a calibrated valve (3). The rotational speed of the disk was 30,000 rpm and was



Experimental installation for the production of urea-formaldehyde compounds and compounds of multifunctional action containing zinc acetate:

- 1 - capacity for the preparation of UFC pulps and drugs of multifunctional action based on them and zinc acetate, 2 - pressure vessel, 3 - valve, 4 - central disk, 5 - spray dryer, 6 - regulator, 7 - amperemeter, 8 - dryers, 9 - fan, 10 - (calorifer) heater, 11 - potentiometer, 12 - temperature controller, 13 - outlet, 14 - cyclone separator, 15 - container

varied by a regulator (6), the control was performed by means of a calibrated amperemeter (7). The pulp was sprayed into the apparatus with the aid of a disk to a foggy state. To dry the pulp through the dryers (8) located in the ceiling of the dryer, a coolant was introduced- hot air with a temperature of 150-350 °C, fed to the unit by a fan (9) through the heater (10). The air temperature was fixed by a potentiometer (11) and regulated by a temperature regulator (12).

By mixing hot air with pulverized pulps, a high intensity of moisture evaporation and the formation of the product in the form of a powder are achieved. Powdered UFC and compounds of multifunctional action together with moist air through the outlet pipe (13) in the conical bottom of the dryer enter the cyclone separator (14), from which they were poured into the container (15), and the moist air entered the stage of dust and gas cleaning. The temperature of the moist humid air was fixed by a thermo couple and controlled by a potentiometer (11).

RESULTS AND DISCUSSION

To determine the optimum temperature regime for the preparation of powdered preparations in a spray dryer, studies were performed in which the temperature of the coolant was varied in the range 150-350 °C. In the framework of the experiment, the concentration of UFC pulps and compounds of multifunctional action on their basis and zinc acetate was 20%, pH 6.8-7.0, loading on the pulp 7-

10 kg/h, air consumption for drying 150-200 m³/h, the rotational speed of the disk is 30000 rpm.

When a coolant with a temperature of 150-200 °C was applied to the spray dryer, caking occurred in the apparatus due to insufficient drying of the compounds having a temperature of 55-60 °C. When the temperature of the drying agent is increased to 250-300 °C, agglomeration and clumping of products are eliminated, the temperature of the material in the apparatus increases to 70-90 °C, which makes it possible to obtain in the spray dryer a well-flowing powdery UFC and compounds of multifunctional action based on them and zinc acetate. When the coolant is supplied to the apparatus with a higher temperature of 300-350 °C, the temperature of the material in the apparatus increases to 95-110 °C, which leads to fusion of mono- and dimethylolurea, to the partial decomposition of UFC and, as a result, to increased losses of formaldehyde to the gas phase.

Thus, the temperature of the coolant when powdered preparations based on UFC is obtained in the spray dryer must not exceed 250-300 °C at the inlet to the apparatus, in which the optimum temperature regime of the process and the minimal thermal decomposition of UFC are maintained in the dryer.

Table 1 displays the composition of the drying product of monomethylolurea pulp and the quantitative characteristics of gas phase to be related to formaldehyde and product dust. It was found that at a pH of 7.0 and a product temperature of 70-90 °C, condensation of the product is excluded and a product of stable composition can be obtained.

Table 1 – Composition of the drying product of the monomethylolurea pulp in a spray dryer and the composition and concentration of gas phase

Parameter		Composition of the product, mass %			Composition and concentration of gas phase, mg/m ³	
pH	Product temperature, °C	Monomethylolurea	Condensation product	Free urea	Formaldehyde	Dust products
7,0	70	97,5	0	2,5	100	200
	90	97,5	0	2,5	100	300
	95	97,5	1,0	2,5	110	400
6,8	70	97,5	0	2,5	100	250
	90	97,5	0,5	2,5	110	350
	95	94,0	3,5	2,5	120	500

Characteristically, with an increase in the temperature of monomethylolurea in the apparatus to 95 °C, a minimal change in its composition occurs, the content of the condensation product is 1.0%, whereas in the production of solid monomethylolurea by the thin layer method, under laboratory conditions, the mass fraction of the condensation product is 3.0-5,0%. This is apparently due to the fact that the drying of UFC solutions in the spray dryer is rapid, within a second they

lose moisture and settle in the form of fine powder particles, this almost instantaneous dehydration of the product leads to a slowdown of the condensation process. The decrease in pH in the supplied monomethylolurea solutions to the apparatus up to 6.8 contributes to the condensation process when drying the product at a temperature of 95 °C, the condensate content is 3.5%.

However, this parameter is 2-3 times less than in case of thin-layer drying of monomethylolurea. This also confirms that rapid dehydration of the product reduces the course of the polycondensation reaction.

In optimal conditions of the technology of production in exhaust gases after spray dryer in the production of powdered monomethylolurea, the formaldehyde concentration is 100 mg/m³ and the dust of the product is 200-250 mg/m³, which must be disposed.

In the production of powdered dimethylolurea in a spray dryer, the product of stable composition was obtained at the range temperature from 220 to 370 °C then supplied to coolant apparatus and the product has temperature about 70-90°C and pH 6.8-7.0 (table 2).

Table 2 – Composition of the product at drying of pulp dimethylolurea in a spray dryer and composition of gas phase

Experiment conditions		Composition of the product, mass %			Composition and concentration of the gas phase, mg/m ³	
pH	Product temperature, °C	Monomethylolurea	Condensation product	Free urea	Formal-dehyde	Dust products
7,0	70	90,9	0	9,1	150	220
	90	90,9	0	9,1	150	340
	95	88,4	2,0	9,6	160	400
6,8	70	91,9	0	8,1	150	260
	90	90,9	0	9,1	150	370
	95	85,0	4,2	10,8	170	500

An increase in the product temperature in the drier to 95 °C promotes the polycondensation of dimethylolurea, the content of the condensation product is 2.0-4.2%. In the gas phase, after the spray dryer under optimal conditions for the production of dimethylolurea powder, 150 mg/m³ of formaldehyde and 220-370 mg/m³ of product dust are contained.

When a powder of methylene-diurea was obtained in a spray dryer at a pH of the pulp of 6.8-7.0, a product of stable composition was obtained in the temperature range 70-95°C, and its condensation was eliminated. In the exhaust gases after the spray dryer, formaldehyde is absent and the product dust contains 220-370 mg/m³.

Thus, the process of obtaining powdered UFC - mono-, dimethylol-, methylene-diurea in a spray dryer was studied. Optimum technological parameters of the process of drying products with residual moisture content of 1.0-1.5% with a high yield of a stable composition product were determined (table 3).

Table 3 – Optimum technological parameters of the process for the production of powdered urea-formaldehyde compounds in a spray dryer

#	Parameters	Unit	Value
1	Temperature:		
	a) of coolant at the inlet to the spray dryer	°C	250-300
	b) of coolant at the outlet from the dryer	°C	80-90
	c) UFC pulp	°C	40-45
	d) powdered product of MPS in the reaction zone	°C	70-90
2	UFC pulp concentration	%	20
3	UFC pulp load	kg/h	7-10
4	pH of the UFC pulp		6,8-7,0
5	The residence time of the product in the reaction zone	minutes	2-5
6	The moisture content in the powdered product	%	1,0-1,5
7	Air consumption for drying	m ³ /h	150-200
8	Productivity	kg/h	2-3

In the process of studies on the preparation of compounds based on low molecular weight UFC and zinc acetate in a spray dryer, the task was also to study the effect of technological process parameters on the composition of finished products, determine the amount and composition of gas emissions after the dryer.

When multifunctional action compounds based on mono- and dimethylolurea and zinc acetate are obtained in the spray dryer in the temperature range of the material in the reaction zone of the apparatus 70-90 °C and pH 6.5-7.0, hydrolysis and condensation of methylol formaldehyde in the composition of binary salts is excluded and it is possible to obtain powdered compounds of stable composition (table 4). It should be noted that an increase in the temperature of the compounds in the drier to 95 °C results in a relatively small degree of polycondensation of mono- and dimethylolurea in the composition of binary salts, as a result of which the mass fraction of methylol formaldehyde in the product based on mono-methylolurea and zinc acetate is reduced to 95.0-98, 5% and the formation of 1,5-5,0% methylene formaldehyde, in the case of the preparation based on dimethylolurea, methylol formaldehyde decreases to 4.5-9.0%. Whereas in the preparation of solid compounds based on mono-, dimethylolurea and zinc acetate under laboratory conditions by drying in thin layers at pH of salts of 6.5-7.0 and a temperature of 95 °C, the mass fraction of methylene formaldehyde in products was 8-10% and 14 -17% respectively. This can be explained by the fact that the drying of pulp compounds based on mono- and dimethylolurea in a spray dryer occurs almost instantaneously, within a fraction of a second they lose moisture and settle in the form of fine powder particles; this rapid dehydration of the products helps to inhibit the condensation process.

Table 4 – The content of methylol and methylene formaldehyde in the pulp drying products of compounds based on mono-, and dimethylolurea, zinc acetate in a spray dryer and the composition of the gas phase

Double connection	Experiment conditions		Mass fraction of formaldehyde in the product, %		Concentration of the gas phase, mg/m ³	
	pH	Product's temperature, °C	Methylol	Methylene	Formaldehyde	Product dust
Monomethylolurea zinc acetate	7,0	70	100,0	0	55	200
		90	100,0	0	55	280
		95	98,5	1,5	70	360
	6,5	70	100,0	0	60	230
		90	100,0	0	60	300
		95	95,0	5,0	80	450
Dimethylolurea zinc acetate	7,0	70	100,0	0	70	240
		90	100,0	0	70	350
		95	95,0	4,5	90	430
	6,5	70	100,0	0	85	250
		90	100,0	0	85	380
		95	91,0	9,0	100	470

In the exhaust gases after the spray dryer for the preparation of powder formulations based on mono- and dimethylolurea, zinc acetate, the concentration of formaldehyde is 55-85 mg/m³ and the dust of the product is 200-380 mg/m³, which must be disposed of.

In the preparation of a preparation based on methylene-diurea and zinc acetate in a spray dryer at a pH of 6.5-7.0 in the temperature range of 70-95 °C, hydrolysis of the product and condensation of methylene-diuria in the composition of the double compound does not occur, and conditions for obtaining a preparation of stable composition are provided. In the exhaust gases after the spray dryer in the preparation of the drug based on methylene-diurea, formaldehyde is absent, contains 200-300 mg/m³ of the product dust. The optimum technological parameters of the drying process of the products were determined, ensuring the preparation of multifunctional action compounds of stable composition based on UFC and zinc acetate (table 5).

Table 5 – Optimum technological parameters of the process for the preparation of powder compounds based on urea-formaldehyde compounds and zinc acetate in a spray dryer

#	Parameters	Unit	Values
1	Temperature:		
	a) of coolant at the inlet to spray dryer	°C	250-300
	b) coolant at the outlet from the dryer	°C	80-90
	c) pulp of the preparation	°C	40-45
	d) a powdered preparation in the reaction zone	°C	70-90
2	Concentration of pulp	%	20
3	Load on the pulp of the preparation	kg/h	6-10
4	pH of the drug's pulp		6,5-7,0
5	The residence time of the preparation in the reaction zone	minutes	2-5
6	The moisture content	%	2,0-4,0
7	Air consumption for drying	m ³ /h	150-200
8	Productivity	kg/h	2-4

Conclusion. Thus, the optimal technological parameters for the preparation of low molecular weight MPS – monomethylolurea, dimethylolurea, methylene-diurea and multifunctional action compounds based on them and zinc acetate in a spray dryer, are obtained in which a qualitative, loose product is obtained: the temperature of the heat carrier is 250-300 °C, the temperature in the reaction zone of the 70- 90 °C, the moisture content of the obtained products is 1-4%. The off-gas contains 55-150 mg/m³ of formaldehyde and 200-380 mg/m³ of product dust, which must be disposed.

The research was carried out according to the scientific and technical program No. BR05234667 within the framework of program-targeted financing CS MES RK.

REFERENCES

- [1] Avtorskoe svidetel'stvo SSSR № 999471 ot 21.10.82. Spособ poluchenija mochevino-formal'degidnogo udobrenija. Budkov V.A., Beglov V.M., Chechetka T.D.
- [2] Avtorskoe svidetel'stvo SSSR № 1048665 ot 15.06.83. Spособ poluchenija mochevino-formal'degidnogo udobrenija. Nabiev M.N., Abdugarimov A.
- [3] Spособ poluchenija modifitsirovannogo karbamida. Iskakov H. Bogdanov A.V., Askarov M.M. B'ulleten' izobretenija №2, 1995 g., opubl. 30.06.95.

Резюме

Ф. Р. Ермаханова, С. Ұсманов, Г. Т. Омарова

ЖЕКЕ МОЧЕВИНО-ФОРМАЛЬДЕГИДТІК ҚОСЫЛЫСТАР МЕН ОЛАРДЫҢ НЕГІЗІНДЕ МЫРЫШ АЦЕТАТЫМЕН ПОЛИФУНКЦИОНАЛДЫ ӘРЕКЕТТІ ПРЕПАРАТТАР АЛУДЫҢ ТЕХНОЛОГИЯСЫН ЗЕРТТЕУ

Мақалада төменмолекулалы мочевино-формальдегидтік қосылыстар мен олардың негізінде мырыш ацетатымен полифункционалды әрекетті препараттарды бұркеуші кептіргіште алу процессінің зерттеулері көрсетілген. Оларды алудың оңтайлы технологиялық параметрлері: жылуұстағыш температурасы 250-300 °С, реакциялық аянда температурасы 70-90 °С, алынған өнімдердің ылғалдылығы 1-4%.

Түйін сөздер: мочевино-формальдегидті қосылыстар, мырыш ацетаты, полифункционалды әрекетті препараттар, кептіру процесі, фазалық құрам өзгерістері, поликонденсация процесі, бұркеуші кептіргіш.

Резюме

Ф. Р. Ермаханова, С. Ұсманов, Г. Т. Омарова

ИССЛЕДОВАНИЕ ТЕХНОЛОГИИ ПОЛУЧЕНИЯ ИНДИВИДУАЛЬНЫХ МОЧЕВИНО-ФОРМАЛЬДЕГИДНЫХ СОЕДИНЕНИЙ И ПРЕПАРАТОВ ПОЛИФУНКЦИОНАЛЬНОГО ДЕЙСТВИЯ НА ИХ ОСНОВЕ И АЦЕТАТА ЦИНКА В РАСПЫЛИТЕЛЬНОЙ СУШИЛКЕ

Исследован процесс получения низкомолекулярных мочевиноформальдегидных соединений, препаратов полифункционального действия на их основе и ацетата цинка в распылительной сушилке. Определены оптимальные технологические параметры их получения: температура теплоносителя 250-300 °С, температура в реакционной зоне 70-90 °С, влагосодержание полученных продуктов 1-4%.

Ключевые слова: мочевино-формальдегидные соединения, ацетат цинка, препараты полифункционального действия, процесс сушки, изменения фазового состава, процесс поликонденсации, распылительная сушилка.

F. R. TASHMUKHAMEDOV, A. Zh. KUTZHANOVA

Almaty technological university, Almaty, Republic of Kazakhstan

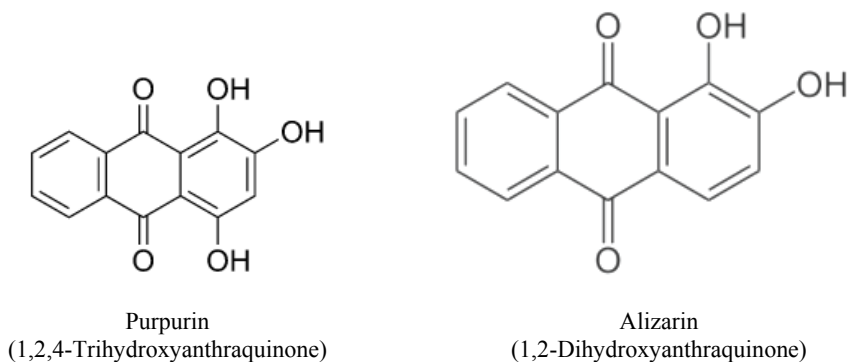
CONTINUOUS DYEING OF CELLULOSIC TEXTILE BY RUBIA TINCTORUM EXTRACT USING SOL-GEL METHOD

Abstract. In this article considers a new method of dyeing cotton fabrics using sol-gel method with natural plant origin dyes. The modified sol-gel method, allowing formation on the fiber a functional barrier coating of silicon oxide, which includes a plant dye. Application of this fixation method allows reducing the yield of the dye from the fiber significantly, as well as introduce additional agents for polyfunctional finishing of textile materials, therefore the method can be referred to the methods of functional depomaterials production. The effect of processing parameters on the intensity and color stability of the obtained materials was studied. The method scanning electron microscopy used for study the surface structure of the treated fibers and to obtain evidence of the presence silica coating. The existence of silicon oxide is also confirmed by the availability of its absorption peaks by Fourier-transform infrared spectroscopy (FTIR).

Key words: sodium silicate, sol-gel, coloring, natural dyes, filer.

Introduction. Developing the chemical industry allows of getting synthetic dyes with the properties and range of colors, which consumer needs for. The undeniable advantages of this dyes type are their low cost, availability of raw materials and, of course, a wide range of colors. However, despite their obvious advantages, they also have disadvantages as their harmful effects on the environment and on humans. The environmental risks of using this type dyes are high, because many of them have carcinogenic properties [1]. In addition, the traditional technology of dyeing with synthetic dyes requires high water resource costs. For example, dyeing one kilogram of cotton fabric carries a flow rate of 70-150 liters of water, about 40 g of active dyes and 0.6 kg of sodium chloride. At the same time, appearance of harmful effect of this type of dye on the environment due to its release into sewage is a known and proven fact [2]. For this reason, in order to create safer textile materials and develop harmless ways of coloring and finishing, it makes sense to return for using natural plant origin dyes particularly. The most complete information about the plants used for these purposes is well studied and presented in previous works [3-6].

The purpose of this work is to develop a technology of coloring cellulose-containing textile materials using a sol-gel method. In this study a water extract of the roots of the madder dye (lat. *Rubiatinctorium*) has been used, so the main coloring substances are porphyrins, namely, alizarin and purpurin (figure 1). The roots of this plant have been used since ancient times for coloring processes silk, cotton and wool. However, with the advent of the era of synthetic dyes, madder plant used for medical purposes as an anti-inflammatory drug mainly.

Figure 1 – Main colorants of *Rubia tinctorum*

The traditional technology of dyeing textile materials with plant dyes uses a periodic dyeing method, there is a long-term presence of the dyed materials in the dyeing solution. It is known that a periodic method of dyeing involves a large expenditure of resources compared to a continuous one. Therefore, using sol-gel dyeing at finishing technology will be better. The name "sol-gel technology" combines a group of methods for synthesizing materials from solutions, so the main result is the preparation of a gel at one stage of the process. Often this process is based on the reaction of controlled hydrolysis of compounds like alkoxides.

Several papers [7-9] about using of the sol-gel method in the coloring of textile materials are known. Most of the precursors of the sol process are alkoxides (TEOS, GMPTS, APTES, TESP-A) and alcohol as solvent with acid, which is a hydrolysis catalyst. In this way the first step is to obtain the sol by reaction of hydrolysis and polycondensation. The second stage is the synthesis of a monolithic gel by the intensive formation of contacts between the particles and the production of a three-dimensional silicon oxide network by increasing the volume of the dispersed phase. The third stage is drying and heat treatment. Products with different levels of density and pore size (xerogels, ambigels, airgels and cryogels) can be obtained. It depends on the method of their implementation. At the textile finishing process there is a tendency of making silicon oxide coatings by sol-gel synthesis on the fiber, which includes a functional substance. In this way it is possible to obtain hydrophobic, fire-resistant, biocide and colored textile materials. The mechanism of functional agent fixation is similar to the technology of printing pigments using a polymer binder, but it has less harm to the environment. Existence of a silicon oxide coatings on the fiber also leads to a decrease photochemical degradation processes under UV radiation [10]. The coloring methods, mentioned above, present an alkoxide sol-gel method, which involves using of a large amount of organic solvents (mainly ethanol). Thus, the method, described in the literature [11, 12] and involves using an aqueous sodium silicate solutions, is most appropriate.

EXPERIMENT

Materials and methods. Samples of 100% bleached cotton fabric, article 1030, with size 200x200mm and surface density of 147 g/m², washed in distilled water at 40 °C, dried in a oven and kept in a desiccators for 24 hours. The precursor of the barrier silica coating is an aqueous solution of sodium silicate (liquid glass of Na₂SiO₃ in the mass ratio of water: Na₂SiO₃ equal to 9: 1) with a density of 1.36 g/m³. As a catalyst of hydrolysis, citric acid (2-hydroxypropane-1,2,3-tricarboxylic acid) was chosen. The raw material for dye extract obtaining was the crushed roots of *Rubia tinctorium*. As a mordant, AlK(SO₄)₂ was chosen.

Extraction of the dye. Pre-dried and shredded roots of the madder dyeing (10 g/l) were poured with an aqueous solution containing NaOH (1-2%), received mixture was heated in a water bath to 80 °C and held for 30 minutes. After removal from the bath, the solution was filtered and held for 12 hours in a cool place. The solution storage process over a long period of time is required to precipitate poorly soluble colloidal impurities in the solution, which can be nuisance for uniform coloration.

Sample preparation and dyeing. Pre-washed and dried samples of cotton cloth with a size of 200x200 mm were impregnated with a solution, containing 10 g/l of AlK(SO₄)₂, for a minute at a temperature of 60-65 °C which followed by 90% padding. At next, tissue samples were impregnated in a second bath with a dye solution, prepared on the basis of an aqueous extract with the addition of liquid glass (50-100 g/l). Impregnation was carried out at a temperature of 65-70 °C for one minute, followed by padding a laboratory padder. After this, the dyed samples were immersed in a third bath, containing an aqueous solution of citric acid (20-50 g/l). Impregnation was carried out at a temperature of 65-70 °C for one minute, followed by padding. Further, it was dried at a temperature of 70-80 °C for 5 minutes and heat treatment at temperatures of 120-160 °C. After heat treatment, the solution was washed with solution, which consists a surfactant containing 2 g/l at 50 °C, and rinsing in distilled water.

Research methods. For determine the color stability to dry and wet friction, the PT-4 device and the gray standards scale were used in accordance with GOST 9733.27-83 "Textile materials. Method of testing the color fastness to friction". For determine the color stability to wet-heat treatments, the stained samples were subjected to repeated washing according to the conditions given in ISO 105-C06-2011 "Textiles. Tests for colour fastness. Part C06: Colour fastness to domestic and commercial laundering". The color intensity K/S of samples were obtained from tabulated data by comparison with the reflection coefficient R%, which measured on a CarlZeiss spectrophotometer. The fact of the availability of coating is one of the reasons for the change in the strength and stiffness parameters in comparison with the original fabric. Determination of the tensile strength of the fabric was carried out on a tensile machine RT-250M in accordance with GOST 3813-72. "Textile materials. Fabrics and piece goods. Methods for determining tensile properties". Determination of the inflexibility parameters of the

processed and untreated samples was carried out with the MT-376 device (Metrotex, Russia) according to the ring method according to GOST 10550-93 "Textile materials. Fabrics. Methods for determining rigidity in bending". For research of chemical compounds and bonds, FTIR method, using Nicolet 6700 spectrometer (USA), was applied. To study the structure of the surface of the processed samples the electron microscopy (SEM) method, using a JEOL JSM-6490LA scanning electron microscope with an energy dispersive analyzer (EDX), was applied.

RESULTS AND DISCUSSION

The results of measuring the intensity of the color of the obtained samples are shown in table 1.

Table 1 – Intensity and color stability

Sample	Concentration of liquid glass, g/l	Concentration of citric acid, g/l	Temperature of heat treatment, °C	K/S			Colour fastness for friction	
				Without washing	After 5 washing	After 10 washing	dry	wet
1	100	50	160	0.9618	0.7225	0.6108	5	5
2	100	50	120	0.7748	0.6255	0.5332	5	5
3	100	20	160	0.9742	0.7403	0.6368	5	5
4	100	20	120	0.8372	0.6843	0.5860	5	5
5	50	50	160	0.9376	0.7181	0.6218	5	5
6	50	50	120	0.8691	0.6640	0.5622	5	5
7	50	20	160	1.0394	0.7726	0.6561	5	5
8	50	20	120	0.8372	0.6561	0.5791	5	5
Untreated				0.009713			5	5

The stability of the stain to dry and wet friction for all samples was 5 points. According to the results of the K/S measurement, it can be seen that samples with a heat treatment at 160 °C have the highest color intensity compared to samples treated at 120 °C, this fact can be explained by the presence of a denser structure of the silica coating, which prevents the dye from desorption. And there is also seen that an increasing of the liquid glass concentration makes it possible to obtain the most stable coloration for wet-heat (laundering) treatments.

The durability of the paint to dry and wet friction for all samples was 5 points, which indicates a sufficient fixation of colorant on the fiber.

Along with the color strength index, the influence of the dyeing conditions on the physical and mechanical characteristics of the fabric was studied, and the inflexibility (toughness) data of the processed samples without the use of a dye was also given. The data obtained during testing of the samples are given in table 2.

Table 2 – Mechanical properties

Sample	Concentration of liquid glass, g/l	Concentration of citric acid, g/l	Temperature of heat treatment, °C	Inflexibility, cN		Tensile strength, N	
				Coloured by sol-gel	Treated by sol-gel, without colorant	Main	Weft
1	100	50	160	11.074	9.741	162	122
2	100	50	120	9.555	11.613	201	148
3	100	20	160	12.769	9.800	162	161
4	100	20	120	10.662	11.437	161	130
5	50	50	160	10.251	8.751	153	110
6	50	50	120	11.250	10.692	163	136
7	50	20	160	10.643	9.016	171	118
8	50	20	120	11.417	9.320	187	115
Clear	0	0	0	7.232	7.232	232	221
Non-coloured, treated by $AlK(SO_4)_2$	0	0	0	9.878	9.898	409	249

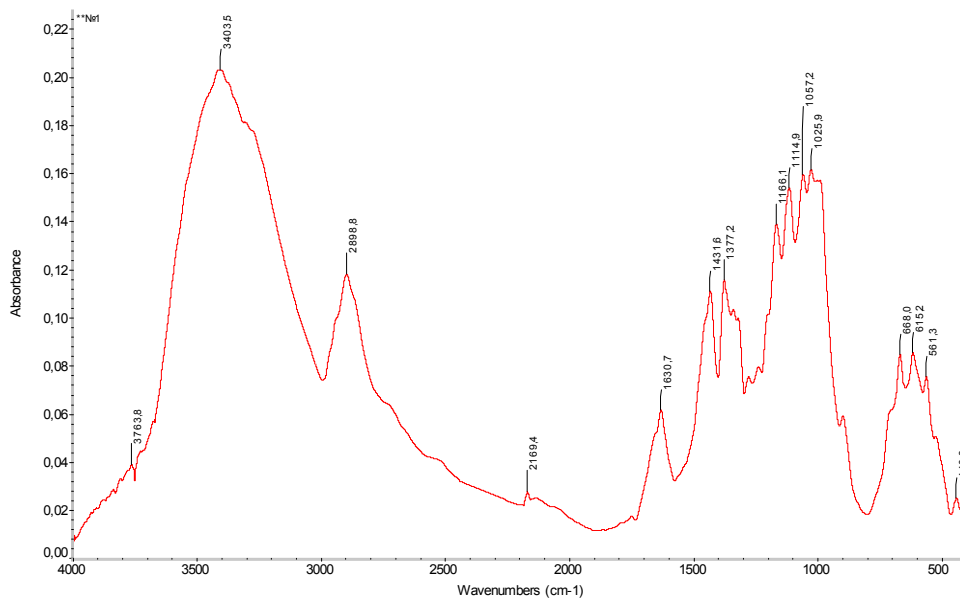


Figure 2 – FTIR absorption spectrum of a coloured sample

Data analysis shows that heat treatment at elevated temperature leads to a decrease in the strength characteristics of the fabric, which is caused both by the dehydration of the cellulose fiber and by decreasing elasticity of the coating and

leads to a decrease in the mobility of the fibers. It can be seen from the table that impregnation with alums before the dyeing process, also leads to strength increasing.

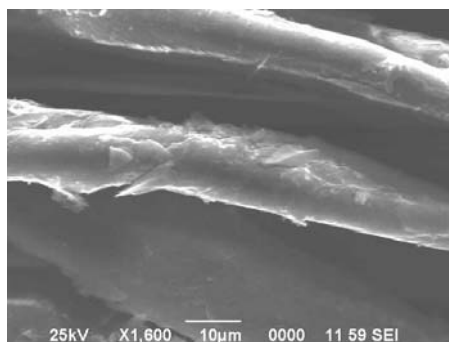
For a more detailed study of the chemical composition and the existence of chemical bonds, an FTIR analysis was made. The results are shown in figure 2. The detailed description of the absorption peaks is presented in table 3.

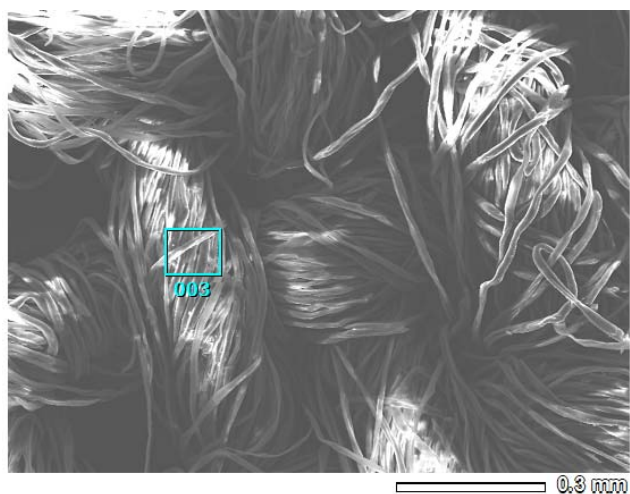
Table 3 – Supposed availability of chemical bonds

Absorption peaks, cm^{-1}	Description	Possible cause
440	-S-S-	Use of alumina potassium alum
561	C-H	–
615	C-Cl or CH-O-N=O	–
668	Presence of benzole ring	Presence of dye
1025	Alkylcyclopropanes or benzole ring existence	Presence of dye
1057	Si-O	Presence of silicon oxide
1115	Acetals	–
1166	Alkylsulfones or disubstituted sulfonides	Due to the reaction of alumacalic alum with a dye, the formation of lacquers
1377	-CH ₃	–
1431	Dimers of carboxylic acids	–
1630	Crystallization Water	Non-full dehydration of Cellulose and Gel Coating
2170	-NH ₃	–
2899	AlK(SO ₄) ₂	Remains of unreduced alumina potassium alum
3403	-OH	Presence of cellulose

The absence of peaks in the region of 1870-1770 cm^{-1} , indicates the absence of sodium citrate salts, the peaks at 559 and 667 cm^{-1} indicate the availability of tetrapyrrol, which confirms the presence of the dye.

Figure 3 –
The SEM image of coloured sample





Memo	C	O	Si	Total(mass%)
3	46.17	48.52	5.32	100

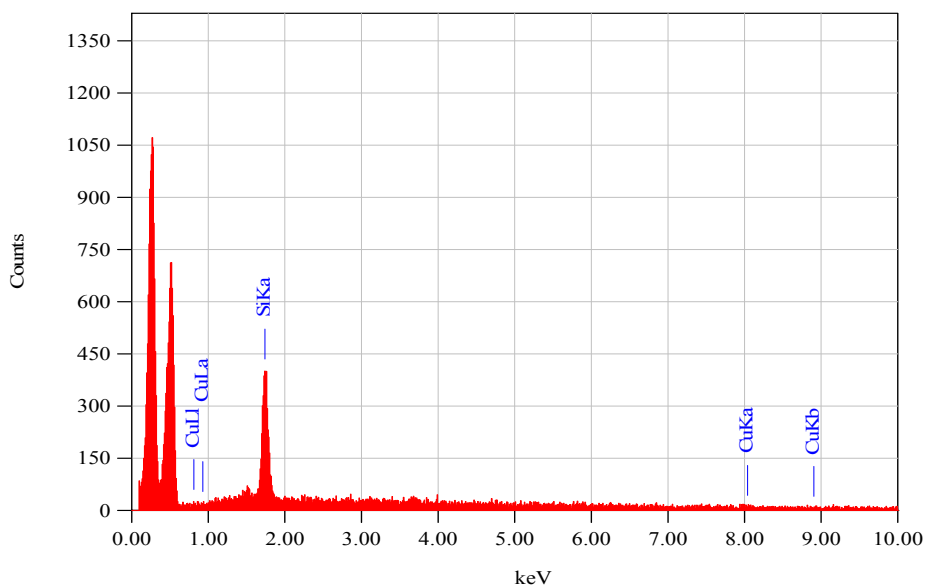


Figure 4 – EDX data of coloured sample

The microstructure and elemental composition of the obtained samples were studied using the scanning electron microscopy method and energy-dispersive elemental analysis. The results of a study of the morphology of the fiber surface are shown in figures 3 and 4.

The presence of a silica coating is seen on the surface images (figure 3) of the material, which is also proved by the presence of peaks for silicon on the energy-dispersion analysis diagram (figure 4).

Conclusion.

1. A new method of dyeing cotton fabrics with plant colourants applying modified sol-gel method, was developed, where a silica coating plays role as a binder and barrier for the dye.

2. The present method makes it possible to increase the storage time of using solution up to several days by applying sequential treatment first in the precursor and then in the catalyst of hydrolysis, with avoiding the premature formation of the hydrogel in the impregnating baths, and being polycondensation reaction occurs at the fiber-solution interface.

3. The use of this method makes it possible to obtain a silica coating, as evidenced by the results of electron microscopy and energy dispersive analysis, as well as to increase the rigidity of the treated materials in comparison with the untreated ones. The study showed that the fixation of pigments by a new method without polymer binders is possible in principle.

REFERENCES

- [1] Zvezdina S.V., Berezin M.B., and Berezin B.D. Natural Dyes Based on Chlorophyll and Protoporphyrin Derivatives // *Russian Journal of Coordination Chemistry*. 2010. Vol. 36, N 9. P. 711-714.
- [2] Robinson T., McCullan G. et al. Remediation of dyes in textile influent: critical review on current treatment technologies // *Bioresource technology*. 2001. Vol. 77, issue 3. P. 247-255.
- [3] Sekar N. Natural colorants-an introduction // *Colourage*. 1999. Vol. 46. P. 57.
- [4] Gupta D. Mechanism of dyeing synthetic fibres with natural dyes // *Colourage*. 2000. Vol. 47. P. 23.
- [5] Ramakrishna E. Into the golden era of natural and vegetable dyes // *Colourage*. 1999. Vol. 46. P. 29.
- [6] Cannon J., Cannon M. *Dye Plants and Dyeing*. London: Herbert, Ltd., 1994. P. 128.
- [7] Mahtlig B., Textor T. Combination of silica sol and dyes on textiles // *Journal of sol-gel science technology*. 2006. Vol. 39. P. 111-118.
- [8] Schramm C., Reanderer B. Dyeing and DP treatment of sol-gel pre-treated cotton fabrics // *Fibers and polymers*. 2011. Vol. 12. P. 226-232.
- [9] Jinyun Liu, Wenqi Huang, Yanjun Xing. Preparation of durables upper hydrophobic surface by sol-gel method with waterglass and citric acid // *Journal of Sol-Gel Science and Technology*. 2011. Vol. 28. P. 18-23.
- [10] Salyakhova M.A., Karasyova I.P., Puhachyova E.N. Fotohimicheskaya distrukciya tekstilnih materialov // *Vestnik Kazanskogo tehnologicheskogo universiteta*. 2013. Vol. 16, N 17. P. 92-93.
- [11] Dyussembiyeva K.Zh. Razrabotka novyh modifitsirovannyh tekstilnyh materialov s antimikrobnymi svoystvami na osnove zol-gel tehnologii: PhD dissertaition, defended 23.12.2016. Almaty: Almaty technological university, 2016.
- [12] Tashmukhamedov F.R. Primenenie zol-gel metoda v krashenii tekstilnyh materialov // *Vestnik ATU*. 2016. N 4(113). P. 5-11.

Резюме

Ф. Р. Ташмухамедов, А. Ж. Кутжанова

**RUBIA TINCTORUM ЭКСТРАКТЫ МЕН
ЗОЛЬ-ГЕЛЬ ӘДІСІН ҚОЛДАНА ОТЫРЫП ЦЕЛЛЮЛОЗАЛЫ
ТЕКСТИЛЬ МАТЕРИАЛДАРЫН ҮЗДІКСІЗ ӘДІСПЕН БОЯУ**

Мақалада целлюлозалы текстиль материалдарын табиғи текті бояғыштармен золь-гель әдісі арқылы бояудың жаңа әдісі ұсынылған. Зерттеу жұмысының негізгі нәтижесі болып маталарды марена бояғышы мен золь-гель әдісін пайдалана отырып экологиялық қауіпсіз бояу технологиясының құрастырылуы болып табылады. Ол текстиль материалының прекурсор мен гидролиз катализаторында сіңіріліп, одан кейін кептіру және термоөңдеу процестері арқылы жүзеге асады. Өңдеу параметрлерінің текстиль материалының физико-механикалық қасиеттері, бояу интенсивтілігі мен беріктілігі зерделенген. Нәтижесінде, 10 жуудан кейін бояу интенсивтілігінің жоғары деңгейі натрий силикатының 100 г/л мөлшеріндегі, 160 °С термоөңдеуден өткен үлгілер көрсетті. Сонымен қатар электронды микроскопия әдісін қолдана отырып функционалды жабын мен бояғыштың бекітілгені зерделенген. Зерттеу нәтижесі целлюлозалы текстиль материалдарын өңдеу өндірісінде пайдалауға болады.

Түйін сөздер: натрий силикаты, золь-гель, колорлау, табиғи бояғыштар.

Резюме

Ф. Р. Ташмухамедов, А. Ж. Кутжанова

**НЕПРЕРЫВНЫЙ СПОСОБ ОКРАШИВАНИЯ ЦЕЛЛЮЛОЗНЫХ
ТЕКСТИЛЬНЫХ МАТЕРИАЛОВ ЭКСТРАКТОМ «RUBIA TINCTORUM»
С ИСПОЛЬЗОВАНИЕМ МЕТОДА ЗОЛЬ-ГЕЛЬ**

В статье приведен новый способ окрашивания целлюлозных текстильных материалов золь-гель методом с применением красителей растительного происхождения. Основным результатом исследования является разработанная экологически безопасная технология колорирования тканей с применением золь-гель метода и экстракта марены красильной, которая состоит в последовательной пропитке текстильного материала в прекурсор и катализаторе гидролиза с последующей сушкой и термообработкой. Исследовано влияние параметров обработки на физико-механические свойства ткани, интенсивность и прочность окраски. Выявлено, что наибольшей интенсивностью окраски после 10 стирок обладают образцы, обработанные при концентрации жидкого стекла, равной 100 г/л, и прошедшие термическую обработку при 160 °С. Так же применен метод электронной микроскопии, результаты которого доказывают наличие функционального покрытия и фиксации красителя в его объеме. Результаты исследования могут быть применены в отделочном производстве текстильных целлюлозосодержащих материалов.

Ключевые слова: силикат натрия, золь-гель, колорирование, растительные красители.

*E. E. ERGOZHIN¹, T. K. CHALOV¹,
B. E. BEGENOVA², T. V. KOVRIGINA¹, YE. A. MELNIKOV¹*

¹JCS « A.B. Bekturov Institute of Chemical Sciences », Almaty, Republic of Kazakhstan
²M. Kozybayev North Kazakhstan State University, Petropavlovsk, Republic of Kazakhstan

STUDY OF SORPTION OF LEAD (II) IONS BY ANIONITE OBTAINED ON THE BASIS OF ANILINE, EPICHLOROHYDRIN AND POLYETHYLENEDIAMINE

Abstract. Polyfunctional anionite based on aniline, epichlorohydrin, and polyamines were synthesized. The composition and structure of the anion exchanger were studied by IR spectroscopy and elemental analysis. Lead sorption was studied by classical polarography. Dependences on the sorption of lead (II) ions on the solution acidity, concentration of metal ions, and duration the contact of resins with solution $Pb(NO_3)_2$ were determined. This anionite exhibits high capacity in sorption of lead ions. The developed sorbents with increased sorption ability can successfully solve problems of removing lead (II) ions from process effluents in nonferrous metallurgy.

Keywords: sorption, lead ions, anion exchanger, sorption capacity.

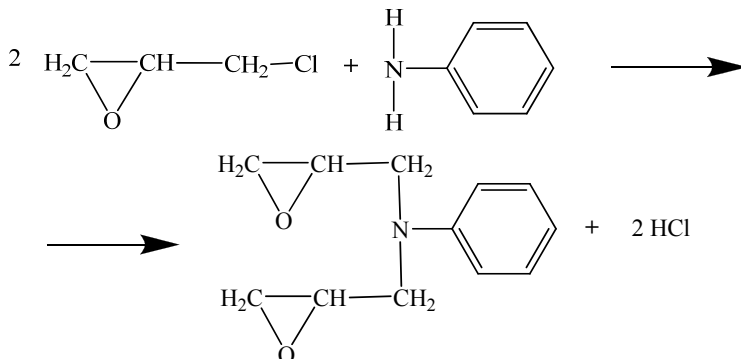
Introduction. Lead is known as a toxic metal that accumulates in the human body throughout the lifetime [1]. The World Health Organization (WHO) has established the maximum allowable limit of 0.01 mg/l for lead in drinking water [2]. Therefore, highly sensitive determination methods of trace lead in environmental samples need to be established and contamination occurs industrial activities such as mining, electricity generation, sewage application, fertilization and petrochemical. Although some of them play important roles in biological function, they are likely to have a potential to destroy ecosystems and human health through the food chain [3-5]. The US Environmental Protection Agency (USEPA) priority list regards Pb pollution as one of the top 20 pollutants. Therefore, the possibility of reducing its contamination must be taken into consideration. Due to the fact that heavy metals are non-biodegradable, they are contained in the soil continually [6]. So it is extremely important to search an environmentally way to harness the environmental pollution of heavy metal, and then reduce the deteriorating effect of heavy metals to the environment [7]. Traditional physical and chemical treatments effective in some cases. The drawback of these methods are that they expensive, disruptive, and impractical under natural environmental conditions. Therefore, ion exchange can be used as a relatively new, economical and highly effective technology to solve the heavy metal problems and restore the fertility of soil. Sorption is also the most advantageous and most promising procedure for purifying and separating substances. The sorbents should be sufficiently selective, exhibit high sorption ability, and be resistant to high temperatures [8, 9].

This study deals with the physicochemical properties of polyfunctional anion exchangers based on aromatic hydrocarbons, epichlorohydrin and polyethylenimine in relation to lead (II) ions onto them.

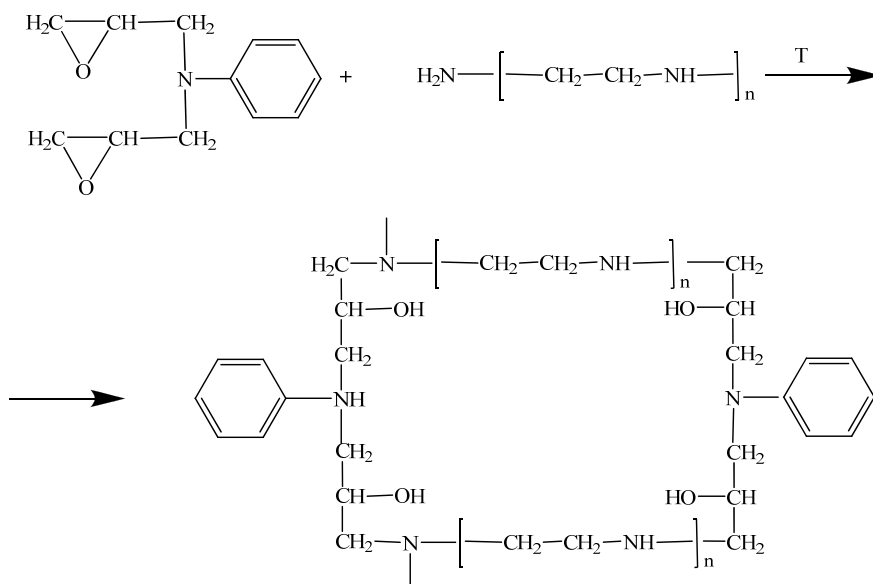
EXPERIMENTAL PART

Epoxy amine was synthesized from aniline (A) and epichlorohydrin (ECH). Polyfunctional anion exchanger A-ECH-PEPA was prepared by condensation of the epoxy amines with polyethylenepolyamine (PEPA).

Glycidyl amine derivatives (epoxy amines) was synthesized in the first step from A and ECH in the presence of NaOH (50°C, 6 h).



In the second step, the condensation of the epoxy amines with PEPA was performed in a dimethylformamide (DMF) solution at different molar ratios of the components at 60– 65°C for 5–6 h, after which the reaction mass was cured at 100°C for 16–24 h. The optimum conditions for preparing the ion-exchange materials were found previously.



The composition and chemical structure of the anion exchanger was studied by IR spectroscopy with a Nicolet 5700 Fourier IR spectrometer (Thermo Electron Corporation, the United States) and by elemental analysis with a CHN628 analyzer (LECO, the United States).

As seen from figure 1, in IR spectra, characteristic bands (cm^{-1}) of epoxy groups (810–920, 1250, 3000–3010) are absent, but N–H bending (1599–1600) and C–N stretching (1020–1220) vibration bands of amino groups appear, suggesting the occurrence of a chemical reaction of aniline diglycidyl derivative with polyamine. The absorption at 1502–1504, caused by stretching vibrations of the benzene ring, confirms the presence of aromatic fragments in the structure of the anion exchangers [10].

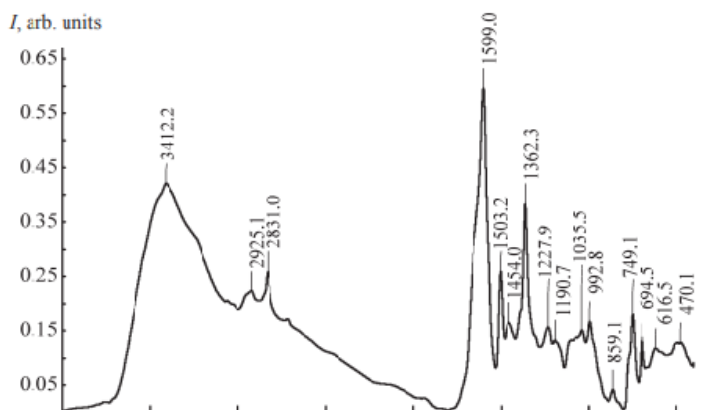
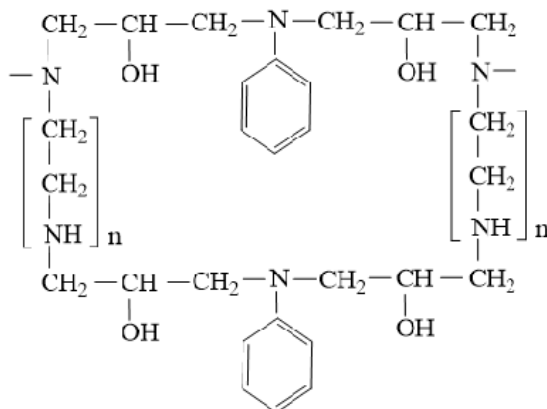


Figure 1 – IR spectra of anion exchanger A–ECH–PEPA.
(I) Intensity and (ν) wavenumber

The elemental composition of the anion exchanger A–ECH–PEPA (found/calculated, %) is as follows: C 74.23/73.84, H 16.32/16.48, N 5.76/5.50, O 3.69/4.18.

The results of chemical and spectroscopic analysis of the synthesized polymers suggests the following structure:



The physicochemical characteristics of the synthesized anion exchanger is given in the table 1.

Table 1 – Physicochemical properties of the synthesized anion exchanger

Anion exchanger	SEC _{HCl} , mg-equiv/g	V _{sp} , ml/g	Chemical stability in solutions, %			Thermal stability in water, %
			5 N H ₂ SO ₄	5 N NaOH	10% H ₂ O ₂	
A-ECH-PEPA	3,03	4,2	89,9	91,4	70,0	91,8

Sorption of lead (II) ions onto A-ECH-PEPA ion exchanger in the OH form was studied in batch experiments under the following conditions: sorbent : solution ratio 1 : 400, room temperature (20 ± 2°C), concentration of lead ions in Pb(NO₃)₂ solutions from 0.227 to 2.072 g/l, pH 1.1–5.8 (adjusted by adding 5 N HNO₃). The pH values were measured with a pH-150 MI pH meter with an accuracy of ±0.05 pH unit. The sorbent–solution contact time was from 0.5 h to 7 days. Model solutions were prepared using chemically pure grade Pb(NO₃)₂.

SC was calculated from the difference between the initial and equilibrium concentrations of the solutions, which were determined by classical polarography in 0.5 M NH₄Cl supporting electrolyte from the Pb (II) reduction wave (E_{1/2} = -0.46 V). The polarograms were recorded with a PU-1 universal polarograph with an accuracy of ±0.5% in a temperature-controlled cell at 25±0.5°C using a dropping mercury electrode. Oxygen was removed from the solutions by argon bubbling for 5 min. A saturated calomel electrode was used as a reference electrode. The conditions of our sorption experiments (sorbent : solution ratio, concentration and pH of molybdenum-containing model solutions, contact time) were close to those of the industrial processes.

RESULTS AND DISCUSSION

To use ion exchangers in the practice, it is necessary to study how the sorption of metal ions depends on the process conditions. To determine the optimum parameters of the sorption, we studied the influence exerted on the sorption of lead (II) ions by the concentration and pH of Pb(NO₃)₂ solutions and by the time of their contact with the ion exchanger (figures 2–4).

From figure 2, can be seen the isotherm of sorption Pb²⁺ ions and the SC anion exchanger is represented, and show increase of SC with the content of lead ions in solutions. The rise of the curve at their small equilibrium concentrations indicates that the anion exchanger extracts lead (II) ions with sufficient completeness. The recovery rate reaches at 91% and maximum SC of A-ECH-PEPA anion exchanger reaches at 228 mg/g.

One of the most important factors controlling sorption of metal ions from solutions is pH of the solution. The pH influences both the metal speciation in the solution and the state of the ionogenic groups [11]. The dependence of the sorption capacity of the anion exchanger for lead ions on the acidity of Pb(NO₃)₂

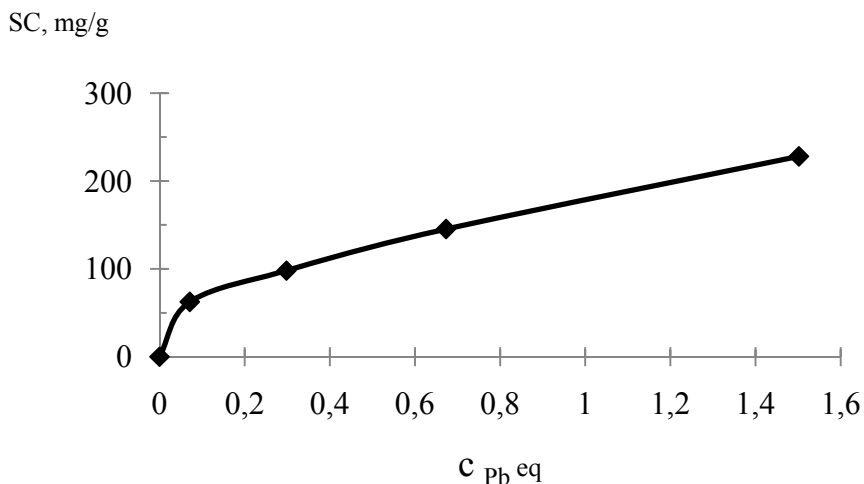


Figure 2 – Isotherm of Pb^{2+} sorption onto A-ECH-PEPA anion exchanger. Contact time 7 days, pH 5.8. SC – sorption capacity (mg/g), $C_{Pb\ eq}$ – equilibrium concentration (g/L)

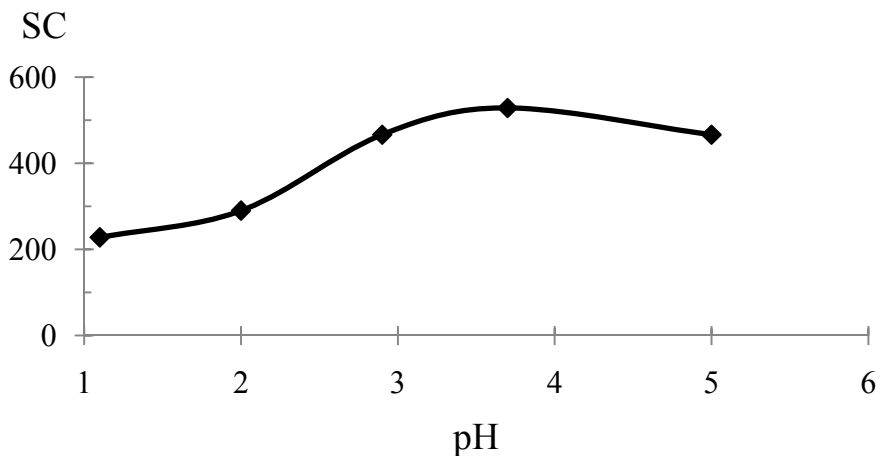


Figure 3 – Dependence sorption capacity of A-ECH-PEPA anion exchanger on the acidity of solution $Pb(NO_3)_2$. $C_{Pb} = 2.072$ g/L; contact time 7 days

solutions is shown in figure 3. As can be seen, the optimum pH for the uptake of lead ions is 3.7. Under these conditions, the uptake of Pb (II) ions and SC of A-ECH-PEPA anion exchanger reach maximal values and SC is 528.4 mg Mo/g.

Figure 4 shows the lead ions sorption isotherm for A-ECH-PEPA anion exchanger. The equilibrium between the resins and solution containing 2.072 g/l Pb and having pH 3.7 is attained in 1 h, and the SC of the A-ECH-PEPA anion exchanger is 528.4 mg/g.

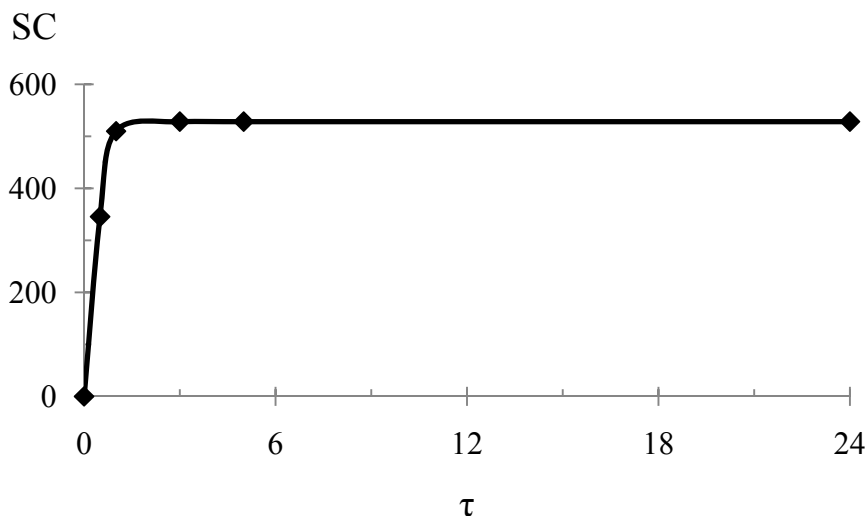


Figure 4 – Dependence sorption capacity of A–ECH– PEPA anion exchanger on the duration contact time (τ) of resin with $\text{Pb}(\text{NO}_3)_2$ solution. $C_{\text{Pb}} = 2.072 \text{ g/L}$; pH 3.7

Conclusion. Thus, the sorption ability of polyfunctional anion exchanger based on aniline, epichlorohydrin and polyethilenpolyamine with respect to lead ions is studied. It is established that it possesses unique sorption properties with respect to Pb^{2+} ions. It is shown that the acidity of the medium has a significant effect on the sorption of lead ions. Thanks to high sorption and kinetic properties, the investigated anion exchanger can be recommended for wastewater treatment of hydrometallurgical production from lead ions.

The research was carried out according to the scientific and technical program No. BR05234667 within the framework of program-targeted financing CS MES RK.

REFERENCES

- [1] Behbahani M., Hassanlou P.G., Amini M.M., Moazami H.R., Abandansari H.S., Bagheri A., Zadeh S.H. Selective Solid-Phase Extraction and Trace Monitoring of Lead Ions in Food and Water Samples Using New Lead-Imprinted Polymer Nanoparticles // *Food Analytical Methods*. 2015. Vol. 8, N 3. P. 558-568.
- [2] World Health Organization. Health Criteria and Other Supporting Information // World Health Organization. Geneva, 1996.
- [3] Dutton J., Fisher N.S. Bioaccumulation of As, Cd, Cr, Hg(II), and MeHg in killifish (*Fundulus heteroclitus*) from amphipod and worm prey // *Science of The Total Environment*. – 2011. Vol. 409, N 18. P. 3438-3447.
- [4] Takahashi C.K., Turner A., Millward G.E., Glegg G.A. Persistence and metallic composition of paint particles in sediments from a tidal inlet // *Marine Pollution Bulletin*. 2012. Vol. 64, N 1. P. 133-137.
- [5] Naseem R., Tahir S.S. Removal of Pb^{2+} from aqueous solution by using bentonite as an adsorbent // *Water Research*. 2010. Vol. 35. P. 3982-3986.
- [6] Bolan N., Kunhikrishnan A., Thangarajan R., Kumpiene J. Remediation of heavy metal(loid)s contaminated soilseto mobilize or to immobilize // *Journal of Hazardous Materials*. 2014. Vol. 266. P. 141-166.

[7] Chandra S.K., Kamala C.T., Chary N.S., Sastry A.R. Removal of lead from aqueous solution using an immobilized biomaterial derived from plant biomass // Journal of Hazardous Materials. 2004. Vol. 108. P. 111-117.

[8] Söderlund M., Lehto J. Sorption of Molybdenum, Niobium and Selenium in Soils. Finland, 2012. 98 p.

[9] F. Granados Correa, J. Serrano Gomez. Kinetic and thermodynamic parameters of ^{99}Mo sorption on thermally treated hydrotalcite // Journal of Radioanalytical and Nuclear Chemistry. 2006. Vol. 268, N 1. P. 95-101.

[10] Böcker J. Spektroskopie: Instrumentelle Analytik mit Atom- und Molekülspektrometrie. Vogel, 1997. 528 p.

[11] Neudachina L.K., Petrova Yu.S., Zasukhin A.S., Osipova V.A., Gorbunova Ye.M., Larina T.Yu. Sorption kinetics of heavy metal ions by polysiloxane functionalized with 2-aminoethylpyridine groups // Analitika i Kontrol. 2011. Vol. 15, N 1. P. 87-95.

Резюме

Е. Е. Ергожин, Т. К. Чалов, Б. Е. Бегенова, Т. В. Ковригина, Е. А. Мельников

АНИЛИН, ЭПИХЛОРИДРИН ЖӘНЕ ПОЛИЭТИЛЕНПОЛИАМИН НЕГІЗІНДЕ АЛЫНҒАН АНИОНИТПЕН ҚОРҒАСЫН (II) ИОНЫНЫҢ СОРБЦИЯСЫН ЗЕРТТЕУ

Анилин, эпихлоридрин және полиэтиленполиамин негізіндегі полифункционалды анионитпен классикалық поляграфия әдісі арқылы қорғасын ионының сорбциясы зерттелді. Ерітінді концентрациясымен рН көрсеткіші қорғасын (II) ионын бөліп алу қасиетін зерттеу барысында, ерітіндідегі Рb концентрациясының көбеюімен иониттің сорбциялық сыйымдылығы артатындығын көрсетті. Аниониттің оңтайлы рН мәні 3.7, тең болған жағдайда сіңіру сыйымдылығы 528.4 мг Рb/г құрайды.

Түйін сөздер: сорбция, қорғасын иондары, анион алмастырғыш, сорбциялық сыйымдылық.

Резюме

Е. Е. Ергожин, Т. К. Чалов, Б. Е. Бегенова, Т. В. Ковригина, Е. А. Мельников

ИЗУЧЕНИЕ СОРБЦИОННОЙ СПОСОБНОСТИ АНИОНИТА, ПОЛУЧЕННОГО НА ОСНОВЕ АНИЛИНА, ЭПИХЛОРИДРИНА И ПОЛИЭТИЛЕНПОЛИАМИНА, ПО ИОНАМ СВИНЦА

Синтезирован полифункциональный анионообменник на основе анилина, эпихлоридрина и полиэтиленполиами́на; были изучены состав и структура анионита методами ИК-спектроскопии и элементного анализа. Исследован процесс сорбции свинца методом классической полярографии и найдены зависимости сорбции ионов Pb^{2+} в статическом режиме от кислотности растворов, концентрации ионов металлов и продолжительности контакта ионитов с раствором $\text{Pb}(\text{NO}_3)_2$. Установлено, что данный ионообменник обладает высокими сорбционными свойствами по отношению к ионам свинца. Научная новизна исследования состоит в том, что впервые была изучена сорбционная зависимость по отношению к ионам Pb^{2+} синтезированным ионитом. Практическая значимость данной работы заключается в том, что разработанный сорбент с повышенной сорбционной способностью может успешно решить проблемы очистки технологических стоков цветной металлургии от ионов свинца (II).

Ключевые слова: сорбция, ионы свинца, анионит, сорбционная емкость.

*SH. N. ATAULLAEV, S. F. FOZILOV,
B. A. MAVLANOV, V. N. AKHMEDOV, A. U. OCHILOV*

Bukhara Engineering-Technological Institute, Bukhara, Uzbekistan

INVESTIGATION OF THE PROCESS OF APPLICATION OF SALTS OF ACTIVE PHASES OF NICKEL AND MOLYBDEN TO THERMOREGENERATED ZEOLITE CaA

Abstract. In this work, studies are carried out the process of applying active phases of nickel and molybdenum compounds to thermoregenerated CaA zeolite and heat treatment of catalytic systems based on it.

Key words: catalyst, thermoregeneration, adsorbent, zeolite, regeneration, application, mixing, activated, thermal analysis, calcinations, chemisorption, endothermic and exothermic effect.

Introduction. It is known that the depth of hydroconversion of the components of the feedstock, the quality and quantity of the target oil depends on the hydrogenating and isomerizing properties of the catalyst used: the more active the contact in these reactions, the deeper the hydroconversion of the raw materials in the low boiling distillates, the higher the quality and the greater the yield of the desired product. The catalysts containing noble metals (Pt, Pd, etc.) possess high hydrogenating and isomerizing properties. But because they have low hydrogenating and isomerizing activity, they are unacceptable for hydroprocessing residual petroleum products containing contact poisons, and the desired results can not be obtained on industrial Al-Ni (Co)-Mo catalysts. At the same time, the catalyst containing a nickel on hydrogenating activity can compete with catalysts based on platinum and palladium, but it is also committed to poisoning with sulfur and nitrogen containing compounds. The use of nickel in combination with molybdenum in the form of nickel molybdate allows the preparation of a catalyst having simultaneously high hydrogenating, isomerizing and cleaving properties. Treatment of the catalyst with sulfur or hydrogen sulphide increases its polyfunctionality in acid catalysis [1, 2].

It has been established that nickel - molybdenum catalysts on various refractory acid carriers exhibit higher activity and stability in oxidation - reduction and acid - base catalysis in the case of exclusion or reduction of the formation of catalytically inactive nickel aluminate by spinel structure.

EXPERIMENTAL PART

To study the processes occurring at the stage of applying active phases to the thermo regenerated and regenerated zeolite and heat treatment of catalytic systems, the following samples were prepared:

Sample 1 (CM). It is prepared by applying the calculated amount of molybdenum salt in the form of an aqueous solution to the thermo regenerated and activated zeolite CaA. After drying in the open air, the sample was subjected to thermal analysis.

Sample 2 (CMN). The air-dry catalyst was obtained by applying the calculated amount of nickel salt in the form of an aqueous solution to a CM sample pre-calcined at 550 °C.

Sample 3 (CN). It is prepared by applying an aqueous solution of a nickel salt to a thermoregenerated zeolite, then the order of the sequence and sequence are the same as for the treatment of a CM sample.

Sample 4 (CNM). It is prepared by calcination of the sample of the CN at 550 °C, followed by applying the calculated amount of the molybdenum salt in the form of an aqueous solution. An air-dry system was subjected to thermal analysis.

RESULTS AND DISCUSSION

On the thermogram of the spent zeolite, an "endothermic" effect at 200 °C with an inflection point at 280 °C, corresponding to the removal of physically adsorbed water is clearly visible. And the stepwise removal of chemisorbed water, localized in various cavities, for CaA type zeolites proceeds most intensively, in the range from 350 to 450 °C. In addition, an "exothermic" effect was observed, due to the removal of organic deposits from the pores of zeolite CaA.

The thermogram of the spent zeolite shows that the intense exothermic effect at 360 °C, from the burnout of organic compounds, overlaps the weaker endothermic effects from the dehydration of the zeolite. The presence of these effects indicates the preservation of the specific crystal structure of the zeolite and its ability to reverse water adsorption. The preservation of crystalline structures was proved by the RFA diffraction method, X-ray diffraction and the weighting method for "adsorption-desorption" of water. The effects on the thermograms of catalyst samples with supported transition metal ions were found to be related. The following effects were observed on the thermogram (figure 1b) of crystalline nickel nitrate: a narrow peak at 65 °C, two more intense broad peaks at 190 and 320 °C, and a small "endoeffect" is observed at 255 °C.

On the thermogram of nickel nitrate deposited on a thermoregenerated zeolite (figure 2b of a sample of CNM) and dried at 20-25 °C, $\tau = 24-26$ hours, a very wide low-intensity endoeffect with a maximum at 150 °C is observed, accompanied by a slight loss of mass on the curve TG, due to the removal of residues of physically adsorbed water. There is no specific narrow endoeffect from the thermal decomposition of crystalline nickel nitrate, the position of higher temperature peaks also does not correspond to the initial substance, all this indicates the occurrence of deep chemical transformations already at the stage of impregnation. Taking into account the strongly alkaline environment during the application of nickel nitrate due to the release of compensating calcium ions into

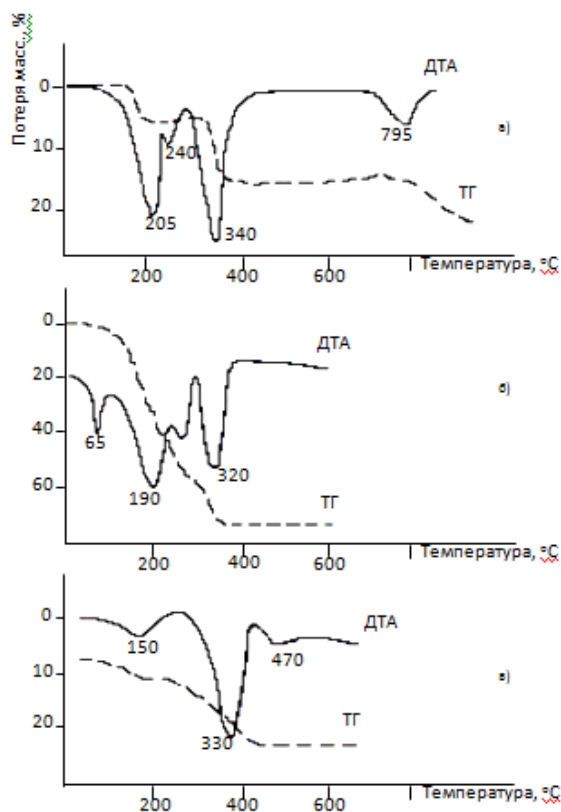


Figure 1 – Thermogram of nickel and molybdenum compounds:
 a) ammonium para-molybdate; b) nickel nitrate; c) nickel hydroxide

the solution, it is possible to assume the formation of the $\text{Ni}(\text{OH})_2$ hydrogel, which is characterized by two little intense broad peaks of the endoeffect at 150 and 470 °C, in addition to the powerful endo-effect, temperature 330 °C, the main weight loss of the sample is observed (figure 1c).

Comparison of the thermogram of the CMN sample with the thermograms $\text{Ni}(\text{OH})_2$ and $\text{Ni}(\text{NO}_3)_2 \cdot 6\text{H}_2\text{O}$ allows us to consider this DTA as a superposition of the stepwise thermal decomposition of the most probable products of basic hydrolysis, namely, hydroxy complexes of nickel nitrate, its basic salts and hydroxides. Apparently, DTA of the investigated sample of CMN is closest to DTA $\text{Ni}(\text{OH})_2$, where there are strongly broadened effects at 150 and 290-330 °C, and "endoeffects" at 400 and 620 °C are most likely due to removal of intracrystalline zeolite water. In the case of thermal decomposition of nickel nitrate deposited on an acid-activated zeolite (figure 2a and a sample of a CN), the thermal effects from the dehydration and thermal fixing of nickel structures on the zeolite are shifted to the low-temperature region.

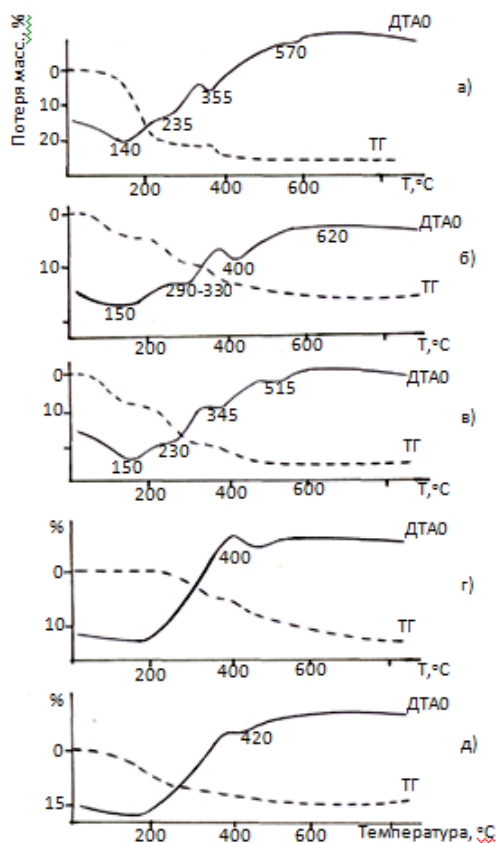


Figure 2 – Thermogram of zeolite catalysts:

a) a sample of the CN, б) a sample of CNM, в) a sample of CMN, г) a sample of CM

This may indicate, according to the ESTD, the prevalence of nickel hydroxo-complexes over nickel hydroxide in a dried but not calcined sample; a variety of nickel structures are observed in the calcined sample. The reaction products of hydrolyzed nickel nitrate with molybdenum compounds thermally fixed on the surface of the activated zeolite dehydrate at lower temperatures than in the case of an activated and the more thermoregenerated sample and may be associated with the dehydration of nickel-molybdate associates. The "exothermic" effect (figure 2, model CM) can be noted on the DTA curve of the CM sample (see figure 2, which is accompanied by a weight loss), which can be explained by the thermal decomposition of the ammonium form of the zeolite formed as a result of ion exchange of the compensating calcium ions with ammonium ions during the impregnation of the zeolite solution of ammonium para-molybdate. On the DTA curve of ammonium para-molybdate, according to (figure 1a), "exoeffect" is not observed, only "endoeffects" at 205, 240, 340 and 795 °C were noted. In our case, the "exothermic" effect of the transition of the ammonium form of the zeolite to

hydrogen does not appear to be due to the fact that during the preliminary application of nickel nitrate followed by calcination (figure 2a), the nickel cations are firmly fixed in the zeolite cavities, and the ion-exchange of Ca^{2+} on NH_4^+ does not occur. The absence of "endoeffects", specific for the thermal decomposition of ammonium para-molybdate, indicates a deep chemical interaction already during impregnation. Smooth weight loss in the temperature range 100-500 °C without pronounced thermal effects is due to the gradual removal of water. Ammonium ions are displaced from ammonium para-molybdate by a stronger base - calcium hydroxide and removed to the drying process of the sample. Due to the fact that the thermal decomposition of the formed calcium molybdate occurs at a temperature of 1000-1100 °C, it does not appear in the investigated range on the DTA curve.

Electronic diffusion reflection spectra (EDS) of molybdenum - nickel and nickel - molybdenum catalysts on a thermoregenerated zeolite are shown in figure 3 and 4.

Spectra of catalysts were taken in the 50-5cm-1 region on a Hitachi-330 spectrophotometer with a diffusion reflection attachment. It follows from figure 3 and 4 when applying an aqueous solution of nickel and molybdenum salts to CaA zeolite, complex processes occur on its surface that promote the formation of various compounds: CaMoO_4 , NiMoO_4 , and other oxygen compounds of nickel and molybdenum. Calcium molybdate clearly appears in the roentgenograms of the calcined catalyst and can overlap the baseline with $d = 3.08\text{\AA}$ from the crystalline nickel molybdate. However, the absence of narrow lines with $d = 2.73$ and 2.06\AA on X-ray diffraction patterns indicates a high dispersion of the nickel-molybdate structures formed. Nickel-molybdate associates appear as broad bands from Ni^{2+} with maxima at 12.9; 20.0; 23.2; 26.6 cm^{-1} . The highly dispersed phase

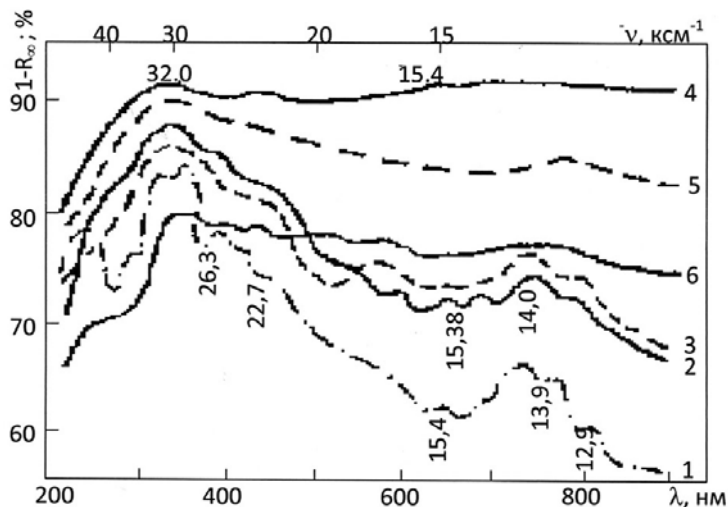


Figure 3 – Electronic spectra of diffuse reflection of nickel-molybdenum catalyst, reduced at 300 °C - (1), 320 °C - (2,3), 360 °C - (4-6) and reoxidized at 25 °C - (3,5) and 360 °C - (6)

of nickel oxide was identified by the pronounced band 13.9 cm^{-1} and a number of diffuse bands at 15.4 ; 21.8 ; 23.2 ; 25.0 cm^{-1} . In a large region at 26.3 and 27.7 ks^{-1} , Mo^{5+} ions are also absorbed, whose presence is confirmed by the decrease of these bands after oxidation of the latter with hydrogen peroxide to Mo^{6+} . Mo^{6+} ions appear in the spectra with a broad absorption band with a maximum of $29.4 \pm 30.7 \text{ ks}^{-1}$ and a shoulder of about 41.7 ks^{-1} . Its high intensity and some shift to the low-frequency region indicate the predominance of structures of the $\text{Mo}^{6+}_{\text{Td}} - \text{O} - \text{Mo}^{6+}_{\text{oh}}$ type, which determine the presence of Brønsted acid sites with $\text{pKa} < -3$ on the surface of the catalyst.

The ESD of the nickel-molybdenum catalyst on the thermoregenerated zeolite is given in figure 4. It follows from the picture that in the catalyst, as in the previous one, CaMoO_4 , NiMoO_4 and other compounds are present. But, the intensity and quantity of CaMoO_4 formed is lower than when nickel is applied to calcined molybdenum-zeolite.

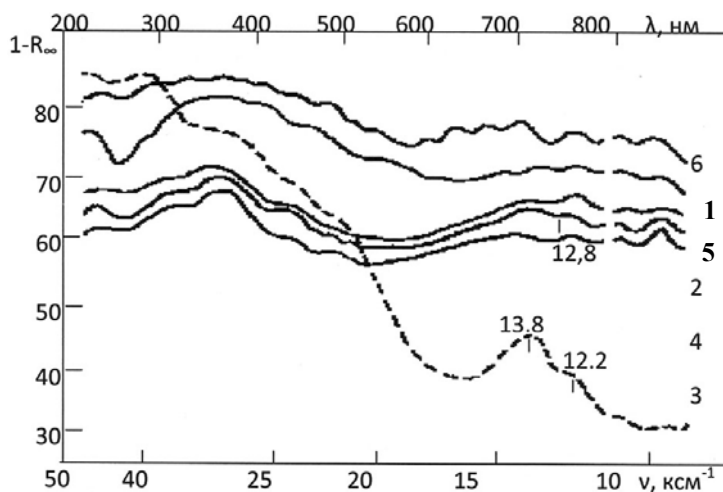


Figure 4 – EDS of catalysts on a thermoregenerated (1-2) and activated by 0.1% HCl zeolite (3-6). Air-dry (1.3), calcined 823 K (2,4-6). The ratio of $\text{NiO} : \text{MoO}_3 = 1 : 1 - (1-4)$

The appearance of new absorption bands in the spectrum of about 12.8 and 12.8 ksm^{-1} is associated with the formation of fragments of nickel-molybdate structures in dried samples when ammonium para-molybdate is applied to calcined nickel-zeolite systems. After calcination, the spectrum consists of an extended absorption band with a maximum of 12.9 ksm^{-1} , moderate bands at 20.0 ; 23.8 ksm^{-1} and an intense wide band of Mo^{6+} ions occupying the entire UV region, which is typical for molybdate-nickel. That is, acid activation and prefixing of nickel structures on the zeolite contribute to the formation of nickel-molybdenum associates. To study the x-ray composition of the nickel-molybdenum catalyst on the thermoregenerated and activated zeolite, the following samples were prepared with the ratio $\text{NiO} : \text{MoO}_3$ 1 : 1 (No. 1), 1 : 2 (No. 2) and 2 : 1

(No. 3). X-ray patterns of the samples are shown in figure. 5. It can be seen from the figure that almost all lines characteristic of CaA zeolite are present in all the samples. Thus, in sample No. 1, CaA exhibits an average degree of crystallinity, which is expressed in the expansion of the lines of 0.338; 0.327 nm.

Figure 5 show that in sample No. 2 enriched with molybdenum oxide, the content of CaMoO_4 and nickel oxide decreases and the degree of crystallization of the zeolite is lower than in sample No. 1. In catalyst No. 3 with an excess of nickel oxide, the crystallinity of the zeolite structure is sharply reduced, this is manifested by a decrease in the intensity of the diffraction lines and their considerable expansion. The amount of phase and the degree of crystallinity of CaMoO_4 are noticeably reduced. In general, the most intense lines appear in the roentgenogram of crystalline calcium molybdate: 4.71; 3.07; 3.09; 2.87; 2.61; 2.25; 1.92; 1,864; 1.628; 1.585; 1.563 Å.

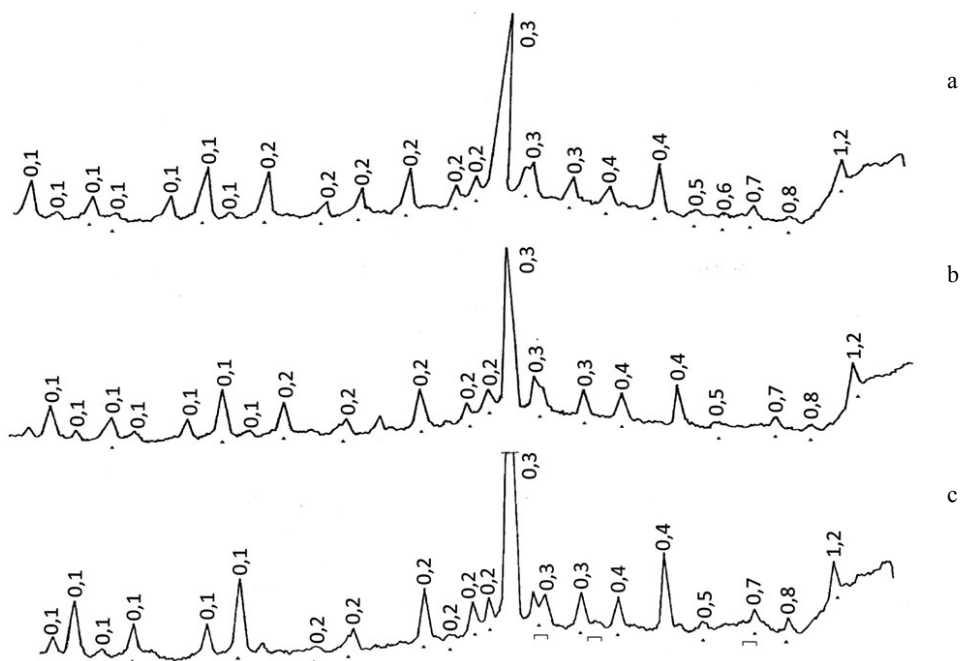


Figure 5 – Radiographs: a) Catalyst (No.1) - NiO: MoO₃ 1: 1;
b) catalyst (No. 2) - NiO: MoO₃ 1: 2; c) Catalyst (No.3) - NiO: MoO₃ 2: 1

The presence of nickel molybdate, found earlier by ESR, can not be determined by X-ray diffraction, in view of its high dispersion and superposition of reflexes. However, molybdate of nickel is more or less present in all samples. The spinel structure of nickel aluminate was not found in the samples studied. According to the EDS, calcium molybdate exhibits acidic properties, so in the catalytic system it can serve as an isomerizing component. In Figure 5. X-ray diffraction patterns of molybdate nickel deposited on a thermoregenerated and activated zeo-

lite are given. The catalyst was prepared by depositing NiMoO_4 on CaA, grinding the system to a powdered state (100-120 mesh), followed by transfer to a paste-like mass, its shaping into extrudates, drying and calcination. It follows from the X-ray diffraction pattern that the finished catalyst consists exclusively of NiMoO_4 and a thermoregenerated CaA zeolite. The results of the EDS and the thermograms of the catalyst showed no interaction of NiMoO_4 with CaA in this system. Elimination of the interaction of the catalyst components - NiMoO_4 and CaA - shows their inherent high catalytic properties in redox and acid-base catalysis.

Conclusion. It was found that nickel molybdate has simultaneously hydrogenating, isomerizing, cleaving, hydrodesulfurizing, hydrodenitrogenating and other properties. The catalyst prepared by deposition of NiMoO_4 on zinc aluminate showed high results in the hydrogenation and isomerization processes. It was found that the NiMoO_4 catalyst on ZnAl_2O_4 is polyfunctional. At the same time, deep hydrogenation, isomerization, dehydrocyclization, cleavage and other reactions take place. A catalyst NiMoO_4 on BaAl_2O_4 manifests in these processes a greater degree of basic properties than acidic ones. Therefore, on this catalyst, deep hydrogenation reactions of hydrocarbons and, in particular, organo-nitrogen compounds of basic character, mainly take place.

Thus, structural studies of the spent CaA zeolite with salts of the active phase of nickel and molybdenum deposited under different thermal conditions have shown that it can be used as a solid carrier for the production of nickel-molybdenum catalysts with additives (promoters). In this case, the catalytic activity of the zeolite can be controlled by selecting it within the pore volume and composition.

REFERENCES

- [1] Kadyrov I. Development of technologies for the preparation of polyfunctional catalysts for hydrogenation and hydromethylation of aromatic compounds of petroleum and petroleum products: Abstract of the dissertation. doc. tech. sien. Tashkent: AS RUZ IONH, 1999. 32 p.
- [2] Ataullov Sh.N., Kadyrov I. Development of a catalyst for destructive hydrotreatment of deasphaltizate into a mixture of basic motor fuels // Uzbek Journal of Oil and Gas. 2004. N 1. P. 36-39.
- [3] Kadyrov I.K., Salimov Z.S., Molodozhenyuk T.B., Manapova R.A., Bekturdiyev G.M., Ataullov Sh.N. Investigation of the processes occurring during the application of molybdenum and nickel to the regenerated zeolite // Processes of petrochemistry and oil refining. 2002. N 2(9). P. 72-75. (Russian).

Резюме

*Ш. Н. Атауллаев, С. Ф. Фозилов,
Б. А. Мавланов, В. Н. Ахмедов, А. У. Очиллов*

**НИКЕЛЬ ЖӘНЕ МОЛИБДЕН ҚОСЫЛЫСТАРЫМЕН БЕЛСЕНДІРІЛІП
ТЕРМОРЕГЕНЕРАЦИЯЛАНҒАН СаА-ТҮРІНДЕГІ ЦЕОЛИТТІ ЗЕРТТЕУ
ЖӘНЕ ҚОЛДАНЫЛУЫ**

Белсенді никель және молибден қосылыстарын пайдалана отырып СаА-цеолитін терморегенерациялау қарастырылады. Осы құрамдас катализаторлардың қыздыруға әсері зерттелінеді.

Түйін сөздер: катализатор, терморегенерация, адсорбент, цеолит, қолдану, араластыру, термиялық талдау, қыздыру, хемосорбция.

Резюме

*Ш. Н. Атауллаев, С. Ф. Фозилов,
Б. А. Мавланов, В. Н. Ахмедов, А. У. Очиллов*

**ИССЛЕДОВАНИЕ ПРИМЕНЕНИЯ
АКТИВНЫХ ФАЗ НИКЕЛЯ И МОЛИБДЕНА
НА ТЕРМОРЕГЕНЕРИРОВАННОМ ЦЕОЛИТЕ СаА**

В этой работе был проведен процесс активных фаз соединений никеля и молибдена на терморегенерированном цеолите СаА и изучены полученные на их основе каталитические системы

Ключевые слова: катализатор, терморегенерация, адсорбент, цеолит, использование, термический анализ, хемосорбция.

ZH. S. AKHMETKARIMOVA¹, Z. M. MULDAKHMETOV¹,
O. A. NURKENOV¹, A. T. ORDABAEVA¹,
M. I. BAIKENOV², D. S. ISABEKOVA²

¹Institute of organic synthesis and coal chemistry of the Republic of Kazakhstan,

²Karaganda state technical university, Republic of Kazakhstan

INFLUENCE OF THE COMPOSITION OF CATALYST SUPPORTED BY ZEOLITE IN THE HYDROGENATION OF FUEL OIL

Abstract. Hydrocarbon raw material consists of condensed aromatic hydrocarbons and other high-molecular compounds, is a complex mixture of organic and mineral substances. The results of the hydrogenation of heavy hydrocarbon feedstocks - fuel oil fraction. In the process of hydrogenation of the fuel oil fraction, in the presence of a zeolite carrier impregnated with highly disperse iron-containing additives, it can be stated that the synthesized catalyst exhibits high activity in hydrogenation processes, hydro destruction of the object of investigation. Determined amount of gas and coke fraction. The amount of gas + fraction is taken as the depth of decomposition. With an increase in the activity of the zeolite more energy intensive coke formation of condensed mechanism increases faster than the polymerization-redistribution mechanism.

Key words: hydrogenation, fraction of oil, temperature, hydrogen pressure, catalyst.

Introduction. The study of the theory and practice of the heavy hydrocarbon feedstock hydrogenation (HFH) in the Common wealth of Independent States (the CIS) and other countries shows that the main reactions of hydrogenation processes which comprise HFH are hydrogenation and dehydrogenation. Analysis showed that the nature of these processes is that they involve movable equilibrium position is determined by factors such as pressure and hydrogen temperature [1-4].

At present, despite the ever-increasing volumes of oil production and refining, not only in the Republic of Kazakhstan, but all over the world, large-scale, intensive research aimed at more efficient use of high molecular weight hydrocarbon feedstock [5].

It should be noted that today in many countries of the world continue to research and pilot projects to improve and improve the performance of the individual stages processes hydrogenation processing HFH and liquefaction products that can significantly improve the efficiency of the method as a whole.

Transformations occurring during the destructive hydrogenation of complex organic substances, which are representatives of oil, fuel oil, coal, etc., are best shown in the individual hydrocarbon compounds.

Previously, the authors synthesized composite catalysts based on Group VIII metal compounds (Fe, Ni, Co) deposited on zeolites (Fe₂O₃/CaA (Fe₂O₃/ZSM),

NiO/CaA (NiO/ZSM), their activity in the hydrogenation of model compounds (anthracene), a number of active catalysts [6].

In order to continue research conducted to study the influence of a catalyst system based on zeolites and compounds of iron and cobalt hydrogenation process heavy hydrocarbon feedstock, particularly heavy fuel oil fraction.

Fuel oil is a liquid hydrocarbon product of dark brown color. A mixture of heavy distillation residues of gasoline, kerosene and gas oil (boiling at temperatures below 350-360⁰C) of oil products or its recycling [7].

EXPERIMENTAL PART

Experiments of hydrogenation fuel oil fraction was carried out in a high pressure autoclave «CJF-0,05» of heat-resistant stainless steel with a capacity 0.05 L. Pre-mixed starting components were placed into the reactor was sealed, purged with hydrogen and the hydrogen was pumped to 4.0 MPa, heated to 400⁰C at a heating rate of 10⁰C per minute. Process duration was 60 minutes after reaching the operating temperature of the autoclave. After the end of the experiment, the reactor was cooled to room temperature the composition of the reaction mixture was determined by chromatography-mass spectrometric (CMS) and gas-liquid (GLC) analysis.

By varying the conditions can be controlled with progress of the hydrogenation process of obtaining target products. Composition of fuel oil fraction identified during the experiment (table 1).

GLC analysis of the initial fraction fuel oil and products of hydrogenation was conducted on a chromatograph "4000 Krystallux M" with PID detector column ZB-5 30 m x 0.53 mm x 1.50 μ m. with the programming of the temperature of the thermostat 60-250⁰C at a temperature rise rate of 6 ⁰C/min. GLC analysis of gaseous products was carried out on a chromatograph "Krystallux 4000 M" (Russia) with the detector module 2DTP/PFID, on a column of CaA 1 -3 m, d-3 mm for constant gases and column Porapak R 1- 3 m, d-3 mm for hydrocarbon gases. GLC analysis of the liquid components was carried out on a chromatograph "Krystallux 4000 M" with a PID detector on a column DB-5 ms 30 mm x 0.250 mm x 0.50 μ m. Data processing was provided by the program "NetChrom v. 2.1" (table 1 and figure 1).

The premixed starting components were placed in a reactor, sealed, flushed with hydrogen, and hydrogen overpressure. The onset of the reaction was the time when the autoclave reached operating temperature. The heating rate of the autoclave was 10⁰C per minute. After the experiment, the reactor was cooled to room temperature the composition of the reaction products was determined by GLC analysis (table 2 and figure 2).

Table 1 – Composition of the fuel oil

#	Component	Time, min	Fraction, %
1	i-octane	4,86	1,40
2	Octane	6,41	2,03
3	1-octene	7,08	1,59
4	1-nonen	9,79	1,10
5	Nonane	10,07	1,97
6	1-decene	13,17	1,13
7	Decane	13,47	2,15
8	1-undecene	16,67	1,35
9	Undecane	16,96	1,84
10	1,2,4,5-tetramethylbenzene	19,09	1,00
11	1-dodecene	20,09	1,01
12	Dodecane	20,37	2,40
13	1-tridecene	23,37	1,08
14	Tridecane	23,62	2,30
15	1-methylnaphthalene	24,16	1,28
16	1-tetradecene	26,47	0,72
17	Tetradecane	26,70	2,55
18	1-pentadecene	29,40	0,74
19	Pentadecane	29,61	2,59
20	1-hexadecene	32,17	0,83
21	Hexadecane	32,36	2,59
22	1-heptadecene	34,81	0,35
23	Heptadecane	34,97	3,27
24	1-octadecene	37,28	0,45
25	Octadecane	37,45	2,58
26	Nonadecane	39,80	2,87
27	Eikozan	42,05	2,84
28	Aneykosan	44,19	2,60
29	Dokozan	46,21	2,32
30	Tricosan	48,22	2,13
31	Tetracosane	50,36	1,79
32	Pentacosane	52,73	1,31
33	Hexacosane	55,58	0,94
34	Heptakosan	58,97	0,62
35	Octacosan	63,08	0,36
36	Nonacosane	68,11	0,34
37	Triacontan	74,42	0,16

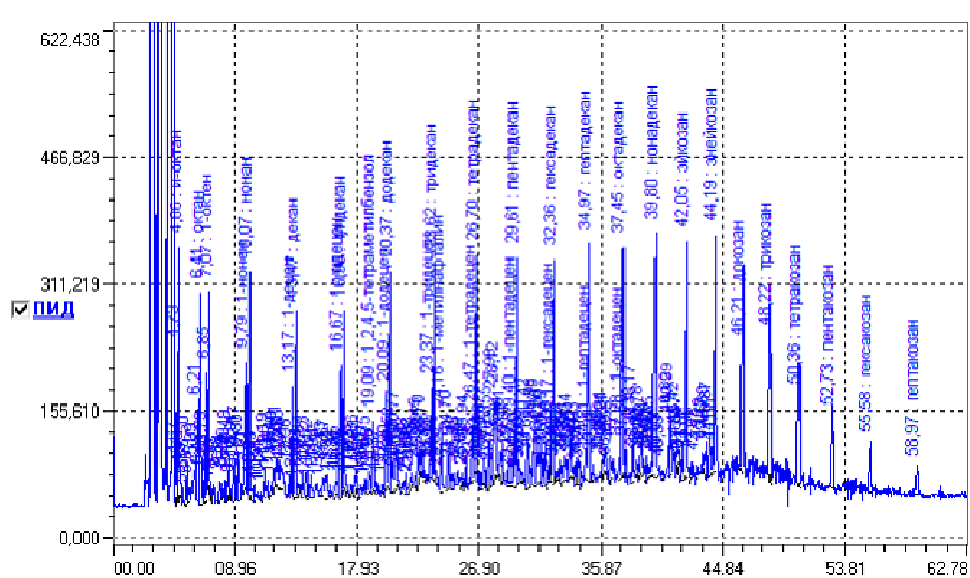


Figure 1 – Chromatogram of the initial fraction of fuel oil

Table 2 – Composition of fuel oil in the hydrogenation at the presence of catalyst Fe_2O_3/CaA

#	Component	Time, min	Fraction, %
1	i-octane	4,87	1,09
2	Octane	6,40	3,892
3	1-octene	7,05	1,8
4	1-nonen	9,73	0,2926
5	Nonane	10,01	2,509
6	1-decene	13,11	0,1329
7	Decane	13,45	1,035
8	1-undecene	16,63	0,6692
9	Undecane	16,90	0,582
10	1,2,4,5-tetramethylbenzene	19,02	0,9559
11	1-dodecene	20,06	0,1592
12	Dodecane	20,31	1,22
13	Tridecene	23,72	0,1928
14	1-tetradecane	26,65	0,7388
15	1-pentadecene	29,56	0,3146
16	Pentadecane	29,74	0,4114
17	1-hexadecene	35,20	0,2119
18	Heptadecane	35,20	0,2119
19	Nonadecane	40,32	0,1373

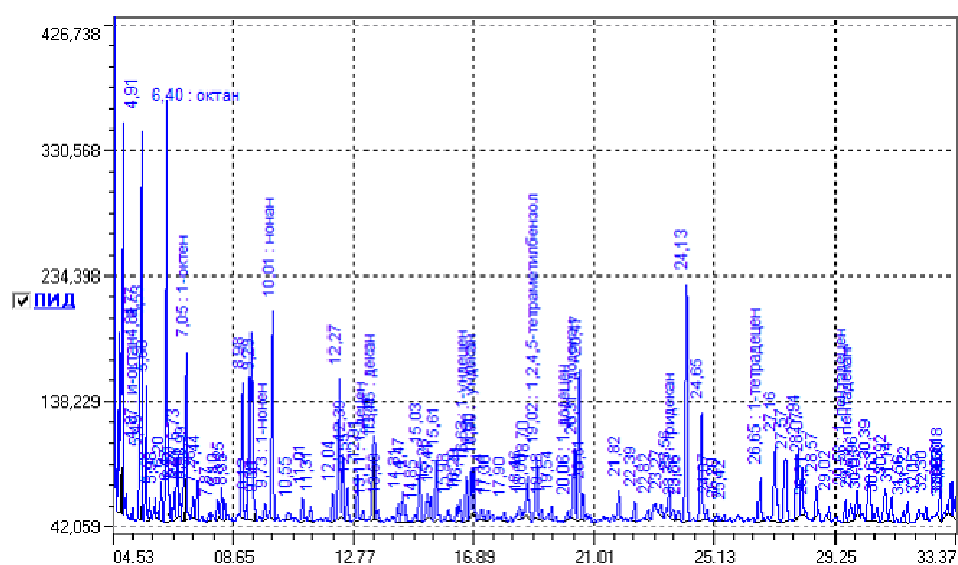


Figure 2 – Chromatogram of fraction in the hydrogenation of fuel oil at presence of catalyst Fe_2O_3/Ca

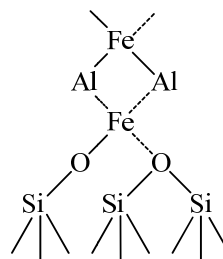
RESULT AND DISCUSSION

Analyzing the chromatogram shown in Figure 2 it was found that there are peaks of saturated hydrocarbon derivatives 12.23%, the amount of iso-derivatives of hydrocarbons was 1.09%. Also tetramethylbenzene is present in an amount of less than 1%.

These data show that at this temperature for all paraffin have stepwise mechanism makes the main contribution to the reaction rate. Relative reaction rate in the range of paraffin in this case changes.

Note that format structures formed by paraffin adsorption on the catalyst surface and decompose sufficiently thermo stable under vacuum at $420^{\circ}C$. At temperatures above $400^{\circ}C$ the main contribution to the rate of catalysis makes stepwise mechanism. This is consistent with the proposed reaction scheme [8], since the thermal decomposition of the surface structures at temperatures above $400^{\circ}C$ should lead to a decrease in the proportion of the associative mechanism and the stepwise transition to a mechanism that is observed the experiments.

We can assume that in the surface complex coordination number of the iron ion is four. In this case, the surface structure of the complex with the iron coordination can be depicted as follows:



In this structure, it is considered that the surface ligands of the iron ion are oxygen, previously associated with a proton carrier and atoms (aluminum silicon). However, this structure may be the dominant, but not the only. It is possible that in the formation of a surface complex, in view of the heterogeneity of the zeolite surface, a certain set of coordination states is realized, the proportion of each of which depends both on the conditions of preliminary dehydration of the carrier and on the amount of the complex. Heterogeneity focal states, apparently increases with increasing temperature and dehydration with increasing concentrations of surface complex; this causes a large number of allowed optical transitions, resulting in a product of almost black color.

Source "cells" size zeolite CaA not more $11,6\text{\AA}$, therefore, should be observed difficulties in penetrating molecules of iron oxide into the inner cavities of the zeolite, especially considering the possibility of adsorption of molecules in the input "cells". Since the nature of the active centers of the zeolite is the same, comparing the results of hydrogenation of fuel oil on iron-containing catalysts on an alumina-silicate substrate allows more clearly to reveal the effects associated with the screening action of the latter.

When Fe_2O_3 converted to aluminosilicate gives less than 1% of the decomposition products, so the depth of hydrogenation was calculated in the weight (%) content of paraffins. Determined amount of gas and coke fraction. For the adopted depth decomposition gas amount + fraction. Reducing the coke yield apparently due to the difficulty of penetration of the molecules of the heavy hydrocarbon feedstock into the inner cavity of the zeolite catalyst Fe_2O_3 . Consequently, with the increase in zeolite activity, the more energy-intensive coke production by the condensed mechanism increases more rapidly than by the redistribution-polymerization mechanism.

Conclusion. Thus, analysis of the data leads to the conclusion that the catalytic oxidation of n-paraffin relative reaction speed depends on recent process mechanism. In the case of stepwise mechanism oxidation rate increases with increasing number of carbon atoms per paraffin molecule. Thus, the reaction rate is limited by the interaction of the hydrocarbon with the surface of the catalyst $\text{Fe}_2\text{O}_3/\text{CaA}$, at which the CH bond in the paraffin molecule.

REFERENCES

- [1] Akhmetkarimova Zh.S. Theory and practice of processing of heavy hydrocarbon raw materials in Central Kazakhstan. Karaganda: Form Plus, 2016. 365 p.
- [2] Muldahmetov Z.M., Ahmetkarimova Zh.S., Meiramov M.G., Ordabaeva A.T., Muldahmetov Zh.K., Baikenov M.I. Calculation of the thermodynamic functions of the light fraction of the primary coal tar resin // Reports of NAS RK. 2015. N 3. P. 80-87.
- [3] Akhmetkarimova Zh.S., Baikenov M.I., MaFengYun. Calculation of the thermodynamic parameters of the primary coal tar fraction // Chemistry of solid fuels. 2016. N 5. P. 3-8.
- [4] Baikenov M.I., Baikenova G.G., Isabaev A.S., Tateyeva A.B., Akhmetkarimova Zh.S., Tusipkhan A., Mataeva A.Zh., Esenbaeva K.K. Influence of New Catalytic Systems on the Hydrogenation of Anthracene // Chemistry of Solid Fuels. 2015. N 3. P. 22-28.
- [5] Muldahmetov Z.M., Akhmetkarimova Zh.S., Meiramov M.G., Ordabaeva A.T., Muldahmetov Zh.K., Baikenov M.I., Dyusekenov A.M. Hydrogenation of anthracene in the Presence of Composite Catalysts // Izvestiya NAS RK. 2017. N 1. P. 33-40.

[6] Ordabaeva A.T., Ahmetkarimova Zh.S., Muldahmetov Z.M., Muldahmetov Zh.Kh., Baikenov M.I., Dyusekenov A.M. Synthesis of binary composite catalysts based on Group VIII metal salts on a zeolite carrier // Chemical Journal of Kazakhstan. 2017. N 2. P. 251-259.

[7] Ordabaeva A.T., Ahmetkarimova Zh.S., Muldahmetov Zh.K., Meiramov M.G. Hydrogenation of anthracene in the presence of a nanocomposite catalyst – Fe_2O_3/KS // Vauch-prak. Conf. with international participation "The Science of the Present and the Future" for students, graduate students and young scientists St. Petersburg, 2017. P. 423-424.

[8] Patent of the Ministry of Justice of the Republic of Kazakhstan No. 1863 for the utility model "Method for producing a composite catalyst based on coal sorbent and iron pentacarbonyl" Meiramov M.G., Fazylov S.D., Ordabaeva A.T., Ahmetkarimova Zh.S., Muldahmetov Z.M. of November 21, 2016.

Резюме

*Ж. С. Ахметкәрімова, З. М. Молдахметов, О. А. Нұркенов,
А. Т. Ордабаева, М. И. Байкенов, Д. С. Исабекова*

МАЗУТ ФРАКЦИЯСЫНЫҢ ГИДРОГЕНИЗАЦИЯ ҮРДІСІНДЕГІ ЦЕОЛИТ НЕГІЗІНДЕ КОМПОЗИТТІ КАТАЛИЗАТОРЛАРДЫҢ ӘСЕРІ

Көмірсутекті шикізат органикалық және минералды заттардың қоспасы болып саналып, конденсирленген ароматикалық көмірсутектерінен және жоғары молекулалық қосылыстардан тұрады. Мақалада ауыр көмірсутегі шикізатының – мазут фракциясының гидрогенизация нәтижелері көрсетілді. Мазут фракциясының цеолит тасымалдағышы қатысында, жоғарыдисперсті темір және кобальт құрамды қосылыстармен импрегнирленген қоспалар қатысындағы гидрогенизация үрдісі нәтижесінде келесі тұжырым жасауға болады, синтезделген катализатор зерттеу нысанының гидрлеу, гидродеструкция үрдістері кезінде жоғары белсенділігін көрсетеді. Газ, фракция мен кокс көлемдері анықталды. Ыдырау тереңдігі ретінде газ+фракциясының қосындысы алынған. Цеолиттің белсенділігінің жоғарлауымен энергоыңғайлы кокс түзілуі қайта бөлу-полимеризациялану механизммен салыстырғанда конденсациялау бойынша тезірек жүреді.

Түйін сөздер: гидрогенизация, мазут фракциясы, температура, сутегі қысымы, катализатор.

Резюме

*Ж. С. Ахметкаримова, З. М. Мулдахметов, О. А. Нуркенов,
А. Т. Ордабаева, М. И. Байкенов, Д. С. Исабекова*

ВЛИЯНИЕ КОМПОЗИТНЫХ КАТАЛИЗАТОРОВ НА ОСНОВЕ ЦЕОЛИТА В ПРОЦЕССЕ ГИДРОГЕНИЗАЦИИ ФРАКЦИИ МАЗУТА

Углеводородное сырье состоит из конденсированных ароматических углеводородов и других высокомолекулярных соединений, является сложной смесью органических и минеральных веществ. В работе представлены результаты гидрогенизации тяжелого углеводородного сырья – фракции мазута. В процессе гидрогенизации фракции мазута, в присутствии цеолитного носителя, импрегнированных высокодисперсными железосодержащими добавками, можно констатировать, что синтезированный катализатор проявляет высокую активность в процессах гидрирования, гидродеструкции объекта исследования. Определялось количество газа, фракции и кокса. За глубину разложения принята сумма газ+фракция. С повышением активности цеолита более энергоемкое образование кокса по конденсированному механизму нарастает быстрее, чем по перераспределительно-полимеризационному механизму.

Ключевые слова: гидрогенизация, фракция мазута, температура, давление водорода, катализатор.

SH. N. ATAULLAYEV, B. A. MAVLANOV, S. F. FOZILOV,
V. N. AKHMEDOV, A. U. OCHILOV, M. M. TILAVOVA*

Bukhara engineering-technological institute, Bukhara

PHYSICAL-CHEMICAL PROPERTIES OF CATALYSTS FOR DESTRUCTIVE HYDROGENIZATION OF OIL DEASPHALTIZATE

Abstract. The physicochemical and catalytic properties of catalysts and their preparation for destructive hydrogenation of asphalt-free oil are found out in the article. Favorable conditions for obtaining effective catalysts of the hydrogenation process were determined. Also, the process of thermal regeneration of the working zeolite and the surface-acid properties of the Ca-zeolite catalyst was studied.

Key words: catalyst, deasphaltizate, destruction, hydrogenization, thermo-regeneration, adsorbent, zeolite, regeneration, sieve, extrudate.

Introduction. It is known that catalysts containing metals of Group VIII of Mendeleev's (Pt, Pd, Co, Ni and etc.) periodic system possess high hydrogenating properties. But their use for hydroprocessing petroleum products with sulfur-, nitrogen-, oxygen- and organometallic impurities is inexpedient, since they are rapidly poisoned. In the hydro processing of residual petroleum products, the depth of their conversion, the quality and quantity of the "light" distillates thus formed depends on the catalytic properties of the using catalysts [1, 2].

It is established that the use of nickel in combination with molybdenum makes it possible to obtain a catalytic system with hydrodehydrogenic and acidic properties, and when this system is converted into a sulphide form, the activity, the functionality of the system in acid catalysis is more increased. Nickel is a molybdenum system because it is the most active catalyst of processes: for hydrogenation, isomerization, dehydrocyclization, hydrodenitrogenation, hydrodesulfuration, it exhibits polyfunctional properties, is stable to the deactivating actions of sulfur-, nitrogen-, oxygen-organic compounds. Treatment of this system with a sulfur organic compound or hydrogen sulphide increases its activity in redox and acid catalysis. In view of the above, the elaboration of polyfunctional catalysts for the destructive hydrogenation of oil deasphaltizate was carried out on the basis of nickel and molybdenum compounds on various refractory acid supports: spent zeolite after thermal regeneration $ZnAl_2O_4$ and $BaAl_2O_4$ [3-6].

Due to their specific surface properties, crystalline aluminosilicates are widely used as a carrier and isomerizing phase in multicomponent catalysts. Depending on the type and concentration of acid sites of zeolites, especially CaA, they are widely used in isomerization, alkylation, polymerization, cracking, hydrocracking processes.

Synthetic zeolites are widely used in various industries. The large-tonnage consumer of zeolite CaA as an adsorbent is the Shurtan gas processing plant. Due to the lack of a local zeolite, it is purchased for foreign currency. At present, a huge amount of environmentally hazardous industrial waste is accumulated in the dumps of the plant - the spent adsorbent CaA, which is subject to regeneration, which can be used for the production of local zeolite. Taking this into account, using modern physicochemical methods of analysis that allow us to study the processes occurring during the processing of the spent zeolite, we have established methods for regenerating the adsorbent in which the zeolite retains its structure and exhibits high surface acidic properties, which makes it possible to use it as a destructive hydrogenation catalyst oildeasphaltizate.

RESULTS AND DISCUSSION

Investigation of the process, thermal recovery of spent zeolite. It is known that the thermal treatment of zeolites allows the removal of impurities, especially of organic nature. The thermograms of spent CaA zeolite obtained from the Shurtan MCC are given in figure 1. As follows from the thermogram, the exoeffect at 200 °C corresponds to the removal of structural water. The pronounced exothermic effect with a maximum at 362 °C refers to the removal of the residual part of organic compounds adsorbed in the purification of natural gas containing sulfur, nitrogen and resinous substances. Weak "Exoeffects" in the region of 500-600 °C are due to the burnout of strongly adsorbed organic substances, which is accompanied by a slight weight loss, and from 700 to 990 °C, zeolite is sintered without losing weight.

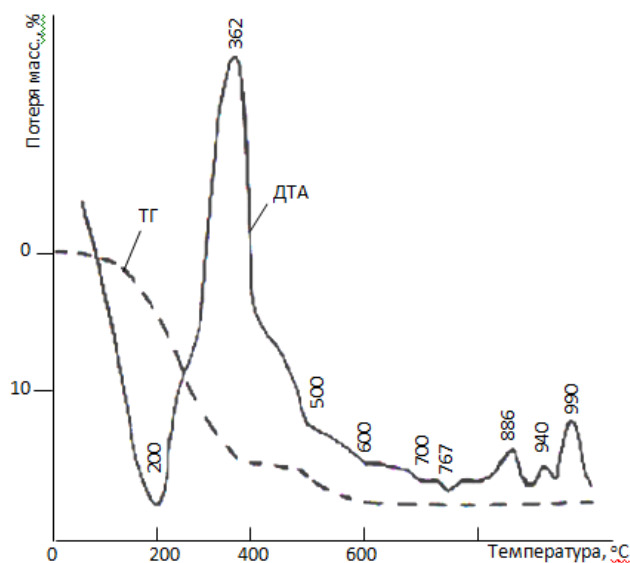


Figure 1 – The thermogram of spent CaA zeolite, obtained from Shurtan MCC

Thus, the temperature ranges for the recovery of the spent CaA zeolite and the limits of the temperature effect on this sorbent were established, and its surface-acid properties were investigated.

In practice, in order to increase the surface acid properties of the zeolite, it is activated by anions of mineral acids. In our case, the thermoregenerated zeolite is activated by an aqueous solution of acids HCl, H₂SO₄ and HNO₃. The activation carried out for 11-12 hours at room temperature. Table 1 shows the results of the study of the change in the surface acid-base properties of the zeolite calcined at 600 °C, depending on the concentration of acid.

Sounding of acid sites by the position of the absorption peak of the indicators was carried out: a) after adsorption on samples without preliminary heat treatment; b) after drying at 200 °C; c) after calcination at 600 °C. The results of the study showed that on hydrated samples phenolphthalein is adsorbed in a colorless acid form, i.e. the main centers with $pK_a \geq 9,3$ are absent. Bromophenolblue - an indicator for weakly acid centers with $pK_a \approx +3,8$ is adsorbed on hydrated samples mainly in two forms. As a result of adsorption on weakly acid and weakly basic centers, ($+3,8 < pK_a < +9$), an absorption band with high extinction is observed in electronic spectra, the maximum of which is about 600-610 nm (the first form), the presence of centers with $pK_a < +3,8$ indicates the appearance of a less intense absorption band at 430 nm (the second form) from bromophenolblue ionized at acid sites. On samples activated with 5% hydrochloric acid, only acid sites with pK_a of less than 3.8 are observed. A similar picture is observed for the indicator benzazolazodiphenilamin $pK_a \leq +1,5$. A study of the surface of the samples dried at 200 °C before the beginning revealed the presence of Brønsted type centers with pK_a about -3. Only the samples treated with 3.0% sulfuric and nitric, as well as 5.0% hydrochloric acid, found stronger Brønsted centers with $pK_a \leq -6$.

The strength and concentration of acid sites is increased by an increase in the pretreatment temperature of the surface to 500 °C. Moreover, in addition to proton ones, Lewis acid sites are also identified on individual samples (table), which disappear at dehydration. It is known that, under equal conditions, the acidity of various types of zeolites increases with an increase in the degree of exchange of metal ions with protons. In the absence of information on the degree of exchange of aluminum and calcium ions, we have attempted to find a correlation between the concentration of acid sites and the concentration of the activating solution containing these ions. From the data of table 1 it can be noted that within each series of samples the maximum concentration of strong acid sites is $-6 < pK_a < -3$, for samples calcined at 600 °C just before probing and $-6 < pK_a < -3$ for samples dried at 200 °C, for activation with a 5.0% solution of hydrochloric acid. At the same time, the concentration of the centers on the samples prepared at 600 °C increases markedly. It is here that aprotic acidic centers are observed, which are particularly pronounced in the case of treatment of sulfuric acid zeolite. As follows from the data in table 1, activation of thermoregenerated zeolite with an aqueous solution of mineral acids enhances its surface-acid properties to a certain

The change of surface of the zeolite calcined at 600 °C depending on the concentration acid and its acid-base properties

Samples and condition	Concentration (mmol/g) of acid-base centers with pKa on the surface of activated solutions and mineral acids with different concentrations							Site type
	-8	-6,3	-5,6	-3,3	+1,5	+3,8	+9,3	
1. Spent (unregenerated)	-	-	-	0,05	0,13	0,38	-	B + L
2. Thermoregenerated (without activation)	-	0,08	0,09	0,24	0,34	0,47	-	B + L
3. Activated by acid at 20-25°C, during 11-12 hour	-	0,20	0,21	0,22	0,32	0,40	-	B
0,1% HCl	0,04	6,07	0,12	0,18	0,27	0,32	-	B
4. 1,0% HCl	0,03	0,24	0,24	0,32	0,37	0,39	-	B
5. 2,5% HCl	-	-	0,03	0,08	0,30	0,30	-	B
6. 5,0% HCl	-	0,8	0,20	0,20	0,21	0,30	-	B
7. 3,0% HNO ₃	-	0,04	0,07	0,13	0,15	0,21	-	B + L
8. 3,0% H ₂ SO ₄	-	-	-	-	-	-	-	-

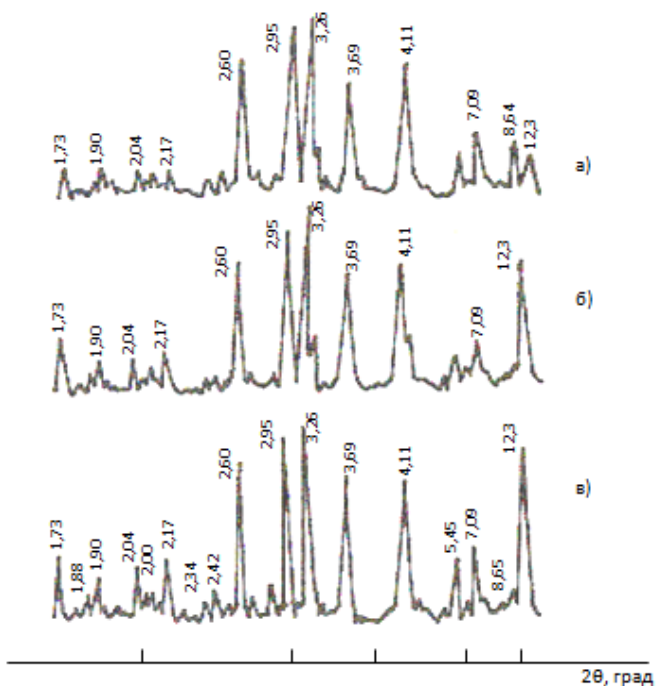


Figure 2 – X-ray patterns:
 a) initial zeolite; b) a thermoregenerated zeolite;
 c) a zeolite activated with hydrochloric acid

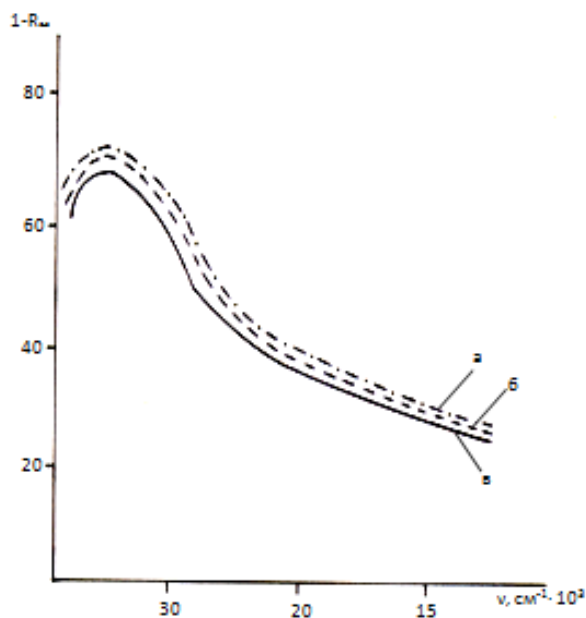


Figure 3 – ESD of zeolite CaA: a) thermoregenerated; b) activated by 1.0; 2.5; 5% HCl solution and dried at 200 °C; c) calcined at 600 °C

extent, which increase with an increase in the concentration of the activating acid to 2.5%, and then decrease. The activating action of solutions of sulfuric and nitric acid is much lower than that of hydrochloric acid. Taking into account that the isomerization reactions proceed mainly on acidic centers with $pK_a = -3,3 \div 3,8$ mmol/g, an aqueous solution of hydrochloric acid with a concentration of 0,1% was used as an activating additive. In the process of processing the thermoregenerated zeolite with this solution, a whole set of acid sites of various strength and concentration appears on the surface of the adsorbent. In the regenerated zeolite, its structure does not change, as evidenced by the X-ray diffraction pattern (figure 2, a, b, c) and ESTD (figure 3, a, b, c).

Conclusion. Thus, when studying the process of thermoregeneration of spent zeolite, the temperature ranges for the recovery of spent CaA zeolite and the limits of the temperature effect on this sorbent were established, the effect of mineral acid anions on the surface-acid properties of CaA zeolite was studied. Based on the data obtained, methods for the preparation of catalysts for the destructive hydrogenation of oildeasphaltizate have been developed and their physicochemical and catalytic properties have been studied.

REFERENCES

[1] Kadyrov I. Development of technologies for the preparation of polyfunctional catalysts for hydrogenation and hydromerization of aromatic compounds of petroleum and petroleum products: Abstract of the dissertation. doct. tech. sci. Tashkent: AS RUZ IONH, 1999. 32 p.

[2] Kadyrov I., Bekturdiyev G.M., Molodozhenyuk T.B., Salimov Z.S., Saidakhmedov Sh.M., Sharafutdinov U.T. Physicochemical properties of spent zeolite and catalysts based on it // Chemistry and technology of fuels and oils. 1999. N 3. P. 34-36. (Russian).

[3] Kadyrov I.K., Salimov Z.S., Molodozhenyuk T.B., Manapova R.A., Bekturdiyev G.M., Ataulloyev Sh.N. Investigation of the processes occurring during the application of molybdenum and nickel to the regenerated zeolite // Processes of petrochemistry and oil refining. 2002. N 2(9). P. 72-75. (Russian).

[4] Ataulloyev Sh.N. Destructive hydrogenation of oildeasphaltizate // The collection of abstracts of the republican scientific-practical conference "Actual problems of chemical processing of mineral raw materials in Uzbekistan. Tashkent, 2003. P. 16-17. (Russian).

[5] Ataulloyev Sh.N., Kadyrov I. Development of a catalyst for destructive hydrotreatment of deasphaltizate into a mixture of basic motor fuels // Uzbek Journal of Oil and Gas. 2004. N 1. P. 36-39.

[6] Ataulloyev Sh.N. Problems of processing deasphalting during the selection of catalysts // "Problems of intensification of technological processes and energy-saving technologies in the conditions of the national economy" Collection of articles of the international scientific-practical conference. Bukhoro, November 20-22, 2003. Vol. 2. – P. 220-221.

Резюме

*Ш. Н. Атауллаев, Б. А. Мавланов, С. Ф. Фозилов,
В. Н. Ахмедов, А. У. Очилов, М. М. Тилавова*

МУНАЙ ДЕАСФАЛЬТИЗАТЫН ГИДРОГЕНИЗАЦИЯЛАУҒА АРНАЛҒАН КАТАЛИЗАТОРЛАРДЫҢ ФИЗИКО-ХИМИЯЛЫҚ ҚАСИЕТТЕРІ

Мұнай деасфальтизатын гидрогенизациялауға арналған катализаторларды алу және олардың физико-химиялық қасиеттері зерттелген. СаА-түріндегі цеолитті қайтақ қалпына келтіру үшін терморегенерациялау және цеолит бетіндегі қышқылдық орталықтар қарастырылған.

Түйін сөздер: катализатор, деасфальтизат, деструкция, гидрогенизациялау, терморегенерациялау, адсорбент, цеолит, қыздыру.

Резюме

*Ш. Н. Атауллаев, Б. А. Мавланов, С. Ф. Фозилов,
В. Н. Ахмедов, А. У. Очилов, М. М. Тилавова*

ФИЗИКО-ХИМИЧЕСКИЕ СВОЙСТВА КАТАЛИЗАТОРОВ ДЛЯ ГИДРОГЕНИЗАЦИИ ДЕАСФАЛЬТИЗАТА НЕФТИ

В работе приведены способы получения катализаторов для деструктивной гидрогенизации деасфальтизата нефти и изучены их физико-химические и каталитические свойства. Также исследованы процесс терморегенерации отработанного цеолита и поверхностно-кислотные свойства катализаторов на основе цеолита СаА

Ключевые слова: катализатор, деасфальтизат, деструкция, гидрогенизация, терморегенерация, адсорбент, цеолит, прокалка.

B. K. KASENOV¹, SH. B. KASENOVA¹, ZH. I. SAGYNTAEVA¹,
M. O. TURTUBAEVA², E. E. KYANYSHBEKOV¹

¹Zh. Abishev Chemical-metallurgy institute, Karaganda, Republic of Kazakhstan,

²S. Toraihyrov Pavlodar State University, Pavlodar, Republic of Kazakhstan

SYNTHESIS OF NEW NANOSIZED (NANOCLUSTER) COBALT (NICKELITE)-CUPRATE-MANGANITES

Abstract. Synthesis of cobalt (nickelite)-cuprate-manganites of the composition LaMgCoCuMnO₆ and LaMgNiCuMnO₆ were carried out by solid-phase interaction of stoichiometric amounts of La₂O₃ (extra-pure grade), NiO, CoO, CuO, Mn₂O₃ and MgCO₃ (analytical grade) in the interval 800-1200 °C for 20 hours. To obtain equilibrium phases at low temperatures, low-temperature annealing was carried out at 400 °C for 10 hours. On a vibrating mill of "Retsch" company (Germany) of the "MM301" brand, polycrystalline samples of new compounds were ground to nanoscale (nanoclusters) particles. The dimensions of the nanoclusters are determined using the "JSPM-5400" Scanning Probe Microscope "JEOL" electron microscope. X-ray phase analysis of new nanosamples were carried out on a DRON-2.0 unit. The analytical method of X-ray indications is established that the synthesized compounds are crystallize in cubic syngony with the following lattice parameters: LaMgCoCuMnO₆ – a=14,12±0,02Å; V^o=2814,87±0,06Å³; Z=4; V^o_{el.cell}=703,72±0,02Å³; ρ_{X-ray}=4,19g/cm³; LaMgNiCuMnO₆ – a=14,38±0,02Å; V^o=2973,56±0,06Å³; Z=4; V^o_{el.cell}=743,39±0,02Å³; ρ_{X-ray}=4,22g/cm³.

Keywords: synthesis, cobalt-cuprate-manganite, nickelite-cuprate-manganite, lanthanum, alkali, alkaline earth metals, X-ray, nanoscale, nanoclusters.

The end of the XX century and the beginning of the XXI century were marked by outstanding discoveries in the field of inorganic materials science: the discovery of superconductivity in cuprates, giant (colossal) magnetoresistance in manganites of rare-earth elements partially replaced by alkaline-earth metal oxides [1, 2]. Along with these discoveries, the effect of a giant value of the dielectric constant in nickelite La_{15/8}Sr_{1/8}NiO₄, has recently been revealed, which opens up good prospects for technological solutions in electronics [3].

In connection with the above, in order to obtain new promising compounds, the results of synthesis of nanoscale (nanocluster) cobalt-cuprate-manganite and nickelite-cuprate-manganite of lanthanum and magnesium LaMgCoCuMnO₆ and LaMgNiCuMnO₆ are given in this paper. Earlier, we studied cobalt-manganites, nickelite-manganites and cuprate-manganites of rare-earth, alkaline and alkaline-earth metals [4-10].

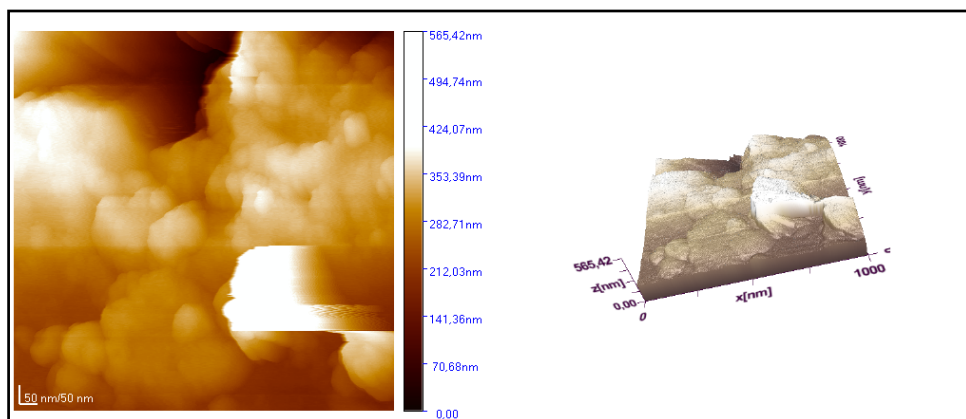
The synthesis of the above LaMgCoCuMnO₆ and LaMgNiCuMnO₆ was carried out by solid-phase interaction of the reagents in the range of 800-1200 °C according to the reactions:



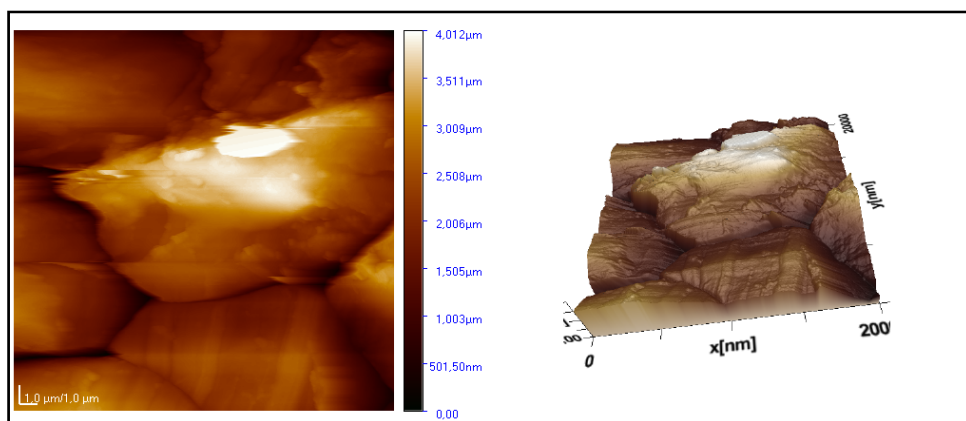
The purity of the starting materials: La_2O_3 – “extra-pure grade” and the rest-qualification “analytical grade”. The annealing time at 800-1200 ° C is 20 hours. Before each increase through 200 ° C (800 ° C, 1000 ° C, 1200 ° C) the mixtures were cooled and thoroughly mixed. For stable at low temperature modifications annealing was carried out at 400 ° C for 10 hours.

Nano-sized particles of synthesized new compounds were obtained by grinding them on a vibratory mill of the company "Retsch" (Germany) of the brand "MM301". Speed from 3 to 30 Hz (180-1800 vibrations per minute). The grinding time is 40-60 minutes.

The sizes of the crushed particles were established on an electronic microscope JSPM-5400 Scanning Probe Microscope "JEOL" (Japan). The electron microscopies of the investigated compounds are shown below (figure 1).



a)



b)

Figure 1 – Electron microscopy of LaMgCoCuMnO_6 (a) and LaMgNiCuMnO_6 (b)

Table 1 – Indication of X-ray patterns of powders of nanoscale (nanocluster) cobalt-cuprate-manganite and nickelite-cuprate-manganite

I/I_0	$d, \text{Å}$	$10^4/d^2_{\text{exp.}}$	hkl	$10^4/d^2_{\text{calc.}}$
LaMgCoCuMnO₆				
18	3,920	650,8	422	651,0
6	2,944	1154	599	1166
100	2,763	1310	444	1302
19	2,503	1596	731	1600
13	2,464	1647	650	1654
4	2,340	1826	733	1817
22	2,251	1973	830	1980
14	2,120	2225	910	2223
29	1,952	2624	940	2630
5	1,745	3284	11.0.0	3281
4	1,695	3481	880	3471
34	1,592	3946	11.5.0	3959
9	1,494	4480	10.8.1	4474
6	1,462	4678	13.2.0	4691
12	1,377	5274	13.5.1	5288
6	1,300	5917	13.7.0	5911
13	1,232	6588	15.3.3	6589
7	1,224	6675	14.5.5	6671
LaMgNiCuMnO₆				
3	4,82	430,4	410	431,0
16	3,89	660,8	510	658,3
3	2,952	1147	630	1139
100	2,756	1317	640	1317
12	2,426	1699	733	1696
8	2,314	1868	750	1874
19	2,249	1977	752	1974
26	2,098	2272	930	2279
29	1,945	2643	10.2.2	2633
5	1,867	2869	10.3.2	2861
8	1,743	3292	11.3.0	3291
3	1,700	3460	11.4.0	3469
13	1,484	4541	11.7.3	4532
15	1,374	5297	10.10.3	5291
4	1,296	5954	15.3.1	5950
7	1,263	6269	14.6.4	6279
13	1,230	6610	16.2.1	6608
7	1,212	6808	16.3.2	6811

X-ray diffraction study of nanophases was carried out on a DRON 2.0. The intensity of the diffraction maxima was estimated from a one-hundred-point scale. The X-ray diffraction patterns of the compounds were determined by the analytical method [11]. Below in table 1 shows the results of the X-ray diffraction.

Based on the indication of the X-ray patterns of the new nanoscale (nanocluster) compounds established that they crystallize in a cubic system with the following lattice parameters: LaMgCoCuMnO_6 – $a=14,12\pm 0,02\text{Å}$; $V^o=2814,87\pm 0,06\text{Å}^3$; $Z=4$; $V^o_{\text{el.cell}}=703,72\pm 0,02\text{Å}^3$; $\rho_{\text{X-ray}}=4,19\text{ g/cm}^3$; LaMgNiCuMnO_6 – $a=14,38\pm 0,02\text{Å}$; $V^o=2973,56\pm 0,06\text{Å}^3$; $Z=4$; $V^o_{\text{el.cell}}=743,39\pm 0,02\text{Å}^3$; $\rho_{\text{X-ray}}=4,22\text{ g/cm}^3$. Satisfactory agreement of $10^4/d^2_{\text{exp}}$ and $10^4/d^2_{\text{calc}}$ shows the correction of the results of the indication.

Thus, nanoscale (nanocluster) cobalt-cuprate-manganite LaMgCoCuMnO_6 and nickelite-cuprate-manganite LaMgNiCuMnO_6 were synthesized for the first time. The type of their syngony and parameters of the lattices were determined.

The work was carried out in accordance with the agreement concluded between the Ministry of Education and Science of the Republic of Kazakhstan and Zh.Abishev Chemical-Metallurgical Institute under the grant of (IRN: AP05131317, AP05131333).

REFERENCES

- [1] Tret'yakov Yu.D., Brylev O.A. Novye pokoleniya neorganicheskikh materialov // Zhurnal RHO im. D. I. Mendeleeva. 2000. Vol. 45, N 4. P. 10-16.
- [2] Tret'yakov Yu.D., Gudilin E.A. Himicheskie printsipy polucheniya metalloksidnykh sverhprovodnikov // Uspehi himii. 2000. Vol. 69, N 1. P. 3-39.
- [3] Erin Yu. Nayideno veshstvo s gigantскими значениями диэлектрической проницаемости // Химия и химик. 2009. Vol. 45, N 4. P. 10-16.
- [4] Kasenova Sh.B., Kasenov B.K., Sagintaeva Zh.I. i dr. Teploemkost' i termodinamicheskie funktsii nanostrukturirovannykh chastits $\text{LaM}_2^{\text{II}}\text{CuMnO}_6$ (M^{II} – Mg, Ca) v intervale 298,15-673 K // Zhurn. fiz. himii. RAN. 2014. Vol. 88, N 5. P. 836-840.
- [5] Kasenova Sh.B., Kasenov B.K., Sagintaeva Zh.I. and etc. Smagulova Heat Capacity and Thermodynamic Functions of New Nanostructured Cuprate-Manganite $\text{NdCa}_2\text{CuMnO}_6$ // Russian Journal of Physical Chemistry A. 2014. Vol. 88, N 10. P. 1802-1805.
- [6] Kasenova Sh.B., Kasenov B.K., Sagintaeva Zh.I. and etc. Synthesis and X-ray diffraction study of nanostructured particles of cuprate-manganites $\text{LaM}_2^{\text{II}}\text{CuMnO}_6$ (M^{II} – Mg, Ca, Sr, Ba) // Russian Journal of Inorganic Chemistry A. 2014. Vol. 59, N 9. P. 1010-1014.
- [7] Kasenov B.K., Turtubaeva M.O., Amerkhanova Sh.K. and etc. Heat Capacity and Thermodynamic Functions of New Cobalt Manganites $\text{LaM}^{\text{II}}_2\text{CoMnO}_6$ (M^{II} – Mg, Ca, Sr, Ba) in the Temperature Interval of 298,15-673 K // Russian Journal of Physical Chemistry A. 2015. Vol. 89, N 6. P. 941-946.
- [8] Kasenov B.K., Kasenova Sh.B., Sagintaeva Zh.I. and etc. Thermodynamic Properties of Zincate Manganites of $\text{LaM}^{\text{II}}_2\text{ZnMnO}_6$ (M^{II} – Mg, Ca, Sr, Ba) Composition // Russian Journal of Physical Chemistry A. 2016. Vol. 90, N 4. P. 739-743.
- [9] Kasenov B.K., Turtubaeva M.O., Amerkhanova Sh.K. and etc. Heat Capacity and Thermodynamic Functions of the New Cobaltic Manganites $\text{NdM}^{\text{II}}_2\text{CoMnO}_6$ (M^{II} – Mg, Ca, Sr, Ba) Within the Temperature Range 298.15–673 K // High Temperature. 2016. Vol. 54, N 4. P. 514-518.

[10] Kasenov B.K., Turtubaeva M.O., Amerkhanova Sh.K. and etc. Heat Capacity and Thermodynamic Functions of New Cobalt Manganites $NdM^{1}_{2}CoMnO_{5}$ ($M^{1} = Li, Na, K$) in the Range of 298.15–673 K // Russian Journal of Physical Chemistry A. 2017. Vol. 91, N 2. P. 282-286.

[11] Kovba L.M., Trunov V.K. Rentgenofazovyi analiz. M.: Izd-vo MGU, 1976. 256 p.

Резюме

*Б. Қ. Қасенов, Ш. Б. Қасенова, Ж. И. Сағынтаева,
М. О. Тұртубаева, Е. Е. Қунышбеков*

ЖАҢА НАНОӨЛШЕМДІ (НАНОКЛСТЕРЛІК) КОБАЛЬТ (НИКЕЛИТ)-КУПРАТ-МАНГАНИТТЕРДІҢ СИНТЕЗІ

Соңғы формуласы $LaMgCoCuMnO_6$ және $LaMgNiCuMnO_6$ болатын кобальт (никелит)-купрат-манганиттердің синтезі La_2O_3 (маркасы «аса таза»), NiO , CoO , CuO , Mn_2O_3 және $MgCO_3$ (квалификациясы «талдау үшін таза») стехиометриялық өлшемдерін 20 сағат бойы 800-1200 °C қатты фазалы әрекеттесу жолымен жүргізілді.

Төмен температурада тепе-тең фазалар алу үшін төмен температуралық қыздыруды 10 сағат бойы 400 °C жүргізілді.

Retsch (Германия) компаниясының «ММ301» маркалы вибрациялық диірменінде үгіту жолымен поликристалдық үлгілер наноөлшемді (нанокластерлік) бөлшекке дейін үгітілді, «JSPM-5400» Scanning Probe Microscope «JEOL» (Япония) электрондық микроскопының көмегімен олардың өлшемдері анықталды.

ДРОН-2,0 дифрактометрінде алынған жаңа наноүлгілерге рентгенофазалық талдау жүргізілді. Рентгенограммаларын аналитикалық әдіспен индицирлеу барысында синтезделініп алынған қосылыстар тор көрсеткіштері келесідей кубтық сингонияда кристалданатыны анықталды:

$LaMgCoCuMnO_6$ – $a=14,12\pm 0,02\text{Å}$; $V^{\circ}=2814,87\pm 0,06\text{Å}^3$; $Z=4$;
 $V^{\circ}_{\text{эл.үя.}}=703,72\pm 0,02\text{Å}^3$; $\rho_{\text{рент.}}=4,19\text{г/см}^3$; $LaMgNiCuMnO_6$ – $a=14,38\pm 0,02\text{Å}$;
 $V^{\circ}=2973,56\pm 0,06\text{Å}^3$; $Z=4$; $V^{\circ}_{\text{эл.үя.}}=743,39\pm 0,02\text{Å}^3$; $\rho_{\text{рент.}}=4,22\text{г/см}^3$.

Түйін сөздер: синтез, кобальт-купрат-манганит, никелит-купрат-манганит, лантан, сілтілі, сілтілі-жер металдары, рентгенография, наноөлшемдер, нанокластерлер.

Резюме

*Б. К. Касенов, Ш. Б. Касенова, Ж. И. Сагінтаева,
М. О. Тұртубаева, Е. Е. Қуанышбеков*

СИНТЕЗ НОВЫХ НАНОРАЗМЕРНЫХ (НАНОКЛАСТЕРНЫХ) КОБАЛЬТО(НИКЕЛИТО)-КУПРАТО-МАНГАНИТОВ

Синтез кобальто(никелито)-купрато-манганитов в пересчете на конечные формулы $LaMgCoCuMnO_6$ и $LaMgNiCuMnO_6$ проводили путем твердофазного взаимодействия стехиометрических количеств La_2O_3 (марки «ос.ч.»), NiO , CoO , CuO , Mn_2O_3 и $MgCO_3$ (квалификации «ч.д.а.») при температурах 800-1200 °C в течение

20 ч. Для получения равновесных фаз при низких температурах проводили низкотемпературный отжиг при 400 °С в течение 10 ч. На вибрационной мельнице компании Retsch (Германия) марки «ММ301» поликристаллические образцы новых соединений измельчены до наноразмерных (нанокластерных) частиц, размеры которых определены с использованием электронного микроскопа JSPM-5400 Scanning Probe Microscope «JEOL».

Рентгенофазовый анализ полученных новых нанобразцов проводили на дифрактометре ДРОН-2,0. Индексированием рентгенограмм соединений аналитическим методом установлено, что синтезированные соединения кристаллизуются в кубической сингонии со следующими параметрами решетки: LaMgCoCuMnO_6 – $a=14,12\pm 0,02\text{ \AA}$; $V^0=2814,87\pm 0,06\text{ \AA}^3$; $Z=4$; $V^0_{\text{эл.яч.}}=703,72\pm 0,02\text{ \AA}^3$; $\rho_{\text{рент.}}=4,19\text{ г/см}^3$; LaMgNiCuMnO_6 – $a=14,38\pm 0,02\text{ \AA}$; $V^0=2973,56\pm 0,06\text{ \AA}^3$; $Z=4$; $V^0_{\text{эл.яч.}}=743,39\pm 0,02\text{ \AA}^3$; $\rho_{\text{рент.}}=4,22\text{ г/см}^3$.

Ключевые слова: синтез, кобальто-купрато-манганит, никелито-купрато-манганит, лантан, щелочные, щелочноземельные металлы, рентгенография, наноразмеры, нанокластеры.

B. D. BALGYSHEVA¹, H. SEYTKALÍ², SH. G. MACABAY¹, ZH. S. SAMET¹

Kazakh national University named after al-Farabi, Almaty, Republic of Kazakhstan,
Kazakh national agrarian University Almaty, Republic of Kazakhstan.
E-mail: beikut2013@mail.ru

OBTAINING ZINC-CONTAINING MICROFERTILIZERS METHOD OF MECHANOCHEMICAL ACTIVATION

Abstract. Glauconite by H_3PO_4 was processed in mechanical-thermal and thermal system in different mass ratios. As a result, it was found that the efficiency of MCA-thermal treatment was higher than thermal treatment. IR spectra and x-ray fluorescence analysis were performed.

Key words: thermal, mechanical, glauconite, microfertilization, phosphoric acid.

Now along with fertilizers, mineral micro-fertilizers composed of macronutrients rise high interest in agriculture. If there is no trace element in the soil, the quality of the product will be low and will lead to plant disease. According to the proven scientific and experimental data, low agricultural production is due to the lack of trace elements in the soil [1]. Trace elements play an important role in the normal functioning of enzymatic systems in the physiological processes of plants [2].

Chloride, manganese, molybdenum, zinc, copper and cobalt play an important role in the nutrition and formation of the plant. Trace elements are present in physiological and biochemical processes. Synthesis of proteins, fats, carbohydrates, phosphorus and compounds occurs along with the presence of zinc. Zinc increases vitamin C, carotene in plants. It strengthens the heat resistance and frost resistance of the plant. Deficiency of zinc elements will lead to fine foliage and fruits. Zinc deficiency is strongly felt especially on the plant grown in carbonate soils: vegetables, maize and fruit trees. Because in this soil, there is a low level of zinc sulphate, villemite, calamine, etc. and they are in the form of compounds. In the soil in the territory of Kazakhstan zinc is between 47-59 mg/kg per kilogram. Different levels of zinc are associated with soil-forming rocks, their mechanical composition and agrotechnical measures [5].

In General, the soil of Kazakhstan is rich in manganese and boron, but has lack of zinc and molybdenum, although copper is provided in an average degree.

For a plant it is useful to have in soil water-soluble compounds of molybdenum and boron, salts of bivalent iron and manganese, as well copper and zinc cations as part of a complex of water-soluble nutrient absorption of soils are useful. When using movable plant types usually fertilizers of micronutrients absorbing types are used and at the same time their size is counted.

Provision of soils with movable trace elements affects the determination of the size of fertilizers which are used in agricultural crops and the growth of this plants.

In the areas of Northern, Southern, Central Kazakhstan usually have black soil, Matt black and brown soil, brown and black soil, light black soil, copper and cobalt have an average level of provision of movable elements, manganese and boron level is higher, level of movable types of molybdenum and zinc are lower. In Almaty and Taldykorgan regions 5-8 mg per kilogram of dark chestnut soil and 2.5-3.0 mg of immovable copper in Zhambyl and South Kazakhstan regions [6].

Polymicrogyria zinc dark gray, contains 25% zinc, produced in powder form. Used seed treatment (repor t 4 kg per 1 ton of seeds) impregnation into the ground (12-20 kg per hectare in the report)

Scientists from Uzbekistan have proved in scientifically-based experience by using glauconitic rocks in the industry and agriculture [7, 8].

Based on the results of long – term experiments, the following conclusions were made: $(R_2O + RO)Re_2O_3 \cdot 4SiO_2 \cdot 2H_2O$ glauconite-valuable, traditional, but there are potassium, R_2O-Na_2O and K_2O , $RO-MgO$, CaO , FeO , ReO , $R_2O_3-Al_2O_3$ and Fe_2O_3 . good effect on plant growth, yield of raw materials. The results of the experiments are good with rice.

Sugar in the Rostov region, the experiment was done on sugar beet, the productivity of culture according to GJI increased by 14-18 t/ha. The results of the experiment with potatoes went well.

Talking about the requirements for glauconite: the requirement of glauconite is still not approved by GOST. The recommendation was presented by the Rostov and Uzbek geologists, also by group of chemists.

In a certain area of production of glauconite and the possibility of application in many works are provided [9].

Summing up the results of the literature review, current problem is to use glauconite fertilizers, especially producing new types of glauconite and glaucopis and glucocare by using production technology can be rational consideration.

Information about the scientific work under glauconite conversion at high temperature is very rare.

Therefore, the aim is to produce fertilizers by activating glauconite phosphoric acid and Zn^{2+} salts.

EXPERIMENTAL PART

As a source of raw materials in Kostanay region Sokolov-Sarbai mine used glauconite $K < 1(Fe^{3+}, Fe^{2+}, Al, Mg)2-3[Si_3(Si, Al)O_{10}][OH]2 \cdot nH_2O$.

As an additive to Glauconite, 40% of orthophosphoric acid was used. Glauconite (G) and 40% phosphoric acid (H_3PO_4) was produced by spraying through batcher in 1:1, 2:1, 3:1, 4:1 mass communication. The ratio of mass of Ball and other ingredients are 25:1, reaction duration is 15 minutes mechanical; rotation frequency is 300 rpm.

Mechanochemical processing of glauconite is made by – modern 2SL brand planetary dirmode in two reels.

Favorable conditions of firing the process were obtained: $T=450\text{ }^\circ\text{C}$, $t=45\text{ min}$.

Heat treatment was carried out in a volume of 45 min mass of the sample.

For the study of fertilizer properties $ZnSO_4 \cdot 7H_2O$ salt was used.

Glaukonit modification was considered in two ways: thermal and mechano-thermal processing (heat treatment and MOSS). The modification was carried out according to the specific methodology.

To detect changes of modified characteristics of the glauconite, structural and electronic microscopic method, x-ray analysis, infrared spectroscopy method, x-ray fluorescence analysis (elemental analysis), differential thermal analysis and atomic absorption analysis methods were used.

Zn^{2+} salt solution 60 $\mu g/ml$, 500 $\mu g/ml$, 1000 $\mu g/ml$ concentration solutions were prepared in three models. In a flask with 200 ml of the prepared solutions on the filling cone, 2g were placed in each three cone kobas. The flask is stoppered and fixed by cone mixer machine for 60 min. At the end of sorption of solutions, are filtered by paper filter of $d=12$ cm "blue ribbon". Chemical analysis were made. As part of the filtrate Zn^{2+} ion concentration of is determined by the atomic absorption analysis method.

RESULTS AND ANALYSIS

The mixture of Glauconite and phosphoric acid obtained by thermal and chemical, mechanochemical way after processing were conducted by a special methodology (tables 1, 2).

Glauconite- H_3PO_4 (40%) of $ZnSO_4 \cdot 7H_2O$ system, obtained by the results of various characteristics after heat treatment of the product salt concentration of Zn^{2+} ions 60; 500; 1000 mg/ml P_2O_5 cit in low concentrations falls. It's also seen obviously during mechanochemical and chemical treatment. P_2O_5 cit.men's. G. significance of the Supreme size is: $H_3PO_4 = 1:1$ mass relationship of Zn^{2+} ions of 60 $\mu g/ml$ of P_2O_5 concentration is observed, the size of 32,07% was revealed (table 2).

Table 1 – Heat treated samples P_2O_5 size

The ratio of the sample	$C_0 (Zn^{2+})$, mkg/ml	P_2O_5 total, %	P_2O_5 the citrate solution, %	$K_{decompose}$. %
G: $H_3PO_4 = 1:1$	60	29,85	22,73	76,14
	500	18,81	13,92	74,00
	1000	12,97	8,86	68,30
G: $H_3PO_4 = 2:1$	60	30,46	20,53	67,39
	500	14,26	9,37	65,70
	1000	14,02	9,16	65,30
G: $H_3PO_4 = 3:1$	60	23,03	15,43	66,99
	500	11,99	8,90	66,99
	1000	11,89	7,28	61,22
G: $H_3PO_4 = 4:1$	60	12,14	6,70	55,18
	500	11,78	5,13	43,54
	1000	12,01	5,82	45,96

Table 2 – Glauconite-H₃PO₄ (40%) system ZnSO₄·7H₂O MOSS concentration of various salts-characteristics obtained after heat treatment of the product

The ratio of the sample	C ₀ (Zn ²⁺), mkg/ml	P ₂ O ₅ total, %	P ₂ O ₅ the citrate solution, %	K _{descompose} , %
G: H ₃ PO ₄ =1:1	60	36.22	32.07	88.54
	500	21.00	17.92	85.33
	1000	16.58	13.86	83.60
G: H ₃ PO ₄ =2:1	60	24.15	19.53	80.86
	500	18.36	16.37	78.82
	1000	13.01	10.46	72.50
G: H ₃ PO ₄ =3:1	60	21.38	18.32	76.33
	500	14.99	11.90	74.42
	1000	11.89	9.28	77.27
G: H ₃ PO ₄ =4:1	60	15.14	11.70	75.29
	500	12.78	10.13	63.00
	1000	8.01	7.82	60.17

IR spectroscopic results of the study:

Phosphoric acid 40% raw glauconite glauconite activated mechanochemically in respect of samples and infrared spectroscopy Specord-M80 installation tabledesign 4000,0 KBr-450,0 cm⁻¹. Identification of the samples was performed by comparison with data debating.

Glaukonit primary δ(O₃PO) in the area of deformation vibrations of when the IR spectrum in this area 471,12 oscillation frequency, cm⁻¹, which look line. A frequency at 875.17, 779.28, 797.13, 713.12 cm⁻¹) line γ (P-OH) and describes the relationship of oscillations (figure 1).

However, 1630.69, 1429.17 cm⁻¹ line δ (P-OH)was characterized by oscillations. And the frequency of 2513.55, 3434.93 cm⁻¹ vibrations of OH groups in the structure of minerals, which characterize the line of interflooroverlappings. The IR spectrum of the frequency fluctuations of securities, the visible 520.06, 648.85, 608.79 cm⁻¹ vibrations sistry PO₄³⁻ ions, are described. But in contrast to the phosphate ions it is possible to trace lines. The frequency of oscillations 460, 471 cm⁻¹, which are composed of silica-oxygen bond quartz, characterizing the line looks dynamic. This line of Si-O fluctuations characterizes the valence bonds. And the frequency 648.85, 694.74, 713.12, 779.28, 797.13, 875.17 cm⁻¹) lines of the Si-O-Si vibrations and characterizes the figure 1. Glauconite primary any IR spectra

Glauconite δ, thermally processed (O₃PO) in the zone of deformation vibrations of the IR spectrum of the curve 471.12 oscillation frequency, cm⁻¹ lines were visible. A frequency 779.08, 797.13 cm⁻¹) line γ (P-OH) and describes the relationship of oscillations (figure 2).

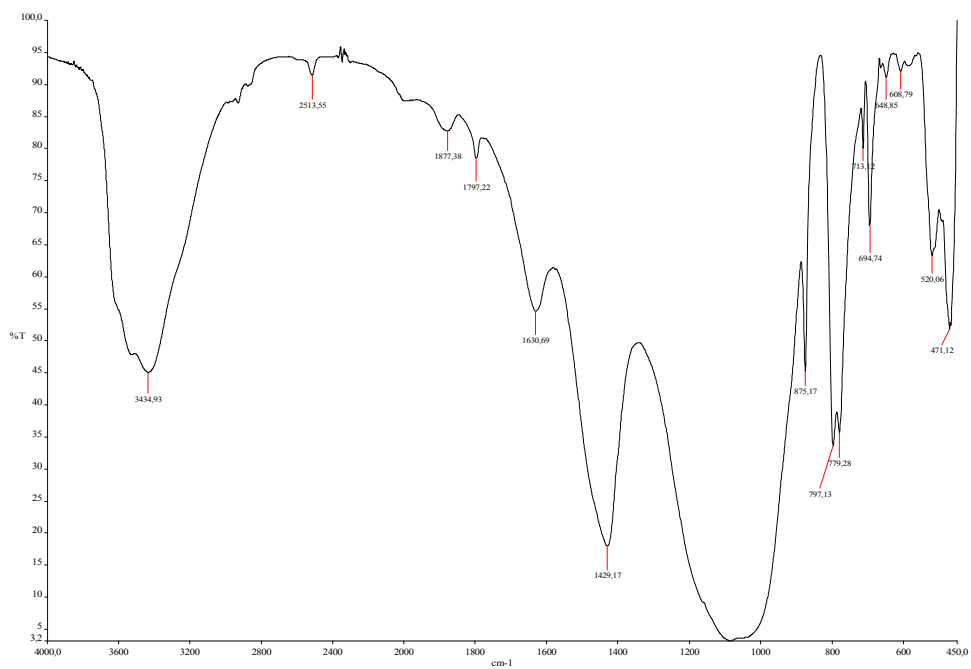


Figure 1 – Glauconite primary any IR spectra

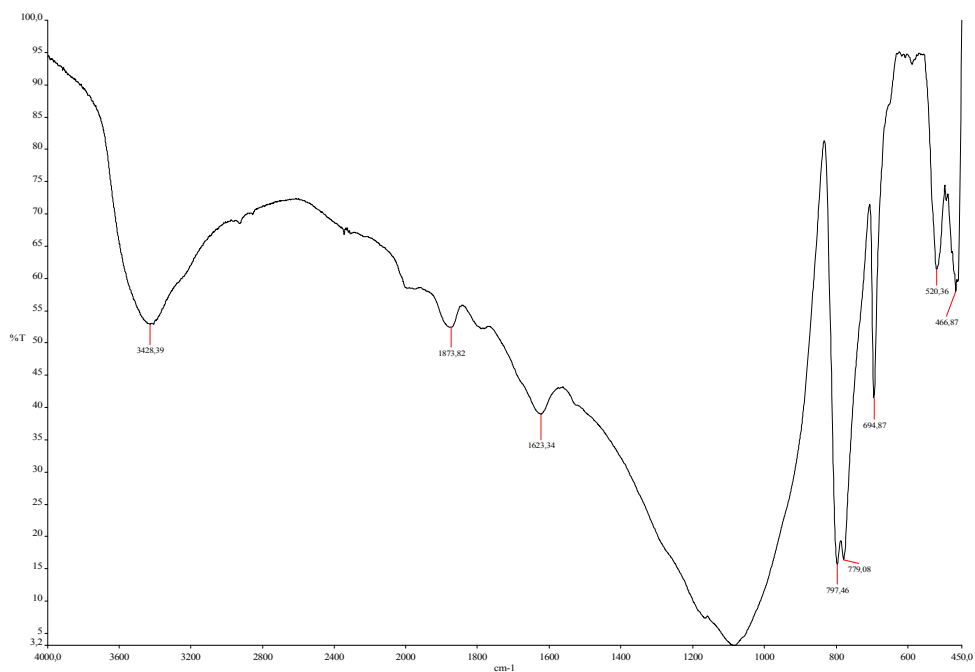


Figure 2 – Glauconite: H₃PO₄ (40%) = 1:1 system Zn²⁺ ions 60 μg/ml, the concentration of the sample after thermal treatment IR spectrum

However, 1623.34 cm^{-1} line $\delta(\text{P-OH})$ and was characterized by oscillations. 520.30 oscillation frequency, 466.87 cm^{-1} vibrations sistery PO_4^{3-} ions, are described. Lines characterize Si-O-Si vibrations. But in contrast to the phosphate ions it is possible to trace lines. Activated mechanochemically has samples IR spectroline 407.66 oscillation frequency, cm^{-1} line, it was evident that glauconite $\delta(\text{O}_3\text{PO})$ was characterized by the deformation vibration of connection with the area (figure 3).

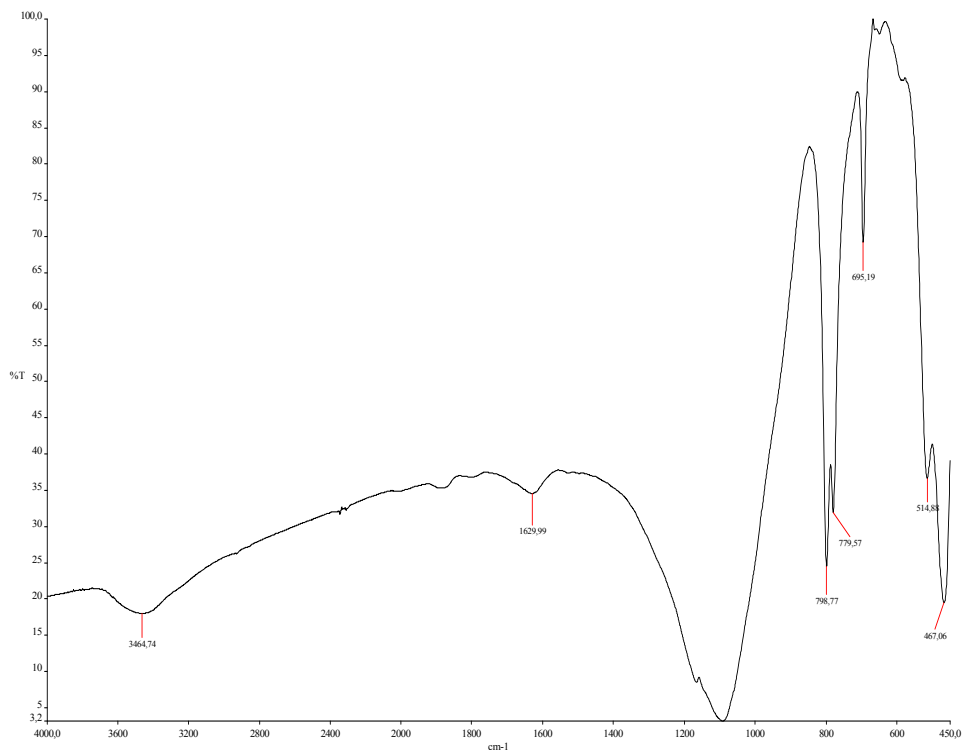


Figure 3 – Glauconite: H_3PO_4 (40%) = 1:1 system Zn^{2+} ions of $60\text{ }\mu\text{g/ml}$ and the concentration of the sample after the heat treatment of MOSS IR range

Figure 3 mechanochemical samples activated IR oscillation frequency spectroline 779.57 , 798.77 cm^{-1} lines of $\gamma(\text{P-OH})$ fluctuations, characterizes the connection. However, 1629.99 cm^{-1} of the $\delta(\text{P-OH})$ line was characterized by oscillations. 514.88 oscillation frequency, 605.19 cm^{-1} vibrations sistery PO_4^{3-} ions, are described. But in contrast to the phosphate ions it is possible to trace lines. Frequency 779.08 , 798.77 cm^{-1} lines characterize the Si-O-Si vibrations. Here you can see that fluctuations in these indicators primary glauconitegilcher. As well as the Silicon-oxygen bond, the relevant abatacept phosphate ions, characterizing the intensity increases the vibration frequency of the oscillation frequencies of floors with lines in the water. Posts (sodium dihydrotres-veils) the

concentration of water in the composition of interflooroverlappingsazip share annually, mostly glauconite, as well as interflooroverlappings that characterize 3464.74 water, cm^{-1} frequency of the oscillation intensity decreases. The floor of the water and the phosphate ions may be the chemical interaction between two. Each reduction in the size of glauconite in the composition of the mixture, mainly in the IR spectrum of water, reduces the intensity of the lines characterizing inter-flooroverlappings. Starting glauconite IR spectrum of vibrations than after heat treatment and the frequency of mechanochemical Vik-range looks like reduced frequency. Hence, there were chemical interactions. That is, as a result of penetration into the structure of glauconite mechano-chemical activation of sodium dihydrophosphate, phosphate ions bind with glauconite water in the composition.

The analysis Rentgen fluorescent glauconite 40% of the samples processed in accordance with the legislation established the elemental composition phosphorus limited mechano-chemically vertical mixing change proportionally. During activation the oxidation of some components and we can say that in connection with mechano-chemical flight was in lesser extent.

Conclusion.

1. G(glauconite) – H_3PO_4 (40%) of the system $\text{ZnSO}_4 \cdot 7\text{H}_2\text{O}$ as a result, identify the optimum temperature for heat treatment. In 450°C colors were turned into light brown beige, also was left free .

2. It was determined by rule that G(glauconite)-mass tinasteride system $\text{H}_3\text{PO}_4(1:1; 2:1; 3:1; 4:1)$ $\text{ZnSO}_4 \cdot 7\text{H}_2\text{O}$ salt (60; 500; 1000 $\mu\text{g/ml}$) whileare increasing the size of the P_2O_5 is decreasing.

3. Were determined the favorable conditions: G: $\text{H}_3\text{PO}_4 = 1:1$ mass relationship of Zn^{2+} ions of 60 mcg/ml concentration 450°C . Kadyrow, 76,14%.

4. G(glauconite) – H_3PO_4 (40%) of the system $\text{ZnSO}_4 \cdot 7\text{H}_2\text{O}$ in the treatment compared to heat treatment with salt K MOSS, 88.54% revealed that.

REFERENCES

- [1] Stefan V.K. Life of plants and fertilizers. M., 1981.
- [2] Artjushin A.M., Derzhavin L.M. Brief Dictionary on Fertilizers. 2nd ed. M., 1984.
- [3] The fundamentals of farming and plant growing. 3rd ed. / Ed. Niklyeva V.S. M., 1990.
- [4] Journal of Chemistry and Business. 2001. N 46.
- [5] Agrochemistry / Edited by prof. A.S. Yagodina. M.: The Ear, 1982.
- [6] Journal Chemistry and Life – XXI century. 1998. N 4.
- [7] Nabiev M.N., Kasymova M.A., Sat "Mineral and Organo-mineral Fertilizers, Structure Formers of Soils and Herbicides". Tashkent: FAN, 1967.
- [8] Vigdorovich V.I., Tsygankova L.E., Nikolenko D.V., Protasov A.S Sorption purification of flowing solutions from copper (II) concentrate glauconite GBMTO // Sorb. and chromatography. Processes. 2013. 13, # 4. P. 442-448. (Rus.).

Резюме

Б. Д. Балғышева, Н. Сейтқали, Ш. Ф. Мағабай, Ж. Самет

**ҚҰРАМЫНДА Zn-БАР МИКРОТЫҢАЙТҚЫШЫН
МЕХАНОХИМИЯЛЫҚ АКТИВТЕУ АРҚЫЛЫ АЛУ**

Глауконит – H_3PO_4 жүйесінің әртүрлі массалық қатынастары термиялық, механохимиялық-термиялық өндеуден өткізілді. Нәтижесінде термиялық өдеуге Қарағанда МХА-термиялық өдеудің тиімділігі анықталды. ИК-спектрлер мен рентген-флуоресцентті талдау жүргізілді.

Түйін сөздер: термиялық, механохимиялық, глауконит, микротыңайтқыш, фосфор қышқылы

Резюме

Б. Д. Балғышева, Н. Сейтқали, Ш. Ф. Мағабай, Ж. Самет

**ПОЛУЧЕНИЕ Zn-СОДЕРЖАЩИХ МИКРОУДОБРЕНИЙ
МЕХАНОХИМИЧЕСКИМ СПОСОБОМ**

Проведена термическая и механохимическая обработка в системе глауконит – H_3PO_4 в разных массовых соотношениях. В результате химического анализа установлено, что механохимическая обработка более эффективна, чем термическая.

Приведены результаты исследований ИК-спектроскопии и рентгенофлуоресцентные.

Ключевые слова: термический, механохимический, глауконит, микроудобрения, фосфорная кислота.

N. M. IVANOVA, YE. S. LAZAREVA, YA. A. VISURKHANOVA, E. A. SOBOLEVA

Institute of Organic Synthesis and Chemistry of Coal of Kazakhstan Republic,
Karaganda, Republic of Kazakhstan

STRUCTURE AND ELECTROCATALYTIC ACTIVITY OF ZINC-CONTAINING COMPOSITES OF POLYANILINE WITH ANILINE-FORMALDEHYDE POLYMER

Abstract. Zinc-containing composites based on polyaniline (PAni) with aniline-formaldehyde polymer (AFP) were obtained by introducing $ZnCl_2$, ZnO or zinc dust treated with ultrasound during the oxidative polymerization of aniline in the presence of AFP. The structure and morphological features of synthesized composites were studied by X-ray diffraction and electron microscopy. It is shown that the use of synthesized composites to activate the cathode in the electrohydrogenation of *o*-nitroaniline is accompanied by the electrochemical reduction of zinc (II) cations and the formation of micro- and nanoparticles of zinc that catalyze the process under investigation.

Keywords: composites of polyaniline with aniline-formaldehyde polymer, zinc chloride (II), zinc dust, zinc oxide (II), electrocatalytic hydrogenation, *o*-nitroaniline

Introduction. Introduction of metal-containing inorganic dopants to polyaniline (PAni), an electrically conductive polymer with a wide range of practical and potential significance, allows to obtain new polymer-metal materials with improved electrically conductive, dielectric, optical, catalytic and other properties. Zinc-containing PANicomposites are no exception. Especially much attention is given to a creation of PANicomposites with zinc oxide (ZnO) nanoparticles. For example, the photocatalytic activity of composites based on copolymers of poly(aniline-*co-p*-phenylenediamine) and poly(aniline-*co-o*-aminophenol) with ZnO nanoparticles (diameter ~ 25 nm) was studied in [1, 2] with respect to the decomposition of methylene blue under effect of UV radiation. It was established in [3] that PAni /ZnO nanocomposites are good sensors for ammonium with the high sensitivity increasing with increase of ZnO content. In [4], the optical and electrical properties of the PAni/ZnO nanocomposite with an electrical conductivity of $3,0 \cdot 10^{-2} \text{ Sm} \cdot \text{cm}^{-1}$, which is less than that of the "pure" PAni, $3,4 \text{ Cm} \cdot \text{cm}^{-1}$, is explained by difficulties in the transport of electrons and electric charge over a polymer matrix interacting with ZnO nanoparticles. The lowering the electrical conductivity of PAni/ZnO composites in comparison with PAni and with ZnO nanoparticles was also shown in [5, 6]. Bactericidal properties were revealed in polyvinyl alcohol/PAni/ZnO nanocomposites [7], while PAni was synthesized in a solution of polyvinyl alcohol sol in the presence of ammonium persulfate.

According to [8], the electrical conductivity is higher, and the anticorrosive effect is better in the PAni/Zn film nanocomposites (zinc particles of size 35 nm) in comparison with the PAni/Zn microcomposites (zinc particles of size 60 μm).

When doping PANi by transition metal ions using the electropolymerization method, a greater effect of Zn^{2+} ions on electrically conductive properties was observed than Ni^{2+} , Co^{2+} and Cu^{2+} ions: in the case the electrical conductivity of the PANi / $ZnCl_2$ composite increases to $6,42 \text{ Sm}\cdot\text{cm}^{-1}$ compared to the PANi in the form of a hydrochloride salt, for which has a value of $1,87 \text{ Sm}\cdot\text{cm}^{-1}$ [9].

In this paper, the results of studies of zinc-containing composites based on the mixed PANi+AFP polymer obtained by the introduction of $ZnCl_2$, ZnO or Zn (zinc dust) in the process of oxidative polymerization of aniline in the presence of aniline-formaldehyde polymer (AFP) in order to study their structure and electrocatalytic activity are discussed. The addition of AFP to polyaniline is an attempt to increase the metal content (in the form of its cations or nanoparticles) by interacting with functional groups of a mixed polymer matrix. Since it is known [10, 11] that AFP participates in a breaking of chains during oxidative polymerization of aniline, its quantity at preparation of the mixed polymer of PANi+AFP was limited to an aniline/AFP ratio of 2:1.

EXPERIMENTAL PART

Zinc-containing PANi + AFP composites were prepared by introducing zinc chloride (II), its oxide ZnO and zinc dust (Zn) in the process of oxidative polymerization of aniline (the oxidizer – ammonium persulfate) in the presence of AFP-polymer in the hydrochloric acid medium. Zinc oxide and zinc dust were pre-treated with ultrasound in distilled water for 20 minutes. Then they were introduced into the reaction mixture after its pH was raised to 7 by addition of 1M NH_4OH solution or 20% NaOH solution. The obtained mixture was left for 24 hours. The precipitate filtered and washed with distilled water, then with acetone. Composites were dried at $80^{\circ}C$ to constant weight. PANi+AFP composites with zinc chloride were also obtained, followed by evaporation of the solvent without and with thermal treatment at $180^{\circ}C$ for 2 hours. The ratio of aniline to AFP was 2:1, and the ratio of aniline / $ZnCl_2$ (ZnO, Zn) was 1:1 and / or 1:2. To fabricate all the composites, a thermally treated AF-polymer was used (at $200^{\circ}C$ for 2 hours).

After synthesizing of PANi + AFP composites the amount of zinc content filtrates was determined by complexometric titration using disodium EDTA in the presence black eriochrome [12].

The structure and phase constitution of synthesized zinc-containing PANi+AFP composites were studied by X-ray diffraction analysis (XRD) on the X-ray diffractometer DRON-2, their morphological features by electron microscopy on the scanning electron microscope TESCAN MIRA 3 LMU.

Experiments on the electrocatalytic hydrogenation of *o*-nitroaniline (*o*-NA) with the use of zinc-containing PANi+AFP composites for cathode activation were carried out in a diaphragm electrochemical cell. The anode was a platinum gauze; the cathode was a copper plate, which closely contacted the bottom of the electrolyzer and served as a substrate for the PANi composite catalyst (1 g). The

current density was $1,25 \text{ kA/m}^2$, the temperature of 30°C was maintained using a thermostat. As an anolyte, 60 ml of 20% NaOH solution was used, as a catholyte—65 ml of 2% NaOH solution with an addition of 15 ml of ethyl alcohol (i.e. in a 4:1 ratio). The amount of hydrogen absorbed (V_i), the rate of hydrogenation reaction (W) and the conversion of the hydrogenated substance (α) were calculated using the volumes of gases (oxygen and hydrogen) evolved. The hydrogenation products were extracted from the catholyte with chloroform, the resulting extracts were analyzed on a Crystal-5000.1 chromatograph.

RESULTS AND DISCUSSION

According to the difference between the initial amount of zinc (as part of its chloride or oxide) introduced to the mixed PANi+AFP polymer and determined by complexometric titration in filtrates after the synthesis. The total composition synthesized composites was calculated, as well as in 1 g of each composite (the values obtained are given below in table 1). According to these data, in PANi+AFP+ZnCl₂ (1:2) composite, after a thorough washing, a relatively low amount of zinc (II) (0,138 g in 1 g of composite) is retained, which affects the electrocatalytic activity of this composite. The addition of an alkaline reagent (NaOH or NH₄OH) to the reaction medium of oxidizing polymerization leads to the formation of zinc-containing compounds precipitated, which contributes to an increase in the zinc content (II) in PANi+AFP+ZnCl₂ composites. The introduction of ZnO and Zn powders as the finished products treated with ultrasound (20 min) is also not accompanied by the preservation of their initial quantity.

Structural-phase changes of the synthesized zinc-containing PANi+AFP composites before and after their application in electrohydrogenation of *o*-NA can be discussed by the results of X-ray analysis. Figures 1 and 2 shows the X-ray patterns of the PANi+AFP+ZnCl₂ (1: 2) composites with the addition of NH₄OH or NaOH. It should be noted that during the oxidative polymerization of aniline using ammonium persulfate, by-products such as H₂SO₄, HCl and (NH₄)₂SO₄ are formed [13]. In the presence of a metal salt, for example, ZnCl₂, this process is also accompanied by the formation of zinc sulfate (II), ammonium chloride and other plausible compounds. The addition of alkaline reagents to the polymerization reaction medium (actually after its completion) leads to the interaction of the formed by-products with them.

Thus, in the case of NH₄OH in PANi+AFP+ZnCl₂ (1:2) composite, according to the X-ray analysis (figure 1, a), there are crystalline phases of the complex salt Zn₄(SO₄)(OH)₆·4H₂O, also possibly Zn(OH)₂, NH₄Cl, and others. After application of this composite in the electrohydrogenation of *o*-NA, only crystalline phases of metallic zinc were found in its constitution (figure 1, b). This indicates the electrochemical reduction of zinc cations (II) from its previous compounds contained in the mixed polymer.

When NaOH is introduced into the reaction medium of oxidative polymerization of aniline, the complex compounds NaZn₄(SO₄)(OH)₆Cl·6H₂O,

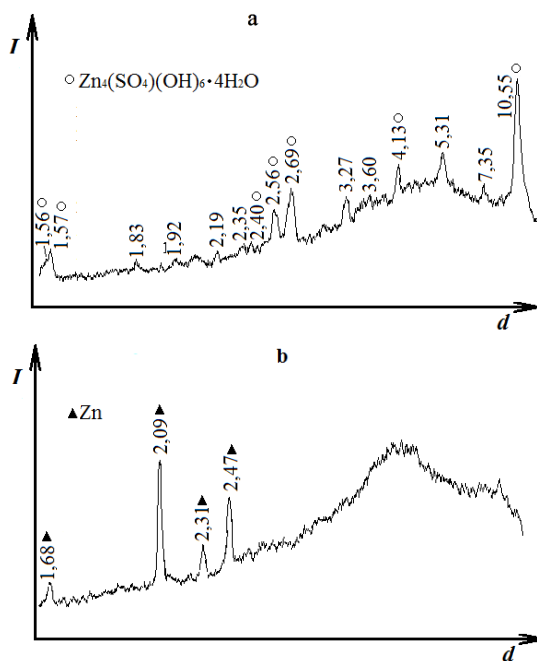


Figure 1 – X-ray patterns of PANi+AFP+ZnCl₂(1:2)+NH₄OH composite before (a) and after (b) the electrohydrogenation of *o*-NA

$6\text{Zn}(\text{OH})_2 \cdot \text{ZnSO}_4 \cdot 4\text{H}_2\text{O}$ are formed in the PANi+ AFP +ZnCl₂(1:2) composite; in addition, there may be present $\text{Zn}(\text{OH})_2$, $\text{Na}_2\text{Zn}(\text{SO}_4) \cdot 4\text{H}_2\text{O}$, and $\text{NaCl} \cdot 2\text{H}_2\text{O}$ (figure 2). There are also a small amount of crystalline Zn^0 phases. After carrying out the electrohydrogenation of *o*-NA on this composite, the zinc content in its constitution increases, and the crystalline phases of its ZnO oxide appear.

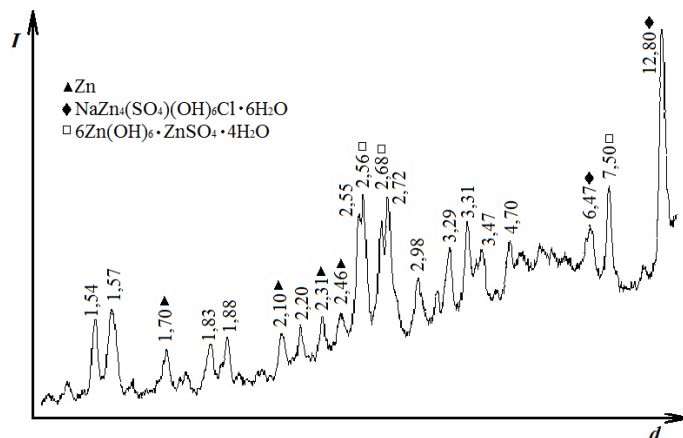


Figure 2 – X-ray pattern of PANi+AFP+ZnCl₂(1:2)+NaOH composite before the electrohydrogenation of *o*-NA

According to the X-ray diffraction pattern of the PANi+AFP+ZnCl₂(1:1) composite prepared with evaporation of the solvent and heat treatment (figure 3, a), it contains crystalline phases of double-salt crystalhydrate of zinc sulphate and ammonium sulfate formed during the oxidative polymerization of aniline.

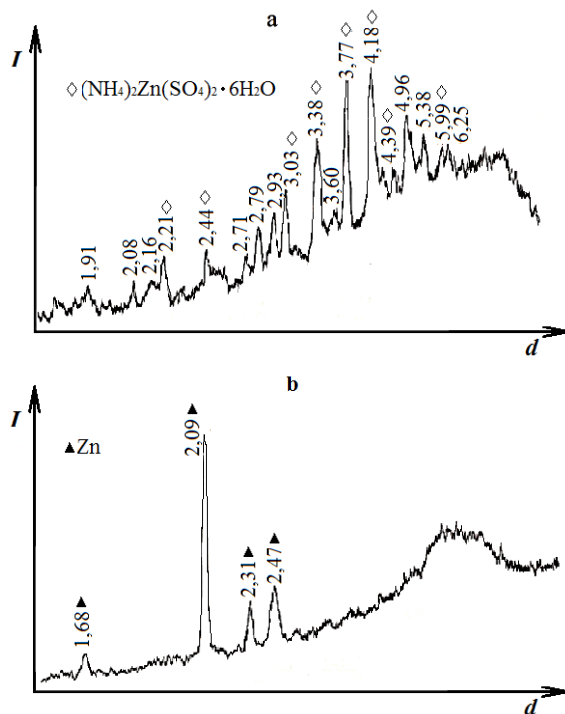


Figure 3 – X-ray patterns of the composite PANi+AFP+ZnCl₂(1:1) (with evaporation) before (a) and after (b) the electrohydrogenation of *o*-NA

In the phase constitution of the composite after its application to activate the cathode in the electrohydrogenation of *o*-NA, there are only crystalline phases of metallic zinc (Zn⁰) (figure 3, b) formed as a result of electrochemical reduction of Zn²⁺ cations from double salt, in addition to the amorphous phase of the mixed polymer.

The highest content of zinc is in PANi+AFP composites (table 1) with the zinc dust introduced. The X-ray diffraction pattern of such a composite synthesized with the addition of NaOH (figure 4, a) shows that in its constitution in addition to the crystalline phases of zinc there are also crystalline phases of its oxide. During the electrohydrogenation process the zinc oxide ZnO is subjected to electrochemical reduction with the formation of zinc in the zero-valence state. It is confirmed by an increase in the intensity of the corresponding peaks and the absence of ZnO crystalline phases in its constitution after electrohydrogenation on its X-ray diffraction pattern (figure 4, b).

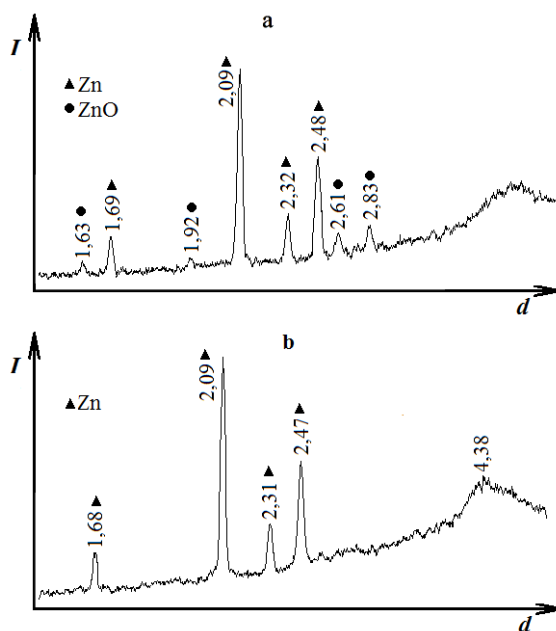


Figure 4 – X-ray patterns of the composite PANi+AFP+Zn(1:1)+NaOH before (a) and after (b) the electrohydrogenation of *o*-NA

The micrographs of PANi + AFP+ZnCl₂ (1:2)+NH₄OH composite (figures 5, 6) were obtained by scanning electron microscope TESCAN MIRA 3 LMU at different scales of scanning. According to the micrographs of this composite before to the electrohydrogenation (figure 5), crystallites of various structure and shape are present on the surface of its particles. First, these are feather-like crystallites and the formations similar to them, bordering "protrusions" on a polymer basis; secondly, they are large bulk and flat semitransparent crystallites, which are apparently the crystallohydrates of Zn₄(SO₄)(OH)₆·4H₂O complex salt (figure 1, a). The polymer basis has both a dense and loose mesh structure consisting from chaotically interconnected nanotubes from 50 to 90 nm in diameter.

As noted above, in the phase constitution of the PANi + AFP+ZnCl₂(1:2) + NH₄OH composite after its application in the electrohydrogenation of *o*-NA, in addition to the polymer basis, only crystalline phases of metallic zinc are present (figure 1, b). The performed electron microscopic studies of this composite showed that it consists from particles with a low content of zinc and particles whose surface is densely covered with grown crystals of zinc (figure 6). In this case, zinc crystals have different shapes: on the surface of dense polymeric particles there are zinc crystals in the form of needles assembled into bundles; on loose particles – in the form of twigs.

X-ray spectral analysis carried out in various parts of particles with different densities is defined a higher percentage content of O and Na elements (obviously

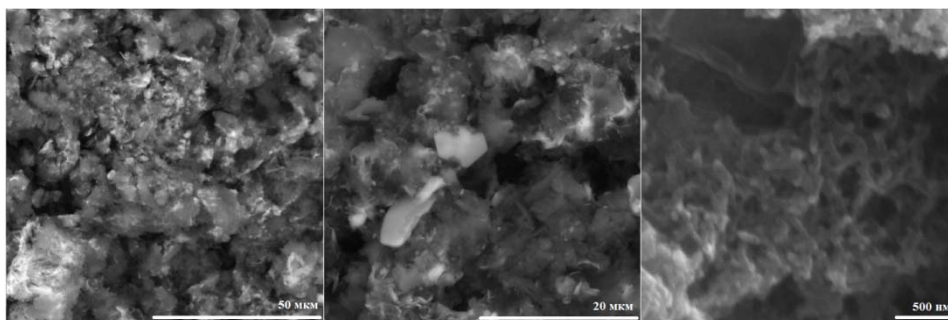


Figure 5 – Micrographs of the PANi(2)-AFP(1)+ZnCl₂(1:2)+NH₄OH composite before the electrohydrogenation of *o*-NA

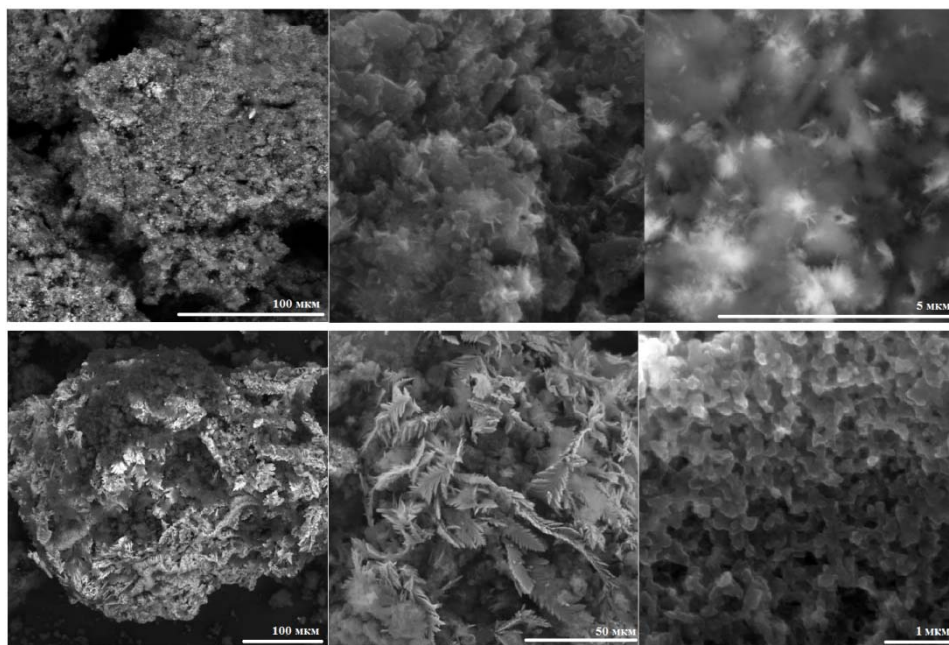


Figure 6 – Micrographs of PANi(2) + AFP(1)+ZnCl₂(1:2)+NH₄OH composite after the electrohydrogenation of *o*-NA

in the form of NaOH) in the near-surface layer of dense particles with needle crystals in comparison with loose particles. Despite the fact that all the particles of this composite were in an alkaline catholyte medium and after electrohydrogenation process they were washed with warm distilled water, more amount of NaOH could be retained in denser particles, than in loose ones. Another explanation is that sodium hydroxide is also used to harden the AF-polymer, and it is retained in the particles of this polymer after synthesis creating a stronger alkaline medium, in which zinc needle crystals are formed. It is quite possible that the

nature of the polymer basis influences the growth of zinc crystals of different shapes.

Synthesized Zn-containing PAni + AFP composites deposited on the surface of copper cathode were investigated for a manifestation of electrocatalytic activity in the electrohydrogenation of *o*-nitroaniline under the conditions described above. There sults are shown in table.

Table 1 – Electrocatalytic hydrogenation of *o*-NA on PAni(2)+AFP(1)+ZnCl₂ (ZnO, Zn) composites

Composites	The zinc content in 1 g of composite	W , ml H ₂ /min ($\alpha = 0,25$)	η , % ($\alpha = 0,25$)	α , %
Cu-cathode	–	3,5	25,0	71,0
PAni(2)+AFP(1)+ZnCl ₂ composites				
PAni+AFP + ZnCl ₂ (1:2)	0,138	3,8	27,1	85,5
PAni+AFP + ZnCl ₂ (1:2) + NaOH	0,243	4,9	34,4	85,0
PAni+AFP + ZnCl ₂ (1:2) + NH ₄ OH	0,270	5,4	39,4	97,7
PAni+AFP + ZnCl ₂ (1:1), with evap.	0,085	6,6	47,7	87,6
PAni+AFP + ZnCl ₂ (1:1), with evap.+ TO	0,089	7,0	50,8	92,1
PAni(2)+AFP(1)+ZnO (Zn) composites				
PAni+AFP+ZnO (1:1) + NaOH	0,285	5,1	33,8	99,9
PAni +AFP +ZnO (1:1) + NH ₄ OH	0,275	4,0	26,7	92,0
PAni+AFP+Zn (1:1) + NaOH	0,384	7,1	52,3	86,4
PAni +AFP+Zn (1:1) + NH ₄ OH	0,370	7,1	51,6	81,2

From the data of table 1 follows that all synthesized Zn-containing composites based on the mixed PAni + AFP polymer possess anelectrocatalytic activity in the electrohydrogenation of *o*-NA. In their presence, the electrohydrogenation of *o*-NA occurs at higher rates and more complete conversion of *o*-NA than in the electrochemical reduction of *o*-NA on the Cu-cathode. As shown by X-ray analysis, under the influence of current the electrochemical reduction of zinc (II) cations to the zero-valence state (Zn⁰) takes place from all of its precursor compounds present in the composites. The zinc micro- and nanoparticles that are formed are the electrocatalyst of the process under study.

Among the PAni + AFP composites with ZnCl₂ introduced, the most electrocatalytic active are composites prepared with evaporation of the solvent, although the zinc content in 1 g of these composites is the least. Apparently, the presence of dissolved components of these composites (ammonium sulfate and chloride, oligomeric polymerization products) in the catholyte promotes the electrocatalytic hydrogenation of *o*-NA on the reduced zinc particles.

From the second group of Zn-containing composites, the most electrocatalytically active are PAni+AFP composites with the introduced zinc dust previously sonicated. The zinc content in the composites is the highest of all synthesized composites (table 1). At the same time, the electrocatalytic hydroge-

nation of *o*-NA with the maximum value of its conversion (99,9%) is run on the composite with ZnO, also activated by a sonication, when the pH is adjusted to 7 with sodium hydroxide. The main product of electrocatalytic hydrogenation is *o*-phenylenediamine, that is confirmed by chromatographic analysis.

Conclusion. Thus, by combined chemical and electrochemical methods, new Zn-containing PAni(2)+AFP(1) composites were produced. Their phase constitution depends upon the synthesis conditions, especially at the introduction of zinc salt (II), and the nature of the zinc-containing compound introduced. It has been established that the use of synthesized composites for cathode activation in the electrohydrogenation of *o*-NA is accompanied by electrochemical reduction of zinc (II) cations and the formation of metallic zinc particles exhibiting electrocatalytic activity in the electrohydrogenation of *o*-NA. The zinc-polymer composites obtained can be also applied as a catalyst or electrocatalyst in other reactions of organic chemistry.

REFERENCES

- [1] Sivakumar K., Kumar V.S., Haldorai Yu. Zinc oxide nanoparticles reinforced conducting poly(aniline-co-p-phenylenediamine) nanocomposite // *Composite Interfaces*. 2012. Vol. 19, N 6. P. 397-409.
- [2] Sivakumar K., Kumar V.S., Shim J-J., Haldorai Yu. Conducting copolymer/ZnO nanocomposite: synthesis, characterization, and its photocatalytic activity for the removal of pollutants // *Synthesis and Reactivity in Inorg., Metal-Org., and nano-Metal Chem*. 2014. Vol. 44, N 10. P. 1414-1420.
- [3] Mehto A., Mehto V.R., Chauhan J., Singh I.B., Pandey R.K. Preparation and characterization of polyaniline/ZnO composite sensor // *Nanomed. Res*. 2017. Vol. 5, N 1. 8 p.
- [4] Alam M., Alandis N.M., Ansari A.A., Shaik M.R. Optical and electrical studies of polyaniline/ZnO nanocomposite // *J. Nanomaterials*. 2013. Vol. 2013. Article ID 157810. 5 p.
- [5] Goyal S.L., Sharma S., Jain D., Kishore N. Study of structural, electrical and thermal properties of polyaniline/ZnO composites synthesized by in-situ polymerization // *Indian J. Pure and Appl. Physics*. 2015. Vol. 53. P. 456-463.
- [6] Mostafaei A., Zolriasatein A. Synthesis and characterization of conducting polyaniline nanocomposites containing ZnO nanorods // *Progress in Natural Science: Materials International*. 2012. Vol. 22, N 4. P. 273-280.
- [7] Samzadeh-Kermani A., Mirzaee M., Ghaffari-Moghaddam M. Polyvinyl alcohol/polyaniline/ZnO nanocomposite: synthesis, characterization and bactericidal property // *Adv. Biol. Chem*. 2016. Vol. 6, N 1. P. 1-11.
- [8] Olad A., Barati M., Shirmohammadi H. Conductivity and anticorrosion performance of polyaniline/zinc composites: Investigation of zinc particle size and distribution effect // *Progress in Org. Coatings*. 2011. Vol. 72, N 4. P. 599-604.
- [9] Zhou S., Wu T., Kan J. Effect of Co^{2+} , Ni^{2+} , Cu^{2+} , or Zn^{2+} on properties of polyaniline nanoparticles // *J. Appl. Polym. Sci*. 2007. Vol. 106. P. 652-658.
- [10] Liu G., Freund M.S. New Approach for the controlled cross-linking of polyaniline: Synthesis and Characterization // *Macromolecules*. 1997. Vol. 30, N 19. P. 5660-5665.
- [11] Liu G. Synthesis and characterization of modified polyanilines. Thesis of Master of Sciences in Chemistry. 1997. 85 p.
- [12] Complexometric titration: methodical instructions for performing laboratory work on the course of quantitative chemical analysis / Pod red. Yakovleva K. I., Stetsenko A. I. St. Petersburg: Izd-vo SPHFA, 2003. 48 p.
- [13] Stejskal J., Gilbert R.G. Polyaniline. Preparation of a conducting polymer // *Pure Appl. Chem*. 2002. Vol. 74, N 5. P. 857-867.

Резюме

Н. М. Иванова, Е. С. Лазарева, Я. А. Висурханова, Е. А. Соболева

ПОЛИАНИЛИННІҢ АНИЛИНФОРМАЛЬДЕГИДТІ ПОЛИМЕРМЕН МЫРЫШҚҰРАМДЫ КОМПОЗИТТЕРІНІҢ ҚҰРЫЛЫСЫ ЖӘНЕ БЕЛСЕНДІЛІГІ

Жұмыста, АФП қатысында анилинді $ZnCl_2$, ZnO немесе мырыш шаңын (Zn) тотықтырып полимерлеу үрдісіне еңгізу арқылы алынған, полианилин (ПАни) және анилинформальдегидті полимердің (АФП) аралас полимерінің негізіндегі мырыш-құрамды композиттерінің құрылысын және электркатализдік белсенділігін зерттеу нәтижелері көрсетілген. Синтездеу жағдайларымен және еңгізілген допанттармен анықталатын, синтезделген композиттердің фазалық құрамдары анықталған. Мырыш катиондарының электрохимиялық тотықсыздануы және оның микро- және нанобөлшектері қалыптасуы нәтижесінде *o*-нитроанилиннің электргидрленуінде, алынған полимер-мырышты композиттері электркатализдік белсенділік көрсететіні анықталған.

Түйін сөздер: полианилиннің анилинформальдегидті полимермен композиттері, мырыш (II) хлориді, мырыш шаңы, мырыш (II) оксиді, электркатализдік гидрлеу, *o*-нитроанилин.

Резюме

Н. М. Иванова, Е. С. Лазарева, Я. А. Висурханова, Е. А. Соболева

СТРОЕНИЕ И ЭЛЕКТРОКАТАЛИТИЧЕСКАЯ АКТИВНОСТЬ ЦИНКСОДЕРЖАЩИХ КОМПОЗИТОВ ПОЛИАНИЛИНА С АНИЛИНОФОРМАЛЬДЕГИДНЫМ ПОЛИМЕРОМ

В работе представлены результаты исследований строения и электрокаталитической активности цинксодержащих композитов на основе смешанного полимера из полианилина (ПАни) и анилинформальдегидного полимера (АФП), полученных введением $ZnCl_2$, ZnO или цинковой пыли (Zn) в процессе окислительной полимеризации анилина в присутствии АФП. Установлены фазовые составы синтезированных композитов, определяемые условиями синтеза и природой вводимого допанта. Показано, что полученные полимер-цинковые композиты проявляют электрокаталитическую активность в электрогидрировании *o*-нитроанилина благодаря осуществлению электрохимического восстановления катионов цинка (II) и формированию его микро- и наночастиц.

Ключевые слова: композиты полианилина с анилинформальдегидным полимером, хлорид цинка (II), цинковая пыль, оксид цинка (II), электрокаталитическое гидрирование, *o*-нитроанилин.

M. M. NYKMUKANOVA¹, B. K. YESKALIYEVA², G. SH. BURASHEVA²

¹S. Amanzholov East Kazakhstan State University, Ust-Kamenogorsk, Republic of Kazakhstan,

²Al-Farabi Kazakh National University, Almaty, Republic of Kazakhstan.

E-mail: nykmukanova@mail.ru

SEPARATION FLAVONOIDS BY SORBENT RP-18 FROM *VERBASCUM MARSCHALLIANUM*

Abstract. Investigating studies of biologically active substances from the ground parts of the family *Scrophulariaceae* genus of *Verbascum marschallianum* growing in the Altai region of Kazakhstan flavonoids were studied. Raw materials (aboveground part *Verbascum marschallianum*) for research are harvested during the budding period in the territory of East Kazakhstan. For the first time, an effective RP-18 sorbent was used for the isolation flavonoid complex from the raw material and the individual compound (cinorazide) was obtained by high-performance chromatography (HPLC). The structure of the compound is solved by chemical (acid hydrolysis) and spectral: ¹H and ¹³C NMR, UV, IR spectroscopy and mass spectrometry.

Key words: *Verbascum marschallianum*, biologically active substances, RP-18 sorbent, high-performance liquid chromatography, acid hydrolysis, flavonoids, 7-O-β-D-glucopyranoside of luteolin (cynorazide).

In the Republic of Kazakhstan there is considerable scientific and technical potential in the field of development and production of herbal medicines, an extensive resource base and the possibilities for its further strengthening. Namely, the Altai territory has such a variety of zonal and intrazonal landscapes in particular, it could not affect the abundance and species diversity of the plant world. The creation of highly effective domestic production facilities, the proposal of new methods for the isolation of biologically active complexes are a priority and actual task.

The genus *Verbascum L.*, common name mulleins, comprises about 370 species of flowering plants in the *Scrophulariaceae* family, predominantly distributed in Asia, Europe and North America [1]. The genus *Verbascum* belonging to the *Scrophulariaceae* family is the richest genus, represented in Turkish flora by 230 species, of which 185 are endemic [2]. In Kazakhstan, there are 9 species of mullein [3] and according to the latest data there are 10 species [4]. *Verbascum marschallianum* not completely investigated.

The object of study – the aboveground part of the genus *Verbascum marschallianum* prepared in phase fruiting in August 2017 from the Altai region of Kazakhstan. By general methodology of research I edition of State Pharmacopoeia of the Republic of Kazakhstan in the study raw materials are defined: loss on drying, extractives, total ash and quantitative of biologically active substances [5]. In plant raw materials by quantitative analysis revealed a large number of flavonoids, iridoids and tannins [6].

For the preparation of biologically active substances dried aerial part (500 g) of plants of the genus *Verbascum* (family Scrophulariaceae) was crushed to size particles of 2-3 mm, extraction was carried out with 100% methyl alcohol in Soxlet. Received the extract was defatted, filtered, concentrated and dried under vacuum. Then the dry extract was treated with hexane, dichloromethane and n-butanol. The n-butanol extract was concentrated dryness on a rotary evaporator at a temperature of 40-45°C and obtained the butanol extract with flavonoid complexes (26.5 g).

The availability of flavonoids in the extract was detected by a yellow stain using two-dimensional paper chromatography (Watman S2 paper grade, Germany) in the system butanol: acetic acid: water (40: 12.5: 29) and 6% acetic acid as an indicator 1% AIS in aqueous solution and by thin-layer chromatography (Silica gel DC-Alugram 60 UV254, Merck firma) in the system dichloromethane: methanol, cerium sulfate was used as an indicator.

For the separation of substances from the butanol extract used adsorption chromatography using silica gel sorbent. Elution of polarity to dichloromethane: methanol solution resulted in 213 fractions. Using a TLC method using specific developers, similar fractions were combined and obtained VB-1 (1.8 g), VB-2 (4.4 g), VB-3 (3.5 g), VB-4 (5.5 g) flavonoid complexes. From the VB-1 fractions, re-chromatography on RP-18 (LiChrospher® 100, Merck firm) (methanol: water 1: 9, 3: 7, 1: 1) yielded VB-A fractions. Fractions VB-A by using NP-HPLC (preparative recycling JAI-LC-908 HPLC, Japan Analytical Industry Co., Tokyo, Japonia) on a Sil-D-60-10 silica gel column (250 × 20 nm × 5 μm) (eluent chloroform: methanol 9.5-0.5) substances **1** (25 mg) were isolated.

According to UV spectra and a result of acid hydrolysis, glycosidic bonds, flavonoid and carbohydrate structures, which are identified with taps [7, 8].

The obtaining 4 polyphenolic complex fractions (figure 1) of the butanol extract were detected in a yellow shade in paper and thin-layer chromatography, then the VB-1 fraction was chromatographed on a RP-18 column, resulting in 6 compounds (figure 2), of which two were similar flavonoids (R_f value).

The spots in the UV light were dark brown. Using of developer of cerium sulfate, the spots were stained from light yellow to dark brown. To obtain 1 substance, was used HPLC with sorbent silica gel (Sil-D-60-10). As a result of three times recrystallization in methanol and an unchanged spot in TLC, it proves that substance 1 is pure (figure 3). According to the Bryant Method, substance 1 refers to glycosides [9].

Luteolin-7-O-β-glucopyranoside - light yellow crystals, $C_{21}H_{20}O_{11}$, ESI-MS, m/z : 471 $[M+Na]^+$ and m/z : 270 $[M]^+$. $T_{\text{melting}} = 259-263^{\circ}C$. The UV spectrum of this compound has a maximum absorption at a wavelength of 254, 338 nm, which is typical for flavones. When sodium acetate is added to the solution of the substance, the shifts do not occur (254, 338 nm), so the 7-OH group is replaced. With sodium hydroxide, we observe a bathochromic shift of band I at 44 nm, band II at 8 nm, hence the molecule contains free phenolic hydroxyl groups.

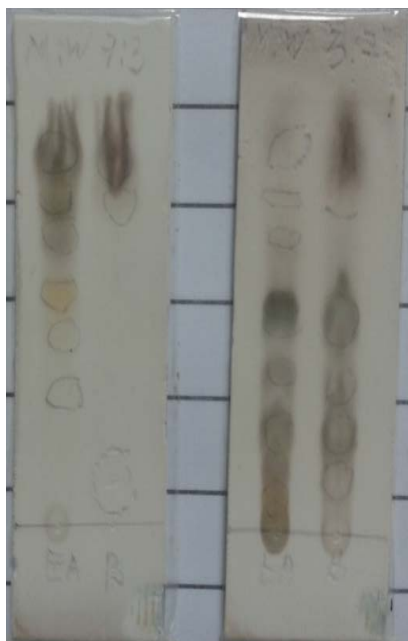


Figure 1



Figure 2



Figure 3

In the IR spectrum, there are bands of vibrations of hydroxyl groups - $3515-3600 \text{ cm}^{-1}$, carbonyl-pyrone 1655 , aromatic $C=C$ bonds 1528 , 1360 , $C-O$ glycoside oscillations 1080 , β -coupling between aglycone and sugar 890 , and $1060, 1040, 1030 \text{ cm}^{-1}$ sugar in glycoside in the form of pyranose, and so according to IR and UV data refers to flavones.

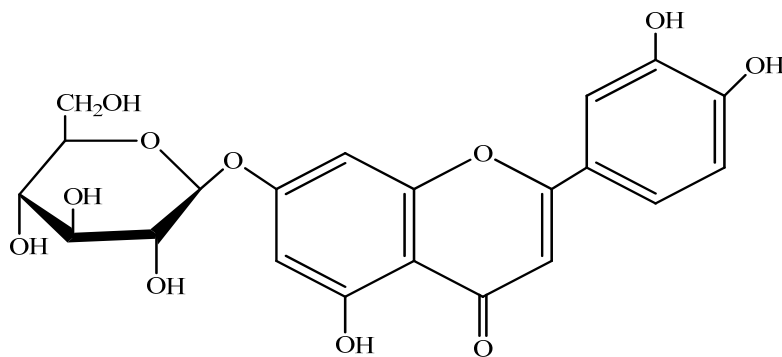
In the $^1\text{H-NMR}$ and DEPT-135 spin system, the lower field is located an anomeric glucose proton $\delta 5.05$ (1H, d, $J = 7.0 \text{ Hz}$) shows that the glycoside in the β -configuration. Chemical shifts of H-6 and H-8 (respectively $0.2 + 0.3 \text{ ppm}$) shows, that C-7 is bonded with sugar.

$^1\text{H NMR}$ spectra (600 MHz, Piridin, δppm) shows signals of 5,7,3',4'-tetrasubstituted flavon and sugar: 6.72 (1H, s, H-3), 6.55 (1H, s, H-6), 6.77 (1H, s, H-8), 7.37 (1H, s, H-2'), 6.81 (1H, d, $J = 8.5 \text{ Hz}$, H-5'), 6.75 (1H, d, $J = 8.8 \text{ Hz}$, H-6'), 5.10 (1H, d, $J = 7.0$, H-1''), $3.19-3.45$ (1H, t, H-2''), $3.19-3.45$ (1H, t, H-3''), 3.31 (1H, t, $J = 8.8$, H-4''), 3.11 (1H, m, H-5''), 3.76 (1H, d, $J = 12.0$, H-6''a), 3.55 (1H, d, $J = 12.8$, H-6''b).

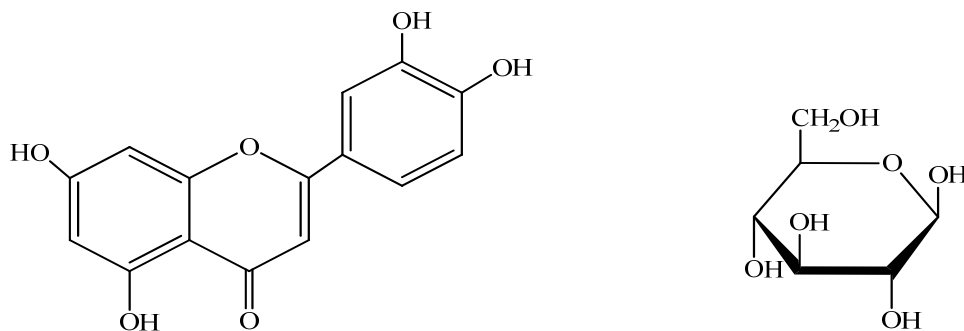
$^{13}\text{CNMR}$ (100 MHz, Piridin, δppm): 165.2 (C-2), 104.3 (C-3), 182.2 (C-4), 159.5 (C-5), 102.5 (C-6), 164.3 (C-7), 95.2 (C-8), 161.8 (C-9), 105.8 (C-10), 122.4 (C-1'), 115.5 (C-2'), 147.6 (C-3'), 151.2 (C-4'), 117.1 (C-5'), 120.0 (C-6'), 100.6 (C-1''), 74.2 (C-2''), 75.9 (C-3''), 70.2 (C-4''), 77.5 (C-5''), 61.5 (C-6'')

A complete acid hydrolysis of the substance was carried out with a mixture of 5 ml of 5% hydrochloric acid and ethanol (1: 1) for 2 hours, and the resulting aglicon was alkaline hydrolysed with 50% potassium hydroxide, using nitrogen

for 20 minutes. As a result, luteolin and glucose were obtained. The hydrolysis products were identified using the TLC method. Based on physicochemical methods of analysis and comparison with the literature data, substance 1 is identified as luteolin-7-O- β -glucopyranoside [10, 11].



Luteolin-7-O- β -glucopyranoside (Substance 1.)



Luteolin β -D-glucose

For the first time from plant of genus *Verbascum marschallianum* growing in Altai region of Kazakhstan was studied chemical investigation and for separation flavonoid complexes an effective sorbent is proposed RP-18 and individual compounds are obtained using high performance liquid chromatography. Luteolin-7-O- β -glucopyranoside (cinorazide) first time obtained from genus of *Verbascum*. The structure of the compound is solved by chemical (acidic, alkaline hydrolysis) and spectral: 1D ($^{13}\text{C-NMR}$, $^1\text{H-NMR}$), 2D (HMBC, HSQC, COSY, NOESY), IR, UV spectroscopy and mass spectrometry (EIMS, ESI-MS, FAB-MS).

REFERENCES

- [1] Fedchenko B.A. Mullein - Verbascum // Flora of the USSR. - Leningrad: Izd. Academy of Sciences of the USSR, 1955. Vol. 22. P. 122. (Rus.).
- [2] Huber A. Morath Flora of Turkey and the East Aegean Islands. 1978. Vol. 6. P. 461.
- [3] Pavlov N.V. Flora of Kazakhstan. Almaty: Academy of Sciences of the Kazakh SSR, 1960. Vol. 8. P. 26-33. (Rus.).
- [4] Baitenov M.S. Flora of Kazakhstan. Almaty: Lent, 1999. Vol. 1. P. 158. (Rus.).
- [5] Silanteva M.M. Abstract of the flora of the Altai Territory. Barnaul, 2013. P. 282-297. (Rus.).
- [6] Nykmukanova M.M., Turalieva A.S., Yeskaliyeva B.K., Burasheva G.Sh. Comparative analysis of the mineral and acid composition of Verbascumthapsus and Verbascummarschallianum // Bulletin of KazNU. Chem. 2017. N 1. P. 27-32. (Rus.).
- [7] Mabry T.S., Markham R.K., Thomson M.B. The systematic identification of flavonoids // Springer-Verlag. Berlin-Heidelberg-New York, 1970. Vol. 29, N 10. P. 151.
- [8] Andersen O.M., Kenneth R. Markham. Flavonoids: Chemistry, Biochemistry and Applications // CRC Press. 2005. Vol. 26. P. 1256.
- [9] Bryant E.T. A note of the differentiation between flavonoid glycosides and their aglycones // J. Amer. Pharm. Assoc. 1950. Vol. 39, N 8. P. 480-488.
- [10] Bonacheva V.M. Drenin A.A. Botirov E.H. Flavonoids Equisetum Arvence L. and LathyrusPratensis L. // Chemistry of plant raw materials. 2014. N 3. P. 195-199. (Rus.).
- [11] Yusifova D.Yu. Movsumov I.S. Flavonoids and triterpenesaponins Scabiosa HyrcanicaStev., growing in Azerbaijan // Chemistry of plant raw materials, 2015. N 2. P. 261-264. (Rus.).

Резюме

М. М. Ныкмуканова, Б. К. Ескалиева, Г. Ш. Бурашева

VERBASCUM MARSCHALLIANUM ӨСІМДІГІНЕН
RP-18 СОРБЕНТІ КӨМЕГІМЕН ФЛАВОНОИДТЫ БӨЛУ

Қазақстанның Алтай өңірінде өсетін *Scrophulariaceae* (сабынкөкгүлділер) тұқымдас құрамындағы биологиялық белсенді заттарды зерттеуді жалғастыра отырып, *Verbascum marschallianum* (Маршалла аюқұлағы) өсімдігінен флавоноидтар кешені алынды. Зерттеуге арналған шикізат (*Verbascum marschallianum* жер үсті бөлігі) Шығыс Қазақстан аймағынан жеміс беру кезінде жиналған. Алғаш рет аталған шикізаттан флавоноидтар кешенін бөлуде тиімді сорбент ретінде RP-18 пайдаланып, жеке зат – лютеолиннің 7-О-β-D-глюкопиранозиді (циноразид) жоғары эффективті сұйықтық хроматография (HPLC) көмегімен бөлінді. Жеке заттың құрылысы химиялық (қышқылдық гидролиз) және спектралды (¹H, ¹³C ЯМР, УК-, ИҚ-спектроскопия және масс-спектрометрия) әдістермен дәлелденді.

Түйін сөздер: *Verbascum marschallianum*, биологиялық белсенді заттар, RP-18 сорбенті, жоғары эффективті сұйықтық хроматографиясы, қышқылдық гидролиз, флавоноидтар, лютеолиннің 7-О-β-D-глюкопиранозиді (циноразид).

Резюме

М. М. Ныкмуканова, Б. К. Ескалиева, Г. Ш. Бурашева

**ВЫДЕЛЕНИЕ ФЛАВОНОИДА С ПОМОЩЬЮ СОРБЕНТА RP-18
ИЗ РАСТЕНИЙ *VERBASCUM MARSCHALLIANUM***

Продолжая исследования биологически активных веществ у представителей семейства *Scrophulariaceae* (Норичниковые), изучены флавоноиды надземных частей *Verbascum marschallianum* (коровяк Маршалла), собранного из Алтайского региона Казахстана в период бутонизации. Для получения флавоноидного комплекса из надземных частей *Verbascum marschallianum* впервые использован эффективный сорбент RP-18 и с помощью высокоэффективной хроматографии (HPLC) выделено индивидуальное соединение (циноразид). Структура выделенного вещества доказана химическими (кислотный гидролиз, щелочное расщепление) и спектральными: (^1H и ^{13}C ЯМР, УФ-, ИК- и масс-спектрометрия) методами.

Ключевые слова: *Verbascum marschallianum*, биологически активные вещества, сорбент RP-18, высокоэффективная жидкостная хроматография, кислотный гидролиз, флавоноиды, 7-О-β-D-глюкопиранозид лютеолина (циноразид).

ZH. M. YERGALYIEVA, G. E. AZIMBAEVA

Kazakh State Women's Pedagogical University, Almaty, Republic of Kazakhstan

METHODS OF DISTRIBUTION OF THE POLYPHENOL EXTRACTS FROM THE LEAVES OF A PLANT CARTHAMUS

Abstract. From the *Carthamus* plant leaf are extracted polyphenol extracts, composition and construction have been proven by methods of IR, UV spectral analysis. Ether extract is 3%, 360 nm wavelength $\epsilon = 4,070$ Rutine, Ethyl Acetate Extract 3,2%, its wavelength 350 nm, $\epsilon = 4,268$ Quercetin compound, 90% ethyl alcohol 2,92%, 365 nm Wavelength, $\epsilon = 4,359$ in the zone of quercetin, and 70% in ethyl alcohol 3,64%, 331 nm wavelength, $\epsilon=4,359$ in the zone of euclidein and the final 50% of ethyl alcohol in the extract was 2,79%, 329 nm, $\epsilon=4,614$ according to the compound of the acid compound.

Key words: carthamus, polyphenol extracts, biologically active substances.

Introduction. Plants are the main source of various organic and biologically active substances, including the most common compounds in nature: flavonoids, caratinoids, polyphenols, ethanols, alkaloids, terpenoids, essential oils, phenolic acids, amino acids, trace elements, vitamins. Natural compounds are widely used in medicine. However, the knowledge and methods of chemistry of natural compounds are very important in their distribution, purification, construction, production and product quality control [1].

Carthamus (translation in Kazakh language – Мақсары) is a plant, oilseed crop, belonging to a sophisticated flower family. The main homeland is Ethiopia and Afghanistan. *Carthamus* grows in Central Asia - in Uzbekistan and Kazakhstan. Today it is grown in Azerbaijan, India, Egypt, Iran, Central and South America, Australia and Western Europe. *Carthamus* plant is one of the most widely studied medicinal plants [2, 3].

According to historical data, the Xinjiang region is one of the earliest cultures of the carthamus. The appearance of the Great Silk Road contributed greatly to the spread of carthamus and its exploration. Today, carthamus includes cuisine, medicine, cosmetics and in other areas.

The southern regions of the republic cultivating of carthamus plant. The main homeland of the Mediterranean coast, the carthamus, has not been long enough to grow and produce products in the country. It's just that recently. The main product from it is gingerbread. The quality of carthamus oil is not less than sunflower and cottonseed. You can not say that the price is as expensive as that. It is much cheaper than cotton oil [4, 5].

Carthamus plant stems are vertical, spruce, lumpy, height up to 90 cm. The leaves are oval, the edges can be the sting. Flower bricks - baskets, from one 5-6 to 30-50 baskets in one plant. The flowers are like a yellow or orange tube. When the seeds ripen, they do not sprout on the ground. Weight of 1000 grains is 20-50 g. *Carthamus* is a heat-resistant, very desert-resistant. The growth period is

90-150 days. The cross is pollinated (by insects and by land), can also spontaneously spray. They do not need a special soil for grow. At a depth of 5-6 cm on a hectare of 6-10 kg per hectare, sow the system intervals 45-60 cm. Products are harvested from each hectare up to 8 centimeters. It is obtained from the seeds of 25-35% of the seeds, 46-60% of the seeds of fat, flower [6, 7].

Flower, leaf, seeds and oils of *Carthamus* plant are widely used in many countries for medical purposes. In Iran, fat is used for hepatic and heart treatments, while safflower is used in Pakistan for treating urinary tract infections with sugar, while carthamus oil in India is used for the treatment of gastric ulcer. China produces medications for various diseases. And we are feeding the cattle as long as we can not handle it.

Therefore, for the cheap and accessible natural home remedy, the study of the composition of medicinal plants grown in the country and the distribution of biologically active substances is one of the topical issues today. Including polyphenol extracts from the *Carthamus* plant.

Polyphenols are a simple potent antioxidant plant pigment. In addition to grapes, polyphenols are found in chocolate, shade, apple, and other coconut fruit, pomegranate juice, cranberries. Polyphenols are found to be in the form of additives with plants similar to those found in the molecular weights of 300-5000. Many of them are dissolved in water, diluted or boiled. Alkaline acids can be obtained on the basis of these sugars together with polyesters or complex dipepsid compounds [8, 9].

At present, about six thousand polyphenols are extracted from the plant composition. Polyphenols, along with useful plants, are contained in vegetables and fruits. In the human body, food contains about 1 g of antioxidant ingredients per day, with a few vitamins, containing about 100 mg of β -carotene, vitamins C, E. Polyphenol is a large number of atomic phenols and their derivatives. It a vital role in the biological role of plants in the world of metabolism. Plants are widely spread in the form of tanning substances (fluogridin, pyrogallol, etc.) and glucosides and essential oils. Polyphenols are found in many nutrients. Their oxidation products (such as quinones) create tasty odor and aromatic texture for the food products. Production polyphenols - catecholomein and some hormones and mediators (adrenaline and noradrenalin) [10, 11].

Polyphenols protect the skin against sunburn, ozone and other toxins and prevent aging. Cranberries can be used in diseases of the kidneys, renal disease. Polyphenols improve cardiovascular disease and bleeding. Polyphenols are important in the treatment of cancer, liver, kidney, diabetes, atherosclerosis, cancer and various diseases. The metabolism participates in photosynthesis process. Performs the function of a fundamental element that holds skin tissues. Therefore, doctors warn that excessive amounts of alcohol can have an adverse effect on the body. In addition, excessive use of polyphenols (such as the daily use of blue or black tea) may cause kidney and liver disease [12]. The aim of the work is determination of composition, composition and structure of polyphenols extracting from *Carthamus* plant leaf.

EXPERIMENTAL PART

The object of the study was leaf from autumn *Carthamus* plant, which was harvested in September and October 2014-2016, Boradilai village, Baydibek district, South Kazakhstan region.

Extraction method is used to extract polyphenols from Leaf leaves of *Carthamus*. It is separated by the fractionation of polyphenols from the *Carthamus* plant.

Polyphenols are extracted by extracting the raw material with water and aqueous alcohol, pure ether or ether alcohol to extract extracts. The resulting product is a cleaner product, followed by separation of the individual substances.

For extraction, first of all, the raw materials are cleaned, dried and sieved, the diameter of the sieve is 3-5 mm. 10 g of raw material are weighed. Extragent is extracted 3 times in 2 hours in hot distilled water, 1:10 in the leaves of the *Carthamus* plant. If the solution is filtered and used for inulin, it extracts the sunflower by the next fraction.

I fraction. For separation from polyphenols, including oxycoric acid and catechin, it is filtered through filter paper to extinction for 30 minutes at room temperature of 200C at 1: 5 with diethyl ether. The solvent is evaporated in a water bath on a porcelain plate. The resulting leaf extract is 3%.

II fraction. In the following fraction extracted leukocancias, dimeric prostanthanidins, oxycoric acid ether and other compounds are extracted with organic solvent 1: 1 or 1:20 at ethyl acetate for 2 hours, filtered by extraction and evaporated in a water bath. The resulting yield of leaf is 3.2%.

III fraction. 90%, 70%, 50% ethyl alcohol for 1 hour to 2 hours to pass to solution in the final fraction of extraction in 90%, 70%, 50% ethyl alcohol in various concentrates to dissolve in many solvents and other phenolic compounds is added to the refrigerant and extracted in a water bath. The extracted extracts account for 90% of ethyl alcohol in 2,92%, and 70% for ethyl alcohol in 3.64% and 50% in ethyl alcohol with 2,79% [13].

RESULTS AND DISCUSSION

The polyphenols were extracted from the I-III fraction by the KBr tablets in the 400-4000 cm^{-1} IR-Bruker ALFA spectrometer, and in UV-SI Analytics Uviline 9400-9100 spectroscopy.

The frequency of oscillations in the IR spectrum of polyphenols derived from *Carthamus* plant varies from 3429 to 3286 cm^{-1} with the aromatic C-H group. The oscillation frequency in the range of 2925-2919 cm^{-1} showed the oscillations of CH_2 groups, oscillations of the O-N groups of carboxylic acid in the range of 2853-2844 cm^{-1} , the oscillation frequency of carbon dioxide C=O in 1633-1710 cm^{-1} , and 1657 The frequency of oscillations of -1597 cm^{-1} corresponds to the groups of aromatic C=C, the frequency of the aromatic group CH_2 is 1455-1414 cm^{-1} , the frequency of aromatic CH_3 is 1381-1373 cm^{-1} , and the frequency of the fluctuation is 1256-1244 cm^{-1} -N group, the pendulum oscillation corresponds to the interval 993-843 cm^{-1} [14].

Table 1 – IR spectra of polyphenols derived from Carthamus leaf, cm⁻¹

Group	Extracts				
	Diethyl ether	Ethyl acetate	90% ethyl alcohol	70% ethyl alcohol	50% ethyl alcohol
ν_{Ar} C-H aromatic	3429	3362	3328	3296	3286
ν CH ₂	2923	2921	2919	2925	2925
ν OH carboxylic acids	2852	2851	2850		
ν C=O carboxylic acids	1733	1733	1713		
ν_{Ar} C=C		1657	1650	1651	1597
δ CH ₂	1455	1454	1453	1415	1414
δ CH ₃	1376	1376	1373	1381	
γ CH	1246	1244	1254	1256	
Pendulum oscillations	973	849	843	993	923

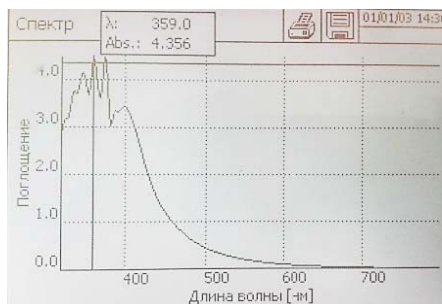
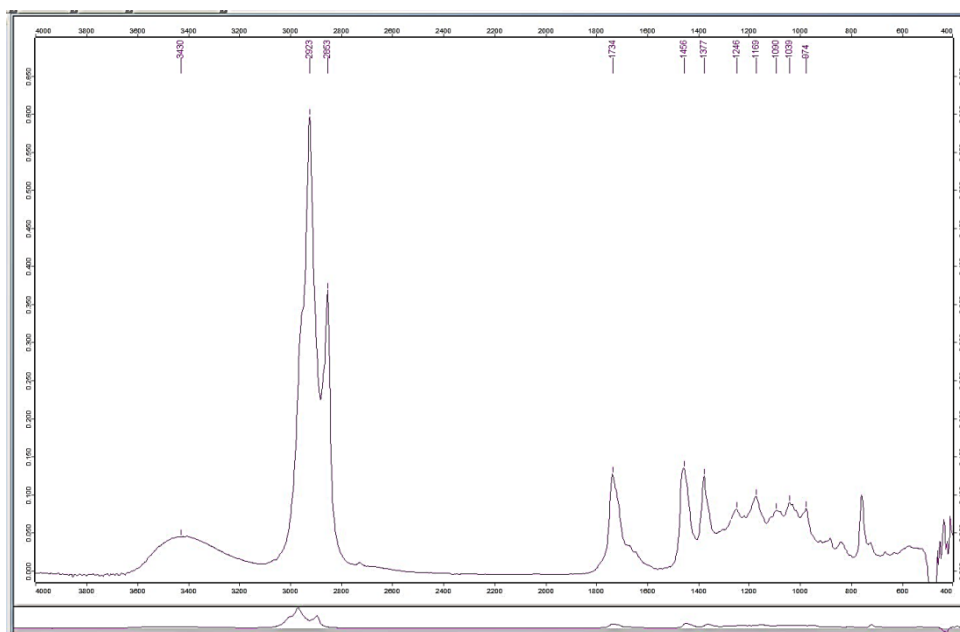


Figure 1 – IR, UV-spectrum extract of diethyl ether of Carthamus

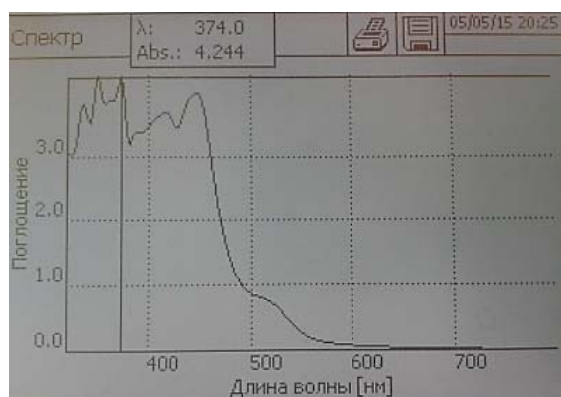
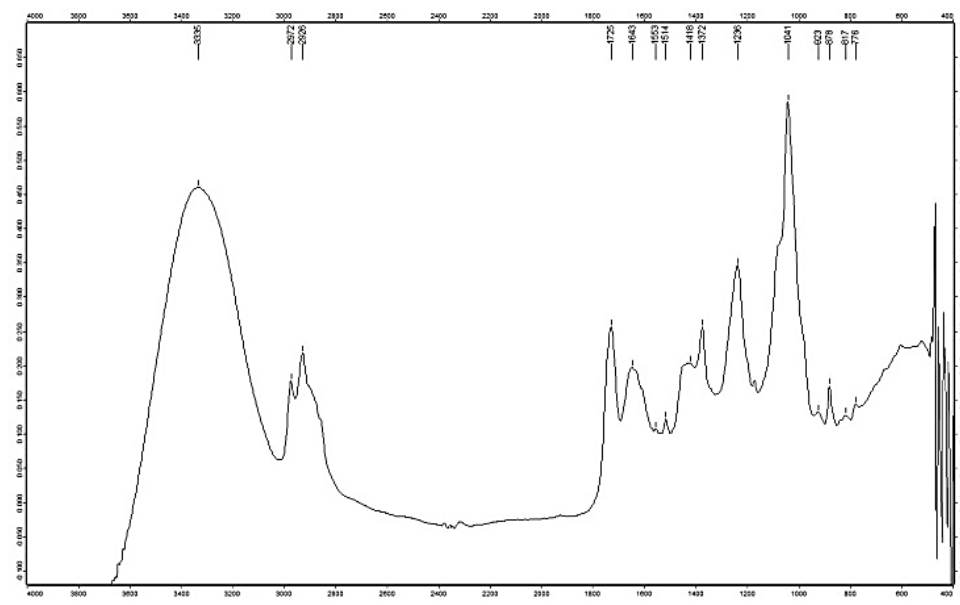


Figure 2 – IR, UV-spectrum extract of carthamus plant in ethyl acetate

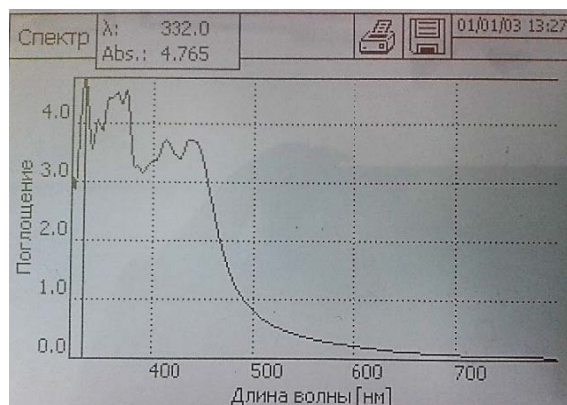
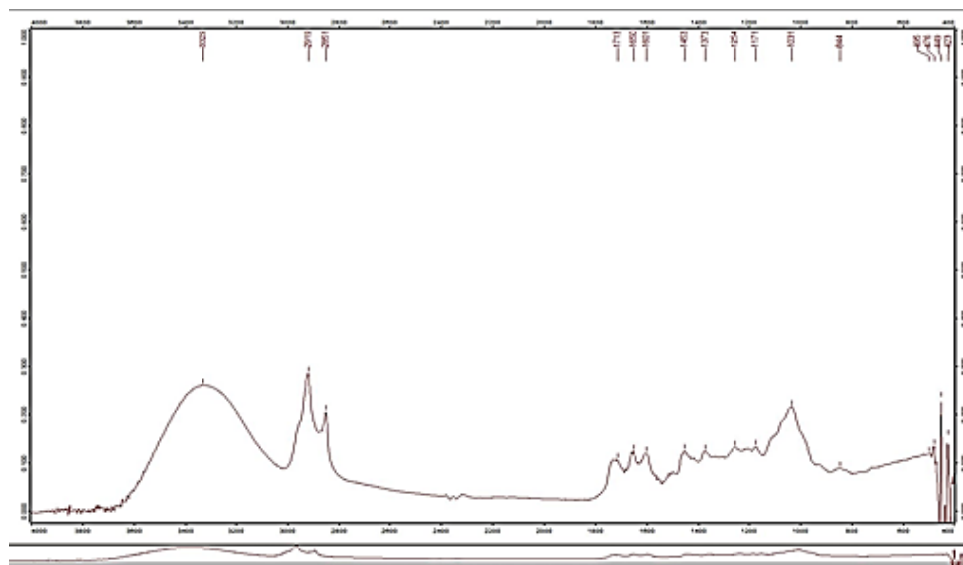


Figure 3 – IR, UV spectrum of 90% ethanol alcohol of Carthamus plant

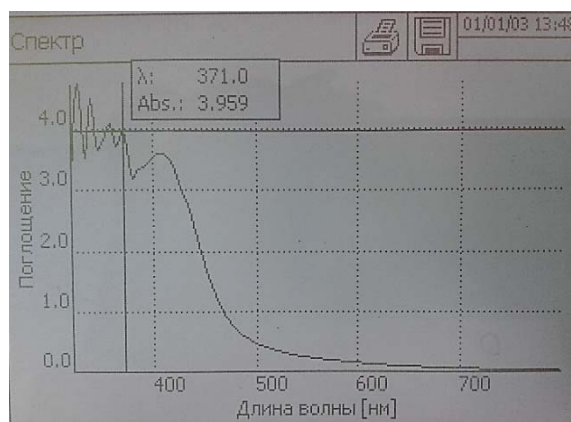
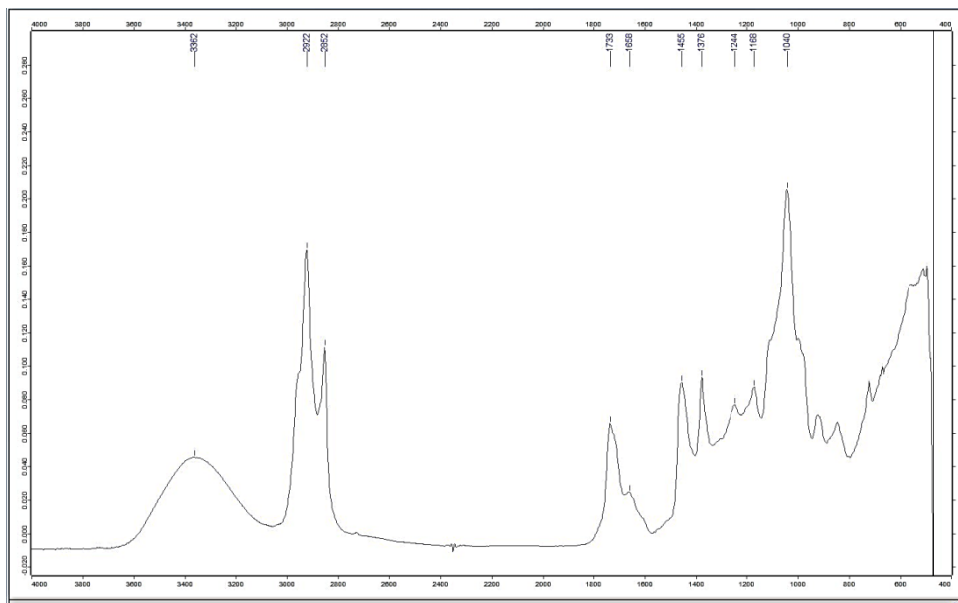


Figure 4 – IR, UV spectrum of extract of ethyl alcohol in 70% of Carthamus plant

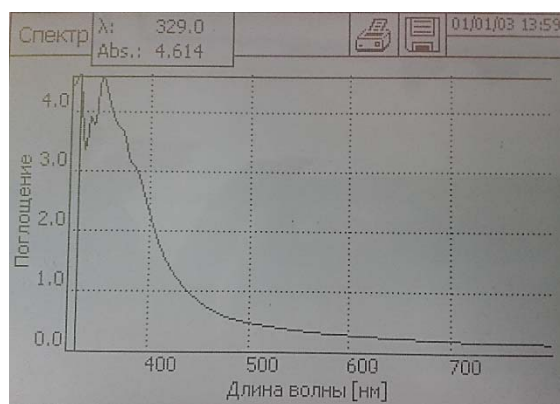
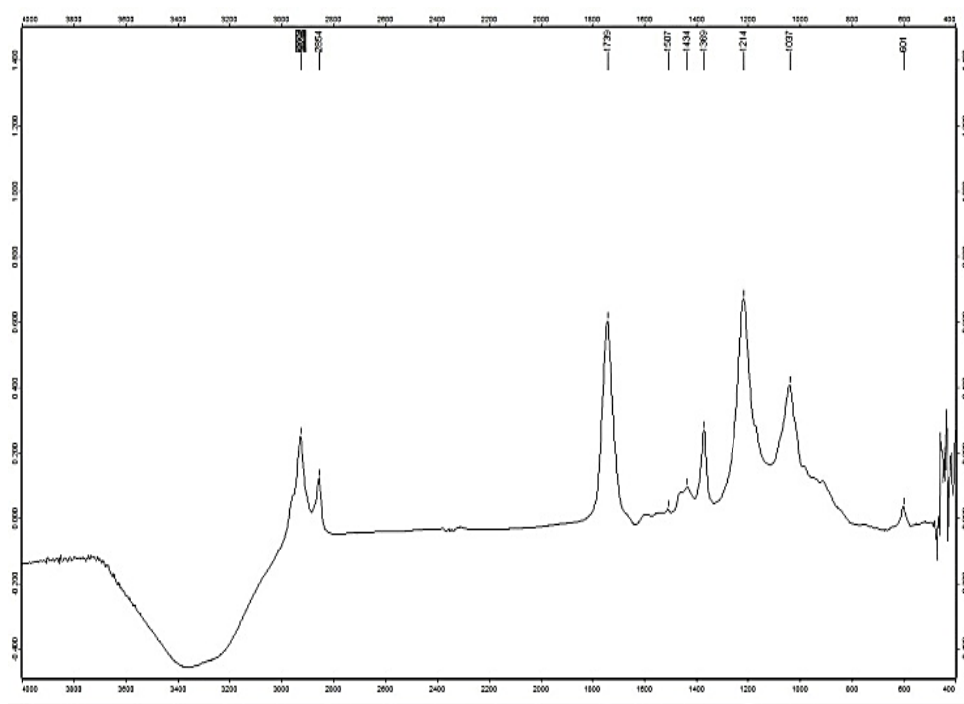
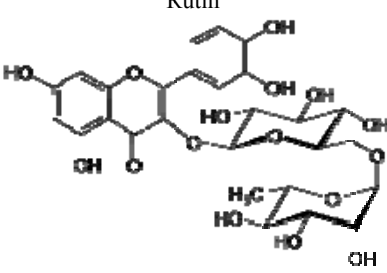
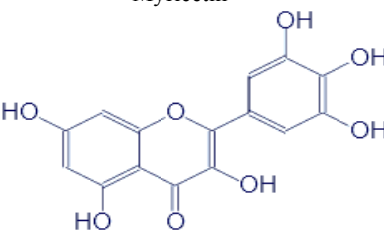
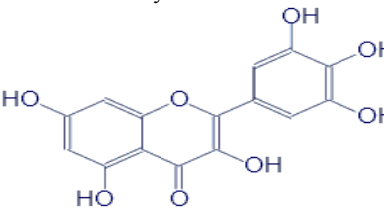
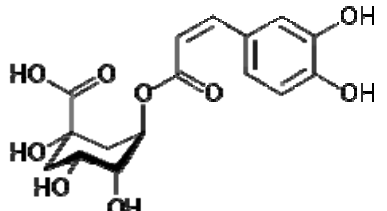


Figure 5 – IR, UV-spectrum extract of 50% of *Carthamus* plant in ethyl alcohol

Table 2 – The UV spectrum of polyphenols derived from Carthamus leaf

#	Specimen name	Wavelength, nm	E	Type of connection
1	Spectrum of extract of diethyl ether 50% sprayed Carthamus plant spray	359	4,356	<p>Rutin</p> 
2	Spectrum of Carthamus plant in ethyl acetate	374	4,244	<p>Myricetin</p> 
3	90% of the flower plant of Carthamus is an alcohol-soluble spectrum	332	4,765	<p>Esculite</p> $3,4(OH)_2C_6H_2 \left\langle \begin{array}{l} CH:CH \\ O-CO \end{array} \right.$
4		371	3,930	<p>Myricetin</p> 
5	50% of the Carthamus plant is an alcohol-soluble spectrum	329	4,614	<p>Chloroanic acid</p> 

The UV spectrum of polyphenols extracted from *Carthamus* leaf corresponds to 359 nm wavelength in diethyl ether, rutine in $\varepsilon = 4,356$ and 374 nm wt. In ethyl acetate, quercetin in $\varepsilon = 4,244$, 90% of the ethyl alcohol spatula with 365 nm wavelength, $\varepsilon = 4,359$ in the zone of quercetin and 70% in alcohol, 331 nm wavelength, $\varepsilon = 4,514$ in the zone of esculite and in the last 50% alcohol spirits, the wavelength range is 329 nm, and $\varepsilon = 4,614$ refers to a chlorogenic acid compound [15].

Conclusion.

1. Polyphenol extracts from the *Carthamus* plant leaf are extracted, composition and structure are proven by methods of IR, UV-spectral analysis.
2. *Carthamus* leaf contains rutin, myricetin, quercetin, esculite, chloroanic acid.

REFERENCES

- [1] The National Encyclopedia of Kazakhstan. Almaty: The Kazakh Encyclopedia, 2009. P. 315. (Kazakh).
- [2] Polymbetova F., Abiyev S., Sarsenbaev B. Travel to the world of useful vegetation Almaty: Science, 1999. P. 46-47. (Kazakh).
- [3] Zimin B.M. The Library of Pharmaceutical Journal, the Comprehensive Medicine and Science. Almaty, 1993. P. 153. (Russian).
- [4] Kenesarina N.A. Plant physiology and basics of biochemistry. Akmola: Agrarian University, 2005. P. 68. (Kazakh).
- [5] Lazurevsky G.V., Terentyeva I.V., Shamshurin Sh.Sh. Practical work on chemical constitution. M.: Search. The Higher School, 1966. P. 17.
- [6] Ayazbekova M.A., Yerzhanov B.K. Chemistry of esophagus products. Almaty: Search. "ATU", 1999. P. 60-60. (Russian).
- [7] Lazurevsky G.V., Terentyeva I.V., Shamshurin Sh.Sh. Practical work on chemical constitution. M.: Search. The Higher School, 1966. P. 17. (Russian).
- [8] Balzarini J. The mannose – specific plant lectin from *Cymbidium hybridum* and *Epipachis helleborine* and the specific plant lectin *Urticadioca* / J. Balzarini, J. Neyts, M. Schols Hosoya // *Antiviral Res.* 1992. Vol. 18. P. 191-207.
- [9] Vegetable resources of the USSR: Spattering, their chemical composition, use: *Semirestia Magnoliaceae - Limoniaceae* / [Redkol: Sokolov PD [gl.] And L.: Nauka, 1984. P. 460. (Russian).
- [10] Korulkin D.U. Polyphenols of *Sedum* in *Rastenia*. Almaty, 1998. (Russian).
- [11] Policarpova T.A. Polyphenols production. Dissection of catechins from the green chay. 2004. P. 25-31. (Russian).
- [12] The National Encyclopedia of Kazakhstan. Almaty: The Kazakh Encyclopedia, 2004. P. 315.
- [13] Yergaliyeva Zh.M., Azimbayeva G.E., Research and distribution of extracts of phenolic compounds of the *Carthamus* plant // International scientific-practical conference on development of science and education in natural sciences. Almaty, 2016. P. 226-229. (Kazakh).
- [14] Tarasevich B.N. IR spectrum of basic classes of organic compounds, M.V.Lomonosov Moscow State University, chemistry faculty, Organic Chemistry Department. Moscow 2012. P. 25. (Russian).
- [15] Ergalieva Zh.M., Azimbayeva G.E. Methods of distribution of polyphenols from flower of *Carthamus* // 3rd international congress on social sciences, China to adriatic. Antalya, 2016. P. 20-24. (Kazakh).

Резюме

Ж. М. Ергалиева, Г. Е. Азимбаева

**CARTHAMUS ӨСІМДІГІНІҢ ЖАПЫРАҒЫНАН
ПОЛИФЕНОЛ ЭКСТРАКТЫЛАРЫН БӨЛУ ӘДІСТЕРІ**

Carthamus өсімдігінің жапырағынан полифенолды экстрактылары бөлініп, құрамы мен құрылысы ИҚ-, УК-спектрлік анализ әдістері арқылы дәлелденді. Өйткені, полифенолды қосылыстар медицинада қабынуға қарсы, уылдыратын, қан тоқтататын, ауруға қарсы және бактерия жойғыш құралы ретінде, қартаю процессін баяулатып, жалпы иммунды жүйені күшейтеді, өсімдікпен және металл тұздарымен уланғанда, ағзадағы радиоактивті заттарды шығаруда, рак ауруларын, асқазан-ішек жолдарының қабынуында, кілегейлі қабықтардың қабынуында және т.б. ауруларды емдеуде қолданылатын таптырмайтын дәрілік препарат.

Түйін сөздер: мақсары, биологиялық белсенді заттар, полифенолды қосылыстар.

Резюме

Ж. М. Ергалиева, Г. Е. Азимбаева

**МЕТОДЫ ВЫДЕЛЕНИЯ ПОЛИФЕНОЛЬНЫХ ЭКСТРАКТОВ
ИЗ ЛИСТЬЕВ CARTHAMUS**

Выделены полифенольные экстракты из листьев Carthamus, состав и структура была подтверждена с помощью ИК-, УФ-методов анализа. Полифенольные соединения применяются в медицине, как противовоспалительные, вяжущие, кровоостанавливающие, как средство замедления процесса старения, для укрепления иммунной системы, связывания солей металлов, радиоактивных веществ в организме, при отравлении, раке, воспалении желудочно-кишечного тракта, слизистых оболочек и т.д.

Ключевые слова: сафлор, биологически активные вещества, полифенольные соединения.

T. P. MIKHAILOVSKAYA, R. KURMAKYZY, D. K. TOLEMISOVA, P. B. VOROBYEV

«A.B. Bekturov Institute of Chemical Sciences» JSC, Almaty, Republic of Kazakhstan

**MODIFYING THE INFLUENCE OF TITANIUM AND
ZIRCONIUM DIOXIDES ON THE PROPERTIES
OF THE VANADIUM OXIDE CATALYST
IN THE VAPOR-PHASE OXIDATION OF 3-METHYLPYRIDINE**

Abstract. The nature of the modifying effect of titanium- and zirconium dioxide on the properties of the vanadium oxide catalyst in the vapor-phase oxidation of 3-methylpyridine is discussed. It was found that the vanadium oxide catalyst, modified by TiO_2 and ZrO_2 additions, showed the highest activity in the studied process. Nicotinic acid was obtained with the yield of 68% at 270 °C and a molar ratio of 3-methylpyridine: O_2 : H_2O = 1:13:94.

Key words: oxidation, 3-methylpyridine, nicotinic acid, catalysts.

Introduction. Nicotinic acid (NA - niacin, vitamin PP, vitamin B₃) is a vitamin that participates in many oxidative reactions of living cells [1]. Nicotinic acid and its derivatives have a wide variety of physiological properties, due to which they are widely used in medicine and agriculture as vitamins, medicines, plant growth regulators. Nicotinic acid is used to enrich food and animal's feed [2].

Several methods for the preparation of nicotinic acid are known [3]: 1) liquid-phase oxidation: a) oxidation of 3-methylpyridine (3-MP) or β -quinoline with KMnO_4 in an alkaline medium. Disadvantages: high expense of expensive KMnO_4 , the difficulty of implementing continuous technology, the complexity of the scheme for processing queen cells, a large amount of MnO_2 waste, the difficulty of mechanization and automation of the process, the high cost of nicotinic acid; b) oxidation with 30% nitric acid. Disadvantages: high aggressiveness of the environment with the use of HNO_3 , which requires the use of expensive corrosion-resistant equipment with special coatings (titanium, cobalt or tantalum), the need for complex absorption systems for nitrogen oxides, complex systems for nitric acid regeneration, a system for cleaning gas emissions, a large amount of waste, acid waste water, a large potential explosion hazard of the process.

Recently, the search for vapor-phase direct oxidation of 3-methylpyridine with air oxygen into nicotinic acid is of special attention. Transition metal oxides are widely used for the preparation of catalysts for the vapor-phase oxidation of methylpyridines. For example, titanium and zirconium oxides are widely used as components of catalytic systems [4-6]. The practical importance of the target product causes interest in finding new effective contacts and studying the effect of oxide additives on the catalytic properties of an oxide-vanadium catalyst.

In this connection, the purpose of this work is to study the effect of titanium dioxide and zirconium dioxide on the catalytic properties of the oxide-vanadium contact in the reaction of vapor-phase oxidation of 3-methylpyridine.

EXPERIMENTAL

In this work used 3-MP, by boiling point 140 °C (692 mm, $d_4^{20} = 0.9568$, $n_D^{20} = 1.5050$) which has been dried and distilled. These characteristics corresponded to the reference data.

As initial components of the catalysts, we used vanadium pentoxide, titanium and zirconium dioxides. The initial oxides in a particular ratio were ground in a porcelain mortar to form a homogeneous batch, which was then compressed into tablets of 15 mm in diameter and 3-4 mm in thickness and calcined at 350 and 640 °C for 4 hours. After cooling, the tablets were crushed into grains of 3-5 mm in size.

The oxidation of 3-MP was carried out in a continuous installation of reaction tube made of stainless steel with a diameter of 20 mm and a length of 150 mm into which 9 ml of a granular catalyst was loaded. The unreacted 3-MP and reaction products were trapped in air-lift type scrubbers filled with water and analyzed by gas-liquid chromatography. NA was titrated with 0,035 N alkali using phenolphthalein.

The deep oxidation products were analyzed by LXM-8MD chromatograph with a thermal conductivity detector. The stainless steel columns had a length of 3,5 m and an inner diameter of 3 mm. The adsorbent for CO detection was an AG-5 mk. activated carbon (0,25-0,50 mm), for CO₂ – polysorbent-1 (0,16-0,20 mm). The temperature of the thermostat was 40 °C.

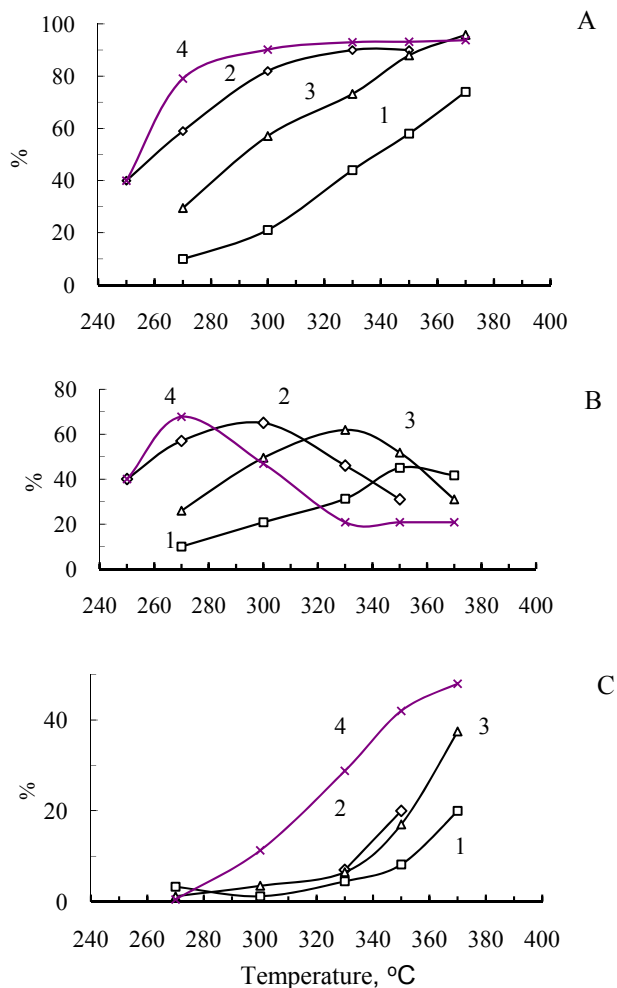
RESULTS AND DISCUSSION

In order to improve the catalytic action of the individual catalyst of vanadium pentoxide in the oxidation of 3-methylpyridine to modify it by adding additives dioxides of titanium and zirconium is of great interest. Binary vanadium-titanium and vanadium-zirconium oxide and three-component vanadium-titanium-zirconium catalysts were prepared and tested.

The general regularities of the reaction, in particular, the effect of temperature, the amount of oxygen (air) fed to the reaction zone and water vapor on the yield of the main reaction products were studied.

The figure shows the results the change in the conversion of 3-methylpyridine and the yield of nicotinic acid (A) on the tested oxide-vanadium catalysts as a function of temperature under comparable conditions. It can be noted that vanadium pentoxide showed the least activity in the oxidation of 3-methylpyridine: the conversion of the starting material even at a temperature of 370 °C was only 70 %. The activity of binary V-Zr-O and V-Ti-O contacts is higher than that of vanadium pentoxide, and the three-component vanadium-titanium-zirconium catalyst of the composition V₂O₅·4TiO₂·4ZrO₂ exhibited the greatest activity.

The main product of oxidation of 3-methylpyridine is nicotinic acid. The figure shows that its yield (B) increases in the following series of oxide-vanadium catalysts: V₂O₅ < V-Zr-O < V-Ti-O < V-Ti-Zr-O. From the presented data, it can



The feed rate of 3-methylpyridine is 36 g, air is 550 l per 1 liter of catalyst per hour.

The molar ratio of 3-methylpyridine:O₂:H₂O = 1:13:94

Effect of temperature on the conversion of 3-methylpyridine (A), the yield of nicotinic acid (B) and CO₂ (C) under oxidation conditions on oxide modifying catalyst V₂O₅ (1), V-Ti (2), V-Zr (3), V-Ti-Zr (4)

be seen that the best catalytic properties in the oxidation of 3-methylpyridine exhibited an oxide vanadium-titanium-zirconium catalyst. On this catalyst, when the starting reagents were fed in a molar ratio of 3-methylpyridine: oxygen:water = 1:13:94, the conversion of 3-methylpyridine at 270 °C was 80%, and nicotinic acid was obtained with the highest yield about 68 %.

Conclusion. Thus, the conducted tests of modified oxide-vanadium catalysts in the reaction of vapor-phase oxidation of 3-methylpyridine showed that the

introduction of titanium and zirconium dioxides contributes to an increase in the activity of the oxide-vanadium catalyst. It has been established that the three-component V-Ti-Zr-O contact directs the oxidation of 3-methylpyridine mainly towards the formation of nicotinic acid: in the low-temperature region (250-270 °C) the selectivity of its formation is higher than 85 %.

The research was carried out according to the scientific and technical program No. BR05234667 within the framework of program-targeted financing CS MES RK.

REFERENCES

- [1] Komov V.P. Biochemistry. M.: Drofa, 2004. P. 640.
- [2] Sarafanova L.A. Food additives: Encyclopedia. 2-nd ed., Rev. and add. St. Petersburg: GIORD, 2004. P. 808. ISBN 5-901065-79-4. (P. 420-221).
- [3] Korotchenkova N.V., Samarenko V.Y. Vitamins of the heterocyclic series. Structure, properties, synthesis, chemical technology: Methodological guidelines. St.-Petersburg: Publishing house SPKhFA, 2006. P. 58
- [4] Petrov I.Y., Tryasunov B.G. Structure and catalytic properties of deposited oxide-molybdenum, oxide-vanadium and oxide-chromium catalysts for the dehydrogenation of hydrocarbons // Vestn. KuzGTU. 2007. N 3. P. 73-84.
- [5] Ibrahim Salem. Recent Studies on the Catalytic Activity of Titanium, Zirconium, and Hafnium Oxides // J. Catal. Rev. Science and Engineering. 2003. Vol. 45, N 2. P. 205-296. doi.org/10.1081/CR-120015740.
- [6] Benjaram M. Reddy. Recent Advances on TiO₂-ZrO₂ Mixed Oxides as Catalysts and Catalyst Supports // Catal. Rev. 2005. Vol. 47, N 2. P. 257-296. doi.org/10.1081/CR-200057488.

Резюме

Т. П. Михайловская, Р. Құрмақызы, Д. Қ. Төлемісова, П. Б. Воробьев

3-МЕТИЛПИРИДИНДІ БУ КҮЙІНДЕ ТОТЫҚТЫРУДАҒЫ ВАНАДИЙ ОКСИДТІ КАТАЛИЗАТОРДЫҢ ҚАСИЕТІНЕ ТИТАН ЖӘНЕ ЦИРКОНИЙ ДИОКСИДТЕРІНІҢ МОДИФИЦІРУШІ ӘСЕРІ

3-метилпиридинді бу фазалы тотықтырудағы ванадий оксидті катализатордың қасиетіне титан және цирконий диоксидтерінің әсері талқыланады.

Түйін сөздер: тотығу, 3-метилпиридин, никотин қышқылы, катализаторлар.

Резюме

Т. П. Михайловская, Р. Курмақызы, Д. К. Төлемісова, П. Б. Воробьев

МОДИФИЦИРУЮЩЕЕ ВЛИЯНИЕ ДИОКСИДОВ ТИТАНА И ЦИРКОНИЯ НА СВОЙСТВА ОКСИДНОВАНАДИЕВОГО КАТАЛИЗАТОРА В ПАРОФАЗНОМ ОКИСЛЕНИИ 3-МЕТИЛПИРИДИНА

Обсуждается влияние диоксидов титана и циркония на свойства ванадийоксидного катализатора в парофазном окислении 3-метилпиридина.

Ключевые слова: окисление, 3-метилпиридин, никотиновая кислота, катализаторы.

*A. N. GURIN^{1,3}, S. G. SOLONINKINA¹, P. RISS²,
B. M. URALBEKOV³, I. V. MATVEYEVA³, E. T. CHAKROVA³*

¹RSE Institute of Nuclear Physics, Almaty, Republic of Kazakhstan,

²University of Oslo, Oslo, Norway,

³Al-Farabi Kazakh National University, Almaty, Republic of Kazakhstan

SELECTION OF MOBILE PHASE SYSTEMS FOR CHROMATOGRAPHIC RESEARCH OF ¹⁷⁷Lu - DOTAELA

Abstract. This paper considered the experimental data on selection of the optimal conditions for separation of free ¹⁷⁷Lu³⁺ cation and labeled ¹⁷⁷Lu-DOTAELA complex by paper chromatography in determining the radiochemical purity of the synthesized preparation. The following issues were also reviewed: the effect of structure and the ratio of mobile phase components, and the type of chromatographic paper on separation quality. The most qualitative separation was observed in application of a mobile phase, representing a buffer solution of sodium citrate with pH 5.0 and sodium chloride with the use of the chromatographic paper.

Keywords: paper chromatography, mobile phase, radiopharmaceutical, lutetium-177, DOTAELA.

Introduction. Receptors for triple negative breast cancer express the gonadotropin-releasing hormones (GnRH) in more than 50% cases. Among several analogues (agonists and antagonists) of GnRH that have been studied for treatment of this type of cancer, the non-peptide antagonist elagolix (ELA) is of greatest interest [1].

Selection of ¹⁷⁷Lu as a radioactive component of the preparation is determined by optimal depth of penetration in human tissue during radionuclide therapy of small tumors, and also by low radiation load for the healthy organs.

In nuclear medicine, radiopharmaceuticals are used for diagnosis and treatment of oncologic, infectious and other pathologies [2]. Radiopharmaceutical preparations contain the substances labeled with radioactive nuclides. During examination of the particular organ, an appropriate radionuclide labeled carrier substance is used in the body. The resulting complex after administration to the patient accumulates in the particular organ. If the unknown amount of the labeled impurity substance in the radiopharmaceutical finds its way to another organ, the capability of correct evaluation of the patient's examination results can be significantly reduced, especially taking into account a wide range of individual metabolic processes

The decisive factor in obtaining good results is that the radiopharmaceutical has the acceptable radiochemical purity [3]. Determination of radiochemical purity is the only guarantee that a drug, administered to a patient, will provide reliable diagnostics or therapy.

Thin layer chromatography (TLC) and chromatography on paper (CP) are widely recognized as reliable quality control methods in determining of radiochemical purity. These methods enable only one or two of impurity components to be recorded. The quantitative results are very sensitive to the details of testing procedure. TLC and CP methods often require about one hour of analysis time [3]. The United States Pharmacopeia (USP) [4] indicates that minimum 90% of total radioactivity corresponds to radiopharmaceuticals, but the monographs do not indicate the method for radioactivity counting.

The aim of the work is the development of the procedure for determining the radiochemical purity of the synthesized substance of antagonistic action of the triple negative breast cancer DOTA-Elagolix (DOTAELA) labeled with lutetium-177.

The advantages of ^{177}Lu as the therapeutic isotope are determined by its nuclear characteristics: maximum β -energy ($\max\beta = 496 \text{ keV}$, $\gamma = 113 \text{ keV}$ (6.4%) and 208 keV (11%)); a half-life of 6.71 days; the optimal depth of penetration into human tissue for radiation therapy of small tumors, a small radiation load on healthy organs [5, 6].

The experiments included the study of the following factors: chromatography paper, mobile phase and its composition.

EXPERIMENT

The chromatographic system was developed for the DOTAELA substance. Radio-labeling was performed with lutetium-177 isotope, obtained by irradiating of $200 \mu\text{g}$ of lutetium chloride, with a thermal neutron flux of $2 \times 10^{14} \text{ n/cm}^2 \times \text{s}$ for 291 hours. After irradiation, the target was exposed for 6 hours and then transported to the Radiochemical Unit of the Scientific Technical Center of Radiochemistry and Isotopes Production (STC RIP) into the hot chamber for ampoule opening, followed by target dissolution in 2 ml of 0.01 M hydrochloric acid solution.

For DOTAELA radio-labeling, $71 \mu\text{l}$ of DOTAELA solution was taken into a 10 ml vial, so that the final concentration was $30 \mu\text{g/ml}$, then $125 \mu\text{l}$ of acetate buffer with pH 4.5 was added, then $8 \mu\text{l}$ of lutetium-177 chloride was added and the volume was adjusted to 2 ml. The final mixture was placed in a glycerin bath at $80\text{-}90 \text{ }^\circ\text{C}$ for 30 minutes. When time was over, the vial was removed and cooled. Then the sample was taken for chromatography.

Chromatographic FN1 type paper and Whatman paper No.3 were used as a stationary phase with the total length of 15 cm for the ascending method and 19 cm for the descending method. Test solution ($5 \mu\text{l}$) was applied to the start line at 3 cm and 6 cm distance from the start of the chromatographic strip. After application, the spots were dried. The strips were then placed in a sealed chamber, and one end of it was immersed in a solvent [7]. The following was used as mobile phases: 10% solution of ammonium acetate in methanol (30:70 v/v); the solution of sodium chloride 0.9%; 0.1 M sodium citrate buffer solution, pH 5.0.

The analysis was carried out using a radio-chromatogram scanner Veenstra VCS-103 base.

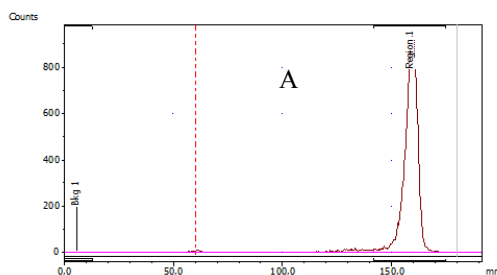
RESULTS AND DISCUSSION

In the course of the chromatograms analysis it was decided to use further the chromatographic paper in the system of solvent descending current due to shorter time of chromatography it provides.

The experimental studies on determination of the optimum conditions for lutetium-177 labeled DOTAELAradiochemical purity showed that this substance is not dissolving in the aqueous solutions. This is confirmed by the chromatograms shown in the figures 1 and 2.

Project: Radiopharmaceutical ¹⁷⁷Lu Method: PC File: Radiopharmaceutical ¹⁷⁷Lu ¹⁷⁷Lu-177 citrate Run 1.Measurement
User: Super User

Chromatogram: ¹⁷⁷Lu



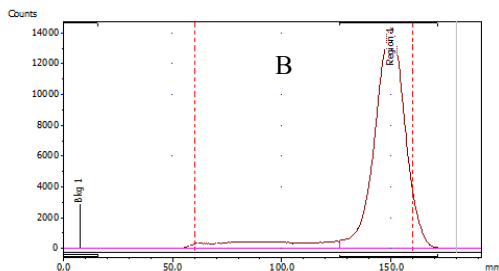
Regions: ¹⁷⁷Lu Detector: PMT

Name	Start (mm)	End (mm)	Retention (RF)	Area (Counts)	%ROI (%)	%Total (%)
Bkg 1	0,0	13,0	-0,453			
Region 1	141,8	174,6	0,823	31148	100,00	96,52
T Peak				31148	100,00	96,52

Total Area: 32270 Counts
Average Background: 0 Counts

Project: Radiopharmaceutical ¹⁷⁷Lu Method: PC File: Radiopharmaceutical ¹⁷⁷Lu/NaCl 0.9 Run 1.Measurement
User: Super User

Chromatogram: ¹⁷⁷Lu



Regions: ¹⁷⁷Lu Detector: PMT

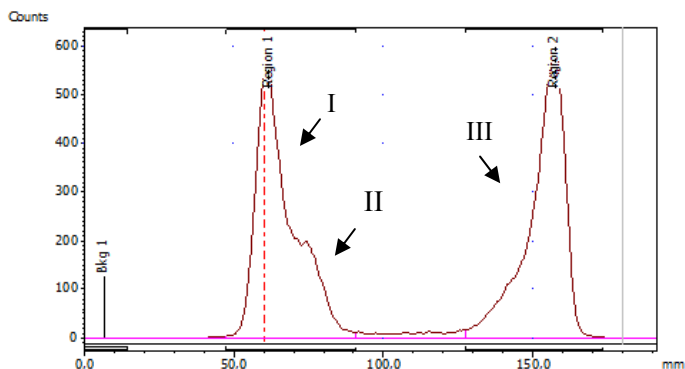
Name	Start (mm)	End (mm)	Retention (RF)	Area (Counts)	%ROI (%)	%Total (%)
Bkg 1	0,0	15,6	-0,520			
Region 1	126,4	171,0	0,902	1141149	100,00	90,33
T Peak				1141149	100,00	90,33

Total Area: 1263367 Counts
Average Background: 0 Counts

Figure 1 – Chromatograms (A and B) of ¹⁷⁷Lu³⁺

Project: Radiopharmaceutical ¹⁷⁷F Method: ¹⁷⁷Lu File: Lu-177(pH-4.5_1 Run 1.Measurement User: Super User
 Project: Radiopharmaceutical ¹⁷⁷Lu Method: PC File: Radiopharmaceutical ¹⁷⁷Lu/citrate Run 1.Measurement User:
 Super User

Chromatogram: ¹⁷⁷Lu



Regions: ¹⁷⁷Lu

Detector: PMT

Name	Start (mm)	End (mm)	Retention (RF)	Area (Counts)	%ROI (%)	%Total (%)
Bkg 1	0,2	14,6	-0,443			
Region 1	47,4	90,8	0,013	39164	50,29	48,99
Region 2	127,4	173,0	0,813	38705	49,71	48,41
2 Peaks				77868	100,00	97,40

Total Area: 79945 Counts
 Average Background: 0 Counts

Figure 2 – Chromatogram of ¹⁷⁷Lu-DOTAELA.
 Peaks (I): ¹⁷⁷Lu-DOTAELA, (II): ¹⁷⁷Lu and (III): fragments of ¹⁷⁷Lu-DOTAELA radiolysis

In figures 1 and 2, the main ¹⁷⁷Lu-DOTAELA peak, detected by the scintillation detector (NaI) after using the aqueous solutions of sodium citrate and sodium chloride as mobile phases, is located on the start line, and the peak, corresponding to the free Lu-177, moves along the chromatogram along with the solvent front. Therefore the important conclusion can be made that ¹⁷⁷Lu-DOTAELA does not prevent determination of unreacted Lu-177 impurity in the reaction mixture.

To obtain the chromatograms in figure 3, the chromatographic strip was placed in a system of organic mobile phase of ammonium acetate in methanol. After chromatography in the organic medium, the analysis of the chromatogram in figure 2 showed that the unreacted Lu-177 remains on the start line and is not moving along with the solvent front, while the ¹⁷⁷Lu-DOTAELA substance is moving with the solvent front and is not characterized by clear peak character, so this system is not suitable for separation.

Conclusion. Thus, it was found that the citrate buffer have the best parameters for studying the behavior of ¹⁷⁷Lu-DOTAELA and obtaining the chromatograms of the products of its interaction with ¹⁷⁷Lu.

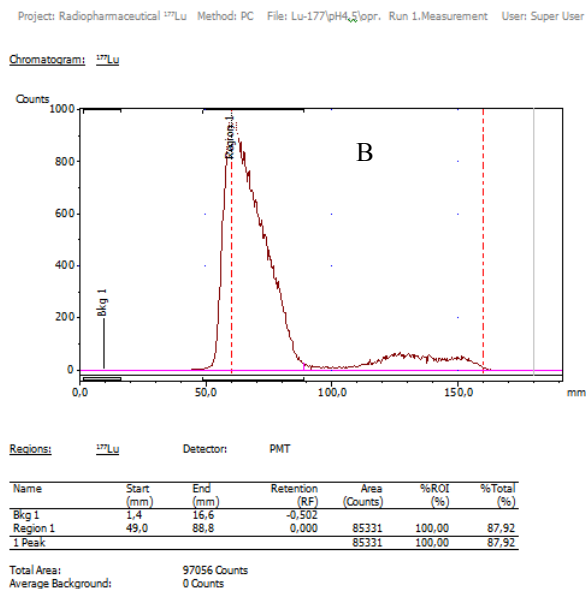
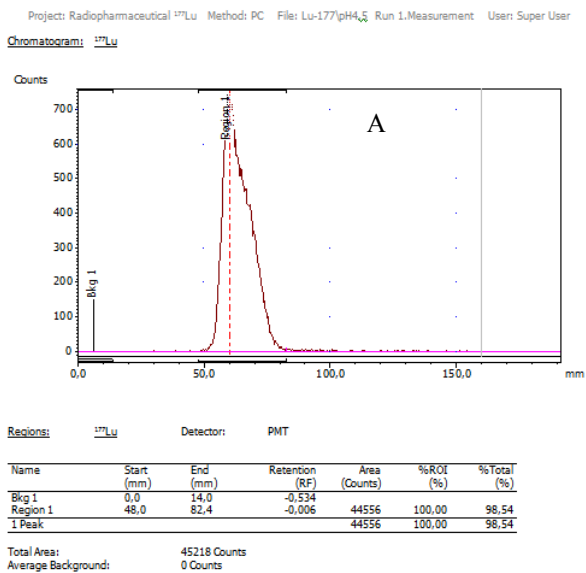


Figure 3 – Chromatograms: A - $^{177}\text{Lu}^{3+}$ and B-(I): $^{177}\text{Lu}^{3+}$ и (II) ^{177}Lu -DOTAELA

It should be noted that the method of chromatography of synthesis products in two mobile phases of sodium chloride and citrate buffer solution provides an accurate estimate of the content of the radio-labeled target product “ ^{177}Lu -DOTAELA”, as well as the radiochemical impurities of unreacted ^{177}Lu .

The work was carried out with the support of G.2018 [No. AP05134384].

REFERENCES

- [1] Mazen Jamous, Uwe Haberkorn, Walter Mier. (2013). Synthesis of Peptide Radiopharmaceuticals for the Therapy and Diagnosis of Tumor Diseases. *Molecules*, 3379-3409
- [2] Radionuclide diagnostics for practical doctors / Ed. Yu.B. Lishmanova, VI Chernov. Tomsk: STT, 2004. 394 p.
- [3] Kumar S., Jyotirmayee K.M. Sarangi (2013) Thin Layer Chromatography: A Tool of Biotechnology for Isolation of Bioactive Compounds from Medicinal Plants. *Int J Pharm Sci Rev Res* 18: 126-132.
- [4] United States Pharmacopeia 36 NF- 29, United States Pharmacopeia Convention, Rockville, United States (2012).
- [5] Knapp F.F., Jr, Mirzadeh S., Beets A.L., Du M. Production of therapeutic radioisotopes in the ORNL High Flux Isotope Reactor (HFIR) for applications in nuclear medicine, oncology and interventional cardiology. *J Radioanal Nucl Chem.* 2005; 263: 503-509. doi: 10.1007 / s10967-005-0083-4.
- [6] Firestone R. Table of Isotopes. 8. New York: Wiley, 1996.
- [7] Eckelman W.C., L evenson S.M. Chromatographic purity of ^{99m}Tc -compounds. In: RHODES BA (editor) Quality control in nuclear medicine: radiopharmaceuticals, instrumentation and in vitro assays. Saint Louis, The CV Mosby Co. 1977. P. 197-209.

Резюме

*А. Н. Гурин, С. Г. Солонинкина, П. Рисс,
Б. М. Уралбеков, Х. В. Матвееваю Е. Т. Чакрова*

ХРОМАТОГРАФИЯЛЫҚ ЗЕРТТЕУЛЕРГЕ АРНАЛҒАН ҰЯЛЫ ФАЗАЛЫҚ ЖҮЙЕНІ ТАҢДАУ ТАҢБАЛАУ ЛЮТЕЦИЙ-177 ҮШІН DOTAELA

Үш рет теріс сүтбезі қатерлі ісігінің рецепторлары гонадотропинді шығаратын гормондарды (GnRH) 50% істердің саны. Раканың осы түрін емдеуге арналған GnRH бірнеше аналогтары (агонисты және антагонисты) арасында пептидті антагонист элаголикс (ELA) еңқызығушылыққа ие. Ядролық физика институты Норвегияның Осло университетінің зерттеушілер командасымен жұмыс істейді ^{177}Lu деп белгіленген DOTAELA негізіндегі радиофармацевтика құрылды. Терапиялық изотоп ретінде ^{177}Lu артықшылығы ядролық сипаттамасымен анықталады: кішкентай ісіктердің радиациялық терапиясы үшін адамның ұлпасына енудің оңтайлы тереңдігі, сау органдарына арналған шағын радиациялық жүктеме. Осы мақалада $^{177}\text{Lu}^{3+}$ мен ^{177}Lu -DOTAELA таңбаланған комплексті қағаз хроматографиясымен бөлуге арналған оңтайлы жағдайларды таңдау туралы эксперименталды деректер келтірілген. Сондай-ақ, композицияның әсер етуі және мобильді фазаның құрамдас бөліктерінің бөліну сапасына, хроматографиялық қағаз түріне қатынасы қарастырылды. Натрий цитратының буферлік ерітіндісін ұсынатын мобильді фазаны пайдалану кезінде ең жоғары сапалы бөліну байқалды, рН 5.0 және натрий хлориді.

Түйін сөздер: қағазхроматографиясы, жылжымалы фазасы, радиофармацевтика, лютеций-177, DOTAELA.

Резюме

*А. Н. Гурин, С. Г. Солонинкина, П. Рисс,
Б. М. Уралбеков, Х. В. Матвеева, Е. Т. Чакрова*

**ВЫБОР МОБИЛЬНЫХ ФАЗОВЫХ СИСТЕМ
ДЛЯ ХРОМАТОГРАФИЧЕСКИХ ИССЛЕДОВАНИЙ
ДОТАЕЛА ДЛЯ ЛЮТЕЦИЯ-177**

Рецепторы для тройного отрицательного рака молочной железы выражают гонадотропин-высвобождающие гормоны (GnRH) более, чем в 50% случаев. Среди нескольких аналогов (агонистов и антагонистов) GnRH, которые были изучены для лечения этого типа рака, наибольший интерес представляет непептидный антагонист elagolix (ELA). Институт ядерной физики работает с командой исследователей из Университета Осло, Норвегия, в создании радиофармацевтического препарата на основе DOTAELA с маркировкой ^{177}Lu . Преимущества ^{177}Lu в качестве терапевтического изотопа определяются его ядерными характеристиками: максимальной оптимальной глубиной проникновения в ткань человека для лучевой терапии малых опухолей, небольшой радиационной нагрузкой на здоровые органы.

В работе представлены экспериментальные данные по выбору оптимальных условий для разделения свободного катиона $^{177}\text{Lu}^{3+}$ и меченого комплекса ^{177}Lu -DOTAELA с помощью бумажной хроматографии. Также были рассмотрены вопросы влияния состава и соотношения компонентов подвижной фазы на качество разделения, тип хроматографической бумаги. Наиболее качественное разделение наблюдалось при использовании подвижной фазы, представляющей буферный раствор цитрата натрия с pH 5,0 и хлоридом натрия.

Ключевые слова: бумажная хроматография, подвижная фаза, радиофармацевтическая, лютеций-177, DOTAELA.

V. D. NAZAROVA, Y. V. AKHANKOVA, A. U. BEKTEMISOVA

M. Kozybayev North Kazakhstan State University, Petropavlovsk, Republic of Kazakhstan

**EXTRACTION OF QUERCETIN
FROM *LINOSYRIS VILLOSA***

Abstract. The chemical composition of the plant *Linosyris villosa* is being investigated for the first time. The following ingredients were extracted from this plant: aglikon quercetin of phlavonoid nature. Different types of chromatography have been applied (column adsorbing, preparational); there was extracted an individual form of quercetin. The physical-chemical methodology analysis was used to prove its structure.

Keywords: quercetin, aglikon, plant *Linosyris villosa*, chromatography, column, preparational, biological activity, antioxidental, immune-modeling, antibiotic.

Introduction. Flavonoids take active part in the cellular circuit processes of a plant. They function as growth regulators, as well as plant development and reproduction regulators. Scientists are interested in flavonoids due to the wide spectrum of their biological activity. A lot of phytopreparations contain flavonoids. While being the safest medicines, these preparations are paid close attention to. Plants contain varied amounts of flavonoids: from 0.5% to 20% (e.g. blossoms of *Styphnolobiumjaponicum*) in average. Flavonoids contained in plants can be of two types: aglycones or glycosides. The *Embryophyta*, such as the family *Compositae (Asteraceae)*, *Polygonaceae* and legumes, are especially rich in flavonoids.

Flavonoid preparations can potentially help to prolong human life, as some of them have anti-sclerotic and anti-oxidant activities, which slow down aging processes. In a human body, flavonoids influence both enzymatic systems and immune processes, causing various effects. A lot of scientists assert that the wide spectrum of biological activity of flavonoids is predetermined by their anti-oxidant activity. Flavonoids, such as quercetin, myricetin and kaempferoland rutin, can not only bind, but also restore or oxidize ions of metals with *variable* valencies. By this way they are able to stimulate or inhibit free radical processes occurring in a human body [1].

The interconnection between the structure and anti-oxidant activity has been studied for most of the flavonoids produced by plants. It has been found out that flavonoids, as well as polyphenols, can serve as a 'trap' for free radicals and inhibit peroxidation of lipids. The most active flavonoids are quercetin, myricetin and morin which inhibit lipid oxidation from 78 to 83%. Being antioxidants the flavonoids play an important part in protecting the structure and functions of the liver in cases of pathologies, quicken the regeneration and restore the functional activity of hepatocytes, especially in cases of complex therapy of acute and chronic hepatitis and liver cirrhosis.

In the modern medicinal practice, flavonoid preparations are widely used in various forms: pills, ointments, tinctures, extracts, powders, dragees and capsules. Much attention is paid to the anti-inflammatory activity of flavonoids which is probably connected to their antiulcerant, wound healing, antipyretic and astringent activities.

The antimicrobial properties of flavonoids are also remarkable. One has detected the negative influence of quercetin and myricetin upon gram-positive bacteria, as well as the influence of flavones and chalconids upon staphylococcus. Gallocatechin, epigallocatechin and the oxidized sum of catechins have antimicrobial properties active for staphylococci and streptococci. Isoflavones, isoflavonoids and flavonols are chemically and biochemically remarkable. All of them have cholesteric, diuretic and antihyperglycemic activity in various degrees. The large therapeutic potential of flavonoids allows to regard them as sources of general treatment activity.

Flavonoids have a valuable property of quick evacuation and the absence of cumulation. Flavonoid preparations are essential not only for treating illnesses, but also for the prevention of vascular problems. Flavonoid preparation treatment has proved effective in cases of cavitory disease in the post-operation period, glaucoma and hyperthyroidism [2].

The anti-oxidant activity of flavonoids has been studied recently. In this regard, the problem of creating medicines with anti-oxidant properties has become topical. Such preparations can be used for the prevention and cure of illnesses which are accompanied by the intensification of free radical reactions. Bioflavonoids are ranked first among exogenous natural antioxidants. The most pharmacologically remarkable are preparations with the high proportion of aglycones and glycosides, such as quercetin, kaempferol, apigenin, luteolin, isorhamnetin and methoxylated 6-oxyflavonols [3].

Such pharmaceutical dosage forms containing quercetin as *Corvitin* and *Lipoflavon* are rather effective in various pathological conditions. The therapeutic effect of using soluble and injection forms become apparent significantly quicker. Due to the wide spectrum of the physiological activity of quercetin, the creation of such forms are of special importance.

Ukrainian scientists have created a new pharmaceutical dosage form – *Corvitin* – which is water-soluble powder for preparing injections on the basis of the synthetic modulator of solubility (polyvinylpyrrolidone). *Lipoflavon* has been created with the help of phosphatidylcholine liposomes. The use of phosphatidylcholine liposomes as carriers allows to inject the preparation into blood. It is possible due to the penetration through the phospholipid bilayer of membranes and the quick transportation of the preparation to the target cells.

As a result of the preclinical trial, it has been found out that *Corvitin* has low toxicity indicators. It does not possess any allergic influence. It has been detected that *Corvitin* has a significant anti-oxidant effect, as well as an inhibiting activity for membrane enzymes, especially lipoxygenases, activating and preserving the

nitrogen oxide level in the affected tissues and blood, protecting membrane-bound enzymes which regulate ion (calcium) homeostasis in the cells.

The wide spectrum of the pharmacological characteristics of *Corviti* has been a major cause for its further testing. Especially significant activities of this preparation are anti-oxidant, anti-inflammatory and membrane-stabilizing actions which are predetermined by the inhibiting influence upon the essential enzyme systems of a cell.

Tests have shown that *Lipoflavin* the 0.1 mg/kg dosage with the parenteral route of administration has a positive effect on the nerve fiber regeneration. Both the number of nerve fibers and the regeneration rates are increased. The therapeutic effect of *Lipoflavin* is predetermined by the liposome form, which is a product of nanotechnology having high affinity rate to the cell membranes, and quercetin, which is an antioxidant protecting nerve cells from the oxidation stress, activating endogenous anti-oxidant protection systems, reducing the inflammation and increasing the axon growth. It contributes to the regeneration processes of the nerve fibers and can prevent degradation processes at the late stages of restoration. The liposome form of quercetin accelerates the emergence and myelination of nerve fibers. Even within a short period of usage (10 days) *Lipoflavin* has an apparent neuroprotective effect [4].

Quercetin is one of the most well-known and profoundly studied flavonols. It is wide-spread in the plant kingdom. The term 'quercetin' stems from the Latin word 'quercus', which means 'oak'. Both oak bark and oak timber contain this substance. The biggest amount of quercetin is in tea (up to 2500 mg/kg of dry leaves). Quercetin belongs to the Vitamin P group. It is found in onions, apples, blueberries, black and green tea, red wine, leafy green vegetables and legumes. For industrial (pharmaceutical) needs, it is extracted by hydrolysis of rutin which is produced from *Styphnolobium japonicum* or buckwheat. Organic fruits and vegetables contain much more quercetin. Thus, tomatoes which have been grown in the natural environment, for instance, contain 79% more of this useful flavonoid than hothouse tomatoes.

Quercetin can be taken as a food additive. However, it is badly digested as a separate substance – most of it is metabolized into inactive phenolic acids or just gets removed from the human body. Nutrients are always better assimilated from whole foods rather than from their separate fragments. This phenomenon can be explained by the fact that any substance naturally exists in a combination with a variety of other synergizing nutrients which increase their assimilation and utilization rates.

By now, there has been extensive research of quercetin preparations for the possibility of their use in order to prevent and cure various illnesses. The summary of the sources available shows a wide spectrum of biochemical and pharmacological properties of quercetin [1, 2].

It is believed that quercetin possesses a wide spectrum of biological activity. It can positively influence metabolism, thus, preventing obesity. It can also

demonstrate an anti-inflammatory effect and prevent atherosclerosis. It is also capable of blocking tumor cell proliferation, decreasing the risk factor expression of cardiovascular diseases. It is regarded as an agent which can inhibit the progress of atherosclerosis-related processes.

Having the ability of inhibiting the activity of 5-lipoxygenase, quercetin demonstrates anti-inflammatory properties and synergism with nonsteroidal anti-inflammatory preparations. The ability to block cell division makes quercetin useful both as an anti-inflammatory preparation and as a cancer prevention means [3].

Quercetin neutralizes aggressive oxygen-containing and nitroxyl radicals, breaks the reaction chains of free radicals. Hence, it can stop pathologic processes in cells. Oxidation products of free radicals are the main agents of the oxidation stress in the cell. They cause various illnesses. Thus, the prevention of free radicals' formation or their neutralization is essential for the successful treatment of illnesses.

The combination of anti-oxidation and membrane-stabilizing properties of quercetin contributes to the decrease in capillary permeability and stabilization. As a result, the increase in energy supply of cardiac hystiocytes due to the anti-oxidation activity and enhanced blood flow predetermines the cardioprotective effect of quercetin.

The selective inhibiting influence upon cell enzymes also lies in the basis of pharmacological and biochemical effects of quercetin. It allows to position quercetin as a specific bioregulator of enzymatic processes occurring in the human body.

Numerous recent researches has proved that quercetin has neuroprotective, anti-oxidation, immunomodulatory, membrane-stabilizing, cardioprotective, antihypoxic and anti-inflammatory actions, it reinforces reparative processes in the organism. Experimenting on volunteers has shown that quercetin is able to produce a positive effect upon patients suffering from inflammatory or oxidation stress, but it does not show any considerable effect when it is used by healthy people [4].

EXPERIMENT

The plant *Linosyris villosa* has been used in the given research. Samples were gathered in its blooming phase in the North-Kazakhstan Oblast. The raw material was dried and crushed till the air-dry state. Then pharmacopoeia indicators were tested. The moisture content in the plant was equal of 8.1% [5].

The raw material was extracted by hexane in the Soxhlet extractor, in the water bath, with the hexane boiling temperature for 10 hours. The ethanolic extract was boiled dry. The dark brown sediment was dissolved in ethanol and then it was applied to the column with aluminium oxide.

Two zones were observed on the column: the upper zone was black, and the lower one was yellow. The elution of the yellow zone was conducted by

96%-ethanol. Three fractions (5 ml of each) were gathered. All fractions were studied with the use of the two-dimensional paper chromatography method in the dissolvent system of butyl alcohol – acetic acid – water with the 4:1:5 ratio (I) and 2%-acetic acid (II). On the chromatogram of the first fraction, there was an oblong spot which had the values $R_f(I) = 0.80$ and $R_f(II) = 0.00$. In the ultraviolet (UV) light, the spot fluoresced showing the yellow colour. In the ammoniavapour, it acquired the bright yellow colour. This fact shows that it is an aglycone of the flavonoid nature. Because the spot was oblong, it was assumed that the chromatogram contained several flavonoid aglycones [6].

The chromatogram of the second fraction also contained an oblong spot. In the UV light, the spot fluoresced showing the yellow colour. In the ammoniavapour, it acquired the bright yellow colour. The position of the spots on the chromatograms of the first and second fractions indicates that the spots are flavonoid aglycones with the values $R_f(I) = 0.80$ and $R_f(II) = 0.00$. The chromatogram of the third fraction contained a spot with $R_f(I) = 0.78$ and $R_f(II) = 0.00$, which also corresponds to a flavonoid aglycone. In the UV light, the spot fluoresced showing the yellow colour. In the ammoniavapour, it acquired the bright yellow colour. The substance on the third chromatogram was identical to quercetin [7, 8].

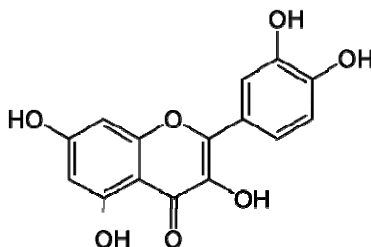
The eluates of Fractions 1 and 2 with Al_2O_3 were combined and boiled. An oily mass was produced which was further processed with distilled water. Then the sediment was dissolved in 96%-ethanol and further chromatographed on the column with aluminium oxide. On the column, there was one yellow zone which was eluated by the mixture of ethanol and chloroform with the ratio 9:1. The produced eluate was yellow. It was boiled dry and crystalized from 80%-ethanol solution [9].

As a result, an amphoteric substance of yellowish brown colour with the fusion temperature of 288-290 °C was produced.

The method of preparation chromatography was used for the further purification of the substance. The dissolvent system of butyl alcohol – acetic acid – water with the 4:1:5 ratios was used and 86 mg of the substance was produced. Aglycone was crystalized from ethanol. A substance of yellowish green colour with the fusion temperature of 304-308 °C was produced. Aglycone was studied with the help of the two-dimensional paper chromatography method in the dissolvent system of butyl alcohol – acetic acid – water with the 4:1:5 ratio (I) and 2%-acetic acid (II). On the chromatogram, there was a spot which had the values $R_f(I) = 0.80$ and $R_f(II) = 0.00$. In the UV light, the spot fluoresced showing the yellowish colour. In the ammoniavapour, it acquired the bright yellow colour. According to the position of the spot on the chromatogram and its colour, the substance was identified as an aglycone of the flavonoid nature.

The infrared (IR) spectrum has been identified for the aglycone using KBr. There are absorption bands in the IR spectrum, in the area of $1,660\text{ cm}^{-1}$, which correspond to the vibrations of the carbonyl group (C=O); in the area of $3,450\text{ cm}^{-1}$, which correspond to the vibrations of the hydroxyl groups(-OH); in the area of $2,850, 2,940\text{ cm}^{-1}$, which correspond to the vibrations of the (C=C) aromatic ring.

Conclusion. Hence, according to the fusion temperature, qualitative reactions, data sources and IR spectroscopy, the produced aglycone has been identified as quercetin with the following structural formula (figure) [10].



Structural formula of Quercetin

REFERENCES

- [1] Tarakhovskiy Y.S., Kim Y.A., Abdrasilov B.S., Muzafarov Y.N. Flavonoids: biochemistry, biophysics, medicine. Pushchino: Synchronbook, 2013. 310 p.
- [2] Flavonoids as anti-oxidant agents: importance of their interaction with biomembranes / Saija A., Scalese M., Lanza M. [et al.] // Free Radic. Biol. Med. 1995. Vol. 19. P. 481-486.
- [3] Rogovskiy V.S. Antihypertensive and neuroprotective activities of quercetin and its derivatives / Rogovskiy, V.S., N.L. Shimanovskiy and A.I. Matyushin // Experimental and Clinical Pharmacology. 2012. Vol. 75, N 9. P. 27-41.
- [4] Slesarchuk V.Y. Neuroprotective properties of the quercetin preparation // Pharmacology and Medical Toxicology. 2014. N 6 (41).
- [5] Kyusev P.A. The complete reference book of medical herbs. M.: Eksmo, 2002. P. 992.
- [6] An introduction to the phytochemical research and identification of the biological activity of plant substances / Ed. Mamonov, L.K. and R.A. Musychkina. Almaty: School of the XXI century, 2008. 215 p.
- [7] Khranova Y.P. The peculiarities of accumulating phenolic compounds in *Potentilla fruticosa* (rosaceae) within the 24-hour limit // Herbal Chemistry. 2017. N 4. P. 97-106.
- [8] Minina S.A., Kaukhova I.Y. Chemistry and technology of phytopreparations. M.: GEOSTAR-MED, 2004. 560 p.
- [9] Vardanyan L.R., Atabekyan L.V., Arapetyan S.A., Vardanyan R.L. The influence of solvents on the extraction degree of antioxidants from the herbal material // Herbal Chemistry. 2018. N 1. P. 83-88.
- [10] Deyneka V.I., Grigoryev A.M., Staroverov V.M. HPLC in the flavonoid research. Identifying rutin // Chemistry and Pharmaceutical Journal. 2004. N 9. P. 23-25.

Резюме

В. Д. Назарова, Е. В. Аханькова, А. Ø. Бектемисова

LINOSYRIS VILLOSA ӨСІМДІГІНЕН КВЕРЦЕТИНДІ БӨЛІП АЛУ

«*Linosyris villosa*» өсімдігінің химиялық құрамы алғаш зерттелуде. Өсімдіктен флавоноидты табиғатты кверцетин агликонын бөліп алдық. Хроматографияның әр түрлерін: бағаналық, адсорбциялық, препаративті қолдана отыра, кверцетинді жеке түрде бөліп алып, оның құрылысын талдаудың физика-химиялық әдістерімен дәлелдедік.

Түйін сөздер: кверцетин, *Lynosyris villosa* өсімдігі, хроматография, бағаналық, препаративті, биологиялық белсенділік, антиоксидантты, иммуномоделирлеуші, қабынуға қарсы.

Резюме

В. Д. Назарова, Е. В. Аханькова, А. У. Бектемисова

ВЫДЕЛЕНИЕ КВЕРЦЕТИНА
ИЗ РАСТЕНИЯ *LYNOSYRIS VILLOSA*

Химический состав растения «*Lynosyris villosa*» изучается впервые. Из растения выделили агликон-кверцетин флавоноидной природы. Применяя разные виды хроматографии, колоночную, адсорбционную, препаративную, выделили кверцетин в чистом виде и доказали его строение физико-химическими методами анализа.

Ключевые слова: кверцетин, растение *Lynosyris villosa*, хроматография, колоночная препаративная, биологическая активность, антиоксидантная, иммуномоделирующая, противовоспалительная.

M. B. UMERZAKOVA, V. D. KRAVTSOVA, R. B. SARIEVA, Zh. N. KAINARBAYEVA

JSC "Institute of Chemical Sciences named after A. B. Bekturov", Almaty, Republic of Kazakhstan

COMPOSITE MATERIALS BASED ON ARYLALICYCLIC COPOLYIMIDE WITH ADDITIVES OF POLYETHYLENE GLYCOL

Abstract. Composite films of various compositions from copolyimide based on tricyclodecene tetracarboxylic and diphenyloxytetracarboxylic acid dianhydrides with polyethylene glycol additives were obtained. Using IR spectroscopy, it was found that polyethylene glycol is well combined with copolyimides, forming H complexes on functional groups of PEG and residual amide acids. The thermal and mechanical properties of the obtained composite films are determined. It is shown that PEG additives contribute to an increase in thermal stability, improve strength properties of composite films in comparison with copolymer, while elasticity has acceptable values for such a material.

Keywords: aromatic dianhydride, alicyclic dianhydride, copolyimide, polyethylene glycol, composition, film.

Introduction. At present time, new polyimide materials developed that possess a set of properties that satisfy the majority of requirements for materials used in the electrical engineering industry, including energy-saving technologies [1, 2]. Among of them there are materials based on polyheterocycles of alicyclic structure, including dianhydrides of tricyclodecene tetracarboxylic acids and various diamines, due to their high hydrolytic stability, resistance to aggressive media, high level of electrophysical characteristics [3, 4]. However, these polymers are characterized by lower thermal stability comparatively to aromatic analogs. To production the composite materials with the necessary properties that facilitate their use as a matrix in micro- and nanoelectronics, electrical engineering, integrated optics and other optical technologies, as products with unusual photosensitive, magnetic, heat-conducting properties, modification of (co) polyimides with various plasticizing and inorganic additives are made [5].

In this work, modification of (co) polyimides based on dianhydrides of tricyclodecene tetracarboxylic, diphenyloxydetetracarboxylic acids and diaminodiphenyl ether by polyethylene glycol was carried out. This approach extends practical possibilities of both alicyclic and aromatic homo- and copolyimides [6].

EXPERIMENTAL PART

4,4'-diaminodiphenyl ether (DADPhE) was purified by sublimation in a vacuum at 0.8 atm. and temperature 202 °C, $t_{\text{melt.}} = 186\text{--}188$ °C.

Tricyclo-(4,2,2,025) dec-7-ene-3,4,9,10-tetracarboxylic acid dianhydride (benzene adduct – AB) was purified by boiling in acetone (grade ch.p.), followed by heating for 2 hours in a vacuum at 0, 8 atm. and a temperature of 200 °C, ($t_{\text{melt.}} = 350\text{--}352$ °C).

Dianhydride 3,3', 4,4'-diphenyloxydetetracarboxylic acid (DFO) was purified by heating in a vacuum of 0.8 atm. at 230 °C, $T_{\text{melt.}} = 220\text{--}221$ °C.

Dimethylacetamide (DMAA), methylpyrrolidone (MP), acetone, ethyl alcohol, dimethylformamide (DMFA) was purified according by known procedures [7, 8].

Polyethylene glycol (PEG) from Aldrich (USA), $M = 2000$ (grade ch.p.), was used without additional purification.

Copolyimides based on AB, DFO and DADPhE at the initial ratio AB:DFO = 90:10 (CPI1) and 85:15 (CPI2) mol. % were prepared by a single-stage copolycondensation in MP in the presence of pyridine (6 wt. %). As catalyst, a gradual increase in the reaction temperature from 90 °C (at this temperature it was held for 0.5 h) to 140 °C (3.5 h, respectively), the monomers concentration in the solution was 40 wt. %.

Compositions based on CPI1, CPI2 with PEG were obtained by adding a solution of PEG in MP (5 wt. %) in the calculation of 0.5–2 % by weight in a solution of CPI1, CPI2 (40 wt. % in MP) at temperature 60 °C with permanent stirring for 1.5 hours.

Films based on CPI and CPI+PEG compositions were formed by watering solutions of copolyimide and compositions based on it on glass surfaces; in order to remove the solvent, the films were pre-dried by heating in a drying oven at the temperature 90 °C during 0.3 hours. After it heat treatment was carried out at the temperature range from 140 to 250 °C in air for 1.5 hours.

IR-Fourier spectra of copolyimide and composite films based on it were recorded on a Nicolet 5700 Spectrometer.

The thermal properties of copolyimide and composite films were investigated by the methods of thermogravimetric analysis (TGA) and differential scanning calorimetry (DSC) on a Mettler Toledo TGA/SDTA 851c and FP85 TA Cell device at constant heating rate of 4 and 8 °C/min, from which the temperature of the beginning of decomposition ($T_{\text{b.d.}}$) and glass transition ($T_{\text{g.t.}}$) of the samples was determined.

The mechanical properties of the films - tensile strength ($\sigma_{\text{t.s.}}$) and elongation (l), for samples measuring 10×10 mm², 0.45–0.55 μm thick, were studied on a Com-Tem Testing Equipment (USA) tensile machine.

RESULTS AND ITS DISCUSSION

PEG was used as the modifying additive to the copolyimide matrix. Polyethylene glycols refer to nonionic surfactants in which polyoxyethylene blocks, as well as terminal hydroxyl groups, can form a composite material [9,10] through a polymer-polymer interaction [11]. PEG is amenable to any methods of processing - casting, extrusion, calendaring, pressing. Yarns and films that have good strength and elasticity can be produced from PEG. Thermo oxidative destruction of PEG lies within the limits of 320–370 °C, which is a good prerequisite for combining with heat-resistant (co)polyimides ($T_{\text{b.d.}} \sim 380$ °C).

The preparation of a composite material based on PEG and CPI was carried out by mechanical mixing of the finished copolymer in which the content of the amide acid groups does not exceed 10–15 % [12], because during the reaction mixture of CPI with PEG, polyamide acid which is formed during copolycondensation of AB, DFO, and DADPhE can be cross linked with terminal hydroxyl groups of the modifier [13].

It was found that by mechanical mixing in alicyclic copolyimide it is possible to introduce up to 2 % by weight of PEG ($M = 2000$). Films in this case are visually smooth, transparent with a smooth surface. The introduction of the molecular weight modifier 8000 in the SPI does not lead to the production of transparent films; compatibility of mixture components is absent.

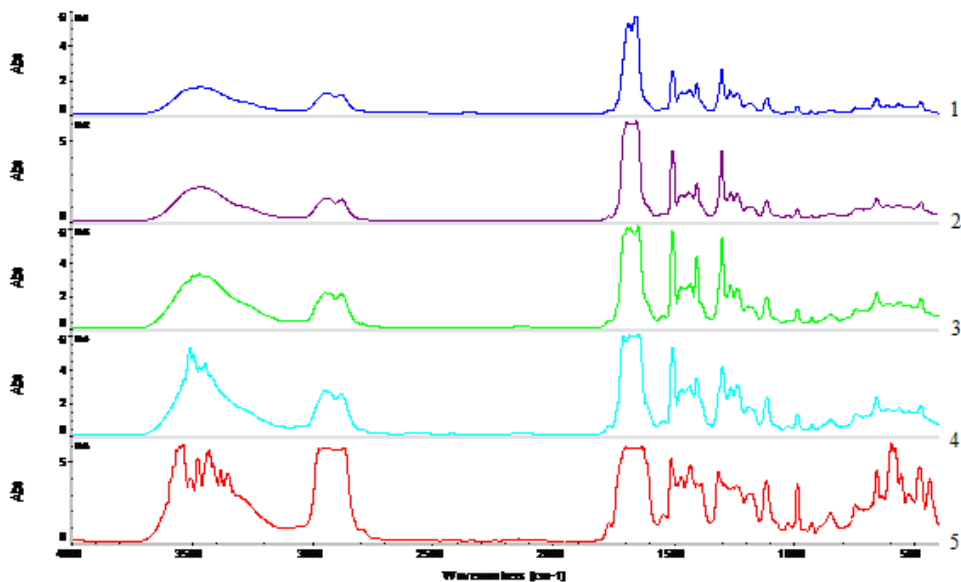
IR spectroscopic study of the obtained compositions and starting polymers was carried out. It was found that when a solution of PEG is introduced into the solution of CPI1 in MP, the characteristic band of the first corresponding to the C–O group is overlapped by the bands of the carbonyl of the imides ring and the amide acid retained in the CPI1 and prescribed by one band in the region of $1681\text{--}1691\text{ cm}^{-1}$.

As the content of PEG in the composite mixture increases, this band expands. In the high-frequency region, the intensity of the broad band ($3200\text{--}3650\text{ cm}^{-1}$) in the spectra of the initial components of the mixture corresponding to the hydroxyl groups of PEG and O–H of the undecycled amido acid groups of the copolymer changes with the addition of PEG. The indicated changes, observed in the spectra during the mixing of polymers, indicate the formation of complexes between the components of the mixture at the level of hydrogen bonds [14]. The formation of H complexes in the mixture is possible between the terminal hydroxyl groups of PEG and the residual acid groups of the amide acid CPI1. Complication in the mixture contributes to the thermodynamic compatibility of the components of the composition.

It was found that containing the PEG in the mixture of polymers about 1–2 wt. % leads to the appearance of copolyimide (1543.5 cm^{-1}) amide groups on the spectra of deformation vibration bands, their intensity increase with increasing PEG in the mixture. This may indicate a decrease in the compatibility of the polymers, i.e. when a PEG of $>1\text{ wt.}\%$ is added to the copolymer, the interaction between the components in the mixture weakens, and bands characteristic of pure polymers are observed in the spectra. In the experiment, however, the revealed decrease in the compatibility of the components does not affect the appearance of the films containing 1.5–2% by weight of PEG, they are obtained in a homogeneous and transparent manner.

The Figure1 shows the IR spectra of SPI2 and compositions based on it, it can be seen that as the PEG content increases, the broadening of the band in the region from $1631\text{ to }1695\text{ cm}^{-1}$, related to the stretching vibrations of the polyethylene glycol C–O and the carbonyl of the imides cycle, is observed in the composition mixture amide acid SPI2. It indicate formation of hydrogen bonds between the residual acid groups of the amide acid in the CPI2 and the terminal

hydroxyl groups of the PEG, as in the case of SPI1. However, in the high-frequency region, for the concentrations of PEG 1 and 2 % by weight, deformation of the absorption bands of stretching vibrations related to the OH groups of the residual amide acid units in the SPI2 and the terminal hydroxyl groups of the PEG in the region 3445–3599 and 3355–3555 cm^{-1} occurs in the composite mixture respectively (figure, curves 4, 5) [14]. This is possible as a result of surface phenomena [10,15,16], manifested in PEG when added to CPI2, since PEG is a non-ionic surfactant. But these phenomena do not reduce the thermodynamic affinity of the two polymers, since films containing 2 % by weight of PEG do not exfoliate [17, 18].



IR spectra:

- 1 – solution of CPI2 in MP on KBr glass; 2 – compositional mixture based on CPI2 + 0.5% by weight PEG; 3 – CPI2 + 0.75% PEG; 4 – CPI2 + 1%PEG; 5 – CPI2 + 2%PEG

Thus, good compatibility of components achieved. Using IR spectroscopy, found that in the composite mixtures based on CPI1, CPI2 and PEG, the interaction of aryl-acyclic copolyimides with PEG on the functional groups of polymers with the formation of hydrogen bonds occurs, and in the case of SPI2 with the maximum content of PEG exhibits surface activity.

To obtain films of acceptable quality on the basis of the developed compositions, the mode of their heat treatment found experimentally. It was found that the films formed from the solutions of the film compositions must be dried in air at the temperature 90 °C during 30 minutes, then successively raise the temperature to 140 and 250 °C, maintaining in each case during 1 hour, to prevent the film material surface from swelling as a result of rapid heating.

The limitation of 250 °C film annealing is due to the fact that PEG at high temperatures tends to form cross linked structures [15], which reduce the elasticity of the composite film, which is not desirable for the resulting material. As a result of this heat treatment, the surface of the films is smooth, the films retain their integrity and transparency.

The thermal and mechanical properties of the obtained film materials based on CPI1, CPI2 and PEG were determined, and presented in the table.

Thermal and physico-mechanical properties of composite films

Film/ composition	T _{g,t} , °C	T _{b,d} , °C	σ _{t,s} , MPa	l, %
PI	114	380	71	30
CPI1/CPI2+ mass% 0.5 PEG	387/381	402/415	145/179	20/19
CPI1/CPI2+mass% 0.75 PEG	393/375	414/417	160/181	25/18
CPI1/CPI2+ mass%1.0 PEG	373/370	398/395	129/120	17/17
CPI1/CPI2+ mass%1.5 PEG	360/352	393/394	125/83	15/13
CPI1/CPI2+ mass% 2.0 PEG	350/355	390/388	82/79	12/11
CPI1/CPI2	388/382	405/408	150/162	20/17

As can be seen from the data presented in the table, increase of both thermal and mechanical properties of the films obtained is observed with an increase of PEG content in the mixture of CPI1 and CPI2 from 0.5 to 0.75 % by weight, further increase the PEG concentration in the mixture provides a certain decrease of these values. Such change in the properties of composite films is due, apparently, to a decrease in the compatibility of the components in the composition.

Thus, new composite films based on CPI1, CPI2 and PEG has been obtained. The optimum content of PEG is 0.75 % by weight, in which the films have improved thermal and strength properties that exceed the similar properties of the original alicyclic polyimide and its copolymer based on AB, DFO and DADPE, and the elasticity is acceptable values for a such material.

The research was carried out according to the scientific and technical program No. BR05234667 within the framework of program-targeted financing CS MES RK.

REFERENCES

- [1] Svetlichny V.M., Kudryavtsev V.V. Polyimides and problems of creating modern structural composite materials // High-molecular Compounds. Ser. B. 2003. Vol. 45, N 6. P. 984-1036.
- [2] Sazanov Yu.N. Applied value of polyimides // J. Appl. Chem. 2001. Vol. 74, issue 8. P. 1217-1234.
- [3] Zhubanov B.A., Kravtsova V.D., Bekmagambetova K.Kh., Akhmettaev D.D. Electrical properties of alicyclic polyimides. Almaty: Nauch. ed. Open Company «Print-S», 2010. 225 p.
- [4] Novakov I.A., Orlinson B.S., Brunilin R.B., Potaenkova E.A. Soluble polyimides and copolyimides with enhanced hydrolytic stability based on [(2-amino)- and (2-aminomethyl)- bicyclo [2.2.1] hept-3-yl] anilines // Vysokomolek. Soed. Ser. A-B. 2010. Vol. 52, N 10. P. 1861-1865.

- [5] Yang C.Y., Hsu S.L.C., Chen J.S. Synthesis and properties of 6FDA-BisAAF-PPD copolyimides for microelectronic application // Appl. Polymer Sci. J. 2005. Vol. 98, N 5. P. 2065-2069.
- [6] Zhubanov B.A., Almabekov O.A., Kravtsova V.D. Synthesis and study of salts of poly-amido acids based on tricyclodecene tetracarboxylic acid dianhydride // Vysokomolek. Soed. 1984. Vol. 26 B, N 5. P. 337-340.
- [7] Weissberg A., Proskauer E., Riddick J., Tups E. Organic solvents. M.: IL, 1958. 519 p.
- [8] Gordon A., Ford R. The chemist's companion. M.: Mir, 1976. P. 437-444.
- [9] Papisov I.M. Polymer-polymer interactions and its role in the formation of macromolecules // Proceedings of the Symposium "Kinetics and Mechanism of Macromolecular Reactions". M., 1971. P. 19.
- [10] Bekturov E.A., Bimendina L.A. Interpolymer complexes. Alma-Ata: Science of the Kazakh SSR, 1977. P. 265.
- [11] Manson J., Speering L. Polymer mixtures and composites. M.: Chemistry, 1979. 439 p.
- [12] Zhubanov B.A., Iskakov R.M., Sariyeva R.B., Abadi M.J. New composite film materials based on alicyclic polyimide // J. Appl. Chem. 2007. Vol. 80, issue 5. P. 856-861.
- [13] Strepikheev A.A., Derevitskaya V.A. Fundamentals of chemistry of high-molecular compounds. M.: Chemistry, 1975. P. 219.
- [14] The chemist's companion. M.: Mir, 1976. P. 208, 202.
- [15] Brief chemical encyclopedia: in 5 vol. M.: Sov. Encyclopedia, 1965. Vol. 4. P. 96, 102.
- [16] Encyclopedia of polymers: in 3 vol. M.: Sov. Encyclopedia, 1974. Vol. 2. P. 430.
- [17] Rabek Ya. Experimental methods in the chemistry of polymers: in 2 parts. M.: Mir, 1983. Part 1. P. 33.
- [18] Rabek Ya. Experimental methods in the chemistry of polymers: in 2 parts. M.: Mir, 1983. Part 2. P. 173.

Резюме

М. Б. Өмірзакова, В. Д. Кравцова, Р. Б. Сариева, Ж. Н. Қайнарбаева

ПОЛИЭТИЛЕНГЛИКОЛЬ ҚОСПАЛАРЫМЕН АРИЛАЛИЦИКЛДІ СОПОЛИИМИД НЕГІЗІНДЕГІ КОМПОЗИТТІ МАТЕРИАЛДАР

Дифенилоксидтетракарбон және үшциклдеценттетракарбон қышқылдарының диангидридтерінің сополиимиді негізінде полиэтиленгликоль қосылумен әр түрлі құрамдағы композициялық қабықшалар алынған. ИҚ-спектроскопия әдісімен сополимердегі қалдық амидоқышқылмен полиэтиленгликольдің функционалдық топтары арқылы Н-комплекс түзе отырып, полиэтиленгликольдің сополиимидпен жақсы әрекеттесетіні анықталды. Алынған композитті қабықшалардың термиялық және механикалық қасиеттері анықталды. ПЭГ қосу композициялық қабықшалардың сополимермен салыстырғанда термиялық және беріктік қасиеттерінің жақсаруына оңықпал ететінін көрсетті, ал серпімділігі осындай материал үшін жарамды болып қала береді.

Түйін сөздер: ароматты диангидрид, алициклді диангидрид, сополиимид, полиэтиленгликоль, композиция, қабықша.

Резюме

М. Б. Умерзакова, В. Д. Кравцова, Р. Б. Сариева, Ж. Н. Кайнарбаева

**КОМПОЗИЦИОННЫЕ МАТЕРИАЛЫ
НА ОСНОВЕ АРИЛАЛИЦИКЛИЧЕСКОГО СОПОЛИИМИДА
С ДОБАВКАМИ ПОЛИЭТИЛЕНГЛИКОЛЯ**

Получены композиционные пленки различного состава из сополиимида на основе диангидридов трициклодецентетракарбоновой и дифенилоксидтетракарбоновой кислот с добавками полиэтиленгликоля. Методом ИК-спектроскопии было установлено, что полиэтиленгликоль хорошо совмещается с сополиимидами, образуя Н-комплексы по функциональным группам ПЭГ и остаточных амидокислот. Определены термические и механические свойства полученных композиционных пленок. Показано, что добавки ПЭГ способствуют повышению термостойкости, улучшению прочностных свойств композиционных пленок в сравнении с сополимером, при этом эластичность имеет допустимые для подобного материала значения.

Ключевые слова: ароматический диангидрид, алициклический диангидрид, сополиимид, полиэтиленгликоль, композиция, пленка.

N. O. AKIMBAYEVA¹, S. A. VIZER¹,
T. M. SEILKHANOV², K. B. YERZHANOV¹

¹JSC "Bekturov's Institute of Chemical Sciences», Almaty, Republik of Kazakhstan,

²Kokshetau State University Sh. Ualikhanov, Kokshetau, Republik of Kazakhstan.

E-mail: akimbaeva@mail.ru

ALKYLATION OF SODIUM ETHANE-1,2-DIYLDICARBAMODITHIOATE

Abstract. Sodium ethane-1,2-diyldicarbamodithioate was obtained by the dithiocarbonylation reaction of ethane-1,2-diamine. Then dialkyl ethane-1,2-diyldicarbamodithioates were synthesized by dialkylation of sodium ethane-1,2-diyldicarbamodithioate with 1-bromo(C₇, C₈, C₉, C₁₀ and C₁₂)alkanes in the good and high yields (63-84%). The structure of the reaction products are confirmed by IR, ¹H and ¹³C NMR spectra data.

Keywords: ethane-1,2-diamine, dithiocarbonylation, alkylation, 1-bromoalkanes, dialkyl ethane-1,2-diyldicarbamodithioates.

Before in [1, 2] we found, that sodium N-(3-phenylprop-2-yn-1-yl)-N-butyl-dithiocarbamate (AN-16) significantly accelerates root formation on black currant cuttings, exceeding the results obtained with known rooting agent - indolylacetic acid (IAA) [3]. At the same time, its working concentration was an order of magnitude lower than the working concentration of IAA. This compound is highly effective for stimulating the bookmarking of generative buds of fruit trees, which makes it promising in innovative technologies for the production of fast-growing seedlings [4], and it is also of practical interest for cultivation of wild medicinal plants, increasing seed germination by three times [5].

In this regard, the search for highly effective plant growth regulators among the new sodium dithiocarbamates of alkylated diamines can let to useful results.

In order to synthesize new hetero-organic compounds and to study their chemical, physico-chemical and biological properties, in particular physiological activity, we carried out the reaction of ethylenediamine with carbon disulphide, which scheme is shown in figure 1. Reactions of ethylenediamine (EDA) with carbon disulphide were carried out in 96% ethanol medium at room temperature and a molar relation of reagents EDA : CS₂ : NaOH = 1:1,4:1,5.

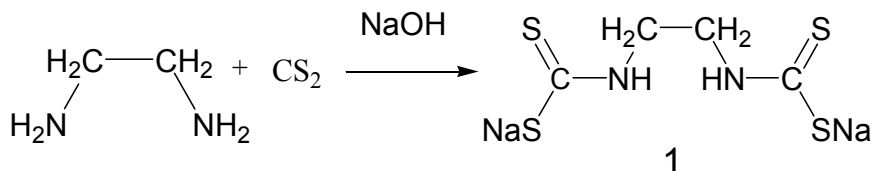


Figure 1 – Reaction of ethylenediamine with carbon disulfide

As a result of the reaction, sodium ethane-1,2-diylldicarbamodithioate **1** was obtained in 90% yield, in the form of a pink crystalline substance with $T_m = 72-73$ °C. The individuality and composition of the synthesized ethane-1,2-dioldicarbamodithioate of sodium **1** are confirmed by thin-layer chromatography and other physicochemical methods. The structure of the compound was established on the basis of IR spectroscopy and ^1H and ^{13}C NMR spectroscopy.

The structure of the synthesized compounds was proved by the methods of IR, ^1H NMR and ^{13}C spectroscopy (the spectra of the synthesized N-octylethane-1,2-diamine **2** are shown in figures 1, 2 - 4, 5).

In the IR spectrum of sodium bisdithiocarbamate **1**, bands of characteristic stretching vibrations of the C-H bonds of methylene groups are in the range 2887 ± 2975 cm^{-1} , stretching vibrations of the NH groups are at $3291, 3401$ cm^{-1} , intense absorption bands of the thioamide group $\text{NC} = \text{S}$ are at 1430 cm^{-1} and 1046 cm^{-1} . Oscillations involving the C-S bond are manifested at 627 cm^{-1} .

In the ^1H NMR spectrum of compound **1**, shown in Fig. 2, the resonance signals of the protons of NCH_2 groups appear at 3.35 ppm, the signal of protons of NH - at 8.26 ppm.

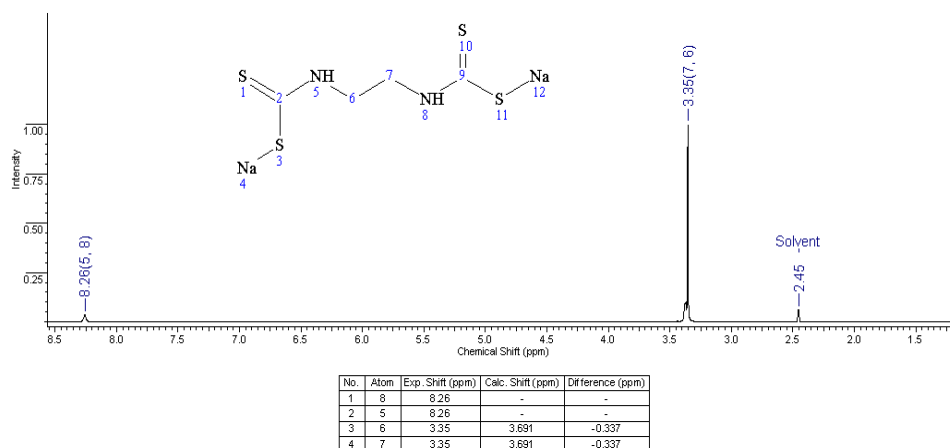


Figure 2 – NMR ^1H spectrum of ethane-1,2-diylldicarbamodithioate sodium **1**

In the ^{13}C NMR spectrum of sodium ethane-1,2-dioldicarbamodithioate **1** obtained which are shown in figure 3, there are resonant signals of carbon atoms of $\text{C} = \text{S}$ groups at 215.0 ppm, confirming the introduction of dithiocarbamate groups into the molecule of a new compound, and the signal of NCH_2 methylene groups at 46.7 ppm.

In order to synthesize and study the properties of the new bisdithiocarbamate derivatives, we investigated the alkylation reaction of bisdithiocarbamate **1** with 1-bromoalkanes (BA) (bromheptane, bromoclotane, bromonanane, bromodecane, bromododecane). The reaction was carried out by interaction of bisdithiocar-

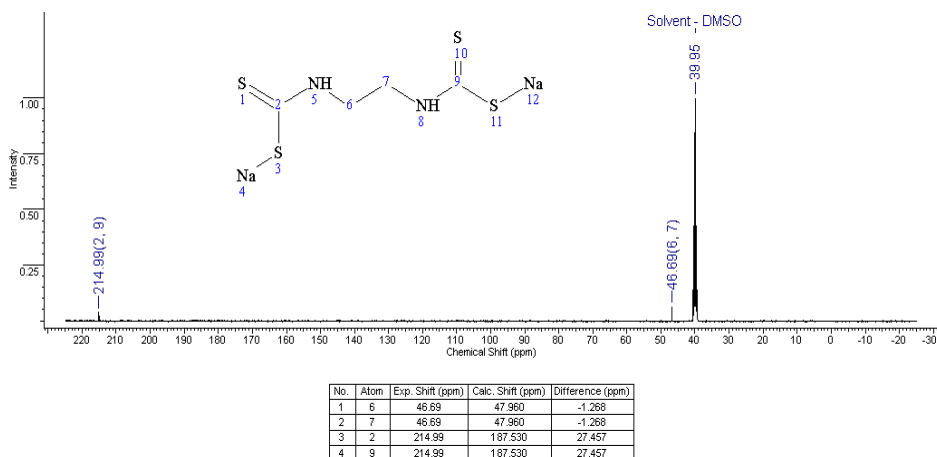


Figure 3 – NMR ¹³C spectrum of sodium ethane-1,2-diyldicarbamodithioate **1**

bamate **1** with 1-bromoalkanes at a temperature of 50-55 °C in acetone medium, at molar ratios of reagents **1**: BA = 1: 1, 1: 2 and 1: 3.

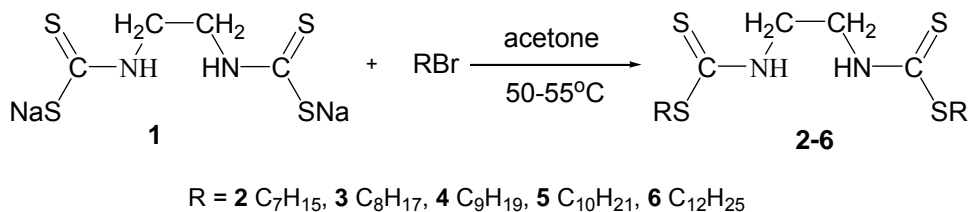


Figure 4 – Scheme of alkylation of sodium ethane-1,2-diyldicarbamodithioate **1**

After appropriate treatment of the reaction mixtures diheptyl, dioctyl, dinonyl, didecyl and dododecyl thiodiesters of ethane-1,2-diyldicarbamodithioic acid **2-6** were isolated in individual yields of 31%, 23%, 17%, 31% and 46% respectively, if the initial reagents were taken in the ratio **1**: BA = 1: 1. As we see, the yields of thiodiesters **2-6** are quite low, so we carried out this reaction at other molar ratios of the reagents. At a molar ratio of reagents **1**: BA = 1:2, the yield of thiodiesters **2-6** increases correspondingly to 50%, 35%, 39%, 36% and 62%, respectively. At a molar ratio of reagents **1**:BA = 1:3, the yield of thiodiesters **2-6** increases to 73%, 78%, 63%, 69% and 84%, respectively.

The composition and individuality of the synthesized compounds **2-6** are confirmed by thin-layer chromatography and other physicochemical methods. The structure of the compounds was established on the basis of IR, ¹H and ¹³C NMR spectroscopy.

In the infrared spectra of synthesized compounds **2-6**, intense absorption bands are observed in the region of 2959-2810 cm⁻¹, corresponding to the vibrations of methyl and methylene groups of alkyl substituents; in the region of 3200-

3400 cm^{-1} , broad absorption bands are observed that correspond for valence vibrations of amide NH groups. The presence of the C=S group is confirmed by the very strong absorption bands in the spectra region of $\sim 1061\text{-}1072 \text{ cm}^{-1}$, the weak bands in the $646\text{-}663 \text{ cm}^{-1}$ region correspond to the C-S bond vibrations, and the presence of an absorption band, characteristic for NH groups, indicates that the reaction was on the C-S group.

Table 1 – Physicochemical characteristics of bisdithiocarbamate **1** and thiodiesters **2-6**

Comp.	Yield, % (1:BA = 1:1)	Yield, % (1:BA = 1:2)	Yield, % (1:BA = 1:3)	mp, °C	IR spectra, ν , cm^{-1}			
					NH	CH ₃ , CH ₂	C=S	C-S
1	60	–	–	72-73	3400 3290	2810-2985	–	–
2	31	50	73	96-97	3237	2581-2951	1061	646
3	23	35	78	78-84	3370	2921	1072	654
4	17	39	63	80-84	3235	2851-2952	1061	646
5	31	36	69	63-65	3212	2850-2952	1059	663
6	46	62	84	96-97	3214	2850-2954	1061	659

The resonance signals from the alkyl substituents are observed in the ^1H NMR spectra of ethane-1,2-diyldicarbamodithioic acid **2-6**: it is a triplet from the protons of the methyl group in the range δ 0.79-0.81, there are the multiplets from the protons of the methylene groups $(\text{CH}_2)_{n-1}$ in the 1.18-3.11 ppm region. The protons of the NCH_2 group resonate at 3.49-3.75 ppm. in the form of a triplet, the proton of the thioamide group resonates at 9.84-9.87 ppm. in the form of a broadened singlet.

In the ^{13}C NMR spectra of alkyl thiodiesters **2-6**, signals in the regions 14.48-14.51 and 22.58-34.54 ppm, corresponding to carbon atoms of CH_3 and $(\text{CH}_2)_n$ groups, are observed. Signal at 197.71-202.36 ppm corresponds carbon atom of C=S group. Signals in the region of 44.57-44.98 ppm belong to the CH_2N groups.

Table 2 – Data of ^1H and ^{13}C NMR spectra for compounds **1-6**

Comp.	NMR ^1H , δ				NMR ^{13}C , δ			
	NH	NCH_2	$(\text{CH}_2)_n$	CH_3	NCH_2	C=S	CH_3	$(\text{CH}_2)_n$
1	8,26	3,35	–	–	47,96	187,53	–	–
2	9,86	3,73	1,20-3,10	0,81	44,98	197,77	14,48	22,58-34,54
3	9,86	3,73; 3,75	1,20-3,10	0,81	44,96	197,74	14,51	22,65-34,52
4	9,87	3,73	1,20-3,11	0,81	44,97	197,76	14,50	22,62-34,52
5	9,85	3,72	1,18-3,07	0,79	44,96	197,71	14,50	22,67-34,51
6	9,84	3,49; 3,74	1,19-3,11	0,81	44,57	202,36	14,50	22,64-33,11

As an example of the experimental NMR spectra, the proton and carbon spectra of diheptyl ethane-1,2-diylldicarbamodithioate **2** are shown in the Figures 5 and 6. In the figures 7 and 8 the two-dimensional HMQC and COSY spectra of the same compound confirming the assignment of the signals in ^1H and ^{13}C NMR spectra are shown.

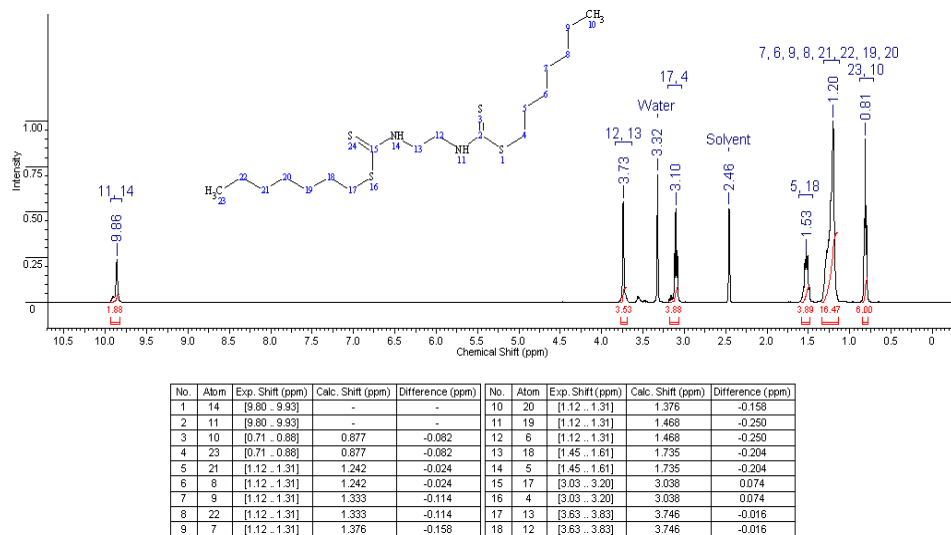


Figure 5 – ^1H NMR spectrum of diheptyl ethane-1,2-diylldicarbamodithioate **2**

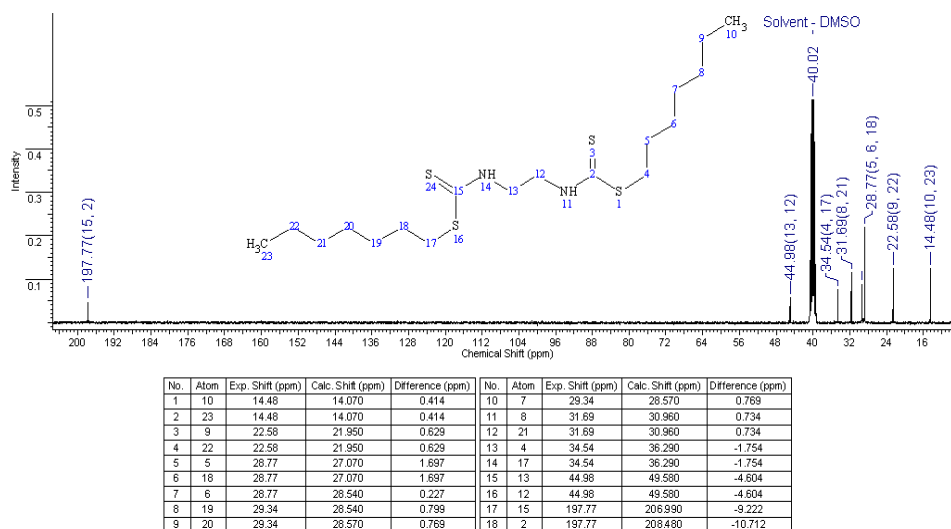


Figure 6 – ^{13}C NMR spectrum of diheptyl ethane-1,2-diylldicarbamodithioate **2**

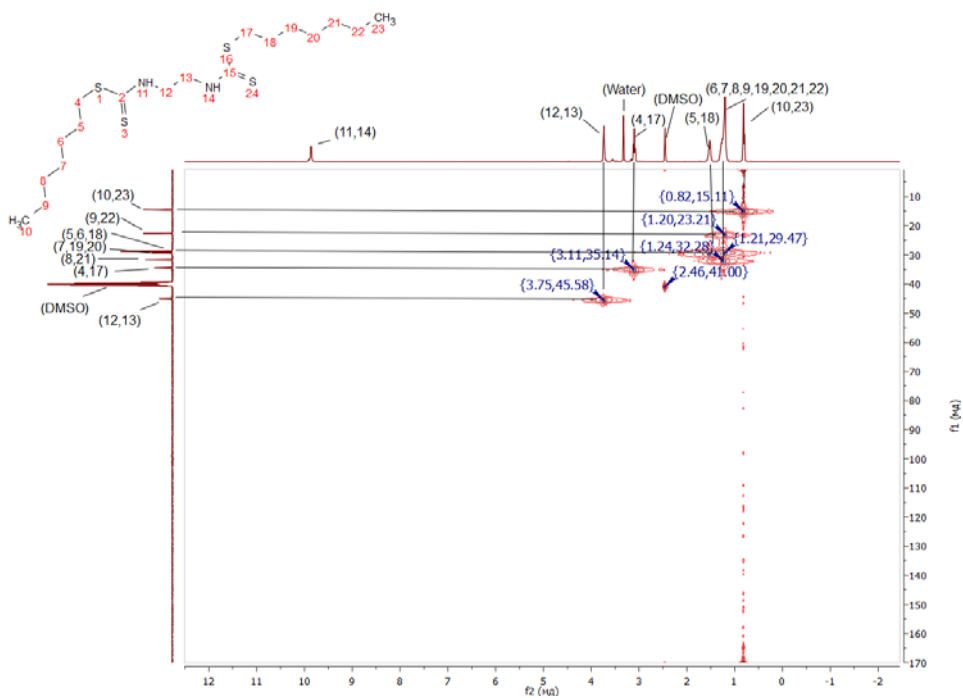


Figure 7 – HMQC NMR spectrum of diheptyl ethane-1,2-diylidicarbamodithioate 2

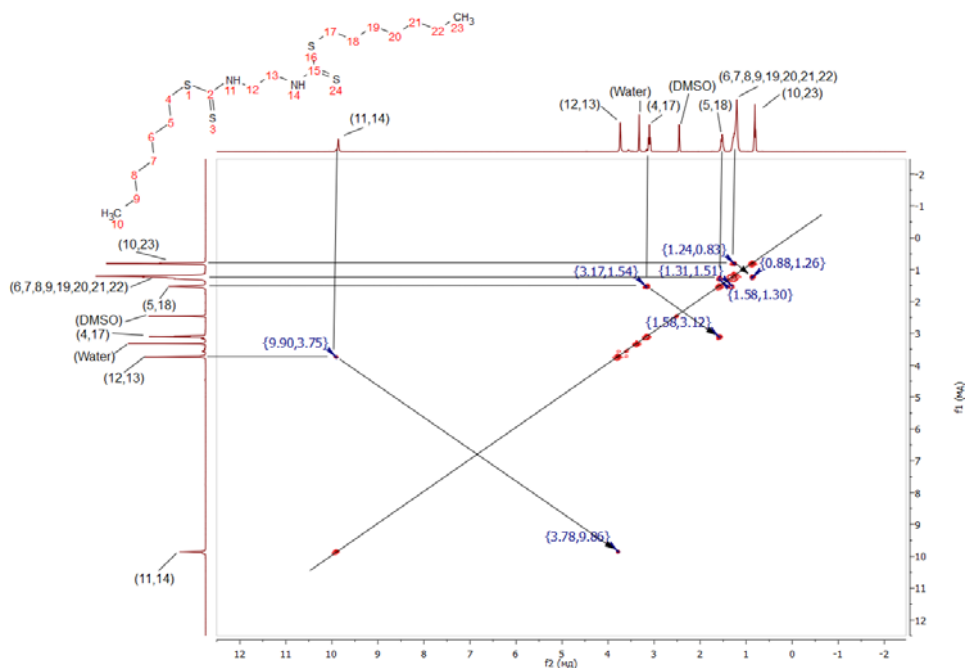


Figure 8 – COSY NMR spectrum of diheptyl ethane-1,2-diylidicarbamodithioate 2

EXPERIMENTAL PART

The spectra of NMR were recorded on a JNN-ECA 400 spectrometer from Jeol (Japan). The working frequency of the spectrometer is 400 MHz on the ^1H and 100 MHz on ^{13}C nuclear cores, respectively. The survey was carried out at room temperature in a solvent of DMSO. Chemical shifts are measured relative to signals of residual protons or carbon atoms of a deuterated solvent.

The melting points of the obtained substances were determined on a Boetius heating table. The IR spectra are recorded on a Nicolet 5700 spectrometer in KBr tablets. The course of the reaction and the purity of the products were monitored by thin-layer chromatography on plates of "Silufol UV-254", eluent - benzene: ethanol, 1:3 with the appearance of spots of substances with iodine vapor.

Sodium ethane-1,2-diylldicarbamodithioate 1. A solution of 10 ml (8.8 g, 0.15 mol) of ethylenediamine in 10 ml of 90% alcohol was introduced into a three-necked flask. The temperature of the reaction mixture was lowered to $-5\text{ }^\circ\text{C}$. and 8.7 g (0.22 mol) of sodium hydroxide dissolved in 2 ml of distilled water was added. After 10 to 15 minutes of stirring, 12.66 ml (15.95 g, 0.21 mol) of carbon disulfide were added dropwise to the reaction flask and stirred at room temperature for 1 hour. Then, alcohol was distilled from the reaction mixture, the remaining precipitate was washed with acetonitrile. As a result, sodium ethane-1,2-diylldicarbamodithioate **1** was obtained as crystals $R_f = 0.04$, mp = $72\text{-}73\text{ }^\circ\text{C}$. Yield 22.8 g (0.09 mole) (90%).

Diheptyl ethane-1,2-diylldicarbamodithioate 2. A solution of 1 g (0.004 mol) of sodium ethane-1,2-diylldicarbamodithioate **1** in 10 ml of acetone was introduced into a three-necked flask. The temperature of the reaction mixture was raised to $50\text{ }^\circ\text{C}$ and 2.15 g (0.012 mol) of heptyl bromide in 10 ml of acetone was added. After the addition of the total amount of heptyl bromide, the reaction mixture was stirred for 2 hours at $50\text{ }^\circ\text{C}$. The reaction was monitored by thin layer chromatography. Then acetone was distilled from the reaction mixture, the remaining precipitate was washed with acetonitrile. As a result, 1.2 g (73%) of diheptyl ethane-1,2-diylldicarbamodithioate **2** with $R_f = 0.04$ was obtained as crystals, mp $96\text{-}97\text{ }^\circ\text{C}$.

According to the developed procedure, 1.36 g (78%) of dioctyl ethane-1,2-diylldicarbamodithioate **3**, mp $78\text{-}84\text{ }^\circ\text{C}$ was obtained from 1 g (0.004 mole) of sodium ethane-1,2-diylldicarbamodithioate **1**, 2.32 g (0.012 mole) of octyl bromide.

According to the developed procedure, 1.17 g (63%) of dinonyl ethane-1,2-diylldicarbamodithioate **4**, mp $80\text{-}84\text{ }^\circ\text{C}$ was obtained from 1 g (0.004 mol) of sodium ethane-1,2-diylldicarbamodithioate **1** and 2.49 g (0.012 mol) of nonyl bromide.

According to the developed procedure, 1.36 g (69%) of didecyl ethane-1,2-diylldicarbamodithioate **5**, mp $63\text{-}65\text{ }^\circ\text{C}$ was obtained from 1 g (0.004 mol) of sodium ethane-1,2-diylldicarbamodithioate **1** and 2.65 g (0.012 mol) of decyl bromide.

According to the developed procedure, 1.75 g (84%) of didodecyl ethane-1,2-diylldicarbamodithioate **6**, mp 96-97 °C were obtained from 1 g (0.004 mol) of sodium ethane-1,2-diylldicarbamodithioate **1** and 2.99 g (0.012 mol) dodecyl bromide.

The research was carried out according to the scientific and technical program No. BR05234667 within the framework of program-targeted financing CS MES RK.

REFERENCES

- [1] Vizer S.A., Akimbaeva N.O., Erzhanov K.B. Plant growth regulators created in the laboratory of chemistry of physiologically active compounds of the Institute of Chemical Sciences. A.B. Bekturov // Chem. f. Kaz. 2016. N 4. P. 10-45.
- [2] Erzhanov K.B., Vizer S.A., Sycheva E.S. Creation of innovative plant growth regulators for a broad spectrum of action. Almaty, 2017. 158 p.
- [3] Pat. 22965 Republic of Kazakhstan. IPC8 A01N 39/02, C07C 49/172. N-(3-phenylprop-2-yn-1-yl)-N-butylldithiocarbamate, which has a root-forming activity / Erzhanov K.B., Akimbaeva N.O., Saurbaeva B.S., Ermagambetov R.R., Oleichenko S.N., Kampitova G.A.; claimed. 28.10.2009; publ. 15.03.2012, Bul. № 3. 3 p.
- [4] I know – the garden of the flowers // Zhailau Journal. The thematic supplement to the magazine AgroAlem. 2009. N 3(3). P. 2-4.
- [5] 5. Inn. 25744 Republic of Kazakhstan. IPC8 C08M 39/18. Regulator of growth of seeds of wild medicinal plants / Erzhanov K.B., Akimbaeva N.O., Anuarbekova I.N., Sultanova Z.K., Sotnikova V.V.; claimed. 30/05/2011; publ. 15.05.2012, Bul. № 5.

Резюме

Н. О. Әкімбаева, С. А. Визер, Т. М. Сейілханов, Қ. Б. Ержанов

ЭТАН-1,2-ДИИЛДИКАРБАМОДИТИОАТ НАТРИЙДІ АЛКИЛДЕУ

Этан-1,2-диаминнің күкіртті көміртектен әрекеттесуін этанол ортасындағы бөлме температурасында, реагенттердің ЭДА:CS₂:NaOH = 1:1,4:1,5 мольдік қатынасында жүргізген реакцияның нәтижесінде 90% шығыммен балку температурасы T_{балку} = 72-73 °C, қызғылт кристалды зат түрінде этан-1,2-диилдикарбамодитиоат натрий (НЭД) алынған. Оны 1-бром(C₇, C₈, C₉, C₁₀ және C₁₂)алкандармен 50-55 °C температурада ацетон ортасында, реагенттердің НЭД: БА = 1:1, 1:2, 1:3 мольдік қатынасында диалкилдеу жолы арқылы жүргізгенде жоғары шығыммен (63-84 %) сәйкес диалкилденген этан-1,2-диилдикарбамодитиоаттар синтезделген. Реакция өнімдерінің құрылысы ИҚ, ЯМР ¹H және ¹³C спектрлердің мәліметтерімен дәлелденген

Түйін сөздер: этан-1,2-диамин, дитиокарбонилдеу, алкилдеу, бромды алкилдер, диалкил этан-1,2-диилдикарбамодитиоаты.

Резюме

Н. О. Акимбаева, С. А. Визер, Т. М. Сейлханов, К. Б. Ержанов

АЛКИЛИРОВАНИЕ
ЭТАН-1,2-ДИИЛДИКАРБАМОДИТИОАТА НАТРИЯ

В результате реакции взаимодействия этан-1,2-диамина (ЭДА) с сероуглеродом, проведенной в среде 96% этанола при комнатной температуре, при мольном соотношении реагентов ЭДА: CS_2 : NaOH = 1:1,4:1,5, получен этан-1,2-диилдикарбамодитиоат натрия (НЭД) с выходом 90 %, в виде розового кристаллического вещества с $T_{\text{пл}} = 72-73$ °С. Путем его диалкилирования 1-бром(C_7 , C_8 , C_9 , C_{10} и C_{12}) алканами (БА) при температуре 50-55 °С в среде ацетона, при мольных соотношениях реагентов НЭД: БА = 1:1, 1:2 и 1:3 синтезированы соответствующие диалкилированные этан-1,2-диилдикарбамодитиоаты с хорошими и высокими выходами (63-84%). Строение продуктов реакций подтверждено данными ИК, ЯМР ^1H и ^{13}C спектров.

Ключевые слова: этан-1,2-диамин, дитиокарбонилирование, алкилирование, 1-бромалканы, диалкил этан-1,2-диилдикарбамодитиоаты.

L. A. KAYUKOVA¹, K. D. PRALIYEV¹, G. T. DYUSEMBAEVA¹,
K. AKATAN², E. SHAYMARDAN², S. K. KABDRAKHMANOVA²

¹JSC «A. B. Bekturov Institute of Chemical Sciences», Almaty, Republic of Kazakhstan,
²S. Amanzholov East Kazakhstan State University, Ust-Kamenogorsk, Republic of Kazakhstan

SYNTHESIZE 1,3,5-SUBSTITUTED ISOXAZOLES AT EXCESSIVE BENZOYLATION OF β -AMINOPROPIOAMIDOXIMES IN PYRIDINE

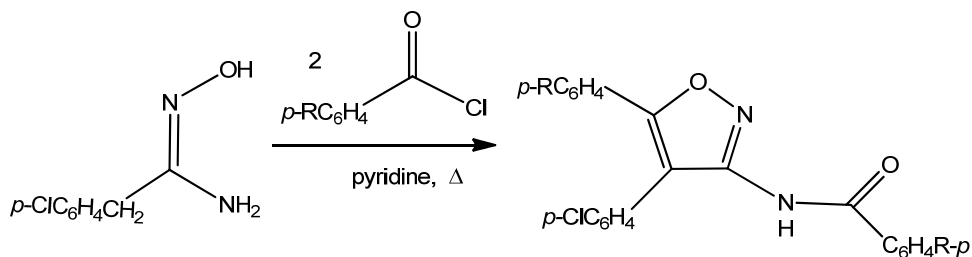
Abstract. Excessive acylation of β -aminopropioamidoximes (β -amino group: piperidin-1-yl, morpholin-1-yl, benzimidazol-1-yl, 4-phenylpiperazin-1-yl, thiomorpholin-1-yl) was carried out with a doubling excess of benzoyl chloride in pyridine at the boiling point of the solvent for 4–8 h. The isolated products are: N,O-dibenzoyl- β -aminopropioamidoxime dihydrochlorides in the case of ерқуу ашықе amidoximes, respectively. Chloride hydrate of 2-amino-1-aza-7-phenylaminospiro(4.5)decane-2-ene-10-ammonium and benzoic acid were the isolated products at using as starting amidoxime β -(4-phenylpiperazin-1-yl)propioamidoxime and hydrochloride of O-benzoyl- β -(thiomorpholin-1-yl)propioamidoxime at using of β -(thiomorpholin-1-yl)propioamidoxime as substrate. The formation of 2-amino-1-aza-7-phenylaminospiro(4.5)decane-2-ene-10-ammonium chloride monohydrate can be represented as the initial formation of O-benzoyl- β -aminopropioamidoxime hydrochloride, its dehydration to 1,2,4-oxadiazole, and the subsequent passing of the Boulton-Katritzky rearrangement to form a spiropyrazolinium compound and benzoic acid.

Key words: β -Aminopropioamidoximes, excessive acylation in pyridine, the Boulton-Katritzky rearrangement, benzoyl chloride, IR spectroscopy, ¹H and ¹³C NMR spectroscopy.

Introduction. Previously, in the series of products of monoacylation of β -aminopropioamidoximes where among the bases and hydrochlorides of O-royl- β -aminopropioamidoximes, and in the array of products of their dehydration – 5-substituted phenyl-3-(β -aminoethyl)-1,2,4-oxadiazoles the compounds possessing with high biological activity were found.

The list of practically useful of β -aminopropioamidoxime derivatives includes such as properties antiarrhythmic, local anesthetic and antitubercular [1, 2]. To modify β -aminopropioamidoximes in potentially biologically active derivatives containing a 3,4,5-substituted isoxazole heterocycle, the conditions for their interaction with a double excess of acylating agents were searched. It is known that the reaction of amidoxime 4-chlorophenylacetic acid with aromatic acid chlorides with a double molar excess of acid chlorides in pyridine leads to the formation of N-[4-(4-chlorophenyl) -5-phenylisoxazol-3-yl]benzamide (scheme 1) [3].

Structural analogs of isoxazole exhibit various types of biological activity and are used for a long time in pharmaceuticals. Sulfamethoxazole is widely known as part of the synergistic sulfonamide bacteriostatic antibiotic biseptol; cyclose-



Scheme 1

rine as an antibiotic agent with anti-tuberculosis, antibacterial activity, and also used in the treatment of leprosy. Biseptol and cycloserine are included in the WHO Model List of Essential Medicines [4]. The antibiotic Co-trimoxazole (sulfamethoxazole and trimethoprim), sulfisoxazole (or sulfafurazole) is used as an agent against a wide range of gram-positive and gram-negative microorganisms [5]. Oxacillin is an antimicrobial drug [6].

EXPERIMENTAL PART

IR spectra were recorded on a NICOLET 5700 FT-IR device in KBr tablets. NMR spectra (^1H and ^{13}C) are recorded on a NMR Avance III 500 MHz Bruker (Germany) device with an internal HMDS standard as solutions of compounds **6–11** in DMSO-d_6 . Chemical shifts are determined with respect to solvent signals (2,51 ppm for ^1H nuclei and 40,0 ppm for ^{13}C nuclei). The melting points was determined in glass capillaries on a TPL device. The purity of the products and the course of the reaction were monitored by TLC on Sorbfil plates (ZAO Sorbopolymer) with a sorbent-loaded silica gel layer CTX-1A with 5–17 μm grain and UV-254 UV indicator. The solvents used in the synthesis and recrystallization of the compounds and for elution in the TLC method (ethanol, *i*-PrOH, benzene) were prepared by standard procedures [11]. The solvent ratio ethanol : benzene in the eluent for TLC amounted to 3 : 1.

The two-step synthesis of the starting β -aminopropioamidoximes [β -amino group: piperidin-1-yl (**1**) and morpholin-1-yl (**2**)], we proposed to carry out in one reactor according to the "one-pot" method [12, 13]. β -Aminopropioamidoximes **3–5** [β -amino group: benzimidazol-1-yl (**3**); 4-phenylpiperazin-1-yl (**4**); thiomorpholin-1-yl (**5**)] were obtained by a two-step synthesis with isolation of β -aminopropionitriles and subsequent reaction of nitriles with hydroxylamine in absolute ethanol [14, 15].

N,O-Dibenzoyl- β -(piperidin-1-yl)propioamidoxime dihydrochloride (**6**). To 1000 mg (53 mmol) of β -(piperidin-1-yl)propioamidoxime (**1**) in 45 ml of pyridine 1,39 ml (106,0 mmol) of benzoyl chloride was added dropwise; then the reaction mixture was kept at room temperature for 2 h with stirring. After that the reaction mixture with TLC control was stirred at 115 $^\circ\text{C}$ for 4 h. The solvent was distilled off in a vacuum of a water jet pump; the residue was recrystallized from

i-PrOH. The yield of colorless crystals of N,O-dibenzoyl- β -(piperidin-1-yl)propioamidoxime dihydrochloride (**6**) amounted to 1300 mg (89%); m.p. 155 °C (i-PrOH); R_f 0,24. Found: C 58,62; H 5,46; Cl 15,30; N 9,07. $C_{22}H_{27}Cl_2N_3O_3$. Calculated: C 58,41; H 6,02; Cl 15,67; N 9,29.

N,O-Dibenzoyl- β -(morpholin-1-yl)propioamidoxime dihydrochloride (7). To 300 mg (17 mmol) of β -(morpholin-1-yl)propioamidoxime (**2**) in 15 ml of pyridine, 0,4 ml (34 mmol) of benzoyl chloride was added dropwise; then the reaction mixture was kept at room temperature for 2 h with stirring. After that the reaction mixture was stirred at 115 °C for 6 h with TLC control. The solvent was distilled off under an oil pump vacuum; the residue was recrystallized from i-PrOH. The yield of a fine white powder of N,O-dibenzoyl- β -(morpholin-1-yl)propioamidoxime dihydrochloride (**7**) was 190 mg (7,5 mmol) (43%); m.p. 110 °C (i-PrOH); R_f 0,40. Found: C 55,78; H 5,20; Cl 15,24; N 9,03. $C_{21}H_{25}Cl_2N_3O_4$. Calculated: C 55,51; H 5,55; Cl 15,61; N 9,25.

N,O-Dibenzoyl- β -(benzimidazol-1-yl)propioamidoxime dihydrochloride (8). To a suspension of 1000 mg (49 mmol) of β -(benzimidazol-1-yl)propioamidoxime (**3**) in 45 ml of pyridine at room temperature 1,39 ml (98 mmol) of benzoyl chloride was added dropwise; then the reaction mixture was kept at room temperature for 2 h with stirring. After that the reaction mixture was heated at 115 °C for 6 h. The end of the reaction is fixed by the presence on the plate for TLC of a single spot of product **8** with R_f 0,69. Pyridine was evaporated in a vacuum of a water jet pump; The precipitate was recrystallized from EtOH. Yield of colorless crystals of N,O-dibenzoyl- β -(benzimidazol-1-yl)propioamidoxime dihydrochloride (**8**) was 370 mg (27%); m.p. 180 °C (EtOH); R_f 0,69. Found: C 59,14; H 4,96; Cl 14,55; N 11,50. $C_{24}H_{22}Cl_2N_4O_3$. Calculated: C 59,39; H 4,57; Cl 14,61; N 11,54.

Chloride of 2-amino-1-aza-7-phenylaminospiro(4.5)decane-2-ene-10-ammonium (9) and benzoic acid (10). To 1000 mg (40 mmol) of β -(4-phenylpiperazin-1-yl)propioamidoxime (**4**) in 45 ml of pyridine 0,93 ml (80 mmol) of benzoyl chloride was added dropwise; then the reaction mixture was kept at room temperature for 2 h with stirring. After that the reaction mixture with TLC control was stirred at 115 °C for 4 h. The solvent was distilled off in a vacuum of a water jet pump; the residue was sublimed in a vacuum of oil pump at 50 °C and 2 mm Hg. At first 420 mg (43%) of a white precipitate of benzoic acid (**10**) with R_f 0,76 was collected on a cooled part of the sublimation apparatus; m.p. 121 °C (EtOH) [colorless needles, m.p. 122 °C (EtOH)] [16]. Found: C 68,95; H 5,22. $C_7H_6O_2$. Calculated: C 68,85; H 4,95. Then the residue in the distillation flask was recrystallized. Yield of light yellow powder of chloride of 2-amino-1-aza-7-phenylaminospiro(4.5)decane-2-ene-10-ammonium (**9**) was 440 mg (39%); m.p. 270 °C (i-PrOH); R_f 0,08. Found: C 54,94; H 7,82; Cl 11,97; N 19,48. $C_{13}H_{21}ClN_4O$. Calculated: C 54,83; H 7,43; Cl 12,45; N 19,67.

O-Benzoyl- β -(thiomorpholin-1-yl)propioamidoxime hydrochloride (11). To 1000 mg (26 mmol) of β -(thiomorpholin-1-yl)propioamidoxime (**5**) in 10 ml of pyridine, with stirring 0,61 ml (52 mmol) of benzoyl chloride was added; then the reaction mixture was kept at room temperature for 2 h with stirring. After that the

reaction mixture was stirred at 115 °C for 8 h and monitored by TLC. The solvent was distilled off in a vacuum of a water jet pump; the precipitate was recrystallized from *i*-PrOH. Yield of *O*-benzoyl- β -(thioforolin-1-yl)propioamidoxime hydrochloride (**11**) was 510 mg (52%), m.p. 119 °C (*i*-PrOH); R_f 0,80. [m.p. 120 °C (*i*-PrOH); R_f 0,79] [15]. Found: C 50,72; H 6,26; Cl 11,02; N 13,06. $C_{14}H_{20}ClN_3O_2S$. Calculated: C 50,98; H 6,11; Cl 10,75; N 12,74.

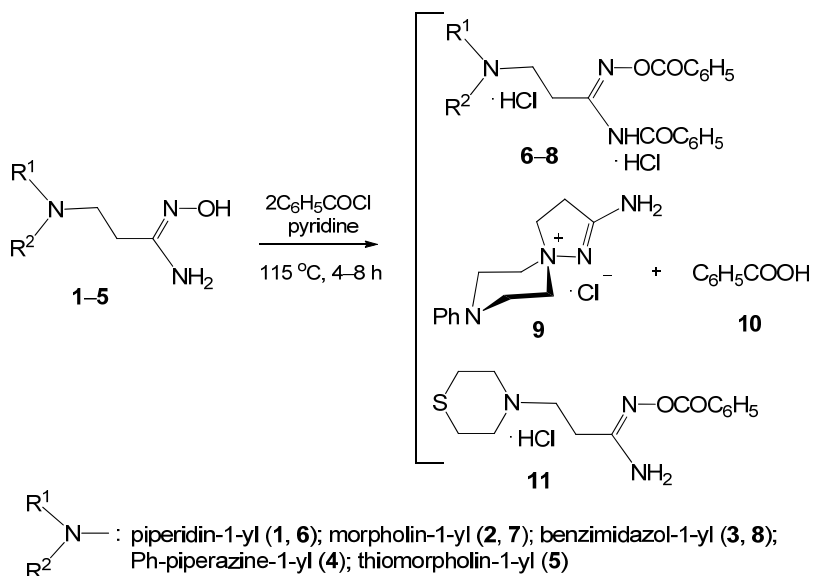
RESULTS AND DISCUSSION

We have not previously studied the acylation of β -aminopropioamidoximes under rigid conditions – with an excess of the acylating agent, in a polar solvent, at the boiling point of the solvent. The preparation of isoxazoles based on β -aminopropioamidoximes by the method [3] would allow us to investigate the little-known question of the excessive acylation of a multifunctional amidoxime group and, in the case of isolating new isoxazole derivatives, to study their biological activity.

When analyzing reaction products based on physicochemical and spectral data (elemental analysis, m.p., R_f , IR spectra and 1H and ^{13}C NMR spectra) (table 1–3), it was found that in the case of amidoximes **1–3** products **6–8** were isolated in the form dihydrochloride of double acylation products on oxygen and nitrogen atoms of the amidoxime group. In the acylation of β -(4-phenylpiperazin-1-yl)propioamidoxime (**4**), a spiropyrazolinium compound **9** and benzoic acid (**10**) were obtained; *O*-benzoyl-(β -thiomorpholin-1-yl)propioamidoxime hydrochloride (**11**) was a single product in the reaction of amidoxime **5** (table 1, scheme 2):

Table 1 – Physico-chemical characteristics of the reaction products of β -aminopropioamidoximes with two equivalents of benzoyl chloride **6–11**

Compound	Gross formula	Found, %				Reaction time, h	Mp, °C	R_f	Output, %
		Calculated, %							
		C	H	Cl	N				
6	$C_{22}H_{27}Cl_2N_3O_3$	$\frac{58,62}{58,41}$	$\frac{5,46}{6,02}$	$\frac{15,30}{15,67}$	$\frac{9,07}{9,29}$	4	155	0,24	89
7	$C_{21}H_{25}Cl_2N_3O_4$	$\frac{55,78}{55,51}$	$\frac{5,20}{5,55}$	$\frac{15,24}{15,61}$	$\frac{9,03}{9,25}$	6	110	0,40	43
8	$C_{24}H_{22}Cl_2N_4O_3$	$\frac{59,14}{59,39}$	$\frac{4,96}{4,57}$	$\frac{14,55}{14,61}$	$\frac{11,50}{11,54}$	6	180	0,69	44
9	$C_{13}H_{19}ClN_4$	$\frac{58,59}{58,53}$	$\frac{7,68}{7,18}$	$\frac{13,49}{13,29}$	$\frac{21,35}{21,00}$	4	270 (decomp.)	0,08	39
10	$C_7H_6O_2$	$\frac{68,76}{68,85}$	$\frac{5,26}{4,95}$	–	–	4	121	0,76	43
11	$C_{14}H_{20}ClN_3O_2S$	$\frac{50,72}{50,98}$	$\frac{6,26}{6,11}$	$\frac{11,02}{10,75}$	$\frac{13,06}{12,74}$	8	120	0,80	52



Scheme 2

The products of N,O-dibenzoylation of β -aminopropioamidoximes (**6–8**) have not been synthesized before. Obviously, the probable subsequent intramolecular splitting off of the water molecule involving protons of the α -methylene group and the carbonyl oxygen atom of the ester group could lead to isoazoles.

IR spectral characteristics of compounds **6–8**: the band of valence bond vibration $\nu_{\text{C=O}}$ is in the range of $1686\text{--}1731\text{ cm}^{-1}$; the stretching vibrations of the $\nu_{\text{C=N}}$ bonds are manifested in the region of $1638\text{--}1686\text{ cm}^{-1}$; the valence bond vibration bands $\nu_{\text{C=C}}$ are present in the region of $1584\text{--}1620\text{ cm}^{-1}$; in the region $1264\text{--}1293\text{ cm}^{-1}$ there are bands of stretching vibrations of the bonds $\nu_{\text{C-O}}$; the stretching vibrations of the $\nu_{\text{N(+)H}}$ ammonium bonds – in the region of $2464\text{--}2835\text{ cm}^{-1}$ (table 2).

Table 2 – Infrared spectra of the products of acylation of β -aminopropioamidoximes (**6–11**) by two equivalents of benzoyl chloride in pyridine

Compound	Valence vibrations of bonds, ν , cm^{-1}						
	$\nu_{\text{C=N}}$	$\nu_{\text{C=O}}$	$\nu_{\text{C=C}}$	$\nu_{\text{Csp}^3\text{-H}}$	$\nu_{\text{Csp}^2\text{-H}}$	$\nu_{\text{C-O}}$	$\nu_{\text{N(+)H}}$ ($\nu_{\text{N-H}}$)
6	1641	1727	1600	2958	3202–3375	1267	2562–2700 (3376)
7	1638	1731	1620	2930	3200–3375	1264	2464–2700 (3375)
8	1650	1730	1601	3063	3250–3416	1246	2500–2680 (3429)
9	1644	–	1600	2846	3116–3220	–	(3300; 3415)
10	–	1675	1600	–	3067; 3235; 3414	1289	3414 ($\nu_{\text{O-H}}$)
11	1640	1714	1611	2907	–	1268	2553; 2582; 2640 (3416; 3488)

In ^1H NMR spectra of N,O-dibenzoylation products **6–8**, in contrast to the literature data [1], the $\alpha\text{-CH}_2$ group signal is retained, which has a triplet structure from the spin-spin interaction with the $\beta\text{-CH}_2$ group (table 3). Signals of α - and β -methylene groups are in the regions δ 2,73–3,50 ppm. and δ 3,10–4,85 ppm, respectively.

The intensity of multiplet signals of aromatic protons in the range of δ 7–8 ppm indicates the presence in the molecules of compounds **6, 7** ten $\text{C}_{\text{sp}^2}\text{H}$ protons, and in the molecule of compound **8** – fifteen $\text{C}_{\text{sp}^2}\text{H}$ protons.

In addition, in the area of δ 6,85–7,50 ppm in the spectra of ^1H NMR compounds **6–8** there is a signal of ammonium protons of the $\text{N}(+)\text{H}_2\text{CO}_6\text{H}_5$ group, and in the range of δ 10,55–12,90 ppm – the signal of the ammonium $\text{N}(+)\text{H}$ proton coordinated on the nitrogen atom of the β -amino group.

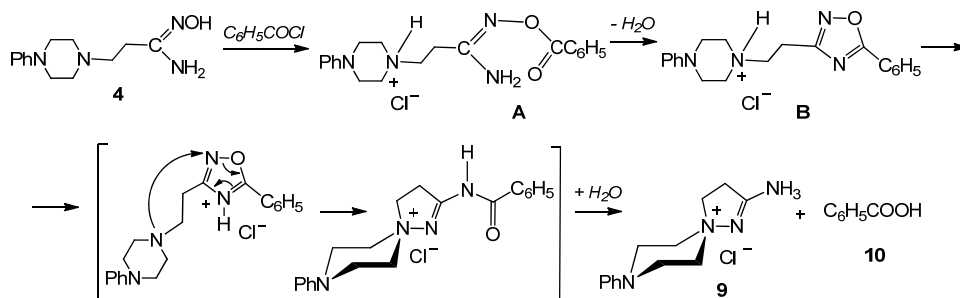
Table 3 – ^1H and ^{13}C NMR spectra of compounds **6–11**, solutions in DMSO-d_6 , δ , ppm*

Compound	Chemical shifts, δ , ppm (J, Hz)	
6	1,39; 1,68; 1,79 [6H, m, $-\text{N}(\text{CH}_2)_2(\text{CH}_2)_3$]; 2,74 (2H, t, $J = 6,0$, $\alpha\text{-CH}_2$); 2,90 [4H, m, $-\text{N}(+)\text{CH}_2(\text{CH}_2)_3$]; 3,30 (2H, t, $J = 6,0$; $\beta\text{-CH}_2$); 6,87 [2H, s, $\text{N}(+)\text{H}_2$]; 7,51; 7,65; 8,11 (10H, m, C_6H_5); 10,74 [1H, s, $\text{N}(+)\text{H}$]	21,82; 22,72; 22,83; 25,87; 52,44; 53,11; 129,01; 129,71; 129,83; 129,88; 133,49; 156,80; 163,88
7	2,76 (2H, t, $J = 7,0$, $\alpha\text{-CH}_2$); 3,15 [4H, m, $-\text{N}(\text{CH}_2)_2(\text{CH}_2)_2\text{O}$]; 3,67 (2H, t, $J = 7,0$, $\beta\text{-CH}_2$); 3,94 [4H, m, $-\text{N}(+)\text{CH}_2(\text{CH}_2)_2\text{O}$]; 6,85 [2H, s, $\text{N}(+)\text{H}_2$]; 7,49–8,12 (10H, m, C_6H_5); 11,65 [1H, s, $\text{N}(+)\text{H}$]	25,55; 25,60; 31,43; 31,45; 51,46; 53,12; 62,08; 62,43; 63,24; 63,65; 129,01; 129,84; 129,88; 133,48; 156,61; 163,86; 169,02; 169,10
8	3,40 (2H, t, $J = 7,0$, $\alpha\text{-CH}_2$); 4,74 (2H, t, $J = 7,0$, $\beta\text{-CH}_2$); 7,48; 7,51; 7,60; 7,65; 7,94; 7,96; 8,04; 8,06; 9,00 [17H, m, $\text{C}_{\text{sp}^2\text{-H}}$ and $\text{N}(+)\text{H}_2$]; 12,95 [1H, s, $\text{N}(+)\text{H}$]	26,35; 43,00; 123,73; 124,61; 124,79; 128,25; 129,00; 129,71; 130,01; 131,27; 133,27; 133,79; 143,54; 167,75; 168,57; 175,57
9	3,19 (2H, t, $J = 6,0$, $\beta\text{-CH}_2$); 3,44 [2H, m, half-width 12,5 mm, $\text{PhN}(\text{CH}_2)_2$ (axial)]; 3,56 [4H, m, $\text{N}(+)\text{CH}_2$]; 3,78 [2H, m, half-width 11 mm, $\text{PhN}(\text{CH}_2)_2$ (equatorial)]; 3,98 (2H, t, $J = 6,0$, $\alpha\text{-CH}_2$); 6,86; 7,02; 7,27 (5H, m, C_6H_5); 7,53 (2H, s, NH_2)	31,57; 44,57; 61,42; 62,91; 116,32; 120,38; 129,58; 149,94; 169,11
10	7,50; 7,63; 7,95 (5H, m, C_6H_5); 12,95 (1H, s, COOH)	129,02; 129,72; 131,24; 133,31; 167,76
11	2,76 (2H, t, $J = 7,0$, $\alpha\text{-CH}_2$); 3,39 (2H, t, $J = 7,0$, $\beta\text{-CH}_2$); 3,35 (4H, m, $\text{S}(\text{CH}_2)_2$); 3,70 [4H, m, $\text{N}(+)\text{CH}_2$]; 6,86 (2H, s, NH_2); 7,51; 7,64; 8,12 (5H, m, C_6H_5); 11,37 [1H, s, $\text{N}(+)\text{H}$]	24,25; 25,61; 53,43; 53,68; 129,00; 129,83; 133,48; 148,56; 156,67; 163,88

*The assignment of the multiplet signals of the protons of the methylene groups of the thiomorpholine heterocycle, having the intensity of two protons which adjacent to the $\text{N}(+)\text{CH}_2$ nitrogen atom of compound **9**, to equatorial and axial is made on the basis of a half-width comparison of the signal. The half-width of the axial signals of the protons is greater than the half-width of the equatorial signals.

In the ^{13}C NMR spectra of compounds **6–8**, the carbon signals of the $\text{C}=\text{N}$ functional groups are found at δ 156,80 (**6**); 156,61 (**7**); 168,57 (**8**), respectively, and $\text{C}=\text{O}$ at 163,88 (**6**), 163,86 (**7**), 175,57 (**8**), respectively.

The formation of 2-amino-1-aza-7-phenylaminospiro(4.5)decane-2-ene-10-ammonium chloride monohydrate (**9**) can be represented as the initial formation of O-benzoyl- β -aminopropioamidoxime hydrochloride (**A**), its dehydration to 1,2,4-oxadiazole (**B**) and the subsequent proton transfer and nucleophilic attack steps, also involving hydrolysis with the formation of spirocompound **9** and benzoic acid (**10**) (scheme 3).



Scheme 3

Such course of the acylation reaction under severe conditions – when the reagents are heated at the boiling point of the polar solvent of pyridine is possible.

Formation of analogous structures under milder conditions – at room temperature in ethanol in the preparation of 5-substituted phenyl-3-[(β -thiomorpholin-1-yl)ethyl]-1,2,4-oxadiazoles hydrochlorides and recrystallization from isopropanol of 5-substituted phenyl-3-[(β -(4-phenylpiperazin-1-yl)ethyl)-1,2,4-oxadiazoles was detected by us earlier [7, 8].

In the IR spectrum of the chloride hydrate of the spiropyrazolinium compound **9**, there are bands of characteristic valence vibrations of the bonds $\nu_{\text{C}=\text{N}}$ and $\nu_{\text{C}=\text{C}}$ at 1644 and 1600 cm^{-1} , respectively. In the ^1H NMR spectrum of the spiropyrazolinium compound **9**, the triplet signals of α - CH_2 and β - CH_2 groups with an intensity of two protons are at δ 3,19 and 3,98 ppm; the signal of the amino group of pyrazolinium ring with an intensity of two protons is present at δ 7,53 ppm.

The carbon atom signal of the $\text{C}=\text{N}$ bond of the compound **9** in the ^{13}C NMR spectrum is observed at δ 169,11 ppm. Benzoic acid **10** was isolated during the treatment of the reaction mixture described in the experimental part. Its physicochemical and spectral characteristics correspond to tabular data.

β -(Thiomorpholin-1-yl)propioamidoxime (**5**) reacts with two equivalents of benzoyl chloride in boiling pyridine with a regiospecific formation of the monoacylation product at the oxygen atom of the amidoxime group, O-benzoyl- β -(thiomorpholin-1-yl)propioamidoxime hydrochloride (**11**). Compound **11** obtained by monoacylation of β -(thiomorpholin-1-yl)propioamidoxime (**5**) at room temperature in chloroform was described by us earlier [9].

Conclusion. Thus, the interaction of β -aminopropioamidoximes with a double excess of benzoyl chloride in boiling pyridine instead of the expected isoxazoles yielded a set of acylation products: N,O-diacylated β -aminopropioamidoxime dihydrochlorides, spiropyrazolinium compound hydrochloride, and O-acylation hydrochloride. The ambiguous direction of the reaction was obviously connected with the electronic influence of the β -aminoheterocyclic substituent and the possibility of thermodynamically light rearrangements of the initially formed products [10].

The research was carried out according to the scientific and technical program No. BR05234667 within the framework of program-targeted financing CS MES RK.

REFERENCES

- [1] Kayukova L.A. Chemistry of azometines of 2-substituted cyclohexanones, β -aminopropioamidoximes and α -chloro- α -isonitrosoketones; their anti-tuberculosis, anti-arithmetic, local-anesthetic and other properties: Author's Abstract of a Doctoral Dissertation in Chemical Sciences. Almaty: JSC «A.B. Bekturov Institute of Chemical Sciences», 2005. 53 p.
- [2] Kayukova L.A., Praliev K.D., Akhelova A.L., Kemel'bekov U.S., Pichkhadze G.M., Mukhamedzhanova G.S., Kadyrova D.M., Nasyrova S.R. Local anesthetic activity of new amidoxime derivatives // *Pharmaceutical Chemistry Journal*. 2011. Vol. 45, N 8. P. 468-471. (Russian Original: Vol. 45, N 8. P. 30-32).
- [3] Vakhitov T.R., Veretennikov E.A., Shtabova O.V. Formation of an isoxazole ring from phenylacetic acid amidoximes // *Chemistry of Heterocyclic Compounds*. 2007. Vol. 43, N 1. P. 118-119. (Russian Original: Vol. 43, N 1. P. 134-135).
- [4] WHO Model list of Essential Medicines 18th edition. April 2013.
- [5] Mashkovskii M.D. Medications. M.: Publishing Ltd New Wave, 2002. Vol. II. P. 282. (Russian).
- [6] Greenwood D. Antimicrobial Drugs. Chronicle of a twentieth century medical triumph. London: Oxford University Press US, 2008. 429 p.
- [7] Kayukova L.A., Orazbaeva M.A., Gapparova G.I., Beketov K.M., Espenbetov A.A., Fashutdinov M.F., Tashkhodjaev B.T. Rapid acid hydrolysis of 5-aryl-3-(β -thiomorpholinoethyl)-1,2,4-oxadiazoles // *Chem. Heterocycl. Compd*. 2010. Vol. 46. P. 879-886. [Russian Original: 2010. Vol. 46. P. 1086-1096.]
- [8] Beketov K.M., Kayukova L.A., Praliyev K.D., Baitursunova G.F. Variety of Boulton-Katritzky rearrangement on the sample of 3- β -(4-phenylpiperazin-1-yl)-5-phenyl-1,2,4-oxadiazole // *Chemical Journal of Kazakhstan*. 2011. N 4. P. 14-19. (Russian).
- [9] Kayukova L.A., Orazbaeva M.A. Synthesis of β -(thiomorpholin-1-yl) propionitrile and amidoxime; preparation of O-aryl- β -(thiomorpholin-1-yl) propioamidoximes as potential antituberculous agents // *Bulletin of NAS RK. Series of Chemistry and Technology Sciences*. 2007. N 5. P. 37-42.
- [10] Kayukova, L.A., Imanbekov K.I., Praliyev K.D. Evaluation of thermodynamic stability of 5-aryl-3-[β -(thiomorpholin-1-yl) and β -(4-phenylpiperazin-1-yl)]ethyl-1,2,4-oxadiazoles and spiro-pyrazolinium compounds in Boulton-Katritzky rearrangement // *Chemical Journal of Kazakhstan*. 2014. N 2. P. 208-212. (Russian).
- [11] Gordon A.J., Ford R.A. The Chemist's Companion. A Handbook of Practical Data, Techniques, and References. M.: Mir, 1976. P. 442-443.
- [12] Innovation Patent of the Republic of Kazakhstan № 28057 / Kayukova L.A., Praliyev K.D., Dusembaeva G.T. A process for the preparation of β -(morpholin-1-yl)propioamidoxime. // *Publ. 25.12.2013. Byul. Izobret. of the Republic of Kazakhstan*. N 12; <https://gosreestr.kazpatent.kz> (Russian).
- [13] Innovation Patent of the Republic of Kazakhstan № 28453 / Kayukova L.A., Praliyev K.D., Dusembaeva G.T., Uzakova A.B. A process for the preparation of β -(piperidin-1-yl)pro-

pioamidoxime // Publ. 15.05.2014. Byul. Izobret. of the Republic of Kazakhstan. N 5; <https://gosreestr.kazpatent.kz> Russian

[14] Akhelova A.L. β -Aminopropioamidoximes as N,O-nucleophiles in the reactions with acylchlorides, α -halogenketones and propargyl haloids; biological properties of the products: Author's Abstract of a Candidate Dissertation in Chemical Sciences. Almaty: JSC «A.B. Bekturov Institute of Chemical Sciences», 2005. 25 p. (Russian).

[15] Orazbaeva M.A. Products of O-arylation, propargylation and heterocyclization of β -aminopropioamidoximes; their antitubercular properties: Author's Abstract of a Candidate Dissertation in Chemical Sciences. Almaty: JSC «A.B. Bekturov Institute of Chemical Sciences», 2008. 25 p. (Russian).

[16] Rabinovich V.A., Khavin Z.Ya. Brief Chemical Reference Book, 2nd. Ed., Revised and Updated. L.: Chemistry Publishers, 1978. P. 131. (Russian).

Резюме

*Л. А. Каюкова, К. Д. Пралиев, Г. Т. Дюсембаева,
К. Акатан, Е. Шаймардан, С.К. Кабдрахманова*

β -АМИНОПРОПИОАМИДОКСИМДЕРДІ ПИРИДИНДЕ АРТЫҚ БЕНЗОИЛІРЛЕУ КЕЗІНДЕ 1,3,5-ОРЫНБАСҚАН ИЗОКСАЗОЛДАРДЫ СИНТЕЗДЕУ

β -Аминопропиоамидоксимдердің шамадан тыс ацелирленуі (β -аминотоп: пиперидин-1, морфолин-1, бензимидазол-1, 4-фенилпиперазин-1, тиоморфолин-1) еріткіштің қайнау нүктесінде 4–8 сағат ішінде пиридиннің бензоил хлоридінің қос тотығымен көбеюімен жүзеге асырылды. Пиперидин, морфолин және бензимидазол амидоксими жағдайында N, O-добензоил- β -аминопропиоамидоксим дихидрохлоридтері ерекше өнім болып табылады; тиісінше, хлоридті гидрат спиропиразолин қосылысының және бензой қышқылы және O-бензоил- β -(тиоморфолин-1-ил)пропиоамидоксим гидрохлоридтеріне субстраттар ретінде β -(4-фенилпиперазин-1-ил)пропиоамидоксим және β -(тиоморфолин-1-ил)пропиоамидоксимдер пайдаланылады.

Түйін сөздер: β -Аминопропиоамидоксимдер, пиридиннің артық ациляциясы, бензоил хлориді, ИК-спектроскопия, ^1H и ^{13}C ЯМР спектроскопиясы.

Резюме

*Л. А. Каюкова, К. Д. Пралиев, Г. Т. Дюсембаева,
К. Акатан, Е. Шаймардан, С.К. Кабдрахманова*

СИНТЕЗ 1,3,5-ЗАМЕЩЕННЫХ ИЗОКСАЗОЛОВ ПРИ ИЗБЫТОЧНОМ БЕНЗОИЛИРОВАНИИ β -АМИНОПРОПИОАМИДОКСИМОВ В ПИРИДИНЕ

Избыточное ацилирование β -аминопропиоамидоксимов (β -аминогруппа: пиперидин-1-ил, морфолин-1-ил, бензимидазол-1-ил, 4-фенилпиперазин-1-ил, тиоморфолин-1-ил) проведено при двукратном избытке бензоилхлорида в пиридине при температуре кипения растворителя в течение 4–8 ч. Выделенными продуктами являются дигидрохлориды N,O-добензоил- β -аминопропиоамидоксимов в случае пиперидинового, морфолинового и бензимидазольного амидоксима; гидрат хлорида спиропиразолиниевое соединения и бензойная кислота и гидрохлорид O-бензоил- β -(тиоморфолин-1-ил)пропиоамидоксима при использовании в качестве субстратов β -(4-фенилпиперазин-1-ил)пропиоамидоксима и β -(тиоморфолин-1-ил)пропиоамидоксима, соответственно.

Ключевые слова: β -Аминопропиоамидоксими, избыточное ацилирование в пиридине, хлористый бензоил, ИК-спектроскопия, спектроскопия ^1H и ^{13}C ЯМР.

M. Kozybayev North Kazakhstan State University, Petropavlovsk, Republic of Kazakhstan

STUDY OF THE DISPERSING EFFECT PRODUCED BY POLYETHER SILOXANE COPOLYMERS IN WATER-DISPERSION SYSTEMS

Abstract. The study resulted in determining the disaggregating effect produced by polyether siloxane copolymers in binary and ternary systems based on water-acrylic dispersion. It exposed the regularities in characteristic changing specific for the dispersed composition of solid-phase particle suspensions, and on this basis the polyester siloxane copolymer costs were optimized to achieve the maximum dispersing effect. The studies contributed to establishing the possibility of using polyether siloxane copolymers in paint coating compositions based on acrylic polymers and titanium dioxide as the modifying additive that produces dispersing effect.

Key words: dispersion, pigment, water-acrylic dispersion, titanium dioxide, polyether siloxane copolymer, suspension, modifier.

Introduction. The solid ingredient combining process, which includes a pigment with a liquid polymer medium, is very important in the paint coating manufacture since the product technological and paint properties depend on it, as well as many coating performance properties. The main thing in this process is the pigment interaction with the polymer at the interface between the solid and liquid phases, since its intensity determines the solid particle dispersion in the given medium and the nature of the resulting combined “solid phase-polymer” structures that form the subsequent properties specific for real materials. This was established in Academician P.A.Rebinder’s publications addressing the structure formation and physicochemical mechanics of dispersed systems [1-3] and was further developed by his school staff, A.B.Taubman and S.N.Tolstaya [4-6], who studied pigments interacting with polymers at the phase interface for a wide range of model and real objects. An important technological characteristic exhibited by paint coating materials, which determine the coating structural and mechanical properties (coverage, hardness, strength), is the disaggregation degree specific for pigments and fillers [1].

It was found that the pigment particle dispersion, when combined with the polymer, may both improve and worsen (which has been shown in Figure 1 schematically), in addition, it depends on the chemical nature of both components.

The component combination where the solid particle dispersion in the given polymer medium increases, i.e. the aggregates gradually disintegrate to smaller aggregates or even to primary particles, which is shown in figure 1, a), b), c), is considered appropriate. Interacting with one another through the surface-active material interlayers, solid particles form a developed structure where, as in the framework, a secondary structure of the oriented (and hence strengthened) polymer is formed [2].

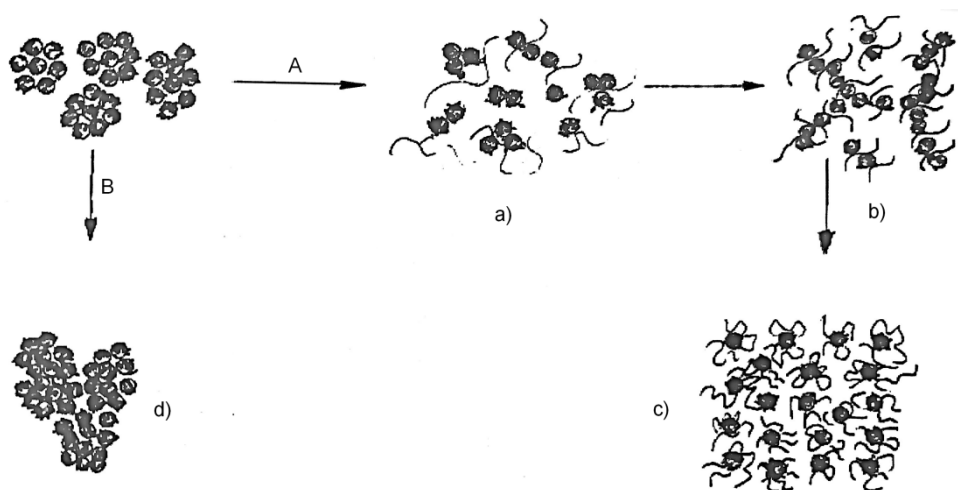


Figure 1 – Change in the pigment dispersion upon its introduction into the polymer medium: A – pigment particle dispersion improvement in comparison with the initial dispersion rate due to natural aggregate peptization: a) separate chain particle formation; b) solid spatial grid formation out of the solid phase particles; c) complete solid particle stabilization. B – pigment dispersion worsening compared with the initial dispersion rate (compact coagulation) – d)

Such combined “solid phase-polymer” structures are called coagulation structures (according to Rebinder); during their formation the system strength increases at the beginning, which is detected by measuring the ultimate statistical shear stress which magnitude is as greater as stronger the solid particle aggregates are peptized in the given medium [7]. Then, after the peptized particles achieve complete stabilization, the strength decreases. Such structures are usually thixotropic, i.e. they are able to recover their physical and mechanical, as well as rheological properties naturally when destructed [3].

Such combined “solid phase-polymer” structures are called coagulation structures (according to Rebinder); during their formation the system strength increases at the beginning, which is detected by measuring the ultimate statistical shear stress which magnitude is as greater as stronger the solid particle aggregates are peptized in the given medium [7]. Then, after the peptized particles achieve complete stabilization, the strength decreases. Such structures are usually thixotropic, i.e. they are able to recover their physical and mechanical, as well as rheological properties naturally when destructed [3].

For the overwhelming majority of paint coating materials, when combining a pigment with polymer solutions, it is necessary to form coagulation-type structures, since in this case it is possible to obtain materials and coatings based on them having the necessary properties.

However, in many cases the pigment particle peptization process does not occur naturally, on the contrary, formation of larger aggregates can be observed in

comparison with the initial particles, i.e. there is a dispersed phase coagulation process in the given medium, as shown in Fig. 1 b, d. The first process occurs under the liqophilicity of the solid phase particle surface against the liquid medium, and the second one occurs under its liophobicity. For example, hydrophobic graphite is well combined with vegetable oils or non-polar rubbers and disperses well in them, whereas hydrophilic inorganic pigments (ZnO , TiO_2 , Fe_2O_3 , SiO_2) poorly combine with such hydrocarbon media, which can lead to compact solid phase particle coagulation [3]. In systems with weak and medium interaction, the process where the pigment and the filler combine with the polymer must be intensified. Using surface-active substances (SAS), fine regulators of interface interactions and finished material properties proves to be the most effective method.

The SAS effect is based on forming the surface pigment and filler of the adsorption layer, whose properties, in turn, are determined due to the forming its inner and outer parts. The inner adsorption layer part is formed resulting from the polar SAS group interaction with active surface centers, which promotes peptizing the aggregated pigment and filler particles and the formation of coagulation structure elements. The adsorption layer outer part is formed when hydrocarbon SAS molecule radicals are oriented to the polymer medium, increasing the liqophilicity of the pigment particle surface that is combined with it [2].

Polar hydrophilic pigments introduction into non-polar hydrocarbon media, provides for using modifiers with long hydrocarbon chains (hydrophobisators), for example saturated carboxylic acids, amines or their salts, as well as quaternary ammonium salts and other compounds. When it comes to polar dispersion media, SAS whose molecules contain polar groups in the hydrocarbon radical that are lyophilic with respect to the polymer dispersion medium (i.e., various bifunctional compounds) are used as pigment surface modifiers [2]. This is applicable to all paint coating material types containing polymer solutions as a binder in organic solvents (or in water for water-soluble polymers), water-dispersed binders. Developed and used in recent years polymeric SAS can be even more effective than their low molecular weight analogues due to their high affinity for the polymer medium.

However, the SAS action in paint coating systems is subject to certain physicochemical laws that must be observed for their effective application. An important role in this is played by the polar SAS group nature and the hydrocarbon radical structure specific for their molecules, as well as the polymer chemical nature and the presence of polar functional groups in its molecules. In the paint coating material suspensions, the development of aggregation and disaggregation processes depends both on the surface properties shown by the solid-phase particles and on the quantitative-qualitative composition of the film-forming agents, solvents and surface-active additives. In this connection, it seemed reasonable to evaluate the dispersing effect performance with respect to the polyether siloxane copolymer against the titanium dioxide in the aqueous dispersion of acrylic polymers.

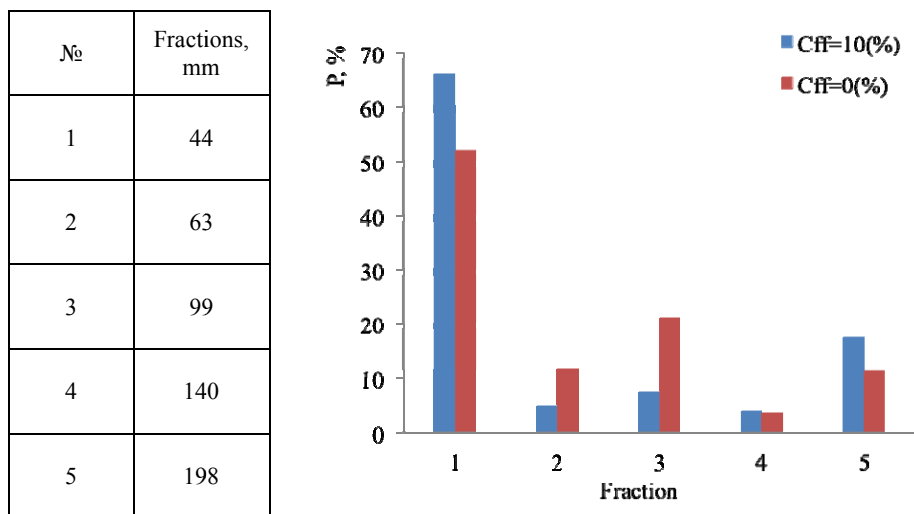


Figure 2 – Differential curves for the particle size distribution of the solid-phase particle fraction in water

by a fine fraction increase to 67%. This process results from the generated disjoining pressure due to the film-forming agent diffusion along the separate particle boundaries; at this stage, the first particles to disaggregate are those bound by point contact mainly and only then those bound by stronger linear and planar contacts [10].

SAS polyether siloxane copolymer introduced into the compositions opens additional possibilities for a purposeful change in the dispersed composition. The depth and direction determined for these changes are shown in figure 3.

In the water-SAS system, the maximum disaggregating effect produced by the modifier was registered when its content stood at 1.0 g/dm³ (figure 3, curve 1), while the average diameter limit was 4.5 μm. Beyond this concentration section

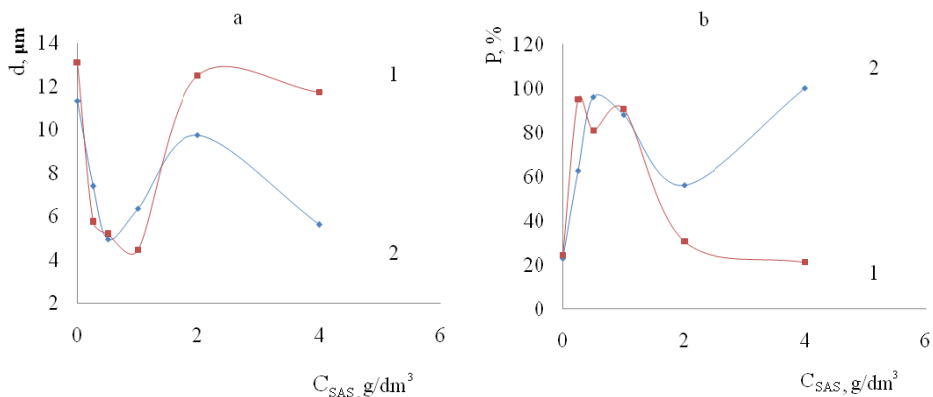


Figure 3 – Changes in the average fine fraction diameter (a) and content (b) depending on the polyether siloxane copolymer concentration

($C_{SAS} > \text{g/dm}^3$), a secondary aggregation process can be observed, accompanied by an increase in diameter from 4.5 to 12.5 μm and a corresponding reduction in the fine fraction content from 91 to 31%.

Similar patterns in the dispersed composition changes under the influence produced by the polyether siloxane copolymer were also noted in the "film-forming agent-SAS" system: the disaggregating effect in the low concentration region and the flocculation process development with its further concentration. In the first place, we should note the intensity in the film-forming solution (figure 3, curve 2), where the secondary aggregation process is less pronounced than in the water, and secondly, the maximal disaggregating effect is shifted to the lower concentration region ($C_{SAS} \leq 0.5 \text{ g/dm}^3$).

Conclusion. Comparatively analyzed dispersing effect produced by the modifier under study in binary and ternary systems showed a deeper dispersion in water, which is due to the deficient competition from the side of the film-forming agent macromolecules.

The performed studies let us establish the possibility of using polyether siloxane copolymers in paint coating compositions based on aqueous dispersion of acrylic polymers and titanium dioxide as the modifying additive that produces dispersing effect. The appropriate SAS concentration is its composition content at 0.25 g/dm^3 .

REFERENCES

- [1] Rebinder P.A. Surface phenomena in dispersed systems: Sat. Scientific works. M.: Nauka, 1979. Vol. 1. 450 p.
- [2] Rebinder P.A. Physico-chemical mechanics of disperse structures. M.: Knowledge, 1958. Ser. 1B. N 34, 49. 64 p.
- [3] Yakovlev A.D. Chemistry and the hedgehogs of the Paint and Varnish Zoatings. L.: Chemistry, 1989. 382 p.
- [4] Taubman A.B., Tolstaya S.N., Borodina V.N. Adsorption modification of fillers and pigments and structure formation in polymer solutions // DAN SSSR. 1962. Vol. 142, N 2. P. 407.
- [5] Tolstaya S.N., Shabanova S.A. The use of surfactants in the paint and varnish industry. M.: Chemistry, 1976. 176 p.
- [6] Abramzon A.A. Surface-active substances. Properties and application. L.: Chemistry, 1975. 248 p.
- [7] Rebinder P.A., Wlodavets I.I. High-molecular dispersed systems // Surface phenomena in disperse systems. M., 1988. P. 61-73.
- [8] Dyuryagina A.N., Ostrovnoy K.A. Evaluation of the disaggregating effect of surfactants in lacquer coating compositions by conjugation of optical microscopy of personal computers // Paint-and-paint materials and their application. M., 2007. N 7-8. P. 77-80.
- [9] Dyuryagina A.N., Lugovitskaya T.N., Ostrovnoy K.A. Fomatizatsiya analysis of powders and suspensions based on computer-optical systems // Collection of proceedings of the third international scientific and practical conference "Research, development and application of high-tech in the industry". SPb., 2007. Vol. 9. P. 47-48.
- [10] Bolatbaev K.N., Dyuryagina A.N., Ostrovnoy K.A. Modification of composites by surfactants. Petropavlovsk, 2005. 184p.

Резюме

А. Н. Дюрягина, А. А. Луценко

ИССЛЕДОВАНИЕ ДИСПЕРГИРУЮЩЕГО ЭФФЕКТА
ПОЛИЭФИРСИЛОКСАНОВОГО СОПОЛИМЕРА
В ВОДНО-ДИСПЕРСИОННЫХ СИСТЕМАХ

Приведены результаты экспериментальных исследований закономерностей развития процессов дезагрегации диоксида титана в водной дисперсионной среде в присутствии полиэфирсилоксанового сополимера. С помощью приложения компьютерно-микрооптического метода к анализу исследуемых суспензий в автоматическом режиме была установлена закономерность развития процессов агрегации твердофазных пигментов и количественные характеристики их распределения по фракциям.

Ключевые слова: диспергирование, пигмент, водно-акриловая дисперсия, диоксид титана, полиэфирсилоксановый сополимер, суспензия, модификатор.

Резюме

А. Н. Дюрягина, А. А. Луценко

ПОЛИЭФИРСИЛОКСАН СОПОЛИМЕРІНІҢ ҚАТЫСУЫМЕН
ТИТАН ДИОКСИДІНІҢ ДИСПЕРСИЯЛЫҚ ҮДЕРІСТЕРІН
ЗЕРТТЕУ

Осы жұмыста полиэфирсилоксан сополимерінің қатысуымен су-дисперсиялық ортада титан диоксидін дезагрегациялау үдерістерінің даму заңдылықтарын эксперименталдық зерттеудің нәтижелері келтірілді. Зерттелетін суспензияларды автоматты тәртіпте талдауға қатысты компьютерлік-микрооптикалық әдістің қосымшасының көмегімен қатты фазалық пигменттердің агрегация үдерістерін дамытудың заңнамалығы, оларды фракциялар бойынша бөлудің мөлшерлік сипаттамалары анықталды.

Түін сөздер: дисперсия, пигмент, су-акрил дисперсиясы, титан диоксиді, полиэфирсилоксан сополимері, суспензия, модификатор.

*H. AVCHUKIR**, *B. D. BURKITBAYEVA*,
A. M. ARGIMBAYEVA, *G. S. RAKHYMBAY*

Al-Farabi Kazakh National University, Almaty, Republic of Kazakhstan.
E-mail: khaisa.avchukir@cfhma.kz

KINETICS OF ELECTRODEPOSITION OF INDIUM ON SOLID ELECTRODES FROM CHLORIDE SOLUTIONS

Abstract. Using the methods of cyclic voltammetry and chronoamperometry, the electroreduction of indium on titanium, platinum and glassy carbon electrodes from perchlorate-containing chloride electrolytes has been studied. The quasi-reversible character of the process under investigation for all the above electrodes are established on the basis of the analysis of the difference in potentials of the peaks on the forward and reverse course of the sweep and the relationship between the current of the reduction peak and the rate of polarization. The overvoltage of indium release in the peak on Pt, GC, Ti electrodes was 158, 111, 64 mV, respectively. The constants of the rate of charge transfer and mass transfer of indium electrodeposition are calculated using the Delahay and Cottrell equations. A comparative analysis of the obtained constants showed that they had large values in the case of a titanium electrode and amounted to $1.06 \cdot 10^{-3}$ and $4.5 \cdot 10^{-4}$ cm/s, respectively. The results obtained indicate the preferred use of titanium in the electrochemical purification of rough indium.

Key words: indium, electrodeposition, mass transfer, charge transfer, diffusion coefficient, quasi-reversibility, rate constant.

Introduction. Electrochemical methods of deep purification of metallic indium have great potentialities and are especially valuable with a low content of micro-impurities. One of the main methods for obtaining high-purity indium is electrochemical refining, the implementation of which requires a deep and detailed study of the processes of discharge-ionization of indium on solid electrodes. This research is devoted to the development of the technology of electrochemical refining of the rough indium of Kazakhstan, which is a by-product of the lead-zinc enterprise Kazzinc JSC [1]. Obtaining domestic high-purity indium is a prerequisite for the development of electronic and semiconductor industry in the Republic of Kazakhstan.

The quality of cathodic precipitation and economic indicators in the process of electrorefining of metals depend on the composition of the electrolyte, substrate nature and electrolysis conditions. A number of publications [2-5] are devoted to the study of indium electrodeposition on various electrodes in chloride and perchlorate electrolytes. In previous works [6, 7] we studied the electroreduction of indium on solid electrodes in acid chloride electrolytes. As a result of these studies, the kinetic characteristics of indium reduction on platinum and titanium electrodes were determined and the nature of the limiting stage was established.

In this paper, the effect of the nature of the electrode and the concentration of the In^{3+} salt in solution on the kinetics of indium electroreduction in perchlorate-containing chloride electrolytes by cyclic voltammetry and chronoamperometry is considered.

EXPERIMENTAL PART

Electroreduction of indium was investigated by the method of cyclic voltammetry, chronoamperometry in a thermostated three-electrode electrochemical cell, using the potentiostat-galvanostat Autolab PGSTAT 302N. Working electrodes were platinum and glass-carbon electrodes 0.3 cm in diameter produced by Metrohm, as well as a titanium electrode 0.25 cm in diameter (of brand Ti BT1-0). The auxiliary electrode was a platinum plate with an area of 12.96 cm², and the reference electrode was a silver chloride electrode. All experiments were carried out at a temperature of 25°C with an accuracy of $\pm 0.1^\circ\text{C}$. Perchlorate-containing chloride electrolytes of composition: 0.025; 0.05; 0.1 M $\text{In}(\text{ClO}_4)_3 + 2.0 \text{ M NaCl}$ (pH = 1.5) were prepared from 1.0 M indium perchlorate solution on the background of 2.0 M sodium chloride solution. Solution $\text{In}(\text{ClO}_4)_3$ was obtained by the interaction of metal indium of brand In-2 (with a 99.98% base metal content) with 60% solution of perchloric acid produced by Sigma Aldrich (99.99%). The basic background electrolyte was a solution of sodium chloride, obtained from a triply recrystallized chemically pure salt (99.9%). The pH values of the solutions (1.5-1.6) were created by acidifying them with perchloric acid. Before each measurement, the platinum and glassy carbon electrodes were purified in a solution of concentrated nitric acid, and the titanium electrode was machined using a micron skin, after which they were thoroughly washed with bidistilled water. To evaluate the reproducibility of the results, each measurement was carried out at least three times.

RESULTS AND DISCUSSIONS

Cyclic Voltammetry. Cyclic voltammetry is a simple and convenient method for studying the kinetics and mechanism of oxidation-reduction processes. In the case of reversible processes, the values of the potentials of the oxidation and reduction peaks that characterize the nature of the electroactive substance are independent of the sweep speed and their difference ($E_{n(\kappa)} - E_{n(a)}$) is a constant value. For irreversible processes this difference is greater than for reversible ones and depends on the sweep speed. When studying the processes of discharge-ionization of indium, cyclic voltammograms were obtained on platinum (Pt), glassy carbon (GC) and titanium (Ti) electrodes from perchlorate-containing chloride solutions. Increase the sweep rate of the potential from 5 mV/s to 40 mV/s induces the displacement of the indium reduction peak ($E_{n(\kappa)}$) in the electrolyte of the following composition: 0.1 M $\text{In}(\text{ClO}_4)_3 + 2.0 \text{ M NaCl}$ (pH = 1.5) into the cathode region for Pt, GC and Ti electrodes at 80, 58 and 54 mV, respectively. This is due to a slow decrease in the surface concentration of the oxidized form of

indium ($C_{In^{3+}}^s$), leading to the maximum value of the concentration gradient of the reagent at a more negative potential [8]. As can be seen from the cyclic voltammograms of the discharge-ionization of indium at different polarization rates of the titanium electrode (figure 1), the beginning of the reduction reaction is shifted, which is apparently related to the features of the formation of the new phase.

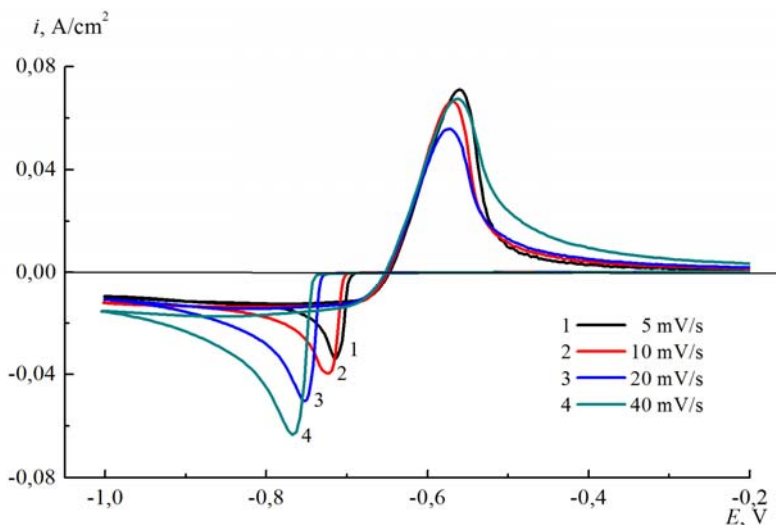


Figure 1 – Cyclic voltammograms of indium at 25⁰C on a Ti electrode in a solution of 0,1 M $In(ClO_4)_3$ + 2,0 M NaCl at different polarization rates

To determine the nature of the observed effect associated with the overvoltage of the formation of a new phase, cyclic voltammograms of indium precipitation and dissolution on an indium electrode were obtained (figure 2). The absence of a delay in indium reduction on an indium electrode indicates a low value of the overvoltage of phase formation. The irreversibility of the process of indium reduction on an indium electrode is reflected in the stretching of the current-voltage curves. In the absence of diffusion restrictions, the shape of the current-voltage curve is affected only by the kinetic parameters, such as the rate constant of charge transfer and the charge transfer coefficient. The potential difference between the peaks in the forward and reverse sweep runs depends on the rate constant of the electronic transition and on the sweep rate of the potential. From the analysis of the presented cyclic polarization curves it can be concluded that at high sweep rates the magnitude of the difference between the potentials of the peaks becomes very large and the degree of irreversibility of electron transfer increases. Consequently, high values of the potential difference of the reduction and oxidation peaks are associated with limitations on the electron transport kinetics.

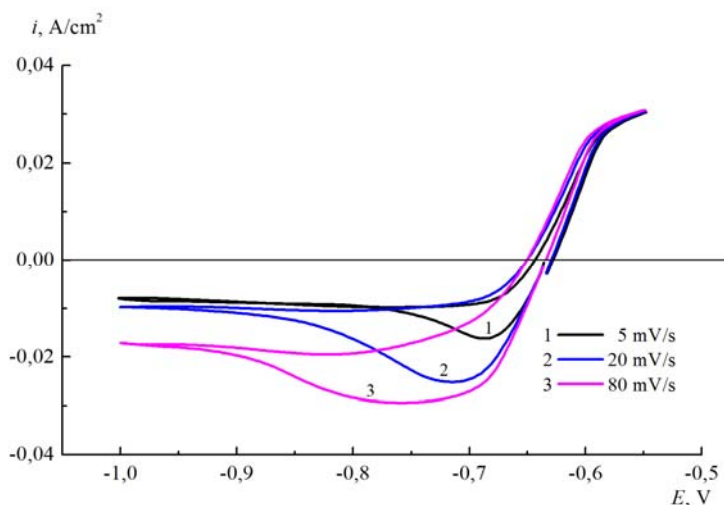


Figure 2 – Cyclic voltammograms of indium at 25⁰C on an indium electrode in a solution of 0.1 M 0,1 M In(ClO₄)₃ + 2,0 M NaCl at different polarization rates

For irreversible processes, the relationship between the reduction peak current and the sweep rate of the potential is described by P. Delahay equation [9]. Analysis of the above experimental results showed a linear dependence of the current density of the reduction peak of indium ($i_{n(\kappa)}$) on the square root of the value of the potential sweep speed (\sqrt{v}) (figure 3), which does not pass through the origin of coordinate, which indicates the quasi-reversible nature of the process under study.

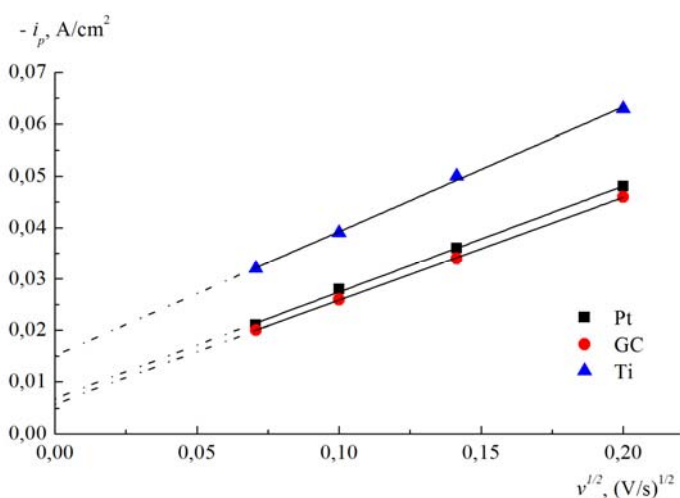


Figure 3 – Dependence of the current density of the indium recovery peak ($i_{n(\kappa)}$) on the \sqrt{v} at 25⁰C on different electrodes in a solution of 0,1 M In(ClO₄)₃ + 2,0 M NaCl

The rate of many electrochemical reactions is very often determined by the rate of charge transfer or mass transfer. The determination of the process regime can be carried out by comparing the orders of the rate constants for the transport of matter and charge. For this purpose, we determined the values of the rate constants of charge transfer and mass transfer of reduction of indium ions in solution on the investigated electrodes.

For irreversible processes, the limiting stage is charge transfer, whose velocity is determined by the rate constant (K^0) and the transport coefficient (α). The Nernst boundary conditions for an irreversible one-stage and many-electron reaction are expressed by the following equations [10]:

$$i = nFk_f(t)C_o(0,t), \quad (1)$$

where

$$k_f(t) = k^0 \exp\left\{-\alpha \frac{nF}{RT} [E(t) - E^0]\right\}. \quad (2)$$

Proceeding from these expressions (1), (2), the peak potential and current density (3) for irreversible reactions can be represented as follows [10]:

$$i_n = (2,99 \cdot 10^5) \alpha^{1/2} n C_0 \cdot D_0^{1/2} v^{1/2}; \quad (3)$$

$$E_n = E^0 - \frac{RT}{\alpha n F} \left[0,780 + \ln\left(\frac{D_0^{1/2}}{k^0}\right) + \ln\left(\frac{\alpha n F v}{RT}\right)^{1/2} \right]; \quad (4)$$

$$i_n = 0,227 \cdot n F C_0^* k^0 \exp\left[-\left(\frac{\alpha n F}{RT}\right) \cdot (E_n - E^0)\right], \quad (5)$$

where E_n - is the peak potential (B), E^0 - is the formal electrode potential (B), i_n - is the cathode current density of the peak (A), k^0 - is the rate constant of the charge transfer stage (cm/s), α - is the transfer coefficient, D_0 - is the diffusion coefficient (cm²/c), C_0^* - is the concentration of ions in the volume of the solution (mol/cm³), C_0 - is the ion concentration in the near-electrode region (mol/cm³), v - is the potential sweep rate (V/s).

As can be seen from equation (4), the reduction peak potential depends on the sweep speed. After logarithm of equation (5) we obtain the following expression [11,12]:

$$\ln i_n = \ln(0,227 n F C_0^* k^0) - \left(\frac{\alpha n F}{RT}\right) \cdot (E_n - E^0). \quad (6)$$

From cyclic voltammograms for the investigated electrodes, varying the rate of the potential sweep and the concentration of indium ions in the solution, a dependence $\ln i_n$ on $(E_n - E^0)$ (figure 4) was obtained, which made it possible to calculate the rate constants of charge transfer during the reduction of indium (table 1).

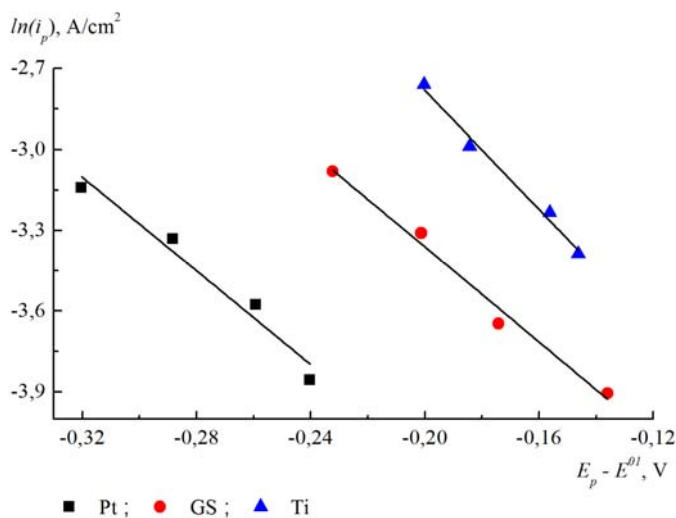


Figure 4 – Dependence of the logarithm of the current density of the cathode indium- $\ln(i_{nuk})$ on $E_{nuk} - E^{0I}$ at 25°C at different electrodes in a solution of 0,1 M $\text{In}(\text{ClO}_4)_3 + 2,0$ M NaCl

Table 1 – The rate constants of charge transfer during the reduction of indium in 2 mol/L NaCl

$C_{\text{In}^{3+}}^*$, mol/l	$k^0, \cdot 10^{-4}$ cm/s		
	Pt	GC	Ti
0,025	3,1	4,1	4,4
0,050	4,2	6,3	6,9
0,100	6,9	7,7	11,6

As can be seen from Table 1, the charge transfer rate constant for indium deposition on a titanium electrode in a 0.1 mol/l indium salt solution is much higher than that for platinum and glassy carbon electrodes. This indicates a greater degree of reversibility of the process on the titanium electrode.

Figure 5 shows cyclic voltammograms of discharge-ionization of indium on electrodes of various nature. The obtained experimental data indicate that the difference in potentials of the cathode and anode indium peaks is 252, 235 and 154 mV for solutions with an indium salt concentration of 0.1 mol/l for Pt, GC and Ti electrodes, respectively. For reversible three-electrode processes, it should not exceed 19.7 mV. The maximum shift to the anode region is observed for the titanium electrode, which also indicates a greater degree of reversibility of the reduction of indium on this electrode.

Overvoltage of the cathodic deposition of indium depends on the nature of the electrode. From the cyclic voltammograms of the discharge-ionization of indium (figure 5), the values of the overvoltage of indium release in the peak at Pt, GC and Ti electrodes, which amounted to 158, 111, 64 mV, respectively, were

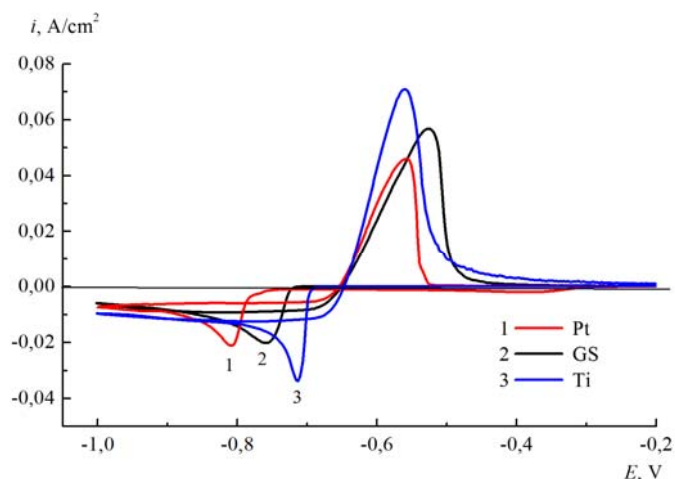


Figure 5 – Cyclic voltammograms of indium at 25⁰C at various electrodes in a solution of 0,1 M $\text{In}(\text{ClO}_4)_3$ + 2,0 M NaCl at a polarization rate of 5 mV/s

determined. This indicates a small value of the energy barrier of the cathodic reaction on the titanium electrode. The results obtained can be related to the values of the electron work function for various metals: 5.12-5.93 eV Pt; 5.0 eV GC; 4.33 eV Ti [13]. However, this is only one of the characteristics of the electrode material, which affects the electrode processes. It is necessary to take into account the peculiarities of the structure of the double electric layer and the processes of specific adsorption.

The displacement of the potential of the indium reduction peak in the anode region depends on the concentration of indium ions in the solution (figure 6). An

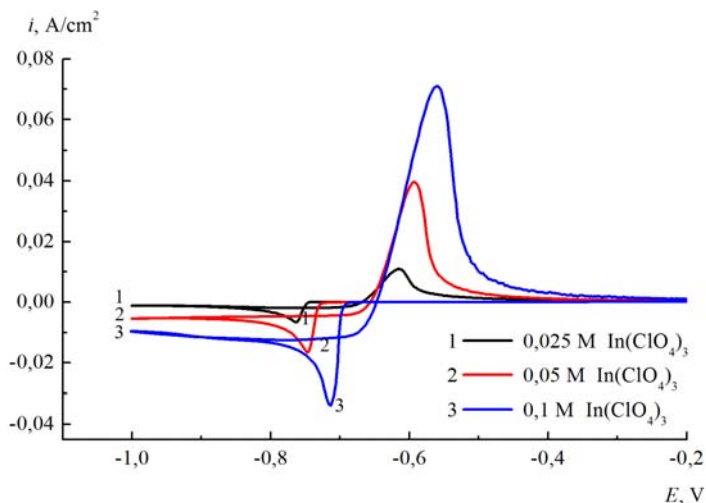


Figure 6 – Cyclic voltammograms of indium at 25⁰C C on a Ti electrode in a 2.0 M NaCl solution with a different content of $\text{In}(\text{ClO}_4)_3$, at a polarization rate of 5 mV/s

increase in the concentration of indium from 0.025 to 0.1 M at a potential sweep rate of 5 mV/s causes a shift in the potential of the reduction peak of indium ions on Pt, GC and Ti electrodes by 15, 11, 48 mV, respectively. The use of electrolytes with a high concentration of the potential-determining ion leads to an increase in the potential difference between the reduction of indium and electro-negative impurities and favors the purification of the base metal from them. Also, the use of titanium as a cathode in the refining of indium will permit electrolysis at relatively high current densities with a high current yield of metal.

Chronoamperometry. Chronoamperometry makes it possible to find the kinetic parameters of the mass transfer stage, such as the effective mass transfer constant and the diffusion coefficient of the potential-determining ion [14]. To determine diffusion coefficients and mass transfer constants, we obtained chronoamperograms of reduction of indium ions on Pt, GC, and Ti electrodes from perchlorate-containing chloride electrolytes by varying the concentration of indium salt (figure 7).

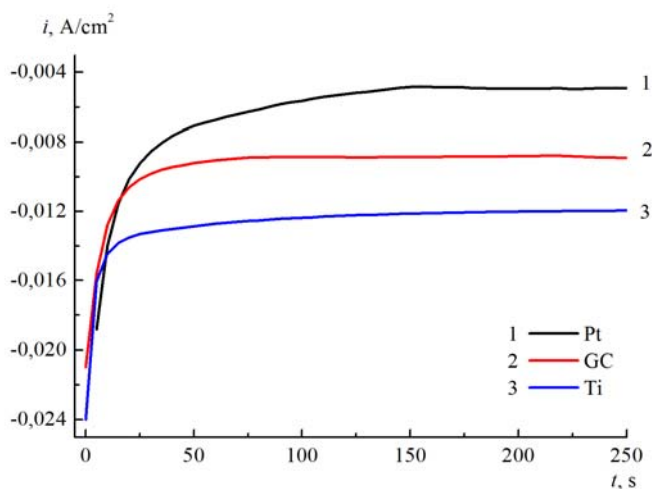


Figure 7 – Chronoamperograms of electrodeposition of indium at 25°C at various electrodes in a solution of 0.1 M $\text{In}(\text{ClO}_4)_3$ + 2.0 M NaCl at $E = -0.9$ V

For the completeness of the reaction during chronoamperometric measurements, it is necessary to supply an electrode with a sufficient jump in potential, which ensures a zero value of the concentration of the oxidized form of the substance on its surface. In our case, it is -0.9 V. In this case, the Cottrell equation, which expresses the dependence of the current density on time for nonstationary diffusion [8, 15], is applicable.

The diffusion coefficient of the electroactive substance is found from the slope of the straight line $i(t) = f(t^{-1/2})$. Table 2 presents the results of an analysis of chronoamperograms of indium reduction on the investigated electrodes from chloride electrolytes containing various concentrations of indium perchlorate.

Table 2 – Values of diffusion coefficients of indium ions in 2 mol / l NaCl solution

$C_{In^{3+}}^*$, mol/L	$D_{In^{3+}}, \cdot 10^{-5} \text{ cm}^2/\text{s}$		
	Pt	GC	Ti
0.025	2.4	1.7	3.2
0.050	1.3	1.6	3.2
0.100	0.6	0.6	0.3

The diffusion coefficient is determined by the properties of the medium and by the type of diffusing particles. The absence of significant differences in the values of the indium diffusion coefficients during its reduction at various electrodes indicates the validity of the application of the Cottrell equation.

From the equation of the limiting diffusion current for nonstationary diffusion, the effective mass-transfer rate constant for three electrodes was calculated (table 3).

Table 3 – The values of the rate constants of mass transfer during electroreduction of indium

Electrode	Pt	GC	Ti
$C_{In^{3+}}^*$, mol/L	$m_{ef}, \cdot 10^{-4} \text{ cm/s}$	$m_{ef}, \cdot 10^{-4} \text{ cm/s}$	$m_{ef}, \cdot 10^{-4} \text{ cm/s}$
0.025	2.4	3.1	3.6
0.050	2.9	3.3	3.9
0.100	3.7	3.5	4.5

Comparison of the values of the constants of the transport of matter and charge testifies to the quasi-reversibility of the system under study. The constant of the mass transfer rate of indium at reduction on a titanium electrode is higher than that of platinum and glassy carbon electrodes, which indicates an accelerated transfer of matter on this electrode and explains the large limiting currents when indium is reduced on the surface of titanium. From the values obtained for the mass transfer constants of indium ions when it is discharged on substrates of various nature, it is clear that the use of titanium in indium refining is preferable.

Conclusion. Based on cyclic voltammograms, the difference in the potentials of the oxidation peak and indium reduction on platinum, glassy carbon and titanium electrodes, as well as a comparative analysis of the calculated charge transport and mass transfer constants, is established that the discharge of indium ions proceeds quasi-reversibly. The greatest degree of reversibility is observed for a titanium electrode.

The values of the overvoltage of indium emission in the peak, at Pt, GC, Ti electrodes can be arranged in descending order as follows: 158, 111, 64 mV. Small overvoltages and the maximum value of the limiting current of indium deposition on a titanium electrode is the rationale for its choice in the refining of indium. With an increase in the $InCl_3$ concentration, the overvoltage of indium

reduction on the titanium electrode decreases, which leads to an increase in the difference in the deposition potential between the parent metal and electronegative impurities, which will improve the purity of the cathodic precipitates.

The values of the rate constant of charge transfer and mass transfer, found from cyclic voltammograms and chronoamperograms, in the process of indium reduction on a titanium electrode at 0.1 mol/L concentration of the potential-determining ion were $1.2 \cdot 10^{-3}$ and $4.5 \cdot 10^{-4}$ cm/s, respectively. The values of the above constants on Pt and GC cathodes are somewhat lower, so the use of the titanium cathode will make it possible to purify indium at high current densities with a high current output.

The work was carried out in the framework of project No. 1580 / GF4 by the support of the Ministry of Education and Science of the Republic of Kazakhstan.

REFERENCES

- [1] Alfantazi A.M., Moskalyk R.R. Processing of indium: a review // Minerals Engineering. 2003. Vol. 16. P. 687-694.
- [2] Munoz A.G., Saidman S.B., Bessone J.B. Electrodeposition of Indium onto Vitreous Carbon from Acid Chloride Solutions // Journal of The Electrochemical Society. 1999. Vol. 146, N 6. P. 2123-2130.
- [3] Saidman S.B., García S.G., Bessone J.B. Electrochemical behaviour of Al-In alloys in chloride solutions // J. Appl. Electrochem. 1995. Vol. 25. P. 2522-2528.
- [4] Breslin C.B., Carroll W.M. The activation of aluminium by indium ions in chloride, bromide and iodide solutions // Corros. Sci. 1993. Vol. 34. P. 327-341.
- [5] Saidman S.B., Bessone J.B. Activation of aluminium by indium ions in chloride solutions // Electrochim. Acta. 1997. Vol. 42. P. 413-420.
- [6] Rakhymbay G.S., Naurzybayev M. K., Burkitbayeva B. D., Argimbaeva A. M., Jumanova R., Kurbatov P., Eyraud M., Knauth P., Vacandio F. Electrochemical deposition of indium: nucleation mode and diffusional limitation // Russian Journal of Electrochemistry. 2016. Vol. 52, N 2. P. 99-105.
- [7] Burkitbaeva B.D., Argimbaeva A.M., Rakhimbai G.S., Beisenova G.S., Avchukur Kh., Kurbatov A.P., Naurzybaev M.K. Study of Electrochemical Transmission in India on Titanium Electrode Method of Cycle Voltammetry // Chemical Journal of Kazakhstan. 2015. N 3 (51). P. 34-41.
- [8] Damaskin B.B., Petri O.A., Цирлина Г.А. Electrochemistry / 2-nd isp. M.: Chemistry, Colosseum, 2006. 672 p.
- [9] Delahay P. Theory of Irreversible Waves in Oscillographic Polarography // J. Am. Chem. Soc. 1953. Vol. 75. P. 1190-1196.
- [10] Allen J. Bard, Larry R. Faulkner. Electrochemical methods: fundamentals and applications. 2nd ed. John Wiley & Sons, Inc. 2001. P. 785-808.
- [11] Protsenko V.S., Kityk A.A., Danilov F.I. Voltammetry study of Cr(III)/Cr(II) system in aqueous methanesulfonate solutions // Journal of Electroanalytical Chemistry. 2011. N 661. P. 213-218.
- [12] Kityk A.A. Use the "Insert Citation" button to add citations to this document.
- [13] Protsenko V.S., Danilov F.I. Voltammetry study of Cr(III)/Cr(II) system in methanesulfonate and sulfate solutions: Temperature dependences // Journal of Electroanalytical Chemistry. 2012. N 689. P. 269-275.
- [14] David R Lide. CRC Handbook of chemistry and physics. English: 89 th. Ed. Boca Raton [etc.] CRC Press-Taylor & Francis cop. 2008. 2736 p.
- [15] Myomandr F., Sadki S. e.a. Electrochemistry = Electrochimie / F. Miomander [and c.]; per. s fr VN Grasevius; sub arch. Y.D. Gamburgue, V.A. Safonova. M.: Techosphere, 2008. 359 p.

[16] Yong-Kook Choi, Boom-Soo Kim, Su-Moon Park. Electrochemical Reduction of Thionyl Chloride Studied by Cyclic Voltammetry, Chronocoulometry, and Chronoamperometry // J. Electrochem Soc. 1993. Vol. 140. P. 11-18.

Резюме

Х. Авчукир, Б. Д. Буркитбаева, А. М. Аргимбаева, Г. С. Рахымбай

ХЛОРИДТІ ЕРІТІНДІЛЕРДЕН ҚАТТЫ ЭЛЕКТРОД БЕТІНДЕ ИНДИЙДІҢ БОЛІНУ КИНЕТИКАСЫ

Құрамында перхлораты бар хлоридті ерітінділерден индийдің электрототықсыздануын циклдің вольтамперометрия және хроноамперометрия әдістерімен титан, платина және шыныкөміртекті электродтарда зерттелді. Тура және кері жолдағы потенциал пиктерінің айырмашылығы, поляризация жылдамдығы мен тотықсыздану пикі тоғымен арасындағы байланыс арқылы зерттеліп жатқан процесстің жоғарыдағы электродтарда квазикайтымды екені анықталды. Pt, ШК және Ті электродтарында индийдің бөліну пикі аса кернеуі 158, 111 және 64 мВ екені анықталды. Делахей және Коттрел теңдеулері арқылы индийдің электр тогы натғысында бөлінуін заряд тасымалдау жылдамдық константасы мен масса тасымалдау жылдамдық константасы есептелді. Анықталған константалардың салыстырмалы анализі нәтижесінде титан электродында жоғары мәндер байқалды: $1,06 \cdot 10^{-3}$ и $4,5 \cdot 10^{-4}$ см/с сәйкесінше. Алынған нәтижелер қаралашты индийдің электрохимиялық тазалау кезінде титанды қолдануын ұтымды екеніне көз жеткізді.

Түйін сөздер: индий, электродтау, массалық трансфер, зарядты беру, диффузия коэффициенті, квази-реверсивтілік, жылдамдық константасы.

Резюме

Х. Авчукир, Б. Д. Буркитбаева, А. М. Аргимбаева, Г. С. Рахымбай

КИНЕТИКА ЭЛЕКТРООСАЖДЕНИЯ ИНДИЯ НА ТВЕРДЫХ ЭЛЕКТРОДАХ ИЗ ХЛОРИДНЫХ РАСТВОРОВ

Методами циклической вольтамперометрии и хроноамперометрии исследовано электровосстановление индия на титановом, платиновом и стеклоглеродном электродах в перхлоратсодержащих хлоридных электролитах. Установлен квази-обратимый характер исследуемого процесса для всех вышеуказанных электродов на основании анализа разности потенциалов пиков на прямом и обратном ходе развертки и взаимосвязи тока пика восстановления от скорости поляризации. Пере-напряжение выделения индия в пике на Pt, Cu и Ti электродах составило 158, 111 и 64 мВ, соответственно. Рассчитаны константы скорости переноса заряда и массопереноса электроосаждения индия с использованием уравнений Делахея и Коттрела. Сравнительный анализ полученных констант показал, что они имели большие значения в случае титанового электрода и составили $1,06 \cdot 10^{-3}$ и $4,5 \cdot 10^{-4}$ см/с, соответственно. Полученные результаты свидетельствуют о предпочтительном использовании титана при электрохимической очистке черногого индия.

Ключевые слова: индий, электроосаждение, массоперенос, перенос заряда, коэффициент диффузии, квазиобратимость, константа скорости.

*G. S. BEISENOVA, B. D. BURKITBAYEVA,
A. M. ARGIMBAYEVA, G. S. RAKHIMBAY, N. N. ESALY*

Al-Farabi Kazakh National University, Almaty, Republik of Kazakhstan.
E-mail: Beisenova.gumi@gmail.com

THE EFFECT OF TEMPERATURE ON THE DEGREE OF PURITY OF INDIUM AT ITS ELECTROREFINING

Abstract. The object of the study was rough indium produced in Kazakhstan. To optimize the conditions for its electrorefining, the effect of temperature on the electro-deposition of indium on a titanium electrode in chloride electrolytes was studied in this paper. From the calculated values of the activation energy of the studied process, it was established that the electroreduction of indium on titanium occurs in a mixed mode ($E_a = 35.7$ kJ/mol). The optimum temperature regime of the process 30-40°C was found, which promotes the formation of qualitative cathode sediments and an increase in their purity during electrolysis (99.9992%).

Keywords: indium, electrolysis, indium electrorefining, cathodic polarization, purity of indium

Introduction. The temperature regime is one of the most important conditions for electrolytic refining of metals. The increase in temperature entails a number of changes: the solubility of salts and the electrical conductivity of the solution are increased, and the passivation of anodes is decreased. In addition, there is a change in the ion discharge potential, namely, reducing the overvoltage of hydrogen and metal evolution. In turn, each of these changes affects the quality of precipitation, so the effect of temperature is complex and under different conditions of electrolysis manifests itself in different ways [1, 2].

The temperature has a double effect on the electrodeposition of metals. With increasing temperature, the diffusion of ions increases, this makes it possible to increase the current density at which the formation of dendrites and spongy deposits is not yet observed. An increase in the temperature of the electrolyte leads to an increase in the growth rate of the crystals, which favors the appearance of a coarse-grained structure [3]. At not too high temperatures, the influence of the first of the factors considered prevails, so that the quality of the coatings is improved. At high temperatures, coatings of inferior quality are formed.

In practice, when examining the effect of the electrolyte temperature on the electrolysis performance, the optimal temperature is selected, at which the maximum possible current output and the minimum power consumption are observed. Usually, the temperature of the electrolyte in the baths is maintained in the range of 36-40 °C. At this temperature, the electrolysis performance is stable, the energy consumption is small and the cathode precipitates are qualitative [4].

In [5], the effect of temperature on the cathodic and anodic yields on current during the electrodeposition of indium on a copper electrode in sulfuric acid

solutions was studied. Brilliant dense precipitation of indium is obtained at higher current densities and elevated temperatures. The temperature does not have a significant effect on the anode current output. The authors of [6] established the influence of the temperature and acidity of the solution on the stability of monovalent indium in sulfuric acid solutions.

When studying the influence of temperature on the processes of electrochemical refining of metals, classical nonstationary methods are used - chronoamperometry and chronopotentiometry. In this paper, the effect of temperature on the kinetics of indium electroreduction on a titanium electrode, the cathode current yield, and the quality of cathodic precipitation are studied.

EXPERIMENTAL PART

The experiments were carried out in a thermostated cell made of organic glass with a volume of 300 cm³ (figure 1). The cathode was a titanium electrode with an area of 40 cm², the anode was indium, and as a reference electrode, chloride-silver electrode was used, connected with the working solution by a salt bridge. The temperature of the electrolyte (30, 40, 50°C) was maintained by thermostating with an accuracy of 0.10°C. Before each measurement, the surface of the titanium electrode was cleaned out with a micron skin, degreased with alcohol and washed with bidistillate. The surface of the anode was renewed by removing the thin layer with a ceramic knife and rinsing with bidistilled water. The pH values of the electrolyte were maintained in the range of 1.5-2.0. The electrolyte was 1 mol/l sodium chloride solution containing 0.5 mol/l indium chloride. The choice of chloride electrolytes is explained by their high electrical conductivity, the activating action on the anode processes and the high rate of discharge-ionization of indium in them.

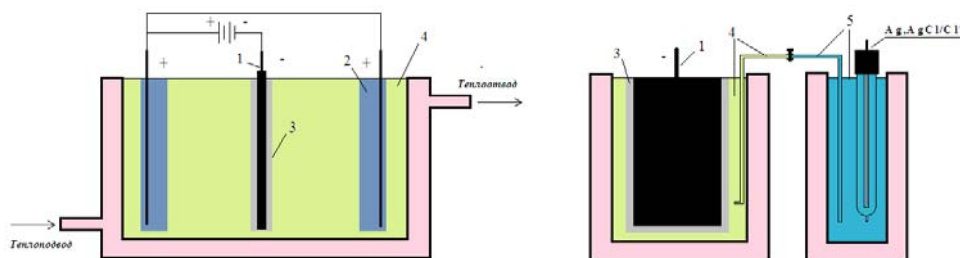


Figure 1 – Electrolysis installation: 1 – Cathode (Titan); 2 – Anode (Rough Indium); 3 – Cathode precipitate (Refined indium); 4 – Electrolyte; 5 – 3.5 M KCl

Analysis of the surfaces of the titanium electrode after cathodic polarization with temperature variation was performed by scanning electron microscopy (SEM) and energy dispersive X-ray spectral analysis (EDX).

Electrolysis was performed in galvanostatic mode. Samples for analysis by ICP-MS method were prepared as follows: after electrolysis, the electrodeposited

indium was dissolved in nitric acid (high purity) and diluted with bidistilled water to a certain volume.

Electrochemical measurements were performed on the device Autolab PGSTAT 302N.

RESULTS AND DISCUSSION

To determine the optimum electrolysis temperature, chronoamperometric measurements of the electrolytic deposition of indium on a titanium electrode at different temperatures were carried out (figure 2).

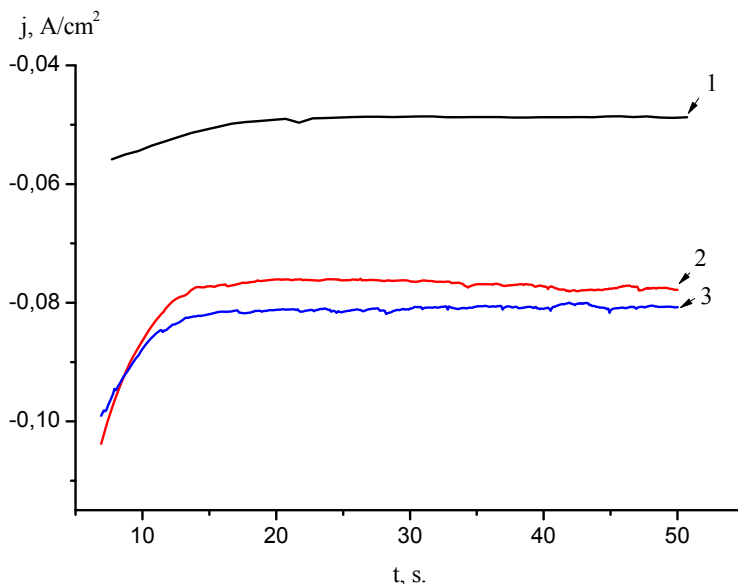


Figure 2 – Chronoamperogram of indium precipitation at a potential of -0.9 V at various temperatures: 1 - 30 °C; 2 - 40 °C; 3 - 50 °C

As the figure shows, with an increase in temperature there is a significant increase in cathodic currents. The chronoamperogram is characterized by the presence of two sections, in the time interval 0–15 s the discharge reaction proceeds in the kinetic regime, and the limiting diffusion current is observed with time. To quantify the effect of temperature on the rate of reduction of indium from chloride electrolytes at a total deposition potential (-0.9 V rel. to the chloride-silver electrode), the values of the activation energy of the process were calculated. For this purpose, the values of the exchange currents were calculated on the basis of the dependence of the magnitude of the current on time. At infinitesimal values of time, the current tends to an infinitely large value, which indicates a high rate of supply of material to the surface of the electrode. Under these conditions, the slowness of the nondiffusive stages of the electrode process is

clearly manifested. At sufficiently small values of time, the dependence of i on \sqrt{t} is linear and allows using the extrapolation method to determine the exchange currents. The linear dependencies shown in figure 3 can be described by the following equation:

$$i = b \sqrt{t} + a \tag{1}$$

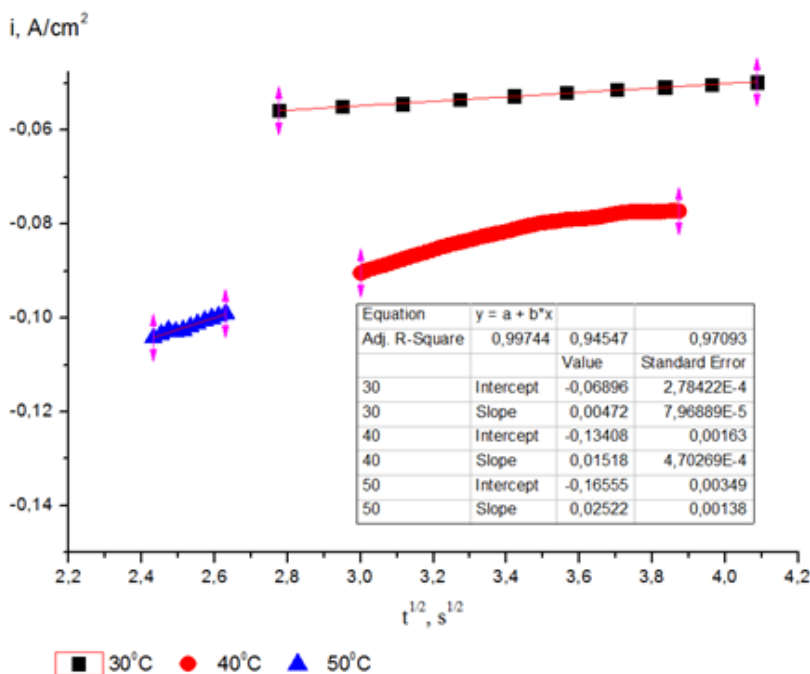


Figure 3 – Chronoamperograms of indium recovery at small values of time on a titanium electrode

The results of processing chronoamperograms are presented in table 1.

Table 1 – The values of the constants a and b, exchange currents (i_0) and correlation coefficients at different temperatures

T, °C	1/T, 10 ⁻³ K ⁻¹	i_0 , A/cm ²	lg(- i_0), A/cm ²	B	a, 10 ⁻³	R ²
30	3,300	-0,069	-1,161	-0,069	4,72	0,99
40	3,194	-0,134	-0,873	-0,134	15,18	0,95
50	3,095	-0,166	-0,781	-0,166	25,22	0,97

Then the values of the activation energy of the process under study at different temperatures were calculated from the exchange currents:

$$\lg i = B - Ea / (2.3 RT) \tag{2}$$

The graph of the dependence $\lg i_0 - 1/T$ allows us to calculate the value of the activation energy (figure 4), which was 35.7 kJ/mol. The value of the activation energy indicates the course of electroreduction of indium on a titanium electrode in a mixed mode.

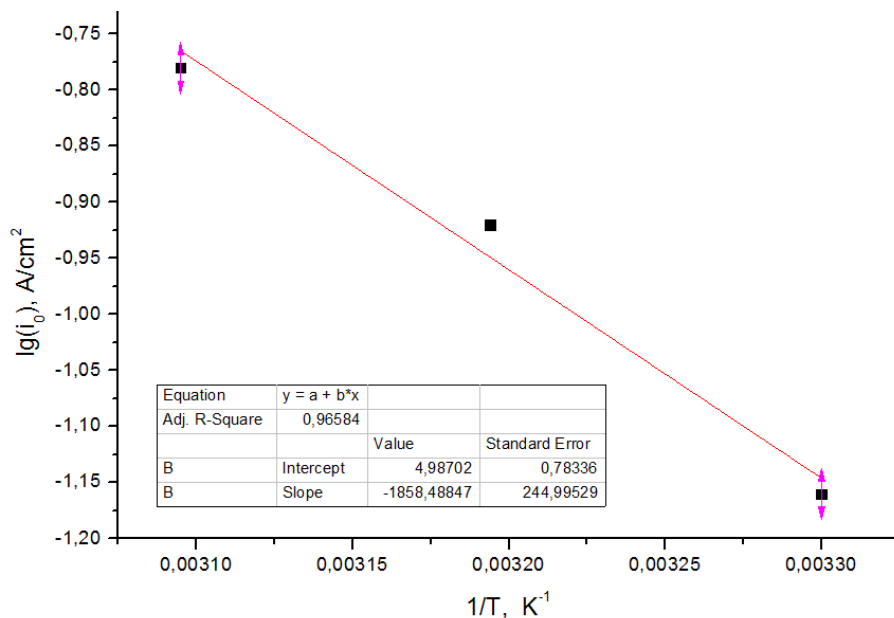


Figure 4 – Dependence of the logarithm of the exchange current $\lg i_0$ on the reciprocal of the temperature $1/T$

The obtained value of the activation energy is in good agreement with the value found from cyclic voltammograms of this process [7]. The obtained results can be used to calculate the rate of the process of electrodeposition of indium on a titanium electrode at other temperatures, which will allow us to optimize the choice of the temperature regime of electrolysis.

To determine the quality of cathode sediments obtained at different temperatures, their analysis was performed by scanning electron microscopy (SEM) and energy dispersive X-ray spectral methods (figure 5).

As can be seen from the photomicrograph, a small increase in temperature accelerates the rate of nucleation, precipitates coarse-grained sediments, which should lead to a decrease in impurities in the precipitated metal. The increase in temperature promotes the consolidation of precipitation, but at a temperature above 40 ° C they become rough and amorphous. This, apparently, is due to the course of the associated hydrogen evolution [8].

In an investigation of the discharge-ionization of indium on a titanium electrode, an optimal range of pH values of the electrolyte was found [9] in the refining of indium (1.5-2.5). This is explained by the fact that the interfering effect of

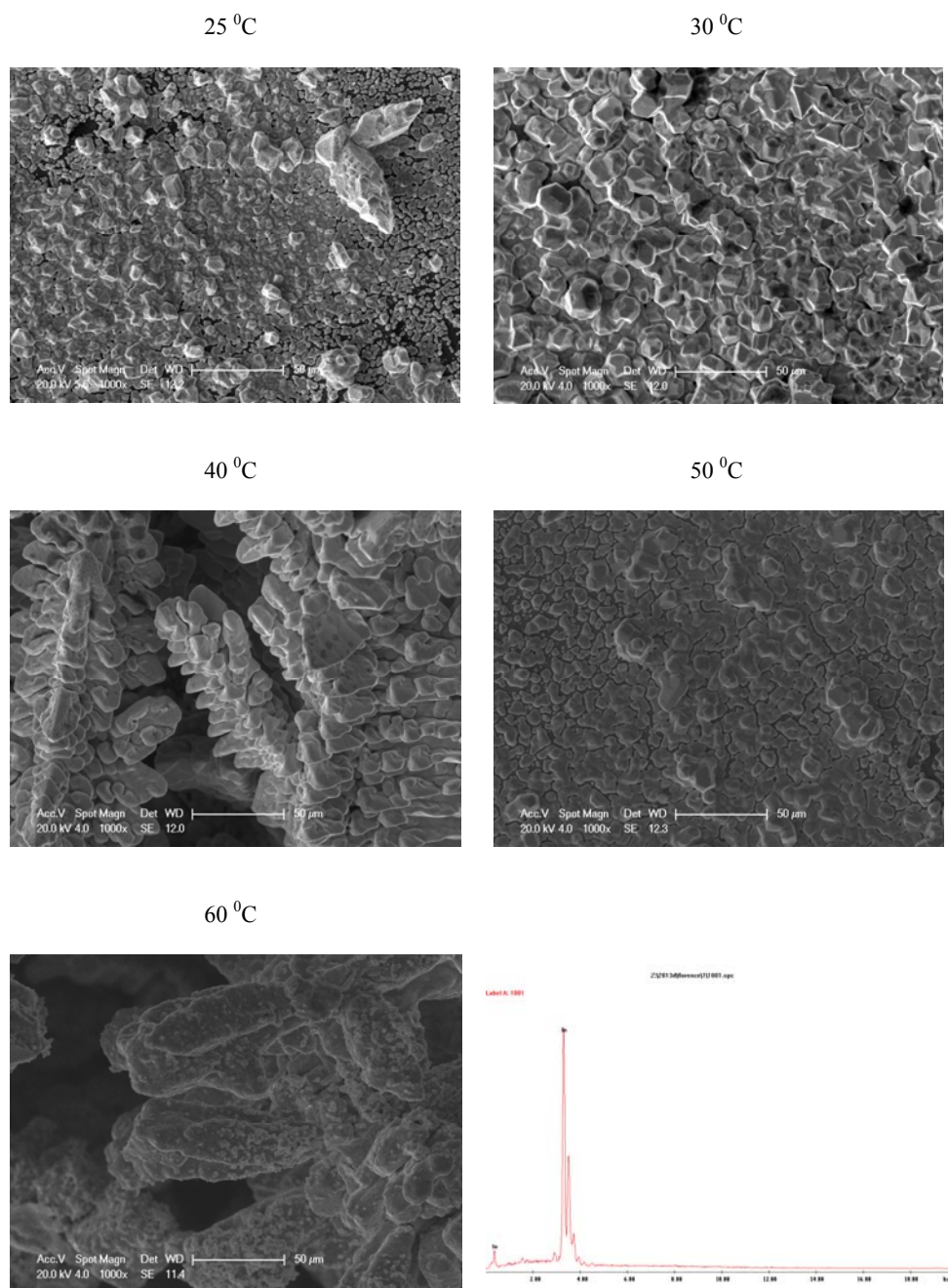


Figure 5 –Microphotographs of the surface of a titanium electrode after cathodic polarization, with temperature variation by SEM and EDX methods

reducing hydrogen ions is enhanced in a strongly acidic medium, and at pH above 3, indium hydroxide is formed. In the same work, the optimum current density (0.01 A/cm^2) was determined during electrolytic refining of indium.

The content of impurity metals and the degree of purity of electrified indium are determined by mass spectrometry (ICP-MS) methods with inductively coupled plasma. The cathode sediments of three experiments on electrolytic purification of rough indium were analyzed in order to evaluate the reproducibility of the experimental results. The results of the analysis are presented in table 2.

Table 2 – Results of analysis of precipitated indium samples by the ICP-MS method

№	The composition of the electrolyte	pH of the medium	The cathode potential (rel.chloride-silver electrode), V	Temperature, °C	VT catode, %	Degree of purity, %
1	0,5M InCl_3 + + 1,0M NaCl	1,5	-0,9	30	100,4	99,9992
					99,8	99,9989
					99,5	99,9990
2				40	100,1	99,9991
					99,7	99,9993
					99,4	99,9994
3				50	114,7	99,9982
					112,5	99,9984
					111,3	99,9987
Rough Indium IN-2						99,9840

As can be seen from the obtained results, there is a significant increase in the purity of cathode sediments during electrolytic refining of indium on a titanium electrode from chloride electrolytes in the temperature range 30-40 °C, which allows us to recommend these conditions as optimal.

Conclusion. The effect of temperature on the electroreduction of indium on a titanium electrode in chloride electrolytes was studied and the optimum temperature regime was determined. It was found that an increase in temperature to 40 °C leads to the enlargement of cathodic sediments and an increase in their purity. Further temperature increases impair the quality of the precipitated indium.

The value of the activation energy ($E_a = 35.7 \text{ kJ/mol}$) of indium electroreduction on titanium, indicating the course of the process in a mixed mode, is determined.

Electrorefining of rough indium at a temperature of 30 and 40 °C was carried out and the purity of indium cathode precipitation was determined, the average value of which was 99.9992%.

REFERENCES

- [1] Gamburg Y.D., Zangari G. Theory and Practice of Metal Electrodeposition New York: Springer, 2011. 375 p.
- [2] 2.Chung Y.H., Lee C.W. Electrochemical behaviors of Indium // Journal of Electrochemical Science and Technology. 2012. Vol. 3, Is. 1. P. 1-13.
- [3] Kolobov G.A. Refining of gallium and indium / G.A. Kolobov, V.V. Pavlov, Yu.V.Moseyko // Theory and practice of metallurgy. 2013. N 3-4(92-93). P. 62-67. (Russian).
- [4] Kazanbaev L.A., Kozlov P.A., Kubasov V.L., Travkin V.F. Indium. Technology of its production. M.: Publishing House "Ore and Metals", 2004. 168 p. (Russian).
- [5] Kochegarov V.M., Zaburdaeva F.I., Zyablova E.A. Research of electrochemical properties of indium // Jour. App. Chem. 1962. Vol. 35, N 6. P. 1376-1379.
- [6] Kozin V.F., Omelchuk A.A. Kinetics and mechanism of formation of ions of univalent indium in the system $\text{In}^0 - \text{In}_2(\text{SO}_4)_3 - \text{In}_2\text{SO}_4$ // Non-ferrous metallurgy. 2006. N 2. P. 45-50. (Russian).
- [7] Avchukir H., Burkitbaeva B.D., Rakhymbay G.S., Argimbayeva A.M., Nauryzbaev M.K. Electrodeposition of indium on titanium from chloride solutions // Conf. Proc. "Theory and Practice of Modern Electrochemical Productions". SPb., 2016. N 1. P. 44. (Russian).
- [8] Rakhymbay G.S., Jumanova R.J., Burkitbaeva B.D., Argimbaeva A.M., Kurbatov A. P., Nauryzbaev M.K. Optimization of condition for electrochemical refining rough indium from chloride electrolytes // International Journal of Biology and Chemistry. 2014. Vol. 7, N 1. P. 27-32.
- [9] Burkitbaeva B.D., Argimbayeva A.M., Rakhymbay G.S., Beisenova G.S., AvchukirKh., Kurbatov A.P., Nauryzbaev M.K. A study of the electrochemical behavior of indium on a titanium electrode by the cyclic voltammetry method // Chemistry Journal of Kazakhstan. 2015. N 3(51). P. 34-41. (Russian).

Резюме

*Г. С. Бейсенова, Б. Д. Буркимбаева,
А. М. Аргимбаева, Г. С. Рахымбай, Н. Н. Есалы*

ЭЛЕКТРОРАФИНИРЛЕУ КЕЗІНДЕГІ
ИНДИЙДІҢ ТАЗАЛЫҚ ДӘРЕЖЕСІНЕ ТЕМПЕРАТУРАНЫҢ ӘСЕРІ

Зерттеу нысаны ретінде Қазақстанда өндірілетін қаралашты индий болды. Оның электрорафинирлеу кезіндегі шарттарын оңтайландыру үшін бұл жұмыста титан электродында хлоридті ерітінділерде индий электрртұнуына температураның әсері зерттелді. Зерттелетін үрдістің активтену энергиясы несептелген мәндерінен индийдің титанда электрртотықсыздануы аралас режимде жүретіні анықталды ($E_a = 35,7$ кДж/моль). Үрдістің оңтайлы темпиралық режимі табылды – 30-40⁰С. Бұл режим катодты тұнбалардың түзілуіне жақсы әсер етіп, олардың электролиз кезіндегі тазалық дәрежесін арттырады (99,9992%).

Түйін сөздер: индий, электролиз, индий рафинирлеуі, катодтық поляризация, индий тазалығы.

Резюме

*Г. С. Бейсенова, Б. Д. Буркитбаева,
А. М. Аргимбаева, Г. С. Рахымбай, Н. Н. Есалы*

ВЛИЯНИЕ ТЕМПЕРАТУРЫ НА СТЕПЕНЬ ЧИСТОТЫ ИНДИЯ
ПРИ ЕГО ЭЛЕКТРОРАФИНИРОВАНИИ

Объектом исследования являлся черновой индий, производимый в Казахстане. Для оптимизации условий его электрорафинирования, изучено влияние температуры на электроосаждение индия на титановом электроде в хлоридных электролитах. Из рассчитанных значений энергии активации исследуемого процесса установлено, что электровосстановление индия на титане протекает в смешанном режиме ($E_a = 35,7$ кДж/моль). Найден оптимальный температурный режим процесса 30-40⁰С, способствующий образованию качественных катодных осадков и повышению их степени чистоты при электролизе (99,9992%).

Ключевые слова: индий, электролиз, рафинирование индия, катодная поляризация, чистота индия.

*K. A. KADIRBEKOV^{1,2}, D. K. ZHAMBAKIN¹, A. K. KADIRBEKOV^{1,2},
K. I. IMANBEKOV², A. U. AITUREEV²*

¹JSC «A.B. Bekturov Institute of chemical sciences», Almaty, Republik of Kazakhstan,

²LLP «Kazatomprom-Sorbent», Almaty, Republik of Kazakhstan.

E-mail: kkairati@mail.ru

LAWS OF FORMATION OF ACTIVE AND SELECTIVE CATALYTIC SYSTEMS ON THE BASIS OF CLINOPTILOLITE FOR HEAVY HYDROCARBONS CRACKING PROCESS

Abstract. Using the modern physical methods (XPS, SEM, TEM, BET) regularities in the formation of catalytic systems based on clinoptilolite by the modification of various by nature acids were revealed. It is shown that as a result of interaction of the modifier with an active surface new structure is created, which lead to a significant increase in specific surface area and catalytic activity. A detailed study of the zeolite surface with TEM HR showed the formation of stable structures of clusters, which are partially embedded in the volume of the zeolite. The sizes of these clusters are 1-2 nm and are available for the reactants. It is believed that as a result of impregnating and calcining the catalytic systems, translation of heteropolyacid particles into highly dispersed state is achieved, where the heteropolyacid particles perform specific adsorption and catalytic properties.

Keywords: clinoptilolit, modification, texture, morphology, acidity, cracking catalytic systems.

Introduction. As an object of research work was natural zeolite from Shankanay region (Kazakhstan) in which the major rock-forming mineral is clinoptilolite, containing from 40 to 84 wt%. It is known, that zeolites being solid acids are basic catalysts of hydrocarbon cracking process [1, 2].

This paper presents the study of the acidic properties, the establishment of textural and morphological changes on the surface of clinoptilolite in the modification of it with different by nature acids or combination of them. We have previously reported that mineral acids carry out ions of alkali and alkaline earth metals from surface of natural zeolite; organic acids form soluble complex compounds with iron ions and mostly carry out ferric ions which catalyze the process of carbon formation from hydrocarbons; and additional modification of the zeolite by heteropolyacid leads to a deep loosening of its surface [3, 4].

EXPERIMENTAL PART

Catalytic systems based on natural Shankanay zeolite were created by modification with mineral, organic acids and heteropolyacids (HPA).

Changes in the composition and structure of the surface samples of natural zeolite in the acid treatment were followed by methods of spectral elemental analysis, BET, XPS, SEM, TEM, XRD and IR.

Oxide and elemental composition of samples of natural Shankanay zeolite was identified by emission-diffraction analysis on diffractometer DFS-13.

XRD analysis of catalytic systems was performed on D8 Advance (Bruker), α -Cu, tube voltage 40 kV, current 40 mA. Data processing and calculation of the diffraction patterns interplanar distances were performed using the software EVA. Deciphering trial and phase search were carried out under the program Search/Match with Database of powder diffractometric data PDF-2 Rel. 2012 (ICDD).

IR study of catalytic systems was conducted by the spectrometer NICCOLET-2700 in the frequency range 400-4400 cm^{-1} . The catalytic systems were formed into a tablet with "thickness" of 60-100 mg/cm^2 . Adsorptions of test gases were carried out at different temperatures, vacuuming 10^{-5} Torr.

BET method by low-temperature nitrogen adsorption at the «AccuSorb» of «Mikromeitics» (USA) was used to identify specific surface area of catalytic systems.

By X-ray photoelectron spectroscopy (XPS) provided information on the qualitative and quantitative composition of the surface area of the test sample and the chemical state of elements. XPS- spectra were recorded on a photoelectron spectrometer ES-300 (KRATOS Analytical) in a mode of constant energy transmission energy analyzer photoelectrons, which is equipped with an automation system based on the IBM PC (held at the G.K. Boreskov Institute of Catalysis SB RAS, Novosibirsk). To capture, source of X-ray was used without monochromator. Radiation energy Mg Ka - was 1253.6 eV. The calibration of the energy scale was carried out on the binding energies of Au4f7/2 equal to 84.0 eV. Quality control of the chemical composition of the surface was carried out on the overview of the spectrum with a range of 0-1100 eV. For the analysis of the composition and chemical state of the elements were shooting narrow areas, and used mode: energy transmission spectrometer HV -25 eV step sweep - 0.1 eV.

C using scanning electron microscopy (SEM) with a spatial resolution of 1 and 10 Å microscope JSM-6X80 transmission and high resolution electron microscopy (TEM HR) microscope JEM-2010 by JEOL accelerating voltage of 200 kV and a resolution of 1,4 Å (0,14 nm) microfeatures and morphology of catalytic systems' surface, elemental composition of the observed point on the surface and the pattern of distribution of elements on the surface, as well as their dispersion were studied. By means of electron microscope Philips CM-20, equipped with EDAX-spectrometer microanalytical experiments were conducted (held at the G.K. Boreskov Institute of Catalysis SB RAS, Novosibirsk).

Using the IR method with low-temperature CO adsorption acidic properties of zeolite catalytic systems were studied [5]. Infrared spectra were recorded on FT-IR spectrometer FTIR-8300 Shimadzu 700-6000 cm^{-1} with resolution of 4 cm^{-1} and the number of scans equal to 100. IR spectra are reported in absorbance units referred to 1 g of catalytic systems per 1 cm^2 of the cross section of the luminous flux and are in units A/ρ , that means optical density A_v at absorbance line ν normalized for tablet thickness sample r (in g/cm^2). Before recording spectra

catalytic systems samples were compressed into tablets without binder. Samples of the catalytic systems were placed in a quartz cell for absorption measurement with windows from CaF_2 , and trained on the vacuum adsorption unit under vacuum ($p < 10^{-6}$ bar) at 500°C , 1 h.

RESULTS AND DISCUSSION

Investigation of textural characteristics of modified samples of natural zeolite. Table 1 shows the textural characteristics of catalytic systems obtained from a natural Shankanay zeolite modified by inorganic, organic, stepwise inorganic and organic acids, and stepwise inorganic acid and heteropolyacid: KI – initial natural zeolite, HKI-1 – zeolite one time modified with a mineral acid, 10% $\text{H}_4\text{EDTA}/\text{KI}$ – natural zeolite modified with ethylenediaminetetraacetic acid, 10% $\text{H}_4\text{EDTA} / \text{HKI-1}$ – zeolite decationized with mineral acid and modified with ethylenediaminetetraacetic acid, 10% Hsal/HKI-1 – zeolite decationized with mineral acid and modified with sulfosalicylic acid, 10% $\text{PW}_{12}\text{-HPA}/\text{HKI-1}$ – decationized with mineral acid and modified with tungsten heteropolyacid of 12 series.

Table 1 – Textural characteristics of catalytic systems obtained by modifying a natural zeolite of Shankanay field

Samples	Specific surface area, m^2/g		Pore volumes, $10^{-3} \text{cm}^3/\text{g}$		Pore size, A°
	S	$S_{\text{micropores}}$	V	$V_{\text{micropores}}$	D_{average}
KI	9,8	2,4	1,76	0,13 (7,4%)	72,2
10% $\text{H}_4\text{EDTA}/\text{KI}$	28,2	–	–	–	–
HKI-1	52,6	38,0	4,86	0,18 (3,7%)	27,7
10% $\text{H}_4\text{EDTA}/\text{HKI-1}$	99,4	–	–	–	–
HSal/HKI-1	78,2	67,8	5,49	3,18 (58,0%)	21,2
10% $\text{PW}_{12}\text{-HPA}/\text{HKI-1}$	257,0	–	–	–	–

The total specific surface of the initial natural Shankanay zeolite is low and ranges of $9.8\text{-}22.1 \text{ m}^2/\text{g}$ (table 1).

After modification specific surface area of the zeolite increases. For example, the specific surface area of clinoptilolite decationized by 1.75N hydrochloric acid increases up to $52.6\text{-}59.0 \text{ m}^2/\text{g}$, and the modification of a natural zeolite with ethylenediaminetetraacetic acid slightly increases the surface to $28.2 \text{ m}^2/\text{g}$ (table 1).

Interesting results are obtained by modifying already decationized zeolite. Since the modification with EDTA leads to an increase in the specific surface area to 99.4, with sulfosalicylic acid up to $100.7 \text{ m}^2/\text{g}$, and the modification with HPA leads to an anomalous increase up to $257.0 \text{ m}^2/\text{g}$.

In figure 1 the adsorption and desorption isotherms of the natural clinoptilolite sample and its modified forms, which are characterized by the presence in

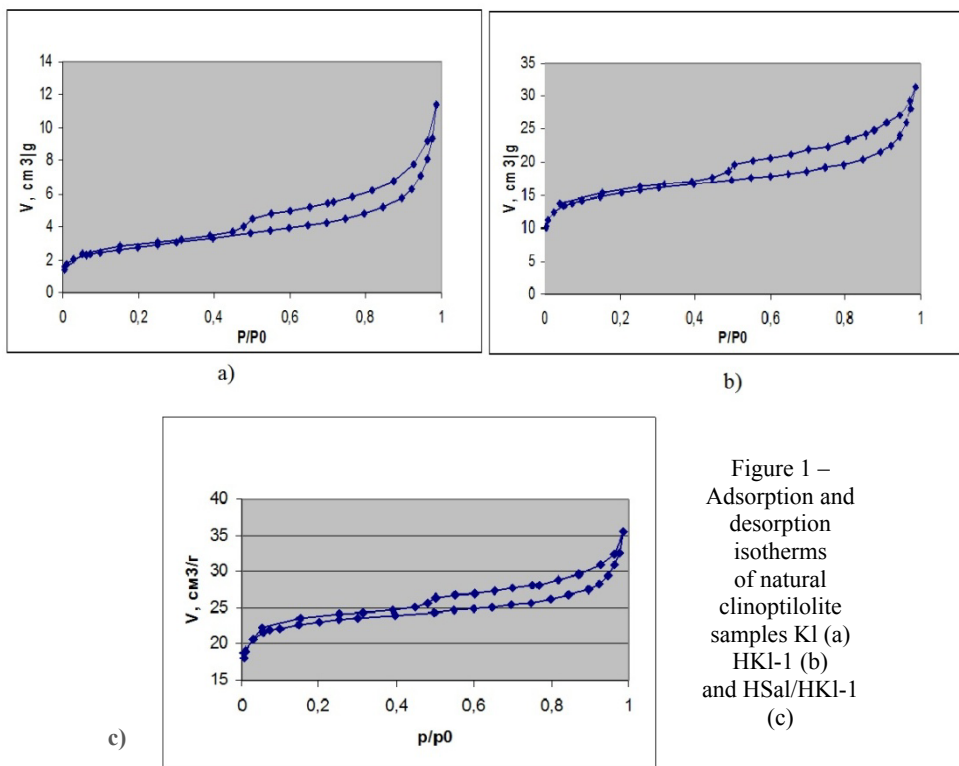


Figure 1 – Adsorption and desorption isotherms of natural clinoptilolite samples K1 (a) HKI-1 (b) and HSal/HKI-1 (c)

all sorption isotherms hysteresis S-shaped type are shown. Sorption hysteresis formed by the capillary condensation of gases and its location usually depends on the method of the modification.

The pore volume after modification initial zeolite by mineral acid increases from $1.76 \cdot 10^{-3}$ to $4.86 \cdot 10^{-3}$ cm³/g, and until $5.49 \cdot 10^{-3}$ cm³/g it is modified by sulfosalicylic acid. This increases relate not only the pore volume, but also increases its number from 7.4% in initial to 58.0% on zeolite modified sulfosalicylic acid (table 1).

In general increasing the number and volume of pores of the modified zeolite average pore size decreases. The average pore size of the initial zeolite is at 72.2 angstroms, hydrochloric acid modification is at 27.7, while for acid modification sulfosalicylic acid reduced to 21.2 angstroms (table 1).

The studies of the surface-modified natural zeolite samples by XPS. Using photoelectron spectrometer ES-300 received XPS-spectra of initial clinoptilolite and its modified forms: K1, HKI-1, H₄EDTA/HKI-1; HSal/HKI-1, PW₁₂-HPA/HKI-1 и PMo₁₂-HPA/HKI-1. A typical photoelectron spectrum of a sample H₄EDTA/HKI-1 corresponding peaks of consisting chemical elements is displayed (figure 2). Quantitative analysis of the composition performed on the basis of calculation of the integrated intensities of the corresponding narrow lines in the spectra of XPS. Correction to the atomic sensitivity of each element of ASF was made.

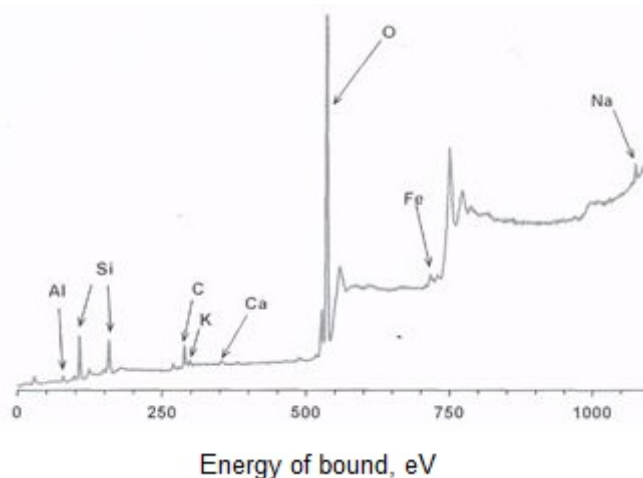


Figure 2 – Photoelectron spectrum of a sample H4EDTA/HK1-1

It can be seen that the sample contains aluminum, silicon, carbon, oxygen, also there is a small amount of potassium, calcium, and iron. These elements are part of almost all samples in this series. Silicon Si2p and aluminum Al2p are presented as peaks with the characteristic binding energy of silicon and aluminum in the composition of zeolites and aluminosilicates. The peaks in the 750-1100 eV are due to the Auger process (electron emission from the outer shell during the process of relaxation after photoionization) and respectively belong to oxygen and carbon. Table 2 shows the elemental content calculated by XPS data normalized by the amount of aluminum.

Table 2 – The chemical composition of the surface of clinoptilolite samples

Sample	Al	Si	C	K	O	Fe	Ca	Na	W	Mo
K1	1	3,0	4,4	0,08	16,8	0,19	0,30			
HK1-1	1	3,7	5,0	0,19	20,4	0,21	0,15			
H ₄ EDTA/HK1-1	1	5,4	5,3	0,16	25,9	0,31	0,13	0,26		
HSa1/ HK1-1	1	7,3	8,3	0,2	34,1	0,39	0,12	0,11		
PW ₁₂ -HPA/HK1-1	1	6,1	7,7	0,22	33,0	0,35			0,58	
PMo ₁₂ -HPA/HK1-1	1	6,5	8,4	0,19	34,8	0,32				0,85

It is also remarkable that impregnating HPA on the surface affect the condition of other elements. From table 2 it is seen that in these zeolite samples the ratio of Si/Al varies quite substantially - from 3 to 6.5. However, given their relatively low concentration, it can be assumed that the change in the state of Al and Si is mainly due to the mutual influence.

XPS spectra of samples PW_{12} -HPA/HK1-1 and PMo_{12} -HPA/HK1-1 showed the presence of tungsten and molybdenum (figure 3). In the original spectrum two doublets W4f with binding energies of the components W4f_{7/2} 34.4 and 36.1 eV could be identified (figure 3a).

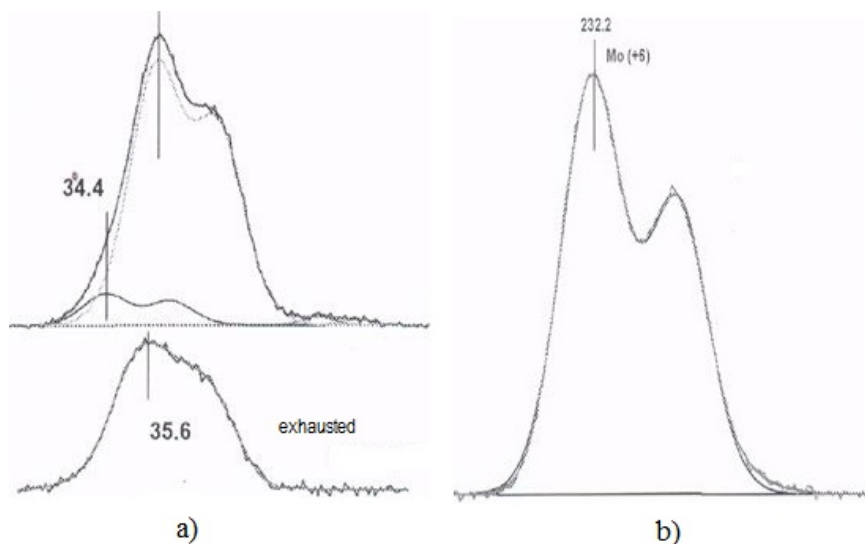


Figure 3 – Spectra of tungsten W4f (a) and molybdenum Mo3d (b)

Such binding energies are characteristic of the oxidized state of tungsten W^{3+} and W^{6+} , respectively. After the reaction only blurred doublet with a binding energy of the first component ~ 35.6 eV is observed, this is also related to the state of W^{6+} . Noticeable broadening of peaks may be due to structural inhomogeneity of HPA after exposure of reaction medium, or the formation of carbon on the surface and its effect on the HPA. The spectrum of molybdenum (figure 3b) can be approximated by only one doublet with a binding energy of component Mo3d_{5/2} equal to 232.2 eV. Such binding energy is characteristic of the charged state of molybdenum (Mo^{+6}).

Thus, the XPS method makes it possible to evaluate energy state of surface elements, which makes it possible to understand the mechanism of action of the active center of the catalytic systems.

The studies of the surface conditions of modified natural zeolite samples by electron microscopy (TEM and SEM). Photographs of various modified natural zeolite samples which were obtained using a scanning electron microscope JSM-6X80 are shown on figure 4.

According to electronic images of natural zeolite granules are irregular in shape (figure 4, a) and are characterized by a specific structure consisting of irregularities and cracks, which causes the penetration of relatively large cations (figure 4, b).

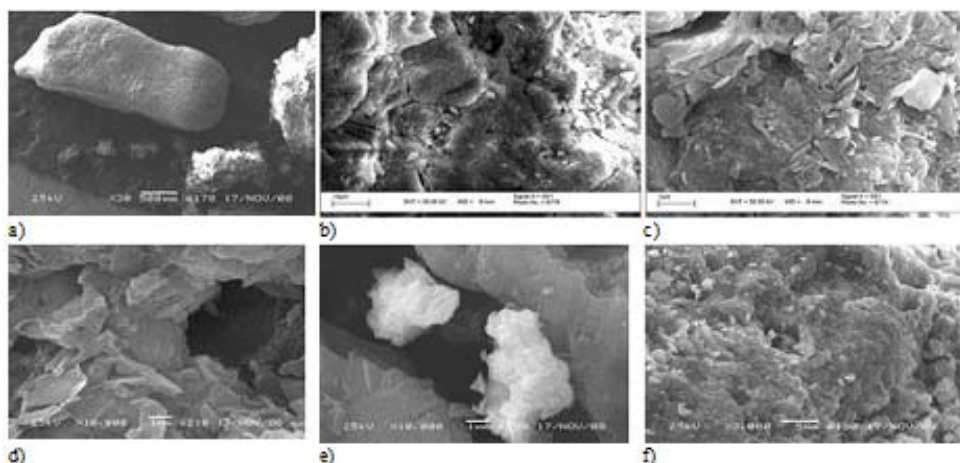


Figure 4 – An electron-microscopic photographs of identified samples of natural zeolite: natural zeolite granules (a) and its outer layer (b); HKI-1 (c); HSAI/HKI-1 (d); PW_{12} -ГПК/HKI-1(e, f)

Surface of decationized clinoptilolite HKI-1, obtained by means of SEM, characterized by inhomogeneity and the presence of multiple shallow channels, which have a layered structure (figure 4, c).

When stepwise modifying with mineral acid as the first step then with organic acid, surface microfeatures are precise and nature of recesses of decationized clinoptilolite layered structures increases, the surface is even more loosened; particularly when modified with sulfosalicylic acid large pores appear and the surface is loosened with peeling whole layers and new pores appear (figure 4, d). Microelement analysis data indicate that the ratio of clinoptilolite basic elements, in particular silicon to aluminum compared with the data of catalytic systems HKI-1 decreases. Wherein the catalytic systems surface HSAI/HKI-1 low iron content was detected.

On figure 4 also photographs of the sample PW_{12} -HPA/HKI-1 are shown. It can be seen that the surface of clinoptilolite layered structures HKI after modification are covered with agglomerates of PW_{12} -HPA, that are evenly distributed and strongly bounded to the surface of clinoptilolite (figure 4, e, f).

In electron-microscopic images of a thin layer of catalytic systems PW_{12} -HPA/HKI-1 obtained by TEM microscope JEM-2010, the spots of different sizes, which have different shapes and contrasts are seen (figure 5). Microanalytical experiments on EDAX-spectrometer showed that the above mentioned spots have the same composition identical with the PW_{12} -HPA (figure 5).

Apparently, this is due to the high degree of dispersion and particle distribution of PW_{12} -HPA on the surface of clinoptilolite. The quality and quantity of the working surface could be mediated from that. Since, the observed point in the surface of the catalytic systems is composed of silicon (1.61%), aluminium (0.74%), oxygen (80.2%), and also phosphorus (1.52%) and tungsten (15.85%)

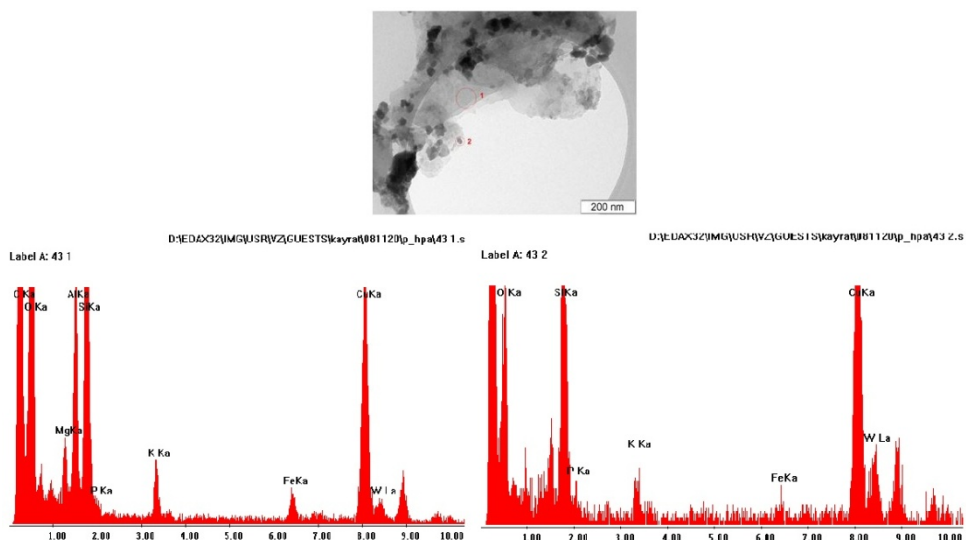


Figure 5 – An electron-microscopic image of the catalytic systems PW_{12} -HPA/HKI-1 obtained by TEM HR, a top under - X-ray spectra of the catalytic systems surface PW_{12} HPA/HKI-1 obtained from EDAX-spectrometer

are found which qualitatively correspond to the composition of the catalytic systems.

A detailed study of the zeolite surface by TEM HR, indeed, showed the formation of stable structures of clusters, which are partially embedded in the volume of zeolite (figure 6). The size of these clusters are 1-2 nm (figure 6). Often

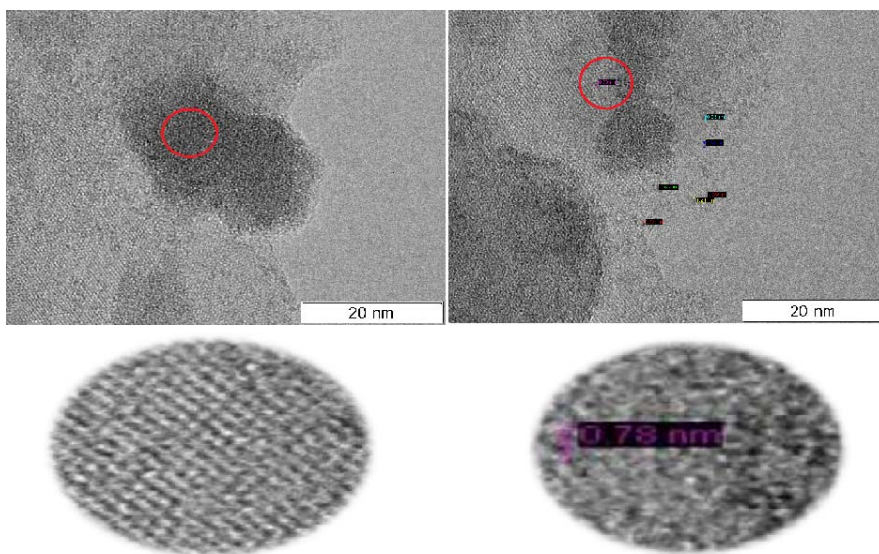
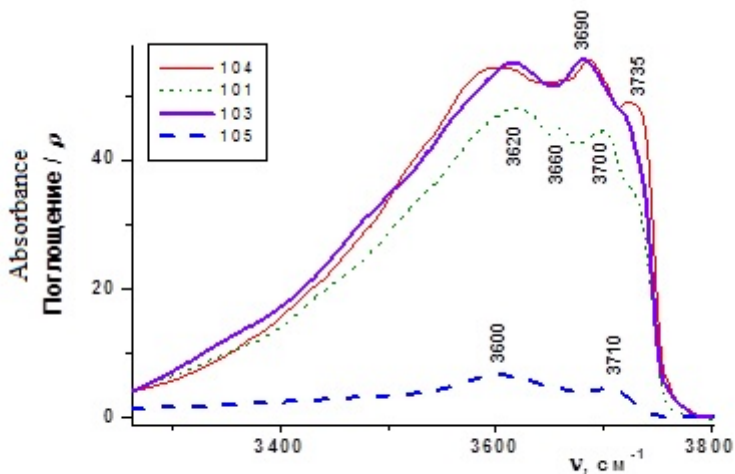


Figure 6 – Electron-microscopic images of the catalytic systems sample PW_{12} -HPA/HKI-1 obtained by TEM HR

occurring lines on images belongs to the clinoptilolite crystal lattice. Thus, clusters are uniformly distributed over the surface of the zeolite and are available for the reactants (figure 6).

In some places of the clinoptilolite surface highly dispersed particles of HPA are arranged as layers in the form of associates - in the pictures appear as a contrasting sites, at the same time the size of the particles clearly evident (0.78-1.32 nm) (figure 6). The compositions of nanostructures according to the EDAX-spectrometer are also identical with PW_{12} -HPA.

Investigation of the acidic properties of surface of modified natural zeolite samples. On the FT-IR spectrometer FTIR-8300 Shimadzu in the 700-6000 cm^{-1} field with a resolution of 4 cm^{-1} and the number of scans of 100 infrared spectra of catalytic systems were recorded; catalytic systems: HKI-1 (spectrum #104), 10% HSal/HKI-1 (spectrum #103), 10% H_4 EDTA/HKI-1 (spectrum #105), 10% PW_{12} -HPA/HKI-1 (spectrum #101), obtained by modifying clinoptilolite samples with 1,75N hydrochloric, 10% sulfosalicylic, 10% ethylenediaminetetraacetic acid and 10% aqueous solution of tungsten of 12 row heteropolyacid ($H_3PMo_{12}O_{40} \cdot nH_2O$) respectively. Their IR spectra in the region of the stretching vibrations of OH groups, obtained by tests using the sequential adsorption of CO at the temperature 77K are shown in figure 7.



#104 - HKI; #101 - 10% PW_{12} HPA/HKI; #103 - 10%HSal/HKI; #105 - H_4 EDTA/HKI

Figure 7 – IR spectra of catalytic systems samples in the region of OH groups' stretching vibrations

In the spectrum of the sample 10% PW_{12} -HPA/HKI peaks related to the absorption of the isolated OH groups at 3620, 3660, 3700 and 3735 cm^{-1} are observed. In the spectrum of the samples HKI and 10%HSal/HKI an increase in the intensity of isolated OH groups peaks as compared with a sample of 10% PW_{12} -HPA/HKI is observed, that may indicate a slight increase in the concentration of hydroxyl-cover. For samples HKI and 10%HSal/HKI compared with

a sample of 10%PW₁₂-HPA/HKl the appearance of intense broad peak at 3680-3690 cm⁻¹ is observed. For a sample of 10%HSal/HKl compared with a sample of 10%PW₁₂-HPA/HKl observed shifting of isolated groups to the low-frequency region (3620→3600 cm⁻¹), and a significant increase in the intensity of 3735 cm⁻¹ region. The sample 10%H₄EDTA/HKl, assumed to have destroyed zeolite structure, in the spectrum of this sample low intense broad peaks at 3600 and 3710 cm⁻¹ are observed. The total concentration of OH groups to sample 10%H₄EDTA/HKl, referred to the sample weight was 8-10 times lower than for the other samples.

Strength of Broensted acid sites can be determined from the magnitude of the shift of the stretching vibrations of OH groups ($\Delta\nu_{OH}^{CO}$) in the presence of adsorbed CO. The greater the shift, the stronger acidic sites. Concentration of Broensted acid sites and their strength, expressed in terms of wavenumber shift amount shown in table 3.

Table 3 – Broensted acid sites (B.a.s.) and their concentration on the surface of hydrocarbons cracking catalytic systems

Catalytic system	SiO ₂ /Al ₂ O ₃	B.a.s. I		B.a.s. II		B.a.s. III	
		$\Delta\nu_{OH}$, cm ⁻¹	C, μ mol/g	$\Delta\nu_{OH}$, cm ⁻¹	C, μ mol/g	$\Delta\nu_{OH}$, cm ⁻¹	C, μ mol/g
10%PW ₁₂ -HPA/HKl		340	4	320	6	220	30
HKl	23,6	340	4	280	20	225	45
10%HSal/ HKl	12,6	340	1	310	15	235	35
10%H ₄ EDTA/ HKl	19,4	–	–	–	–	–	–

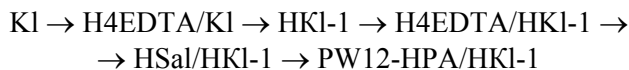
Thus, there are three types of the acidic centers on samples of catalytic systems that differ in strength and concentration, which is determined by the magnitude and intensity of the shift. When the adsorption of CO on the catalytic systems the greater the shift of the OH groups' stretching vibrations ($\Delta\nu_{OH}$, cm⁻¹), the stronger the acid sites. Strong acid sites are found on 10%PW₁₂-HPA/HKl and HKl. On 10% HSal/HKl their concentration is 4 times lower, and on 10% H₄EDTA/HKl shift is not observed, giving rise to talk about the absence of surface Brönsted acid sites.

Bronsted sites of the second type on 10% PW₁₂-HPA/HKl stronger by the shift than on the other catalytic systems, although the concentration is less. Acid sites of the third type on the catalytic systems approximately the same amount, but they apparently do not determine the activity when cracking. The total concentration of strong acid sites on 10%PW₁₂-HPA/HKl is greater than on the other catalytic systems samples.

Discussions. Modification of natural zeolite sample with various acids leads to structural changes of clinoptilolite. Acid activation of clinoptilolite increases its surface and pore volume, decreases average pore diameter, which in turn directly affect the properties of the active acid sites of the zeolite, which are responsible

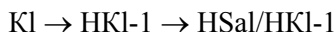
for acid-base reactions, as well as their distribution on the catalytic systems surface.

The study found that the catalytic systems obtained by modification of natural zeolite with various substances, by the specific surface area, starting from the lowest arranged in a row:

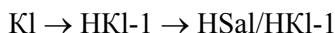


Special attention deserves the significant growth of the surface when the modification with 10% PW12-HPA to 257.0 m²/g, since this value is much higher than for pure zeolite and HPA. Obviously, when HPA applied on the surface of the zeolite there is a deep interaction occurs. In addition, this increase is due to the formation of new nanostructures that have been shown by TEM and SEM.

In a row of samples:



area of hysteresis loop decreases and the amount of gas adsorbed on the surface of clinoptilolite increases. This fact can be attributed to an increase in pore volumes of the samples. By volume of pores the catalytic systems starting from the lowest may be arranged in a row:



The pore distribution on the samples of catalytic systems surface shifts toward micropores, or in other words, on the surface mainly micropores are found.

Obviously, the surface growth of the samples of catalytic systems is due to the formation of new micropores. Determination of surface micropores (S_{mc}) also shows their growth from 2.49 to 38.07 m²/g after modification with hydrochloric acid and to 67.84 m²/g with sulfosalicylic acid.

Using the method of XPS information about the qualitative and quantitative composition of the surface area of the samples and the chemical state of elements was obtained. Since the samples were subjected to severe impacts of acid there might be amorphization of their surfaces. Applying HPA on the surface affect the condition of the other elements. However, given their relatively low concentration, it can be assumed that the change in the state of Al and Si is mainly due to the mutual influence. At the same time, purely qualitatively it can be concluded that the decrease in binding energy due to the transition Al2p of aluminosilicate type structures to aluminum rich structures. This is also supported by earlier data of IR and XRD.

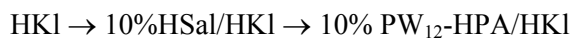
As a result of the XPS study it was found that when impregnating heteropolyacids of molybdenum and tungsten series, the zeolite framework partially decomposed with the formation of individual and Al-O- and Si-O- structures. Since conditions of the main elements of the zeolite varies a little. Molybdenum and tungsten in catalytic systems are in present as Mo (6+) and W (6+), respectively, which evidence of retaining heteropoly-like structure.

Morphology and microfeatures, elemental composition in the observed point, the distribution pattern of elements on the surface of initial clinoptilolite and its acid-modified forms examined by electron microscopy.

Thus, in particular, using an SEM indicated that after step-modifying by mineral acid then heteropolyacid, heteropolyacid particle dispersion on the surface of the zeolite are high; the layered structure of the zeolite covered with uniformly distributed and tightly bounded to its surface a heteropolyacid agglomerates.

When modification of zeolite with decationized HPA of Tungsten 12 series, as already mentioned above, there is a sharp increase in the specific surface area of the catalytic systems. Obviously, when HPA impregnated on the surface of the zeolite there is a deep interaction. Thus on the TEM HR images of catalytic systems homogeneous structures of HPA interspersed into the pores of the zeolite are visible. The dimensions of these structures are a few nanometers. Obviously, the occurrence of these nanostructures alters the catalytic properties, particularly cracking activity of the catalytic systems considerably increases, consequently the yield of liquid products of the cracking reaction, constituting mainly of the long-chain α -olefins increase.

By means of CO adsorption method of strength and concentration of acid sites of the samples of catalytic systems were identified. In the series starting from lowest:



there is a significant increase in the proportion of strong and very strong Bronsted acid sites. The total concentration of strong acid sites on 10%PW₁₂-HPA/HKI and sum of shifts at 340 cm⁻¹ and 320 cm⁻¹ is higher than on HKI. It should be noted that the increase in acidity correlates with high silicate modulus (SiO₂/Al₂O₃) of the zeolite sample.

Conclusions. Thus it is clear that the occurrence of nanostructures and the large number of strong acid sites leads to increase of cracking activity catalyst systems based on clinoptilolite in the cracking of heavy hydrocarbons.

The research was carried out according to the scientific and technical program No. BR05234667 within the framework of program-targeted financing CS MES RK.

REFERENCES

- [1] Abdallah A. Al-Shammari, Syed A. Ali, Nabil Al-Yassir, Abdullah M. Aitani, Kehinde E. Ogunronbi, Khalid A. Al-Majnouni, Sulaiman S. Al-Khattaf, Catalytic cracking of heavy naphtha-range hydrocarbons over different zeolites structures, *Fuel Processing Technology*, 122 (2014). P. 12–22.
- [2] Xiao F.S., Meng X., *Zeolites in Sustainable Chemistry Synthesis, Characterisation, Catalytic Applications*, Springer 2016.
- [3] Kadirbekov K.A., Zhambakin D.K., Nurbaeva R.K., Aitureev A.U., Kadirbekov A.K., Imanbekov K.I., Design of active and selective catalyst systems on the basis of clinoptilolite for hydrocarbon cracking, [in] *Abstracts of EuropaCat 2015 XII European Congress on Catalysis “Catalysis: Balancing the use of fossil and renewable resources” Kazan, Russia, 2015. P. 557-558.*
- [4] Konuspayev S.R., Kadirbekov K.A., Salanov A.N., Nurbayeva R.K., Sarsekova A.T., Nurlybayev I.T., The synthesis of nanocatalysts of oil treatment from natural zeolites, [in] *14th ICC Pre-conference School Nanocatalysis Fundamental & Applications, Dalian, China, 2008. P. 190.*
- [5] Paukshtis E.A. *Infrared Spectroscopy in Heterogeneous Acid-Base Catalysis*. Novosibirsk: Nauka, 1992.

Резюме

*Қ. А. Кадирбеков, Д. Қ. Жамбакин, А. Қ. Кадирбеков,
А. У. Айтуреев, Қ. И. Иманбеков*

**АУЫР КӨМІРСУТЕКТЕРДІ КРЕКИНГЛЕУ ПРОЦЕСТЕРІНІҢ
КЛИНОПТИЛОЛИТ НЕГІЗІНДЕГІ АКТИВТІ ЖӘНЕ СЕЛЕКТИВТІ
КАТАЛИТИКАЛЫҚ ЖҮЙЕЛЕРІН ҚАЛЫПТАСТЫРУДЫҢ ЗАҢДЫЛЫҚТАРЫ**

Заманауи физикалық әдістерді (РФЭС, СЭМ, ПЭМ, БЭТ) қолдана отырып ауыр көмірсутектерді крекинглеу процестерінің клиноптилолит негізіндегі активті және селективті каталитикалық жүйелерін оны табиғаты әртүрлі қышқылдармен модифицирлеу арқылы қалыптастырудың заңдылықтары анықталды. Модификаторлар мен клиноптилолиттің беткі қабатының белсенді әрекеттесуінің нәтижесінде жаңа құрылымдар түзіліп, олардың каталитикалық жүйенің беткі қабаты ауданы мен каталитикалық активтілігін біршама өсіретіндігі көрсетілді. Модификатор ретінде гетерополиқышқылдар қолданылған жағдайдағы цеолит бетін кең шешімді ПЭМ әдісімен тиянақты зерттеу цеолиттің ішкі көлеміне жартылай енген қышқылдың тұрақты кластерлік құрылымдары түзілетіндігін айқындады. Бұл кластерлердің өлшемдері 1-2 нанометр құрайды және олар әрекеттесуші реагенттерге қолжетімді. Модификатор ретінде гетерополиқышқылдарды цеолитке отырғызып және алынған катализаторлық жүйені қыздырып шынықтырғанда гетерополиқышқыл бөлшектері жоғары дисперсті күйге ауысады, соның нәтижесінде олар ерекше адсорбциялық әрі каталитикалық қасиеттер көрсетеді деп қорытынды жасалды.

Түйін сөздер: табиғи цеолит, модифицирлеу, текстура, морфология, қышқылдық, крекинг катализаторлары.

Резюме

*К. А. Кадирбеков, Д. К. Жамбакин, А. К. Кадирбеков,
А. У. Айтуреев, К. И. Иманбеков*

**ЗАКОНОМЕРНОСТИ ФОРМИРОВАНИЯ АКТИВНЫХ И СЕЛЕКТИВНЫХ
КАТАЛИТИЧЕСКИХ СИСТЕМ НА ОСНОВЕ КЛИНОПТИЛОЛИТА
ДЛЯ ПРОЦЕССОВ КРЕКИНГА ТЯЖЕЛЫХ УГЛЕВОДОРОДОВ**

С применением современных физических методов (РФЭС, СЭМ, ПЭМ, БЭТ) выявлены закономерности формирования каталитических систем на основе клиноптилолита для процессов крекинга углеводородов при модифицировании их различными по природе кислотами. Показано, что в результате активного взаимодействия модификаторов с поверхностью образуются новые структуры, которые ведут к значительному росту удельной поверхности и каталитической активности. Детальное изучение поверхности цеолита методом ПЭМ ВР показало образование устойчивых структур кластеров, которые частично внедрены в объем цеолита. Размеры этих кластеров составляют 1-2 нанометров и они доступны для реагирующих веществ. Считается, что при нанесении и в результате прокаливании катализатора достигается перевод частиц гетерополикислоты в высокодисперсное состояние, при котором у частиц гетерополикислоты появляются особые адсорбционные и каталитические свойства.

Ключевые слова: природный цеолит, модифицирование, текстура, морфология, кислотность, катализаторы крекинга.

G. S. AKHMETOVA¹, U. B. ISSAYEVA¹, V.K. YU¹, K. D. PRALIYEV¹,
YE. M. SATBAYEVA², D. M. KADYROVA², M. K. AMIRKULOVA²,
G. S. SMAGULOVA², T. M. SEILKHANOV³

¹A.B.Bekturov Institute of Chemical Sciences, Almaty, Republic of Kazakhstan,

²S.D. Asfendiyarov Kazakh National Medical University, Almaty, Republic of Kazakhstan,

³Sh. Ualikhanov Kokshetau State University, Kokshetau, Republic of Kazakhstan.

E-mail: gulgakhmet@mail.ru

FLUOROBENZOATES OF 1-PROPYL-4-KETOXIMEPIPERIDINE AS POTENCIAL LOCAL ANESTHETICS

Abstract. p-Fluoro-, m-fluoro-, o-fluorobenzoates of 1-propyl-4-ketoximepiperidine, displaying a local anesthetic activity in varying degrees, have been synthesized. An introduction of fluorine leads to the formation of local anesthetics of different efficiency. Depending on the position of a fluorine atom in the phenyl ring, the greatest activity has been displayed by p-isomers, then o-isomers, whereas m-fluorobenzoates have proved to be less active.

Key words: p-fluoro-, m-fluoro-, o-fluorobenzoylcarbonylchloride, N-propylpiperidine-4-ketoxime, esters, 1-propyl-4-(p-fluoro-, m-fluoro-, o-fluorobenzoyloxyimino)piperidine, local anesthetic activity.

Elimination and prevention of a pain syndrome is a pressing problem of medicine. One of the most important directions for its solution is the development and creation of medicinal preparations of a local anesthetic activity. In surgery, when general anesthesia is not the only possible anesthetic method, it is expedient to apply the methods of infiltration and conduction anesthesia as the simplest and most secure ones. In recent times, the proportion of local anesthesia has especially increased, which is connected with the new notions of the role of local anesthesia, as well as the emergence of new effective “green” local anesthetics [1, 2].

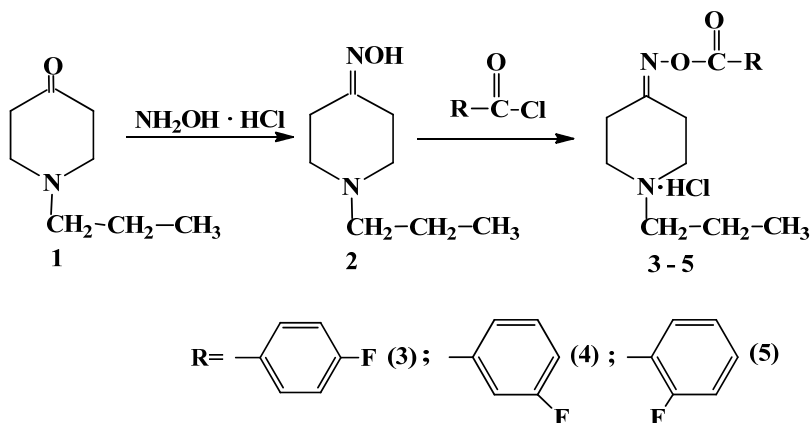
The modern period of the development of organic chemistry demonstrates not only a potential of organic synthesis, but also its importance for the development of both chemistry in general and many related fields of science and practice, in particular, the provision of the mankind with medicines. Due to a high physiological activity of azacyclanes, in particular, piperidine derivatives, these studies acquire the status of one of the topical tasks of modern chemistry, biology and medicine [3, 4].

The most characteristic derivatives of 4-oxopiperidines are azomethins, including oximes. Oximes of carbonyl compounds and their derivatives are well known as one of the main classes of organic substances, which are promising in searching for new biologically active preparations of broad spectrum [5-7].

In this connection, the task of this work has been defined as the synthesis of oxime and its acyl derivatives, in particular, fluorine-containing derivatives on the basis of N-propyl-4-oxopiperidine (1).

Upon the interaction of hydrochloric hydroxylamine with 1-propyl-piperidine-4-one (1) in the presence of alkali in isopropanol, an oxime has been obtained (2).

With the purpose to determine the effect of the introduction of a fluorine atom on a pharmacological activity of the compounds, the corresponding esters (3-5) have been synthesized by acylation of the obtained oxime (2) with 4-fluorobenzoyl chloride, 3-fluorobenzoyl chloride and 2-fluorobenzoyl chlorides. The reaction has been carried out in absolute dioxane upon heating, with the ratio of ketoxime : acylating agent as 1:1.5.



The obtained appropriate hydrochlorides of aminoesters (3-5) represent white crystalline substances.

The yields, melting points, R_f and IR spectra data (absorption bands of ester carbonyl as the most characteristic features for esters and C=N) are presented in table 1.

Table 1 – The yields and physical and chemical characteristics of hydrochlorides of 1-propylpiperidin-4-ketoxime fluorobenzoates.

Compound	Yield, %	R_f	Melting point, °C	IR-spectrum, cm^{-1}		Molecular formula
				C=N	C=O ester	
3	61.0	0.72	170-172	1639.3	1751.2	$\text{C}_{15}\text{H}_{20}\text{N}_2\text{O}_2\text{FCl}$
4	46.8	0.7	159-161	1659.8	1740.2	$\text{C}_{15}\text{H}_{20}\text{N}_2\text{O}_2\text{FCl}$
5	44.5	0.69	169-171	1654.4	1752.4	$\text{C}_{15}\text{H}_{20}\text{N}_2\text{O}_2\text{FCl}$

It has turned out that oximes of N-substituted 4-ketopiperidines are most easily acylated with *p*-fluorobenzoyl chloride; fluorine in the *o*-position of the benzene ring deactivates the process to the greatest extent. Accordingly, *p*-fluorobenzoates have been obtained with the best yields, *m*-fluorobenzoates have fallen in between, *o*-fluorobenzoates have been formed with the least yields. The optimum ratio of alcohol/oxime:fluorobenzoate is 1:1.5. The best yields of fluorobenzoates have been obtained when using dioxane as a solvent.

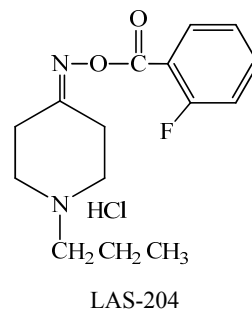
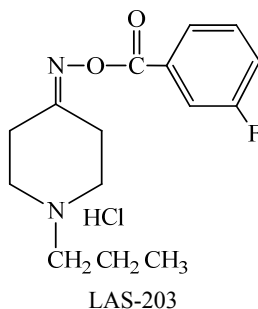
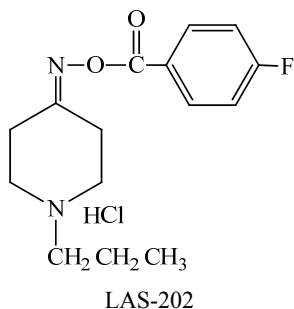
^{13}C NMR spectra have proved to be most informative for the determination of the structure of hydrochlorides of ketoxime fluorobenzoates of 1-propylpiperidine-4-one (table 2).

The occurrence of a signal of carbonyl carbon in the weak field (153-172 ppm) testifies to the formation of ester. The C_4 atom of the piperidine cycle of ketoxime fluorobenzoates also resonates in this field. The different position of a fluorine atom is confirmed by a shift of a signal of the corresponding aromatic carbon to the weak field (160 ppm). The carbon atoms of the piperidine cycle and substituents at the nitrogen atom appear in the expected field.

Table 2 – The values of chemical shifts of the carbon atoms in the ^{13}C NMR spectra of hydrochlorides of 1-propylpiperidine-4-ketoxime fluorobenzoates (δ , ppm.)

Compound	$\text{C}_{2,6}$	$\text{C}_{3,5}$	C_4	$\text{C}=\text{O}$	$\text{C}_6\text{H}_4\text{F}$	$\text{C}-\text{F}$	N-R
3	50.51; 49.60	27.92; 23.91	162.92	162.42	16.56- 132.82	<i>n</i> -F 167.15	$\text{CH}_2\text{CH}_2\text{CH}_3$ 57.07;17.39;11.51
4	50.47; 49.63	27.91; 23.95	163.28	161.32	116.36- 131.04	<i>m</i> -F 162.28	$\text{CH}_2\text{CH}_2\text{CH}_3$ 57.05;17.39;11.52
5	50.55; 49.48	27.84; 24.11	162.70	153.30	117.65- 132.45	<i>o</i> -F 161.23	$\text{CH}_2\text{CH}_2\text{CH}_3$ 57.07;17.48;11.50

Study of a biological activity. An experimental study of a specific activity of hydrochlorides of 1-propylpiperidine-4-ketoxime fluorobenzoates under the laboratory codes LAS-202 – LAS-204 (LAS – Local Anesthetic Substance) has been carried out upon infiltration and conduction anesthesia at the Department of Pharmacology of S.D. Asfendiyarov Kazakh National Medical University, using the methods of primary screening, recommended by the RK Pharmacological Committee and Guidelines for experimental (pre-clinical) study of new pharmacological substances [8].



It has been established that all studied compounds display a certain effect (table 3). The greatest most activity is marked in case of LAS-202 (hydrochloride of 1-propyl-(4-fluorobenzoyloxy)-4-ketoximepiperidine), which in 0.25% solution by its strength (anesthesia index) is equal to trimecaine, and statistically sig-

nificantly exceeds the indices of lidocaine and novocaine by a factor of 1.4 and 1.3, respectively.

The duration of total anesthesia under the effect of LAS-202 has made up 19.6 min, like that of trimecaine, exceeding the values of lidocaine and novocaine by a factor of 1.38 and 19.6, respectively. The “transfer” of fluorine to the *m*- and *o*- positions results in the reduction of an anesthetic effect of the fluorobenzoates of piperidineketoximes.

The duration of total anesthesia is approximately the same for all studied compounds. The compounds LAS-202, LAS-203, LAS-204 are statistically significantly more active than trimecaine by a factor of 1.4, have the same effect as that of lidocaine, and are more efficient as compared with novocaine by a factor of 1.9. The total effective duration of LAS-202 is within the range of 162 min, which is 2.9 times higher than that of trimecaine, lidocaine and novocaine. The compound LAS-203 falls in between by its activity.

Table 3 – Activity and effective duration of action of LAS-199 – LAS-204

Compounds	Infiltration anesthesia			Conduction anesthesia	
	0.25%			1.0 %	
	Anesthesia index, M±m	Total anesthesia duration, min	Effective duration, min	Total anesthesia duration, min	Effective duration, min
LAS-202	32.7±0.8	19.6±2.38	53,33±1,66	69.16±2.37	161.3±13.6
LAS-203	30.2±1.32	13.8±0.91	40.8±3.01	65.0±3.1	145.8±11.7
LAS-204	28.8±2.98	15.0±3.42	46.7±8.26	67.5±3.19	84.1±4.2
Trimecaine	33.6±0.33	20.0±1.7	38.3±1.05	47.3±8.4	56.9±12.8
Lidocaine	23.1±0.9	14.2±0.8	30.8±0.8	65.0±18.4	90.8±18.4
Novocaine	25.0±1.0	10.0±1.2	29.1±1,5	35.2±7.1	42.3±13.6

Thus, fluorobenzoic esters of piperidineketoximes cause profound and prolonged anesthesia, the introduction of fluorine leads to the formation of local anesthetics of different efficiency. Depending on the position of a fluorine atom in the phenyl ring, the greatest activity has been displayed by *p*-isomers, then *o*-isomers, whereas *m*-fluorobenzoates have proved to be less active.

EXPERIMENTAL CHEMICAL PART

The course of the reaction and individuality of the compounds are controlled by TLC on aluminum oxide of the III degree of activity, with the development of spots by iodine vapors. The IR spectra are recorded on a Nicolet 5700 spectrometer in KBr tablets and between KBr plates. ¹³C NMR spectra of the studied compounds in CDCl₃ are recorded on a JNM-ECA400 spectrometer, manufactured by JEOL firm, with an operating frequency 100 MHz at the carbon nuclei. An internal standard is HMDS. The data of elemental analysis of all synthesized compounds are presented in the corresponding tables in the experiment discussion.

Hydrochloride of 1-propyl-4-(p-fluorobenzoyloxyimino)piperidine. 1.5 g (0.01 mol) of oxime of 1-propylpiperidine-4-one is dissolved in a small quantity of absolute dioxane, then 2.27 l (0.02 mol) of hot solution of *p*-fluorobenzoylchloride in absolute dioxane is slowly added dropwise, while stirring, to the solution. Herewith, a white precipitation is immediately observed. The reaction mixture is held for 24 hours at the room temperature. The course of the reaction is controlled by TLC. The reaction mixture is washed by diethyl ether and the precipitation is filtered, recrystallized from isopropyl alcohol. 1.93 g (61 % of the theoretic value) of hydrochloride of *1-propyl-4-(p-fluorobenzoyloxyimino)piperidine* is obtained, mp of 170-172⁰C, R_f of 0.85 (Al₂O₃, eluent - benzene : dioxane - 4:1).

Found, %: C 56.99; H 6.32. C₁₅H₂₀ClFN₂O₂.

Calculated, %: C 57.23; H 6.40.

Hydrochloride of 1-propyl-4-(m-fluorobenzoyloxyimino)piperidine. 1.5 g (0.01 mol) of oxime of 1-propylpiperidine-4-one is dissolved in a small quantity of absolute dioxane, then 2.27 l (0.02 mol) of *m*-fluorobenzoylchloride in absolute dioxane is slowly added dropwise, while stirring, to the solution. As the solution is cooled the white precipitation is observed. The reaction mixture is held for 24 hours at the room temperature. The course of the reaction is controlled by TLC. The reaction mixture is washed by diethyl ether and the precipitation is filtered, recrystallized from isopropyl alcohol. 1.47 g (46.8 % of the theoretical value) of hydrochloride of *1-propyl-4-(m-fluorobenzoyloxyimino)piperidine* is obtained, mp 159-161⁰C, R_f of 0.7 (Al₂O₃, eluent - benzene : dioxane - 4:1).

Found, %: C 57.59; H 6.29. C₁₅H₂₀ClFN₂O₂.

Calculated, %: C 57.23; H 6.40.

Hydrochloride of 1-propyl-4-(o-fluorobenzoyloxyimino)piperidine. 1.5 g (0.01 mol) of oxime of 1-propylpiperidine-4-one (2.2) is dissolved in a small quantity of absolute dioxane, then 2.27 l (0.02 mol) of hot solution of *o*-fluorobenzoylchloride in absolute dioxane is slowly added dropwise, while stirring, to the solution. The reaction mixture is held for 24 hours at the room temperature. Several drops of diethyl ether are added to the solution, and a white precipitation is formed. The course of the reaction is controlled by TLC. The reaction mixture is washed by diethyl ether and the precipitation is filtered, recrystallized from isopropyl alcohol. 1.4 g (44.5 % of the theoretic value) of hydrochloride of *1-propyl-4-(o-fluorobenzoyloxyimino)piperidine* is formed, mp of 169-171⁰C, R_f of 0.7 (Al₂O₃, eluent - benzene : dioxane - 4:1).

Found, %: C 57.09; H 6.35. C₁₅H₂₀ClFN₂O₂.

Calculated, %: C 57.23; H 6.40.

EXPERIMENTAL BIOLOGICAL PART

The studies have been carried out on guinea-pigs by the Bulbring and Wade method and on rats by the "tail flick" method. The infiltration method is based on the principle of summation of the threshold mechanical stimuli, applied with a

certain rhythm, and allows one to estimate the intensity of an anesthetic effect. Each concentration has been tested on 6 animals. The average values of the results of the studies during 30 min have been taken as an anesthesia index. Compounds and reference preparations (novocaine, lidocaine, trimecaine) have been compared by the time of anesthesia onset, the duration of total anesthesia, and the total duration of an anesthetic effect of the preparation.

1. *An infiltration anesthetic activity* has been studied by the Bulbring and Wade method on guinea-pig males with the weight of 200-250 g. 0.2 ml of isotonic solutions of the compound under study and reference preparations have been introduced intracutaneously in four points (at the angles of a square 3 cm on a side) in the dorsal area of each animal, having preliminarily removed the hair covering. A local anesthetic activity has been estimated 6-8 times for each of the selected concentrations. Sensitivity at the place of introduction has been determined by touching with an obtuse injection needle, in series of 6 touches with the intervals of 3-4 after each 5 min, during 30 min. The profundity of anesthesia, expressed in ‘anesthesia indices’ (the average of 6 experiments, the maximum index – 36), the duration of total anesthesia and the total duration of an anesthetic effect have been determined. The activities of the compounds have been compared with that of the reference preparations – trimecaine, lidocaine and novocaine in the corresponding concentrations. The compound and reference preparations have been tested in 0.25% solutions.

2. *Conduction anesthesia model. The modified “tail flick” method on rats.* The “tail flick” method has been developed at the of Pharmacology of I.P. Pavlov St. Petersburg State Medical University. This method allows one to determine the rate of anesthesia onset, its profundity, the duration of total anesthesia, and the total duration of an anesthetic effect of the preparation. The activities of the compounds and reference preparations have been studied in 1% solutions. The study has been carried out on white outbred rat males with the weight of 200-250 g.

The research was carried out according to the scientific and technical program No. BR05234667 within the framework of program-targeted financing CS MES RK.

REFERENCES

- [1] The most essential in anesthesiology / Translation from English; under the general editorship of A.P. Zilber, V.V. Maltsev. M.: MEDpress-inform, 2007. P. 272.
- [2] Bguasheva B.A. Directed screening of locally anesthetic substances among the new derivatives of indole // Success of modern natural science. 2009. N 7. P. 45-47.
- [3] Praliyev K.D. C- and N-substituted mono- and bicyclic piperidines: synthesis, stereochemistry, transformations and properties. New synthetic analgesics and anesthetics. // Nitrogenous heterocycles and alkaloids. 2001. The Proceedings of the First International Conference. Moscow, October 9-12, 2001. P. 130-138.
- [4] RF Patent No. 1704415. 1-(2-ethoxyethyl)-4-ethinyl-4-benzoyloxypiperidine, possessing a local anesthetic activity (KAZCAINE) // K.D. Praliyev, Zh.I. Issin, V.K. Yu et al. Published 08.07.96.
- [5] Nauryzova B.Zh., Baimurzina M.A., Poplavskaya I.A., Praliyev K.D. Synthesis of oximes and their derivatives on the basis of simple ethers of 1-(2-ethoxyethyl)-4-acetyl-4-hydroxypiperidine // Izv. of NAS RK. Chemical series. 2003. N 2. P. 3-10.

[6] USSR Certificate of Authorship No.1220298. Hydrochloride of O-benzoyloxime of 1,2,5-trimethylpiperidone-4, possessing an antagonistic activity in relation to morphine, promedol and ethanol. // L.M. Sharkova, L.M. Andronova, V.A. Zagorevskiy, N.K. Barkov; Published 25.07.84, Bul. No.7.

[7] Praliyev K.D., Yu V.K., Akhmetova G.S. Synthesis of some oximes of the piperidine series // Izv. of MES RK, NAS RK. Chemical series. 2000. N 1. P. 96-101.

[8] Kuzdenbayeva R.S., Rakhimov K.D., Shin S.N. Pre-clinical study of a local anesthetic activity of new biological substances. (Textbook of Methods for Pharmacologists). The RK State Pharmacological Committee. Almaty, 2000. P. 28.

Резюме

Г. С. Ахметова, У. Б. Исаева, В. К. Ю, К. Д. Пралиев, Э. М. Сатбаева, Д. М. Кадырова, М. К. Амиркулова, Г. С. Смагулова, Т. М. Сейлханов

ЖЕРГІЛІКТІ АНЕСТЕЗИЯЛЫҚ БЕЛСЕНДІ 1-ПРОПИЛ-4-КЕТОКСИМПИПЕРИДИН ФТОРБЕНЗОАТТАР

Түрлі деңгейдегі жергілікті анестезиялық белсенділік көрсететін 1-пропил-4-кетоксимпиперидиннің п-фтор, м-фтор, о-фтор-бензоаттары синтезделді. Фторды енгізу жергілікті анестетиктерге әртүрлі тиімділік дәрежесімен әкеледі. Фенил сақинасында фтор атомының орнына байланысты ең көп белсенділікті пара-изомерлер көрсетті, содан кейін орто- және аз белсенді метафторобензоаттар болды.

Түйін сөздер: п-фтор, м-фтор, о-фтор-бензоилкарбонилхлорид, N-пропилпиперидин-4-он, күрделі эфирлер, 1-пропил-4-(п-фтор-, м-фтор-, о-фторбензоилоксиимино)пиперидиндер, жергілікті анестезиялық белсенділік.

Резюме

Г. С. Ахметова, У. Б. Исаева, В. К. Ю, К. Д. Пралиев, Э. М. Сатбаева, Д. М. Кадырова, М. К. Амиркулова, Г. С. Смагулова, Т. М. Сейлханов

ФТОРБЕНЗОАТЫ 1-ПРОПИЛ-4-КЕТОКСИМПИПЕРИДИНА С МЕСТНОАНЕСТЕЗИРУЮЩЕЙ АКТИВНОСТЬЮ

Синтезированы п-фтор, м-фтор, о-фтор-бензоаты 1-пропил-4-кетоксимпиперидина, проявившие в разной степени местноанестезирующую активность. Введение фтора приводит к местным анестетикам с различной степенью эффективности. В зависимости от положения атома фтора в фенильном кольце наибольшую активность показали пара- изомеры, затем орто- и менее активными были мета- фторбензоаты.

Ключевые слова: п-фтор, м-фтор, о-фтор-бензоилкарбонилхлорид, N-пропилпиперидин-4-он, сложные эфиры, 1-пропил-4-(п-фтор-, м-фтор-, о-фторбензоилоксиимино)пиперидины, местноанестезирующая активность.

*R. M. CHERNYAKOVA, A. A. AGATAYEVA, R. A. KAYINBAYEVA,
K. Ye. YERMEKOVA, N. N. KOZHABEKOVA, U. Zh. ZHUSSIPBEKOV*

JSC «Institute of Chemical Sciences named after A.B. Bekturov», Almaty, Kazakhstan

SORPTION OF LEAD CATIONS (II) BY ACID-MODIFIED ZEOLITE IN ALKALINE MEDIUM

Abstract. A systematic analysis of the sorption properties of acid-modified zeolite was carried out in alkaline (pH 8.5) medium with respect to Pb^{2+} cations. The interaction of time, temperature and concentration of lead on the sorption capacity of acid-modified zeolite was established. The sorption curves depending on temperature and concentration of Pb^{2+} ions have extreme character. The appearance of the maximum or minimum on the lead sorption curves probably due to saturation of modified zeolite with lead cations under these conditions, consequence, a decrease in its sorption properties. This process, in turn, is caused by the desire of the system to equilibrium, where the concentration of lead is equalized in both phases. The optimal conditions for sorption of Pb (II) cations in an alkaline medium with an acid-modified zeolite corresponding to the maximum degree of their absorption (99.8-99.9%) were determined.

Keywords: alkaline medium, lead cations (II), heavy metals, acid-modified zeolite, sorption.

Introduction. In recent years sorption methods for the purification of aqueous media and wastewater by using of modified natural zeolites have become widespread [1, 2]. The acid activation of natural zeolites is accompanied by the process of dealumination, as a result, the channels of zeolite framework are unblocked, which leads to an increase in Si/Al ratio, the formation of silanol groups, an increase in the effective size of micropores, and an increase in exchange capacity of zeolite [3-9]. The exchange acid centers appear in the zeolite structure due to acid activation. When acid is activated by appearance of active in the process of sorption of H^+ exchange acid centers and the displacement of aluminum (Al^{3+}) into exchange positions, more favorable arrangement of active sites for the interaction of reacting substances are created. In addition, at acidic treatment of zeolite the silica increases the specific surface area and porosity of the activated samples and removed impurities blocking the channels [10]. The stability of silica-alumina skeleton of high-silica zeolites to the action of acids has increased the possibilities of regulating their properties by decationization and dealumination under various conditions of acid treatment.

It has been found that acid-activated clinoptilolite tuffs are shown high sorption properties, for example with respect to phenylalanine [11, 12] and formaldehyde [13, 14], which is their practical application in the purification of contaminated media. A method for extracting α -tocopherol from vegetable oils based on high selectivity of acid-activated clinoptilolite to α -tocopherol from an ethanol

solution was developed and proposed [15]. Modification of natural zeolites with acids increases their efficiency of extracting NH_4^+ ions from various media [16, 17]. It was shown that acid-activated natural clinoptilolite (Sokirnitsky deposit, Ukraine) shows a growth in sorption capacity with respect to SO_2 molecules [18]. Obviously, this is due to the reduction in the main (donor) surface centers (potential centers of adsorption of acceptor molecules SO_2), as a result of action of protonic acid. Detailed studies by the authors of [19] and carried out in [18] showed that the samples of Bulgarian clinoptilolite, treated by boiling for 4 hours in 2N, 4N, 6N and 8N hydrochloric acid behave differently in the adsorption processes of SO_2 . For H-Cl (4N HCl) samples protective action time and amount of adsorbed SO_2 were maximum. However for the sample of H-Cl (8N HCl), these values were lower than natural clinoptilolite. The authors associate the obtained results with an increase in the degree of dealumination and partial destruction of the zeolite crystal lattice [19]. Acid treatment of natural zeolite allows to obtain more efficient sorbents in relation to phosphates, fluorine, cations of iron (III), aluminum (III), and heavy metals [20-22].

A negative influence of temperature on the process of acid activation of clinoptilolite was revealed in [23]. Activation of clinoptilolite of Bigadis deposit (Turkey) with 5 M hydrochloric acid at 25, 40 and 100 °C reduces the content of cations in aluminosilicate, the amount decrease by increase of the temperature. However, there is no complete removal of exchange cations and aluminum.

A number of alkaline production effluents contain in dissolved form inorganic impurities such as Fe, Mg, Pb, As, Cu, Mn, Ni, etc. Lead ions among previous cations-impurities are toxic, which are capable to concentration and accumulation in soil, wastewater, groundwater, and in the human body [24-26]. For the purification of contaminated alkaline media application of acid-modified zeolites is perspective due to an increased exchange capacity.

From the review it is clear that acid modification of natural zeolites of various deposits increases their sorption properties. However, the sorption capacity of obtained sorbents is determined by the nature of used zeolite, temperature and other factors of the process.

The aim of the work was to study the influence of the sorbent norm, time, temperature and concentration of Pb^{2+} cations on the process of their sorption from an alkaline medium by acid-modified zeolite.

EXPERIMENTAL PART

In this research was used zeolite of the Shankanay deposit modified by 15% hydrochloric acid. The sorption capacity of acid-modified zeolite with respect to lead was studied under stirring conditions in thermostat reactor which was evaluated by change in content of Pb^{2+} cations in solution, i.e. with the difference in the initial and residual concentration of lead (after the completion of the process). The degree of sorption (extraction) is the ratio of difference between the initial and reached concentration of Pb (II) cation at fixed time to its original content.

Initial and final concentrations of lead ions in solutions were analysed by using an atomic absorption spectrophotometer (AA-7000, Shimadzu Corporation, Japan), № A30664901456.

Studying of sorption process of lead (II) cations was carried out in lead-containing aqueous solution with pH of 8.5, which created with 1 N sodium hydroxide solution. The predetermined concentration of Pb^{2+} cations was obtained by introducing in the alkaline solution estimated quantity of acetic acid-lead $Pb(CH_3COO)_2 \cdot 3H_2O$.

The effect of the norm of acid-modified zeolite on its sorption capacity was investigated by an alkaline solution at room temperature where concentration of Pb equal to 49.1 mg/l. The sorbent consumption was varied from 2.5 to 30 g per 100 g of purified alkaline solution. The sorption process was carried out at room temperature for 30 minutes.

The degree of purification of various media significantly depends on time, temperature, and concentration of Pb^{2+} cations. Quantitative determination of such a complex dependence carried out by method of mathematical planning of the orthogonal rotatable 3 factorial experiment of the 2nd order [27]. Variable (input) factors of the process were: time (Z_1 , min), temperature (Z_2 , °C), and C_{Pb} (Z_3 , mg/l). The selected levels of factors and range of their variation are given in table 1.

Table 1 – Coordinate center of the plan, levels of variation

Parameters	Z_1 , min	Z_2 , °C	Z_3 , mg/L
Upper level (+1)	48,9	59,9	81,8
Center of the plan - zero level (Z_i^0)	32,5	45	55
Lower level (-1)	16,1	30,1	28,2
Interval of variation along the axis (ΔZ_i)	16,4	14,9	26,8
Star point (+1,682)	60	70	100
Star point (-1,682)	5	20	10

The changes in the concentration of Pb (II) cations indicated in the table correspond to possible range of their presence in contaminated solutions and wastewater.

Defined (output) parameter Y_1 (response) was residual content of Pb^{2+} ions in studied system "Pb²⁺ - alkaline medium - acid-modified zeolite" after sorption of lead by sorbent.

RESULTS AND DISCUSSION

Studying of effect of the norm of acid-modified zeolite on its sorption capacity with respect to Pb (II) cations in an alkaline medium (pH 9) revealed, increasing in the sorbent consumption from 2.5 g to 5 g per 100 g of purified solution the sorption rate risen from 98.28 % to 99.95% (by 1.67%). Further increase in sorbent consumption practically has no effect on the degree of alkaline purification from lead. The optimal ratio "modified zeolite (T): alkaline solution (G)" is 5:100.

Studying of the sorption of Pb^{2+} cations depending on its concentration, time and temperature carried out at constant ratio of S:L equal to 5:100.

Based on the coordinates of the center of plan, variation levels and planning matrix (table 1, 2), experiments carried out with the appropriate conditions for studying of Pb^{2+} cations sorption by an acid-modified zeolite in an alkaline medium. The results are shown in table 2.

Table 2 – The residual content of Pb^{2+} cations and degree of their sorption by acid-modified zeolite in alkaline medium

#	The natural value of experiments			The content of Pb^{2+}	
	X_1 , min	X_2 , °C	X_3 , mg/l	The residual content of Pb^{2+} , mg/L	K_s , %
1				0,03	99,88
2	48,9	30,1	28,2	0,09	99,65
3	16,1	59,9	28,2	0,03	99,88
4	48,9	59,9	28,2	0,03	99,88
5	16,1	30,1	83,7	0,03	99,96
6	48,9	30,1	83,7	0,03	99,96
7	16,1	59,1	83,7	0,79	99,06
8	48,9	59,1	83,7	0,93	98,95
9	5	45	55	1,03	98,19
10	60	45	55	0,93	98,37
11	32,5	20	55	1,06	98,14
12	32,5	70	55	6,78	87,95
13	32,5	45	10	2,25	79,73
14	32,5	45	100	14,8	84,10
15	32,5	45	55	0,06	99,89
16	32,5	45	55	1,21	97,87
17	32,5	45	55	1,02	98,21
18	32,5	45	55	1,18	97,93
19	32,5	45	55	0,86	98,49
20	32,5	45	55	1,65	97,11

After the processing of the results and the elimination of insignificant coefficients, obtained by regression equation allows calculating the residual content of Pb (II) cations in the alkaline medium after the end of the sorption process by acid-modified zeolite also describes dependence of the residual content of Pb (II) cations on investigated process parameters:

$$Y_{pb} = 0,339+0,089X_2+0,106X_3+0,136X_1^2+0,109X_2^2+0,158X_3^2+0,200X_2X_3$$

The regression equation checked with Fisher criterion by comparing the variances. It is found that $F < F_{1-p}(f_1, f_2) = Y_{Pb^{2+}}$ 1,204 < 4,699, so that the equation adequately describes the experiment.

Analysis of regression equation showed that cleaning the solution with an acid-modified zeolite, the residual content in the liquid phase of system "Pb²⁺ - alkaline medium - acid-modified zeolite" is a function of all investigated variables. However their effect is different. Thus, in the regression equation, the time effect is represented only by positive quadratic value (X_1^2). The time factor affects independently on the output parameter and increasing coefficient by value higher than the coefficient of temperature factors (X_2) and concentration of lead cations (X_3).

The considered interference of factors and their effect on the response is well demonstrated by following graphs. It can be seen from Figure 1a, b by increasing purification process duration of an alkaline solution with a low concentration of Pb²⁺ (10-28 mg/L) at all temperatures reduces its residual content in liquid phase of the system. The most intensive sorption process takes up to 30 minutes. Increasing of process time from 30 to 50 min has no effect on the change of lead concentration in solution with $C_{Pb} = 10$ mg/L (figure 1, a), but leads to an increase in its residual content in the solution of $S_{Pb} = 28$ mg/L (figure 1, b). Thus, at 20°C after 5 min of process there is 0.92 mg/L of Pb²⁺, after 16 min - 0.72 mg/L of Pb²⁺, after 32 min - 0.46 mg/L of Pb²⁺, after 60 minutes - 0.60 mg/L Pb²⁺. Accordingly, the degrees of sorption are 96.7; 97.44; 98.36 and 97.87%, i.e. with the increase in the duration of the process, there is a tendency to reduce the sorption capacity of sorbent.

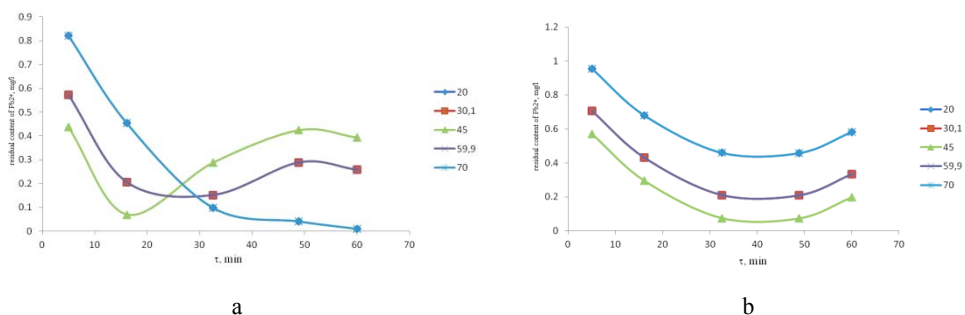
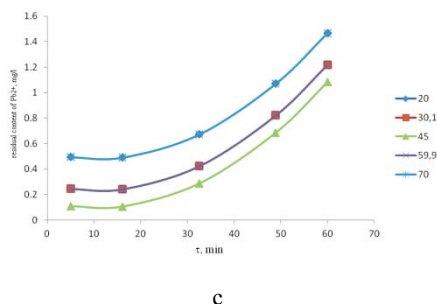


Figure 1 –
Influence of time on residual content
of Pb (II) cations
in liquid phase of system "Pb²⁺ - alkaline
medium - acid-modified zeolite":
a – 10 mg/L; b – 28 mg/L; c – 82 mg/L



Increasing of process time has a detrimental effect on the purification of more concentrated lead-containing alkaline solutions (81.8-100 mg/L Pb), which contributes to the growth of the residual content of Pb^{2+} ions in the liquid phase of system (figure 1, c). For example, the process starting from 16-20 minutes and up to 60 minutes in an alkaline solution containing 100 mg/L of Pb cations at 20°C, the degree of lead sorption by an acid-modified zeolite decreases by 1.4%. In this case, increasing the process time has a negative effect on the sorption of lead.

According to the regression equation describing the dependence of the residual content of Pb (II) cations on investigated process parameters, it follows that temperature effect on the degree of sorption of Pb^{2+} ions is complex and is represented by positive values of the linear factor X_2 , quadratic X_2^2 , double interaction of temperature and concentration of Pb cations (X_2X_3). Since in equation before the coefficient of variable X_2 there is a “plus” sign, the temperature factor affects the output parameter not only as double interaction with the third factor (C_{pb}), but also independently and directly proportional with. Comparison of coefficients of considered factor X_2 shows its practically equivalent effect along with the first X_1 (time) and the third X_3 (C_{pb}) factors. A somewhat larger effect is exerted by the factor of double interaction X_2X_3 (temperature and C_{pb}). Apparently, lead adsorption is exerted by influence of temperature and concentration of Pb^{2+} cations.

Analysis of the obtained results revealed that the curves dependence of residual content of Pb^{2+} cations on temperature have extreme character (figure 2). At the same time, the influence of temperature, lead concentration and time on purification of alkaline solutions with low (10 mg/L) and high (100 mg/L) concentrations are noted (figure 2, a, c). Wherein the sorption curves at 45°C in the range of 5-16 min in solutions with $C_{pb} = 10$ mg/L have a minimum, and in the range of 32-60 min have maximum, while in solutions with $C_{pb} = 100$ mg/L on sorption curves in the indicated time limits are characterized by the presence of maximum and minimum. In the first case growth of temperature up to 45°C has a positive effect, as the residual content of Pb^{2+} cations decreased (the degree of sorption increases), and in the second case - negative one, since the concentration of Pb^{2+} ions in the system raised (the sorption degree decreases).

In systems the sorption curves throughout the studied time interval are characterized by a minimum at 45°C when C_{pb} equal to 28-82 mg/L (figure 2, b). Raising of temperature to 45°C has positive effect. Above noted temperature the degree of sorption of lead decreased. For example, 97.63% Pb is sorbed in 16 minutes at 20°C, at 45°C - 98.98% Pb and at 70°C - 97.55% Pb.

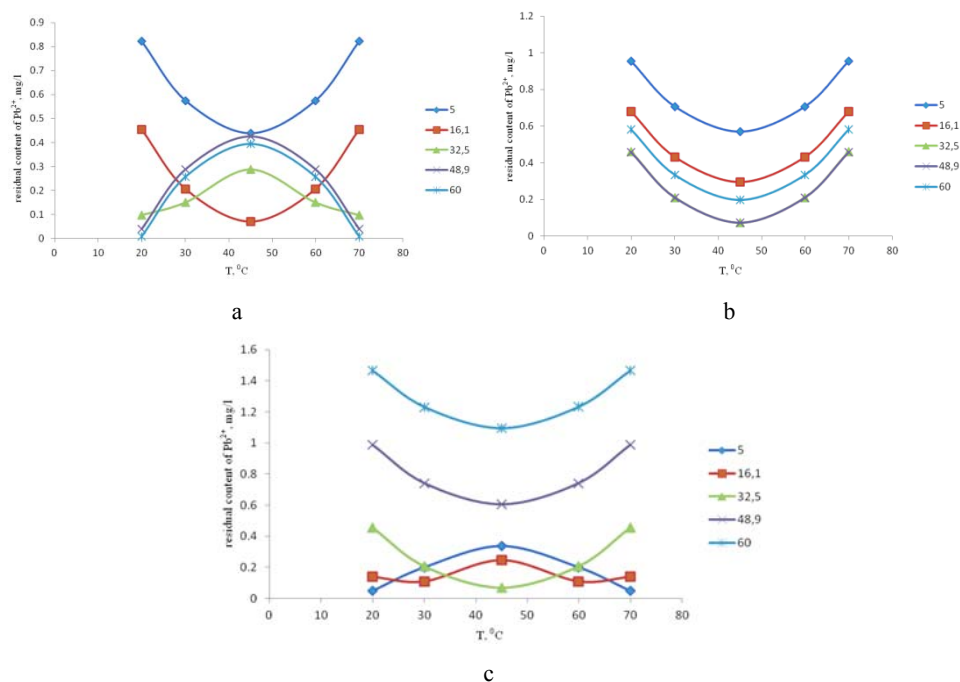


Figure 2 – Effect of temperature on residual content of Pb (II) cations in the system "Pb²⁺ - alkaline medium - acid-modified zeolite":
 a – 10 mg/L Pb²⁺; b – 28 mg/L Pb²⁺; c – 100 mg/L

Appearance of the maximum or minimum on the sorption curves is probably due to the saturation of acid-modified zeolite with lead cations under these conditions, consequence, deterioration of its sorption properties. This process caused aspiration of system to equilibrium where the concentration of lead in both phases is equalized.

According to the regression equation, the effect of concentration of Pb²⁺ cations on their sorption by an acid-modified zeolite is represented by positive linear (X_3) and quadratic (X_3^2) factors. Compare with contact duration of the sorbent with purification of alkaline solution this suggests a more complex effect of concentration of lead in solution on the process of their sorption. If we compare the values of lead concentration factors X_2 and time X_1^2 , then for X_1^2 (time) its value is several higher, but this is somewhat balanced by the close values at coefficients (X_3) and (X_3^2) corresponding to the concentration of lead ions.

The sorption curves of lead depending on their concentration (figure 3) have similar character to the sorption curve by temperature (figure 2). So the curves have extreme character with min or max at 55 mg/L Pb. Moreover, the sorption curves at low temperatures (20°C) obtained in the interval of 5-50 min, which characterized by the presence of min and at 60 min - max (figure 3, a), at higher temperature (70°C) is prescribed min on the curves in the interval of 15 -60 min, and max - at 5 min of the process (figure 3b).

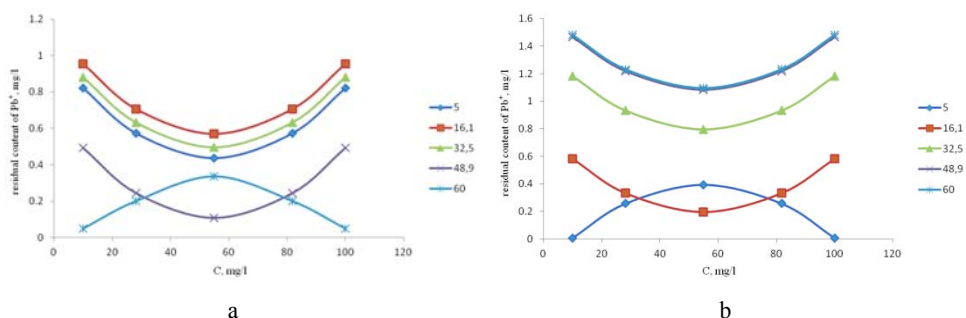


Figure 3 – The effect of Pb (II) cations concentration on its residual content in the system of "Pb²⁺ - alkaline medium - acid-modified zeolite":
a – 20°C; b – 70°C

So, at 20°C up to 50 min with increasing of C_{Pb} to 55 mg/L, lead sorption degree (K_c) increased, and with a further increase K_c C_{Pb} decreased. However, simultaneous increase in C_{Pb} and time (60 min) decreased the sorption degree reaching to minimum at 55 mg/l Pb, then increased with raising of C_{Pb} .

At higher temperature (70°C), the maximum degree of Pb sorption is also reached in solutions with their concentration of 55 mg/L. However, for 15-60 min and the minimum - for 5 min of the process.

The presence of maximum or minimum on the sorption curves is due to the saturation of the zeolite, consequence, due to the deterioration of its sorption properties. This process, in turn, may be caused by the desire of the system to equilibrium, where the concentration of copper in both phases is equalized. So that the appearance of maximum on the sorption curves is due to the desorption process, when under these conditions took place exit of the sorbed cations from zeolite back to solution [28].

When determining the optimum conditions for sorption of Pb²⁺ cations by an acid-modified zeolite from an alkaline medium, it is necessary to consider temperature, lead concentration and the process time. Thus, the greatest degree of sorption of Pb cations is achieved at 20 and 70°C in an alkaline solution with C_{Pb} equal to 10 and 100 mg/L, respectively, in 60 and 5 minutes (99.8-99.9%) and with C_{Pb} equal to 55 mg/L for 16 and 48 min, respectively, at 20 and 70°C (99.6-99.8%).

The research was carried out according to the scientific and technical program No. BR05234667 within the framework of program-targeted financing CS MES RK.

REFERENCES

- [1] Razmakhnin K.K., Khatkova A.N. Modification of properties of zeolites for the purpose of widening the areas of their application // Mining information-analytical bulletin. 2011. N 4. P. 246-252.
- [2] Shevchenko T.V., Klimov E.S., Buzaeva M.V. Wastewater treatment with non-traditional sorbents. Ulyanovsk: UISTU, 2011. 201 p.

[3] Kowalczyk P., Myroslav S., Artur P.T. Porous structure of natural and modified clinoptilolites // *J. of Colloid and Interface Science*. 2006. Vol. 297. P. 77-85.

[4] Garcia-Basabe Y., Rodriguez-Iznaga I., Menorval M. Step – wise dealumination of natural clinoptilolite: Structural and physicochemical characterization // *Microporous and Mesoporous Mat.* 2010. Vol. 135, N 1-3. P. 187-196.

[5] Sprynskyy M., Golembiewski R., Trykowski G., Buszewski B. Heterogeneity and hierarchy of clinoptilolite porosity // *J. of Physics and Chemistry of Solids*. 2010. Vol. 71. P. 1269-1277.

[6] Moreno P.V., Arellano J.J.C., Ramirez H.B. Characterization and preparation of porous membranes with a natural Mexican zeolite // *J. Phys.: Condens. Matter*. 2004. Vol. 16. P. 2345-2352.

[7] Groen J.C., Peffer L.A., Perez J.R. Pitfalls and limitation in gas adsorption data analysis pore size determination in modified micro- and mesoporous materials // *Microporous and Mesoporous Mater.* 2003. Vol. 60. P. 1-17.

[8] Khankhalaeva S.T., Badmaeva S.V., Dashinamshilova E.T. Influence of modification on structural, acidic and catalytic properties of layered aluminosilicate // *Kinetics and catalysis*. 2004. Vol. 45, N 5. P. 748-753.

[9] Kurama H., Zimmer A., Reschetilowski W. Chemical Modification Effect on The Sorption Capacities of Natural Clinoptilolite // *Chemical Engineering Technology*. 2002. N 25. P. 301-309.

[10] Garcia-Basabe Y., Rodriguez-Iznaga I., Menorval M. Step – wise dealumination of natural clinoptilolite: Structural and physicochemical characterization // *Microporous and Mesoporous Materials*. 2010. Vol. 135. P. 187-196.

[11] Kotova D.L., Do Thi Long, Krysanova T.A., Selemenev V.F. Effect of acid activation on the sorption of phenylalanine on clinoptilolite tuff // *Journal of Phys. Chem.* 2011. P. 85. N 12. P. 2365-2369.

[12] Do Thi Long, Kotova D.L., Krysanova T.A., Bolotova M.S., Dolgopolova E.A., Beke-tov B.N. Immobilization of phenylalanine on acid-activated clinoptilolite tuff // *Sorption and chromatographic processes*. 2010. Vol. 10. P. 736-740.

[13] Belchinskaya L.I., Tkacheva O.A., Lavlinskaya O.V., Anisimov M.V. Adsorption of formaldehyde by activated fillers of carbamide-formaldehyde resins. Voronezh, 2014. 224 p.

[14] Belchinskaya L.I. Study of structural and adsorption characteristics in the activation and modification of natural silicates // *Sorption and chromatographic processes*. 2007. Vol. 7. P. 571-576.

[15] Vasylieva S.Yu. Equilibrium sorption of α -tocopherol on modified clinoptilolite: dis. ... cand. of chem. sc.: 02.00.04. Voronezh: The Voronezh State University, 2014. 138 p.

[16] Aref A., Abdullateef I., Amer M. Xinrong L., Hongquan W., Chunjie Y. The investigation into the ammonium removal performance of Yemeni natural zeolite: Modification, ion exchange mechanism, and thermodynamics // *Powder Technology*. 2014. Vol. 258, N 1. P. 20-31.

[17] Leikin Yu.A., Myasoedov B.F., Losev V.V. Modified sorbents for selective extraction of ammonia and its derivatives // *Chemical physics*. 2007. Vol. 26, N 10. P. 18-32.

[18] Rakitskaya T.L., Raskola L.A., Kiose T.A., Yarchuk A.V., Korotkova A.S. Adsorption and protective properties of modified clinoptilolite relative to sulfur dioxide // *News of ONU. Chemistry*. 2014. Vol. 19. P. 52-58.

[19] Allen S.J., Ivanova E., Koumanova B. Adsorption of sulfur dioxide on chemically modified natural clinoptilolite. Acid modification // *J. Chem. Eng.* 2009. Vol. 152, N 2-3. P. 389-395.

[20] Jie Xie, Zhe Wang, Da Fang, Chunjie Li, Deyi Wu. Green synthesis of a novel hybrid sorbent of zeolite/lanthanum hydroxide and its application in the removal and recovery of phosphate from water // *J. of Colloid and Interface Science*. 2014. N 423. P. 13-19.

[21] Rahmani A., Nouri J., Kamal Gh., Mahvi A.H., Zare M.R. Adsorption of fluoride from water by Al^{3+} and Fe^{3+} pretreated natural Iranian zeolites // *Int. J. Environ. Res.* 2010. Vol. 4, N 4. P. 607-614.

[22] Arutyunyan R.S., Arutyunyan L.R., Petrosyan I.A., Badalyan G.G., Sergsyan A.O., Kuznetsova T.F., Ivanets A.I. Sorption of iron (III) ions from wines by zeolites treated with acid // Applied chemistry and biotechnology. Irkutsk: Ir. Nat. Res. TU, 2017. Vol. 7, N 1. P. 111-118.

[23] Çakicioglu-Ozkan F., Ülkü S. The effect of HCl treatment on water vapor adsorption characteristics of clinoptilolite rich natural zeolite // Microporous and Mesoporous Mat. 2005. Vol. 77. P. 47-53.

[24] Sukiasyan A.R., Tadevosyan A.V., Pirumyan G.P. Migration of a number of heavy metals in the soil-plant system // Natural and technical sciences. 2016. N 3. P. 32-34.

[25] Kentbaev E.Zh., Kentbaeva B.A. Accumulation of heavy metals in leaves of wood species of Astana city // Vestnik of the Nizhny Novgorod state agricultural academy. 2014. Vol. 4. P. 151-155.

[26] Serdyukova A.F., Barabanshikov D.A. Effects of soil contamination with heavy metals // Young scientist. 2017. N 51. P. 131-135.

[27] Akhnazarova S.L., Kafarov V.V. Optimization of the experiment in chemistry and chemical technology. M.: Higher School, 1985. 327 p.

[28] Kats E.M., Nikashina V.A., Bychkova Ya.V. Kinetics of sorption of heavy metals from surface water on natural and modified polyethyleneimine clinoptilolite of the Kholinsky deposit // Sorption and chromatographic processes. 2016. Vol. 16, N 1. P. 36-43.

Резюме

*Р. М. Чернякова, Р. А. Қайыңбаева, А. А. Ағатаева,
Қ. Е. Ермекова, Н. Н. Қожабекова, Ө. Ж. Жүсіпбеков*

СІЛТІЛІК ОРТАДА ҚЫШҚЫЛМЕН МОДИФИКАЦИЯЛАНҒАН ЦЕОЛИТ АРҚЫЛЫ ҚОРҒАСЫН (II) КАТИОНДАРЫН СОРБЦИЯЛАУ

Қышқылмен модификацияланған цеолиттің сілтілік ортада (рН 8,5) Pb^{2+} катиондарына қатысты сорбциялық қасиеттерін жүйелі түрде талдау жүргізілді. Уақыт, температура және қорғасын концентрациясының қышқылмен модификацияланған цеолиттің сорбциялық қабілетіне өзара әсер ететіні анықталды. Температура мен Pb^{2+} иондары концентрациясына тәуелді сорбциялық қисықтар айрықша сипатқа ие. Қорғасынның сорбциялық қисықтарында максимум немесе минимумның пайда болуы осы жағдайларда модификацияланған цеолиттің қорғасын катиондарымен қанығуына, соның салдарынан оның сорбциялық қасиеттерінің төмендеуіне байланысты болуы мүмкін. Бұл процесс өз кезегінде жүйенің тепе-теңдікке ұмтылуы салдарынан туындайды, нәтижесінде қорғасын концентрациясы екі фазада да теңеседі. Сілтілік ортада Pb (II) катиондарының қышқылмен модификацияланған цеолит арқылы сорбциялану процесінің оңтайлы жағдайлары анықталды. Pb (II) катиондары ең жоғарғы сорбциялану дәрежесіне Pb концентрациясы 10 және 100 мг/л (99,8-99,9 %) тең ерітіндіде 5 және 60 минутта, сондай-ақ Pb концентрациясы 55 мг/л (99,6-99,8 %) тең ерітіндіде 16 және 48 минутта 20 және 70°C температурада жетеді.

Түйін сөздер: сілтілік орта, қорғасын (II) катиондары, ауыр металдар, қышқылмен модификацияланған цеолит, сорбция.

Резюме

*Р. М. Чернякова, Р. А. Кайынбаева, А. А. Агатаева,
К. Е. Ермекова, Н. Н. Кожобекова, У. Ж. Джусупбеков*

**СОРБЦИЯ КАТИОНОВ СВИНЦА (II)
КИСЛОТОМОДИФИЦИРОВАННЫМ ЦЕОЛИТОМ
В ЩЕЛОЧНОЙ СРЕДЕ**

Проведен системный анализ сорбционных свойств кислото- модифицированного цеолита в щелочной (рН 8,5) среде по отношению к катионам Pb^{2+} . Установлено взаимовлияние времени, температуры и концентрации свинца на сорбционную способность кислото-модифицированного цеолита. Сорбционные кривые в зависимости от температуры и концентрации ионов Pb^{2+} носят экстремальный характер. Появление на кривых сорбции свинца максимума или минимума, вероятно, обусловлено насыщением в этих условиях модифицированного цеолита катионами свинца и, как следствие, снижением его сорбционных свойств. Данный процесс, в свою очередь, вызван стремлением системы к равновесию, при котором происходит выравнивание концентрации свинца в обеих фазах. Определены оптимальные условия процесса сорбции катионов Pb (II) кислотомодифицированным цеолитом в щелочной среде. Наибольшая степень сорбции катионов Pb (II) достигается в растворе с C_{Pb} , равной 10 и 100 мг/л (99,8-99,9 %) за 5 и 60 мин и с C_{Pb} , равной 55 мг/л за 16 и 48 мин (99,6-99,8 %) при температурах 20 и 70°C.

Ключевые слова: щелочная среда, катионы свинца (II), тяжелые металлы, кислотомодифицированный цеолит, сорбция.

*M. T. OSHAKBAEV, E. A. TUSUPKALIEV, M. N. BAIMBETOV,
ZH. N. KAINARBAYEVA, G. D. BAIBATYROVA, ZH. S. ALIMBEKOV*

JSC "Institute of Chemical Sciences named after A. B. Bekturova", Almaty

NATIVE CONDITIONS AND FEATURES OF THE GEOLOGICAL STRUCTURE OF THE TERRITORY JSC «OZENMUNAIGAS» AND CHARACTERISTICS WORK

Abstract. Production activities of extraction and preparation of hydrocarbon raw materials JSC "Ozenmunaigas" has a certain impact on the components of the environment. Improvement of the ecological situation and rational economic use of natural resources is becoming the most important state problem of the region. In this regard, the timely assessment of the environmental condition of the territory and chemical and environmental studies actual.

Key words: production, environment monitoring, emission, JSC "Ozenmunaigas", geological structure, climatic conditions.

Introduction. Conducting industrial environmental control including its monitoring is the obligatory in the use of natural resources of the Republic of Kazakhstan.

Over the past few years, a number of important changes have occurred in the legislation of the Republic of Kazakhstan concerning the issues of environmental monitoring. A number of legislative and regulatory acts, such as the Law "Environmental protection of the Republic of Kazakhstan" (1997), the Law "Protection of atmospheric air" (2002), "Rules of organization and maintenance of the Unified state system of monitoring of the environment and natural resources" (2001), "Model rules of conducting industrial monitoring" (2007) and a lot of other acts, no longer valid in connection with the introduction of the Environmental Code of the Republic of Kazakhstan in 2007.

The item 137 of the Environmental Code of the Republic of Kazakhstan provides the concept of environmental monitoring: "State environmental monitoring (monitoring of the environment and natural resources) is a comprehensive system of monitoring the state of the environment, natural resources in order to assess, forecast and control changes in their state under the influence of natural and anthropogenic factors [1]. "Thus, the Environmental Code identifies the terms "ecological monitoring" and "monitoring of the environment and natural resources".

The content of the state Unified monitoring system of the environment and natural resources consist of the following subsystems:

- environmental monitoring;
- monitoring of natural resources;
- special types of monitoring.

The unified state system for monitoring the environment and natural resources is implemented at three levels (item 144 of the Environmental Code):

- local (industrial monitoring and monitoring on specific areas of settlements, water bodies and rivers, especially protected natural areas);
- regional;
- Republican.

According to the Environmental code of the Republic of Kazakhstan, industrial monitoring (IM) of the environment (monitoring, which is carried out by the nature user) is an element of industrial environmental control.

Environmental Code of the Republic of Kazakhstan, divides the production environmental monitoring into the following types:

- Operational monitoring includes monitoring of the parameters of the production process in order to ensure proper project operation and compliance with the conditions of the production process regulations;

- Monitoring of emissions to the environment involves monitoring emissions from sources of emissions and discharges in order to comply with the maximum permissible emissions (MPE) and maximum permissible discharges (MPE) standards. The choice of measurement points is determined by the location of specific sources of OS pollution;

- Impact monitoring. Monitoring of impacts is carried out when it is necessary to monitor compliance with environmental legislation of the Republic of Kazakhstan and regulations.

According to the project: № ARO05131111 JSC "Institute of Chemical Sciences A. B. Bekturova" will be carried out work on the theme. "Production monitoring of waste oil production for the development of resource-saving technologies." Production monitoring will be carried out in JSC "Ozenmunaigas".

Administrati on management of JSC "Ozenmunaigas" is located in the of Karakiyan district on the Mangistau region.

Among the offices of JSC "Ozenmunaigas", there are the main production management, which includes, first of all, the oil and gas production management (NGDU) and the management of oil preparation and production support, perform secondary functions that are ancillary or service nature. The main fields of the production branch are oil and gas fields Uzen and Karamandybas with a single field infrastructure.

In General, the branch production is growing. The water content of the extracted oil under the PF "Ozenmunaigas" does not increase significantly over time and is steadily maintained at the level of 80%.

In the produced oil fluid, its component, is associated gas. Production of associated gas has increased significantly over the past four years, which is probably due to the increase in gas caps of oil reservoirs.

The state of the well stock is largely reflected in the performance of field development. As oil production increases, the operating Fund of producing wells gradually increases, while part of the production Fund is transferred to other categories, this is due to the fact that with a significant decrease in the production rate of the producing well or a large water content of the produced fluid, the well is transferred to another category or goes to liquidation.

Table 1 – Monitoring objects of PF " Ozenmunaigas»

Branch	Control	
PF «OMG»	NGDU-1	Oil and gas production Department №1
	NGDU-2	Oil and Gas production Department №2
	NGDU-3	Oil and Gas production Department №3
	NGDU-4	Oil and Gas production Department №4
	UPN&PO	Oil preparation and production support
	UH&E	Department of ecology and chemialiration
	OEN	UzenEnergoNeft
	УРНО и ТК	Management Whie Management of chemicals and the environment
	UOC-1-UOC-5	WellServiceControls
	UAT	AutomationandTelecommunicationsDepartment
	UTT	Departmentoftechnologicaltransport
	UPTO&KO	Management of production and technical services and equipment

Mining technology for oil-1, oil-2, oil-3, oil-4 is typical. Oil production at Uzen and Karamandybas fieldsproduced by mechanized method, with the bulk of the production wells (98%), equipped with deep well pumps.

This method of production is basic and is used on all oil and gas branch. At the same time, production wells are equipped with wellhead platforms, foundations for rocking machines, shgn control stations and transformer substations. It should be noted that more than half of the production wells are in operation for more than 15 years.

Technological scheme of oil and gas gathering oil-1, oil-2, oil-3, oil-4 also is a model, and implemented the following scheme.

The fields use a single-tube pressurized system for collecting the extracted oil, through which the extracted fluid is supplied to the measuring unit (storage). Measurement of the flow rate of producing wells in the storage is carried out by the "Sputnik" installations. The number of wells connected to the measuring unit" Sputnik " is from 6 to 20 wells.

After the installation of the metering fluid flows in the group installing GU. At each site GU comes fluid from 2-5 measuring units. Technological equipment GU provides the primary preparation of oil and gas, transportation of oil flooded in the axial collector, transportation of associated gas in the axial collector.

Then on the center manifold the oil flows on UPSV NDA and to prepare it to the quality of commodity oil.

Collection and preparation oil at NGDU (CDG-1 and CGDU somewhat different from the considered technological scheme and implemented according to the project of reconstruction of the Uzen field on Blocks 2A and 3.

At the CDNG oil production is carried out mainly mechanically by means of pumping machines, from which the extracted fluid is extracted along the single –

tube beam closed-loop system on the swing lines to the measurement unit "ASMA" installed on the manifold station or GU.

The oil and gas mixture is collected from a group of wells connected to the corresponding gas or storage facility at the manifold stations (MS). From where the averaged flow is directed to the site of the preliminary separation of the oil and gas mixture (NS). Further, oil is sent through the pipeline for further preparation to UPSV-1.

On CDNG-10 at the flow lines of the downhole products are supplied to three-phase metering installation with 14 taps. After the parameters are determined, the extracted oil is transported to the General reservoir to the GU. At the group installation, all the collectors are combined into one collector, from where the fluid enters the separator, where the separation occurs (oil, gas, water).

The dehydrated oil is pumped by pumps through the communications of the group installation, where it is heated by a radiant furnace, to the axial collector, and then to the UPSV-1.

Dedicated passing gas through pipelines is transported to Kazgppz. Part of the gas is used for own production needs as fuel for furnaces and heating of premises in winter.

Management of preparation of oil and production supply. Oil preparation for the purpose of ensuring commodity conditions, preparation of reservoir water and provision of fields with necessary transportation means (field collectors) for pumping of oil and water through the fields Uzen and Karamandybas is carried out in management of oil preparation and production support. This management:

- installation preliminary water UPSV – 1 and UPSV – 2;
- workshop of preparation and pumping oil;
- oil transportation and equipment repair shop;
- plant transport of process liquids.

Pre-discharge water installations UPSV-1 and UPSV-2 are designed to separate free and partially bound water from oil by thermochemical action on water-oil emulsion entering the pre-discharge water installation (UPSV) from the fields of NGDU-1, NGDU-2, NGDU-3, and NGDU-4 .

Water-oil emulsion where water consisting over 80% from oil fields is fed to the sedimentation tanks, where there is a preliminary dehydration of oil from water 30 – 40%. Separated water up to 30-40%. Separated water from the sedimentation tanks enter the RVS.

Dehydrated oil, with water content about 5%, is supplied to the KSU under excess pressure, where gas is separated from oil. Gas is sent to the compressors, and oil is sent to the centred preliminary preparation of oil pipeline.

From RVS produced water is supplied to the filtration, and then to RVS №2/1 and №2/2 and further from these tanks is pumped by pipeline to the system of PPD.

Caught oil, RVS, No. 1/1, no 1/2 is returned to the head process.

The released gas from the KSU is sent to the compressor station and then to the GPP.

The main production indicators of the CCA are presented in table 2.

Table 2 – Production indicators of UWWR

Indicators	The project, m ³ / day	Actual, m ³ /day
The plant capacity	45 000	63 000
By oil	15 000	15 000
By water	30 000	48 000
Product water content		70-80%
Input	40%	5%
Output	5%	

Shop of preparation and pumping of oil (zppn). Oil treatment at the cppnis carried out by the method of thermochemical dehydration of oil-water emulsion coming from the UOC-1, UOC-2 units.

Shop of preparation and pumping of oil (zppn). Oil treatment at the cppn is carried out by the method of thermochemical dehydration of oil-water emulsion coming from the UOC-1, UOC-2 units.

From above units obtain following commercial products:

- commercial oil;
- gas terminal stages of separation;

Here is also waste water.

Characterization of the product oil are presented 3.

Table 3 – Characteristics of commercial oil and gas

The name	GOST or TU	Indicators GOST or TU		Note
		1 group	for the group of norm	
Marketable oil GOST	GOST 9965-76	Water, %	0,5	GOST -21534-76
		Content of chlorine salts, mg/kg	100	GOST – 6370 -83
		The content of mechanical impurities, %	0,05	ГОСТ- 6370-83
Gas end stage separation		Density, kg / m ³	0,79	

REFERENCES

[1] Environmental code of the Republic of Kazakhstan (with amendments and additions). Astana, 2007.

[2] Law of the Republic of Kazakhstan "on subsoil and subsoil use" (with amendments and additions). Astana, 2010.

[3] The law of the Republic of Kazakhstan "on protection, reproduction and use of animal world" (with amendments and additions). ASTA-on, 2004.

[4] Water code of the Republic of Kazakhstan (as amended. Astana, 2003.

[5] Code of the Republic of Kazakhstan "on health of the people and health care system" (with amendments and additions). Astana, 2009.

[6] The law of the Republic of Kazakhstan "on radiation safety of the population" (with amendments). Astana, 1998.

[7] Law of the Republic of Kazakhstan No. 461-IV of July 15, 2011 "on amendments and additions to some legislative acts of the Republic of Kazakhstan on improvement of the licensing system. Astana, 2011.

[8] The law of the Republic of Kazakhstan № 505-IV dated December 3, 2011 "on amendments and additions to some legislative acts of the Republic of Kazakhstan on environmental issues". Astana, 2011.

[9] Order of the Minister of environmental protection of the Republic of Kazakhstan from April 24, 2007 № 123-p On approval of Rules of coordination of programs of industrial ecological control and reporting on results of industrial ecological control.

Резюме

*М. Т. Ошакбаев, Е. А. Тусупкалиев, М. Н. Баимбетов,
Ж. Н. Кайнарбаева, Г. Д. Байбатырова, Ж. С. Алимбеков*

«ӨЗЕНМҰНАЙГАЗ» АҚ АУМАҒЫНЫҢ ГЕОЛОГИЯЛЫҚ ҚҰРЫЛЫМЫНЫҢ ЕРЕКШЕЛІКТЕРІ МЕН АЙМАҚТЫҢ ТАБИҒИ ШАРТТАРЫНЫҢ СИПАТТАМАСЫ

«Өзенмұнайгаз» АҚ көмірсутегі шикізатын өндіру және дайындау нысандарының өндірістік қызметі қоршаған ортаның компоненттеріне айтарлықтай әсер етеді. Экологиялық жағдайды жақсарту және табиғи ресурстарды ұтымды пайдалану өңірдегі ең маңызды мемлекеттік міндетке айналды. Осыған байланысты аумақтың экологиялық жай-күйін және химиялық-экологиялық зерттеулерді уақтылы бағалау қажет.

Түйін сөздер: өндірістік мониторинг, шығарындылар мониторингі, «Өзенмұнайгаз» АҚ, геологиялық құрылым, климаттық жағдайлар, НГДУ.

Резюме

*М. Т. Ошакбаев, Е. А. Тусупкалиев, М. Н. Баимбетов,
Ж. Н. Кайнарбаева, Г. Д. Байбатырова, Ж. С. Алимбеков*

ХАРАКТЕРИСТИКА ПРИРОДНЫХ УСЛОВИЙ РАЙОНА РАБОТ И ОСОБЕННОСТИ ГЕОЛОГИЧЕСКОГО СТРОЕНИЯ ТЕРРИТОРИИ АО «ОЗЕНМУНАЙГАЗ»

Производственная деятельность объектов добычи и подготовки углеводородного сырья АО «Озенмунайгаз» оказывает определенное воздействие на компоненты окружающей среды. Оздоровление экологической обстановки и рациональное хозяйственное использование природных ресурсов становится сейчас важнейшей государственной задачей региона. В этой связи актуальны своевременная оценка экологического состояния территории и химико-экологические исследования.

Ключевые слова: производственный мониторинг, мониторинг эмиссий, АО «Озенмунайгаз», геологическое строение, климатические условия, НГДУ.

T. K. JUMADILOV, R. G. KONDAUROV

JSC «Institute of chemical sciences after A. B. Bekturov», Almaty, Republic of Kazakhstan

SELF-ORGANIZATION OF POLYMER HYDROGELS OF POLYACRYLIC ACID IN INTERGEL SYSTEMS IN CERIUM IONS SORPTION PROCESS

Abstract. Sorption process of cerium ions by intergel systems hydrogel of polyacrylic acid (hPAA) – hydrogel of poly-4-vinylpyridine (hP4VP) and hydrogel of polyacrylic acid (hPAA) – hydrogel of poly-2-methyl-5-vinylpyridine (hP2M5VP) is studied. Found that self-organization of PAA hydrogels is in significant influence from structure of basic hydrogel. Absence of bulky methyl substituent in the structure of hP4VP provides faster ionization of the hydrogels in intergel system hPAA-hP4VP in comparison with system hPAA-hP2M5VP. Extraction degree of cerium ions of individual hydrogels of PAA, P4VP and P2M5VP is 63.33%, 56.67% and 50.00% respectively. At 17%hPAA-83%hP4VP and 33%hPAA-67%hP2M5VP ratios 92.33% and 90.67% cerium is extracted. PAA, P4VP, P2M5VP polymer hydrogels have not very high values of polymer chain binding degree (52.53%, 47.00% and 41.47% respectively). Maximum values of polymer chain binding degree in the intergel systems are observed at ratios: 17%hPAA-83%hP4VP (binding degree is 76.59%) and 33%hPAA-67%hP2M5VP (polymer chain binding degree is 75.21%).

Keywords: intergel system, self-organization, sorption, Ce^{3+} ions, hydrogels, polyacrylic acid, poly-4-vinylpyridine, poly-2-methyl-5-vinylpyridine.

In result of previous investigations [1-6] it was found that remote interaction of polymer hydrogels provides significant changes of their self-organization. In this regard goal of the present work is study of impact of second component (polybasis) on self-organization of polyacrylic acid polymer hydrogels in intergel systems as well as study of sorption properties of intergel systems hPAA-hP4VP and hPAA-hP2M5VP in relation to cerium ions.

EXPERIMENTAL PART

Equipment. Measurements of optical density for further calculation of cerium ions concentration were carried out on spectrophotometer Jenway-6305 (UK).

Materials. Studies were carried out in 0.005 M solution of 6-water cerium nitrate. Hydrogels of polyacrylic acid were synthesized in presence of cross-linking agent N,N-methylene-bis-acrylamide and red-ox system $\text{K}_2\text{S}_2\text{O}_8\text{-Na}_2\text{S}_2\text{O}_3$. Hydrogel of poly-4-vinylpyridine (hP4VP) (2% of cross-linking agent) was synthesized by «Sigma Aldrich» company. Hydrogel of poly-2-methyl-5-vinylpyridine (hP2M5VP) was synthesized in dimethylformamide medium in presence of cross-linking agent epichlorohydrin. Synthesized hydrogels were put together to create intergel pairs hPAA-hP4VP and hPAA-hP2M5VP. Swelling degrees of the hydrogels are: $\alpha_{(\text{hPAA})}=27.33$ g/g; $\alpha_{(\text{hP4VP})}=3.27$ g/g; $\alpha_{(\text{hP2M5VP})}=3.20$ g/g.

Experiment. Experiments were made at a room temperature. Study of the intergel systems was made as follows: calculated amount of each hydrogel in dry state was put in special glass filters, pores of which permeable for low-molecular ions and molecules, but non-permeable for hydrogels dispersion. Then the filters were put in glass in which salt solution presents. After that, aliquots were taken.

Methodology of cerium ions determination. Methodology of cerium ions determination in solution is based on formation of colored complex compound of organic analytic reagent arsenazo III with rare-earth metals ions [7].

Cerium ions extraction degree (sorption degree) was calculated in accordance with equation:

$$\eta = \frac{C_{\text{initial}} - C_{\text{residual}}}{C_{\text{initial}}} * 100\%$$

where C_{initial} – initial concentration of metal in solution, g/L; C_{residual} – residual concentration of metal in solution, g/L.

Total polymer chain binding degree was calculated as follows:

$$\theta = \frac{v_{\text{sorbed}}}{v} * 100\%$$

where v_{sorbed} – quantity of polymer links with sorbed metal, mol; v – total quantity of polymer mass (if there are 2 hydrogels in solution, it is calculated as sum of each polymer hydrogel mass), mol.

Effective dynamic exchange capacity was determined by calculations in accordance with equation:

$$Q = \frac{v_{\text{sorbed}}}{m_{\text{sorbent}}}$$

where v_{sorbed} – amount of sorbed metal, mol; m_{sorbent} – sorbent mass (if there are 2 hydrogels in solution, it is calculated as sum of their masses), g.

RESULTS AND DISCUSSION

Sorption of cerium ions by the intergel systems hPAA-hP4VP and hPAA-hP2M5VP occurs by ionic and coordination mechanisms. Process of rare-earth elements sorption (on lanthanum example) is clearly described in previous works [8-10].

Extraction of cerium ions by intergel system hPAA-hP4VP. Dependence of cerium ions extraction degree of the intergel system hPAA-hP4VP from hydrogels molar ratios in time is presented on figure 1. Maximum quantity of cerium ions is sorbed by the intergel system at hydrogels ratio 17%hPAA-83%hP4VP. Extraction degree at 48 hours is 92.33%. Obtained results show that extraction degree of cerium ions of individual hydrogels of polyacrylic acid and poly-4-vinylpyridine is not high, values of the parameter are 63.33 and 56.67 respectively. The rest intergel pairs in the intergel system hPAA-hP4VP also have

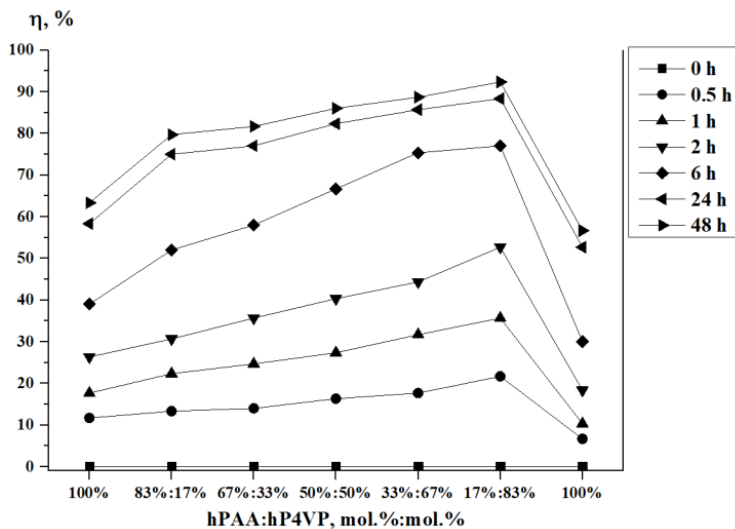


Figure 1 – Dependence of cerium ions extraction degree of the intergel system hPAA-hP4VP from hydrogels molar ratios in time

significantly higher values of cerium ions extraction degree comparatively with individual hydrogels of PAA and P4VP.

Figure 2 represents dependence of polymer chain binding degree (in relation to cerium ions) of the intergel system hPAA-hP4VP from time. Maximum values of binding degree in the intergel system at 48 hours are observed at hydrogels

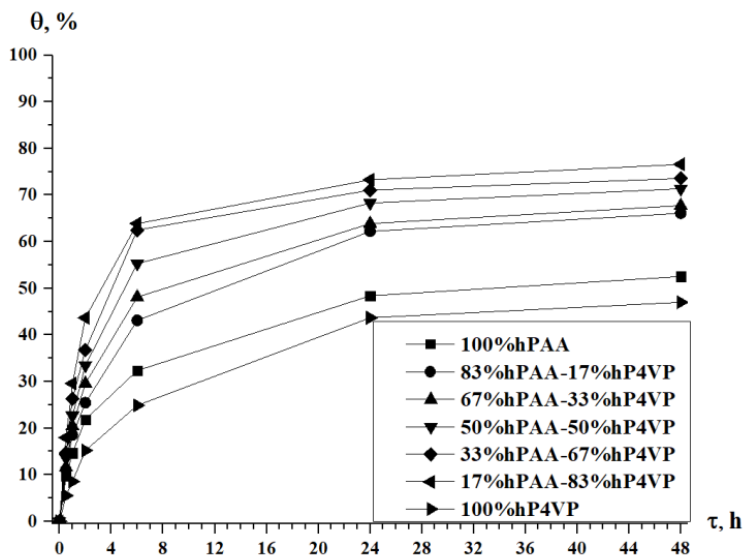


Figure 2 – Dependence of polymer chain binding degree of the intergel system hPAA-hP4VP from time

ratio 17%hPAA-83%hP4VP, it is 76.59%. High values of polymer chain binding degree are also observed at ratios 33%hPAA-67%hP4VP and 50%hPAA-50%hP4VP. It indicates to high ionization degree of the macromolecules in results of mutual activation of hydrogels of polyacrylic acid and poly-4-vinylpyridine. Polymer chain binding degree of the individual hydrogels of PAA and P4VP at 48 hours is 52.53% and 47.00%.

Dependence of effective dynamic exchange capacity of the intergel system hPAA-hP4VP from hydrogels molar ratios in time is shown on figure 3. Obtained data point to the fact that mutual activation of the polymer hydrogels in intergel pairs provides significant increase of values of exchange capacity in comparison with initial hydrogels. This is particularly pronounced at 6 hours of remote interaction. As seen from the figure, at this time of hydrogels interaction at ratio 17%hPAA-83%hP4VP values of exchange capacity are in 2.5 times higher than values of capacity of the individual hydrogels of PAA and P4VP. Further remote interaction of the polymers indicates that the intergel system hPAA-hP4VP approaches to equilibrium state, what is evidenced by not strong increase of effective dynamic exchange capacity as it was in the beginning of the hydrogels remote interaction. Maximum values of effective dynamic exchange capacity are reached at ratio 17%hPAA-83%hP4VP at 48 hours of remote interaction.

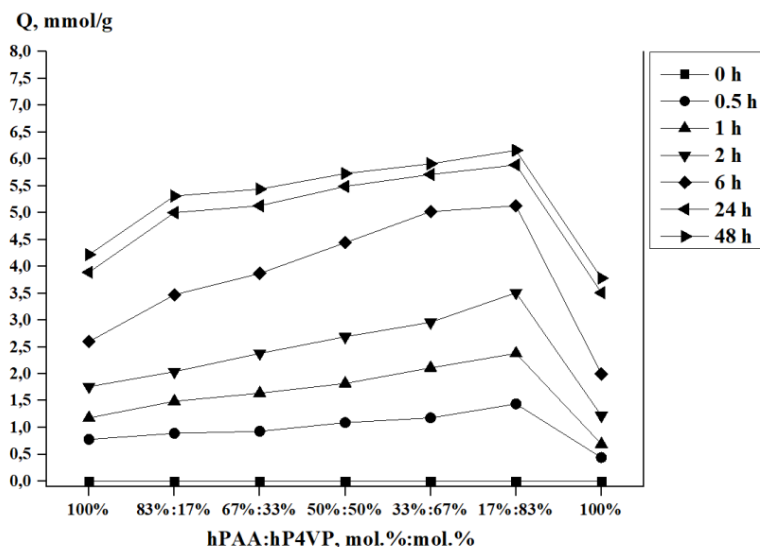


Figure 3 – Dependence of effective dynamic exchange capacity of the intergel system hPAA-hP4VP from hydrogels molar ratios in time

Extraction of cerium ions by intergel system hPAA-hP2M5VP. Figure 4 shows dependence of cerium ions extraction degree of the intergel system hPAA-hP2M5VP from hydrogels molar ratios in time. Extraction degree increases with time in intergel system. It should be noted that transfer of polymer

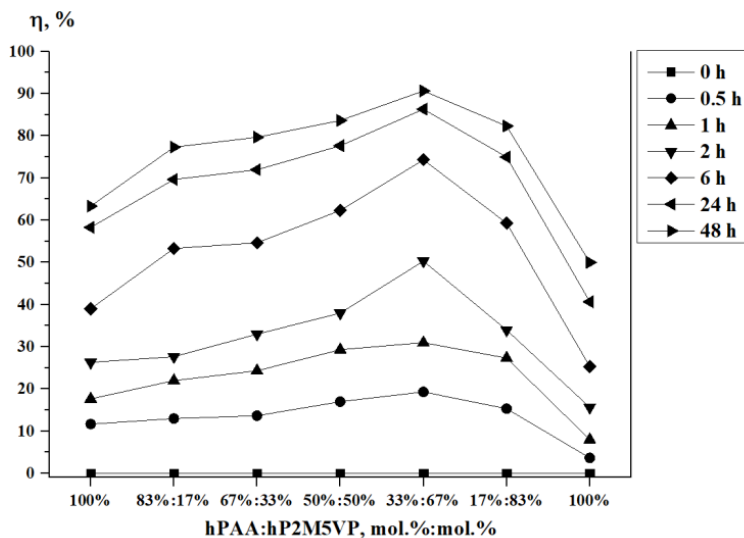


Figure 4 – Dependence of cerium ions extraction degree of the intergel system hPAA-hP2M5VP from hydrogels molar ratios in time

macromolecules into highly ionized state due to their mutual activation provides strong increase of extraction degree of cerium ions of polymer hydrogels in the intergel pairs comparatively with initial polymers. Maximum values of extraction degree of cerium ions in the intergel system are observed at ratio 33%hPAA-67%hP2M5VP. Extraction degree at this ratio is 90.67%. Sorption degree of cerium ions of individual polymer hydrogels of PAA and P2M5VP is 66.33% and 50.00% respectively.

Dependence of polymer chain binding degree (in relation to cerium ions) of the intergel system hPAA-hP2M5VP is presented on figure 5. Individual hydrogels of polyacrylic acid and poly-2-methyl-5-vinylpyridine have not sufficiently high values of binding degree (52.53% and 41.47% respectively). Maximum values of polymer chain binding degree in the intergel system hPAA-hP2M5VP are reached at 48 hours of PAA and P2M5VP hydrogels remote interaction at ratio 33%hPAA-67%hP2M5VP, binding degree is 75.21%.

Effective dynamic exchange capacity of the intergel system hPAA-hP2M5VP is shown on figure 6. The highest values of the parameter the intergel system hPAA-hP2M5VP reaches at 48 hours of PAA and P2M5VP remote interaction at ratio 33%hPAA-67%hP2M5VP. Minimum values of exchange capacity are observed in presence of only individual hydrogels of PAA and P2M5VP, what is result of absence of polymer hydrogels mutual activation phenomenon.

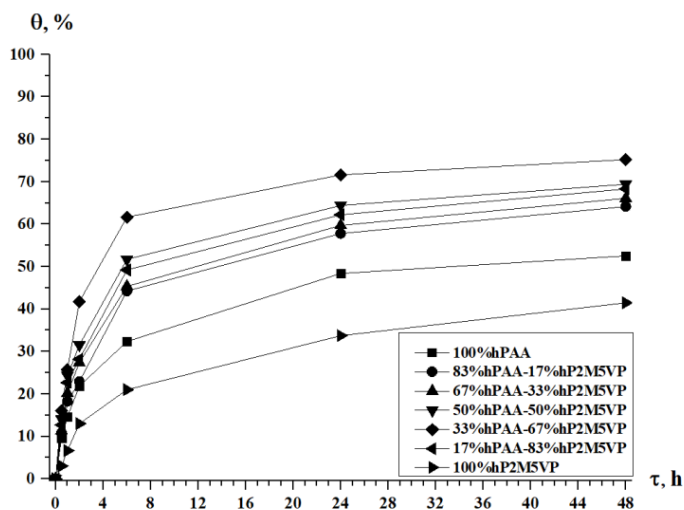


Figure 5 – Dependence of polymer chain binding degree of the intergel system hPAA-hP2M5VP from time

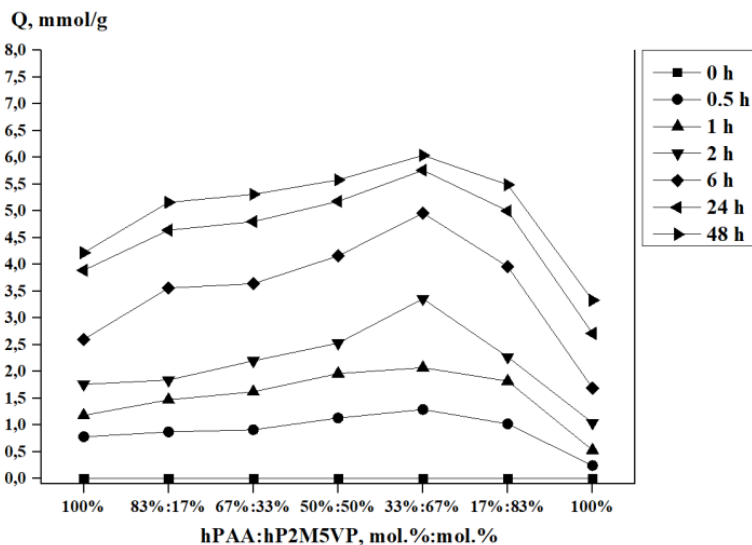


Figure 6 – Dependence of effective dynamic exchange capacity of the intergel system hPAA-hP2M5VP from hydrogels molar ratios in time

As seen from the obtained data, self-organization of polyacrylic acid hydrogels is significantly impacted by the structure of second component (polybasis). Absence of bulky methyl substituent in the structure of hP4VP provides faster ionization of the hydrogels in intergel system hPAA-hP4VP in comparison with system hPAA-hP2M5VP.

Conclusion.

1. Individual hydrogels of PAA, P4VP, P2M5VP do not have high values of sorption properties. Cerium ions extraction degree of hPAA, hP4VP, hP2M5VP is 63.33%, 56.67%, 50.00%.

2. Significant increase of extraction degree in intergel systems hPAA-hP4VP and hPAA-hP2M5VP is result of mutual activation of polymers. Extraction degree of cerium ions in the intergel system hPAA-hP4VP reaches maximum values (92.33%) at ratio 17%hPAA-83%hP4VP at 48 hours. In intergel system hPAA-hP2M5VP maximum extraction of cerium ions occurs at ratio 33%hPAA-67%hP2M5VP, at 48 hours 90.67% of the metal is sorbed.

3. Polymer chain binding degree of hPAA, hP4VP, hP2M5VP is not high (52.53%, 47.00% and 41.47% respectively). This is consequence of absence of mutual activation between the polymers.

4. Maximum values of polymer chain binding degree in the intergel systems are observed at the following ratios: 17%hPAA-83%hP4VP (binding degree is 76.59%) and 33%hPAA-67%hP2M5VP (binding degree is 75.21%).

Acknowledgment. The work was financially supported (the work was made due to the grant funding of 2 Projects: AP05131302 and AP05131451) by the Committee of Science of Ministry of education and science of the Republic of Kazakhstan.

REFERENCES

[1] Alimbekova B., Erzhet B., Korganbayeva Zh., Himersen H., Kaldaeva S., Kondaurov R., Jumadilov T. Electrochemical and conformational properties of intergel systems based on the cross-linked polyacrylic acid and vinylpyridines // Proceedings of VII international scientific-technical conference "Advance in petroleum and gas industry and petrochemistry" (APGIP-7). Lviv, Ukraine, May 2014. P. 64.

[2] Alimbekova B.T., Korganbayeva Zh.K., Himersen H., Kondaurov R.G., Jumadilov T.K. Features of polymethacrylic acid and poly-2-methyl-5-vinylpyridine hydrogels remote interaction in an aqueous medium // Journal of chemistry and chemical engineering. 2014. Vol. 3. P. 265-269.

[3] Jumadilov T.K., Abilov Zh.A., Kaldayeva S.S., Himersen H., Kondaurov R.G. Ionic equilibrium and conformational state in intergel system based on polyacrylic acid and poly-4-vinylpyridine hydrogels // Journal of Chemical Engineering and Chemistry Research. 2014. Vol. 1. P. 253- 261.

[4] Jumadilov T.K., Abilov Zh.A., Kondaurov R.G., Himersen H., Akylbekova M.A. Remote interaction of hydrogels in intergel system hydrogel of polyacrylic acid – hydrogel of poly-2-methyl-5-vinylpyridine // Chemical journal of Kazakhstan. 2015. N 2. P. 79-84.

[5] Akylbekova M.A., Kondaurov R.G., Jumadilov T.K., Umerzakova M.B. Features of swelling and electrochemical properties of polyacrylic acid gel // Chemical journal of Kazakhstan. 2015. N 4. P. 31-37.

[6] Jumadilov T.K., Kondaurov R.G., Khakimzhanov S.A., Himersen H., Yeskaliyeva G.K. Influence of initial state of hydrogels on self-organization of polymer networks of polymethacrylic acid and poly-4-vinylpyridine at their remote interaction in an aqueous medium // Chemical journal of Kazakhstan. 2018. N 1. P. 42-48.

[7] Petruhin O.M. Practice book on physical and chemical methods of analysis. M.: Chemistry, 1987. P. 77-80.

[8] Jumadilov T.K., Kondaurov R.G., Abilov Zh.A., Grazulevicius J.V., Akimov A.A. Influence of polyacrylic acid and poly-4-vinylpyridine hydrogels mutual activation in intergel system on their sorption properties in relation to lanthanum (III) ions // Polymer Bulletin. 2017. Vol. 74. P. 4701-4713. doi:10.1007/s00289-017-1985-3.

[9] Jumadilov T., Abilov Zh., Grazulevicius J., Zhunusbekova N., Kondaurov R., Agibayeva L., Akimov A. Mutual activation and sorption ability of rare cross-linked networks in intergel system based on polymethacrylic acid and poly-4-vinylpyridine hydrogels in relation to lanthanum ions // Journal of Chemistry and Chemical Technology. 2017. Vol. 11, N 2. P. 188-194.

[10] Jumadilov T.K., Abilov Zh.A., Kondaurov R.G. Intergel systems: highly effective instruments for rare earth elements extraction from industrial solutions / Jumadilov T.K. // Chemical engineering of polymers. Production of Functional and Flexible Materials composites / Omari V. Mukbaniani, Marc J.M. Abadie, Tamara Tatrishvili. AAP press, 2017. P. 267-279.

Резюме

Т. Қ. Жұмаділов, Р. Г. Кондауров

ЦЕРИЙ ИОНДАРЫН СОРБЦИЯЛАУ БАРЫСЫНДА ИНТЕРГЕЛДІ ЖҮЙЕДЕГІ ПОЛИАКРИЛ ҚЫШҚЫЛЫНЫҢ ПОЛИМЕРЛІК ГИДРОГЕЛДЕРІНІҢ ӨЗІН-ӨЗІ ҰЙЫМДАСТЫРУЫ

Аннотация. Полиакрил қышқылы гидрогелі (ПАҚГ) – поли-4-винилпиридин гидрогелі (П4ВПГ) және полиакрил қышқылы гидрогелі (ПАҚГ) –поли-2-метил-5-винилпиридин гидрогелі (П2М5ВПГ) интергелді жүйелерімен церий иондарын сорбциялау процесі зерттелді. Полиакрил қышқылы гидрогелінің өзін-өзі ұйымдастыруына негізгі гидрогелдің құрылымы анағұрлым әсер ететіні анықталды. ПАҚГ-П2М5ВПГ жүйесімен салыстырғанда ПАҚГ-П4ВПГ интергелді жүйесінде П4ВПГ құрылымында үлкен метил алмастырғыштың болмауы гидрогелдердің неғұрлым жылдам ионизациялануына әкеледі. ПАҚ, П4ВП және П2М5ВП жекелеген гидрогелдерінің церий иондарын шығару дәрежесі сәйкесінше 63,33%, 56,67% және 50,00% құрайды. 17%ПАҚГ-83%П4ВПГ және 33%ПАҚГ-67%П2М5ВПГ қатынастарында 92,33% және 90,67% церий шығарылады. ПАҚ, П4ВП және П2М5ВП полимерлік гидрогелдері полимерлік тізбектердің байланысу дәрежесінің салыстырмалы төмен мәндеріне ие (сәйкесінше 52,53%, 47,00% және 41,47%). Интергелді жүйелердің мына қатынастарында полимерлік тізбектердің байланысу дәрежесі анағұрлым жоғары мәнге ие: 17%ПАҚГ-83%П4ВПГ (байланысу дәрежесі 76,59%-ға тең) және 33%ПАҚГ-67%П2М5ВПГ (полимерлік тізбектің байланысу дәрежесі 75,21%-ды құрайды).

Түйін сөздер: интергелді жүйе, өзін – өзі ұйымдастыру, сорбция, Ce^{3+} иондары, гидрогелдер, полиакрил қышқылы, поли-4-винилпиридин, поли-2-метил-5-винилпиридин.

Резюме

Т. К. Джумадилов, Р. Г. Кондауров

САМООРГАНИЗАЦИЯ ПОЛИМЕРНЫХ ГИДРОГЕЛЕЙ
ПОЛИАКРИЛОВОЙ КИСЛОТЫ В ИНТЕРГЕЛЕВЫХ СИСТЕМАХ
ПРИ СОРБЦИИ ИОНОВ ЦЕРИЯ

Аннотация. Изучен процесс сорбции ионов церия интергелевыми системами гидрогель полиакриловой кислоты (гПАК) – гидрогель поли-4-винилпиридина (гП4ВП) и гидрогель полиакриловой кислоты (гПАК) – гидрогель поли-2-метил-5-винилпиридина (гП2М5ВП). Установлено, что значительное влияние на самоорганизацию гидрогелей ПАК оказывает структура основного гидрогеля. Отсутствие объемного метильного заместителя в структуре гП4ВП приводит к более быстрой ионизации гидрогелей в интергелевой системе гПАК-гП4ВП по сравнению с системой гПАК-гП2М5ВП. Степень извлечения ионов церия индивидуальных гидрогелей ПАК, П4ВП и П2М5ВП составляет 63,33%, 56,67% и 50,00% соответственно. При соотношениях 17%гПАК-83%гП4ВП и 33%гПАК-67%гП2М5ВП извлекается 92,33% и 90,67% церия. Полимерные гидрогели ПАК, П4ВП, П2М5ВП обладают относительно невысокими значениями степени связывания полимерной цепи (52,53%, 47,00% и 41,47% соответственно). Наиболее высокие значения степени связывания полимерной цепи в интергелевых системах наблюдаются при соотношениях: 17%гПАК-83%гП4ВП (степень связывания равна 76,59%) и 33%гПАК-67%гП2М5ВП (степень связывания полимерной цепи составляет 75,21%).

Ключевые слова: интергелевая система, самоорганизация, сорбция, ионы Ce^{3+} , гидрогели, полиакриловая кислота, поли-4-винилпиридин, поли-2-метил-5-винилпиридин.

CONTENTS

Certificate Springer Nature. Springer nature training Ergozhin Edil.....	4
ІСНТЕ-2018. 2018 Technology&Equipment. Сертификат участника.	
Награждается АО «Институт химических наук им. А.Б.Бектурова».....	5
ІСНТЕ-2018. 2018 Technology&Equipment. Диплом участника.	
Награждается Байдуллаева Айнаш Кайратовна.....	6
КУЭЛЖК Ф.0796. Бейорганикалық, органикалық, полимерлі қосылыстардың, қасиеттері белгілі жүйелер мен материалдарды алудың физика-химиялық негіздері. Физико-химические основы создания неорганических, органических, полимерных соединений, систем и материалов с заданными свойствами.....	7
Благодарственное письмо от ректора Северо-Казахстанского государственного университета им. Манаша Козыбаева С. Омирбаева.....	8
Благодарственное письмо от ректора, профессора А. А. Абжаппарова и коллектива кафедры химии и биотехнологии Кокшетауского государственного университета им. Ш. Уалиханова.....	9
Информационное сообщение.....	10
<i>Bektenov N.A., Ergozhin E.E., Ryspaeva S.B., Sadykov K.A., Moldagalyeva I.S., Maratova A.A.</i> Ecology of oil and oil sorbents.....	11
<i>Anuarbekova I.N., Akimbayeva N.O., Vizer S.A., Yerzhanov K.B.</i> Selective monoalkylation and dithiocarbonylation of ethylenediamine.....	28
<i>Temirgaziev B.S., Seilkhanov T.M., Tyanakh S., Kozhanova A.M., Seilkhanov O.T., Minayeva Ye.V., Sal'keeva L.K., Tuleuov B.I., Adekenov S.M.</i> Obtaining and investigation of supramolecular inclusion complex of 2-deoxy-20-hydroxyecdysone with γ -cyclodextrine by NMR spectroscopy method.....	36
<i>Yermakhanova F.R., Usmanov S., Omarova G.T.</i> Physical and chemical properties of the production technology of individual urea-formaldehyde compounds and multifunctional compounds on the basis of those compounds and zinc acetate.....	45
<i>Kairbekov Zh.K., Jeldybayeva I.M., Yermoldina Ye.T.</i> Application natural ore materials as catalysts at hydrogenation of Kenderlyk coal.....	54
<i>Yermakhanova F.R., Usmanov S., Omarova G.T.</i> Study of the technology for the production of individual urine-formaldehyde compounds of multifunctional action on the basis of urea and zinc acetate in spray dryer.....	60
<i>Tashmukhamedov F.R., Kutzhanova A.Zh.</i> Continuous dyeing of cellulosic textile by rubia tinctorum extract using sol-gel method.....	68
<i>Ergozhin E.E., Chalov T.K., Begenova B.E., Kovrigina T.V., Melnikov Ye.A.</i> Study of sorption of lead(II) ions by anionite obtained on the basis of aniline, epichlorohydrin and polyethylenepolyamine.....	77
<i>Ataullaev Sh.N., Fozilov S.F., Mavlanov B.A., Akhmedov V.N., Ochilov A.U.</i> Investigation of the process of application of salts of active phases of nickel and molybden to thermoregenerated zeolite CaA.....	84
<i>Akhmetkarimova Zh.S., Muldakhmetov Z.M., Nurkenov O.A., Ordabaeva A.T., Baikenov M.I., Isabekova D.S.</i> Influence of the composition of catalyst supported by zeolite in the hydrogenation of fuel oil.....	93
<i>Ataullaev Sh.N., Mavlanov B.A., Fozilov S.F., Akhmedov V.N., Ochilov A.U., Tilavova M.M.</i> Physical-chemical properties of catalysts for destructive hydrogenization of oil deasphaltizate.....	100
<i>Kasenov B.K., Kasenova Sh.B., Sagyntaeva Zh.I., Turtubaeva M.O., Kyanyshbekov E.E.</i> Synthesis of new nanosized (nanocluster) cobalt(nickelite)-cuprate-manganites.....	106
<i>Balgysheva B.D., Seytkali H., Macabay Sh.G., Samet Zh.S.</i> Obtaining zinc-containing microfertilizers method of mechanochemical activation.....	112


<i>Ivanova N.M., Lazareva Ye.S., Visurkhanova Ya. A., Soboleva E.A.</i> Structure and electrocatalytic activity of zinc-containing composites of polyaniline with aniline-formaldehyde polymer.....	120
<i>Nykmukanova M.M., Yeskaliyeva B.K., Burasheva G.Sh.</i> Separation flavonoids by sorbent RP-18 from <i>Verbascum Marschallianum</i>	130
<i>Yergalyieva Zh.M., Azimbaeva G.E.</i> Methods of distribution of the polyphenol extracts from the leaves of a plant <i>carthamus</i>	136
<i>Mikhailovskaya T.P., Kurmakyzy R., Tolemisova D.K., Vorobyev P.B.</i> Modifying the influence of titanium and zirconium dioxides on the properties of the vanadium oxide catalyst in the vapor-phase oxidation of 3-methylpyridine.....	147
<i>Gurin A.N., Soloninkina S.G., Riss P., Uralbekov B.M., Matveeva I.V., Chakrova E.T.</i> Selection of mobile phase systems for chromatographic research of ¹⁷⁷ Lu-DOTAELA.....	151
<i>Nazarova V.D., Akhankova Y.V., Bektemissova A.U.</i> Extraction of quercetin from <i>LINOSYRIS VILLOSA</i>	158
<i>Umerzakova M.B., Kravtsova V.D., Sariyeva R.B., Kainarbayeva Zh.N.</i> Composite materials based on arylalicyclic copolyimide with additives of polyethylene glycol.....	165
<i>Akimbayeva N.O., Vizer S.A., Seilkhanov T.M., Yerzhanov K.B.</i> Alkylation of sodium ethane-1,2-diyldicarbamodithioate.....	172
<i>Kayukova L.A., Praliyev K.D., Dyusembaeva G.T., Akatan K., Shaymardan E., Kabdrakhmanova S.K.</i> Synthesize 1,3,5-substituted isoxazoles at excessive benzoylation of β-aminopropioamidoximes in pyridine.....	181
<i>Dyuryagina A.N., Lutsenko A.A.</i> Study of the dispersing effect produced by polyether siloxane copolymers in water-dispersion systems.....	190
<i>Avchukir H., Burkitbayeva B.D., Argimbayeva A.M., Rakhymbay G.S.</i> Kinetics of electrodeposition of indium on solid electrodes from chloride solutions.....	197
<i>Beisenova G.S., Burkitbayeva B.D., Argimbayeva A.M., Rakhymbay G.S., Esaly N.N.</i> The effect of temperature on the degree of purity of indium at its electrorefining.....	208
<i>Kadirbekov K.A., Zhambakin D.K., Kadirbekov A.K., Imanbekov K.I., Aitureev A.U.</i> Laws of formation of active and selective catalytic systems on the basis of clinoptilolite for heavy hydrocarbons cracking process.....	217
<i>Akhmetova G.S., Issayeva U.B., Yu V.K., Praliyev K.D., Satbayeva Ye.M., Kadyrova D.M., Amirkulova M.K., Smagulova G.S., Seilkhanov T.M.</i> Fluorobenzoates of 1-propyl-4- ketoximepiperidine as potencial local anesthetics.....	230
<i>Chernyakova R.M., Agatayeva A.A., Kayinbayeva R.A., Yermekova K.Ye., Kozhabekova N.N., Zhussipbekov U.Zh.</i> Sorption of lead cations (II) by acid-modified zeolite in alkaline medium.....	237
<i>Oshakbaev M.T., Tusupkaliev E.A., Baimbetov M.N., Kainarbayeva Zh.N., Baibatyrova G.D., Alimbekov Zh.S.</i> Native conditions and features of the geological structure of the territory JSC «Ozenmunaigas» and characteristics work.....	248
<i>Jumadilov T.K., Kondaurov R.G.</i> Self-organization of polymer hydrogels of polyacrylic acid in intergel systems in cerium ions sorption process.....	254

Редактор *Н. Ф. Федосенко*
Верстка на компьютере *Д. Н. Калкабековой*

Подписано в печать 12.07.2018.
Формат 70x100 ¹/₁₆. 16,5 п.л. Бумага офсетная. Тираж 500.



«УТВЕРЖДАЮ»
Главный редактор,
академик НАН РК

 Е.Е. Ергожин
«3» января 2018 г.

Требования для оформления статей в журнале «ХИМИЧЕСКИЙ ЖУРНАЛ КАЗАХСТАНА»

Научный журнал открытого доступа «Химический журнал Казахстана» издается ордена Трудового Красного Знамени Институтом химических наук имени А.Б. Бектурова с периодичностью 4 номера в год.

Цель Журнала – освещение новых научных результатов и идей, проблемных вопросов науки и техники, последних разработок и исследований по актуальным проблемам фундаментальных и прикладных исследований в области неорганической и органической химии, химии и технологии мономеров и высокомолекулярных соединений, ионного обмена, нефтехимии и нефтехимического синтеза, химии лекарственных веществ и физиологически активных соединений, химической экологии, химии удобрений и солей, физической химии для широкого круга специалистов. В Журнале публикуются научные статьи и обзоры ученых, докторантов, магистрантов, производственников, имеющие теоретическое и практическое значение.

Статьи, представленные в редакцию Журнала, должны удовлетворять следующим требованиям:

Общие требования. Редакционная коллегия принимает статьи, набранные в текстовом редакторе MS Word в электронном виде, а также на бумажном носителе, причем, последняя страница подписывается всеми авторами с проставлением даты.

Рисунки представляются с разрешением минимум 300 dpi, в формате *.bmp, .tiff. Схемы, графики выполняются во встроенной программе MS Word или в MS Excel.

Язык статьи. Статьи принимаются на казахском, русском или английском языках, однако, в целях популяризации Журнала, редакционной коллегией приветствуется прием статей на английском языке.

Параметры страницы. Формат страницы: А4 (210x297 мм).

Поля: верхнее – 2 см, нижнее – 2 см, левое – 3 см, правое – 1,5 см. Расстановка переносов не допускается. Фбзацный отступ – 1,0 см.

УДК. В начале статьи, в верхнем левом углу указывается номер по Универсальной десятичной классификации (УДК), соответствующий заявленной теме. Далее, после отступа строки, указываются инициалы и фамилии автора(-ов), еще через строку следуют названия организации(-й), в которой(-ых) работают авторы, название города и страны. Еще ниже, через строку указывается название статьи прописными буквами. Шрифт - полужирный.

Аннотация. Предоставляется на языке статьи (объем не менее 150 слов).

Ключевые слова. Слова и словосочетания (6-8), обеспечивающие наиболее полное раскрытие содержания статьи, представляются на языке статьи.

Гарнитура. Текст статьи набирается в гарнитуре Times New Roman, размер кегля 14 пт, межстрочный интервал - одинарный, форматирование - по ширине.

Структура и объём статьи. Структурирование статьи производится в соответствии с общепринятыми стандартами: "**Введение**" (должно включать в себя пояснение, в связи с чем проведено данное исследование, обзор актуальной литературы, обоснование выбора методологии исследований), "**Экспериментальная часть**" (описание проводимых исследований), "**Результаты и их обсуждение**" (полученные в ходе исследования результаты), "**Выводы**" (касательно полученных результатов, в том числе соответствуют ли они ожиданиям или нет). Объем статьи, включая аннотацию и список литературы: от 6 до 10 страниц. Обзорные статьи могут быть до 20 страниц.

Ссылки на использованные источники. Ссылки на использованные источники приводятся после цитаты в квадратных скобках, с указанием порядкового номера источника цитирования, в соответствии с ГОСТ 7.1–2003 «Библиографическая запись. Библиографическое описание. Общие требования и правила составления».

Список литературы. Располагается после текста статьи. Нумерация начинается с первого номера, предваряется словом «ЛИТЕРАТУРА» и оформляется в порядке упоминания или цитирования в тексте статьи. Рекомендуемое количество ссылок – не менее 20, в том числе не менее 50% – ссылки на международные источники (журналы, входящие в международные базы данных Clarivate Analytics, Scopus, Springer Nature). Далее в том же порядке приводится транслитерация списка. Под одним номером указывается только один источник. Список литературы должен быть представлен наиболее свежими и актуальными источниками.

Резюме. После списка литературы должны быть представлены резюме. К примеру, если статья написана на казахском языке, то на русском и английском языках даются резюме, состоящие из ФИО автора (-ов), названия, текста (не менее 150 слов), ключевых слов, организации, где выполнялась работа.

Сопроводительные документы, прилагаемые к статье. К статье прилагаются сопроводительные документы (на казахском или русском языке):

1. Письмо-направление в редакционную коллегию Журнала от организации, в которой данное исследование выполнено.

2. Акт экспертизы.

3. Сведения об авторах: Фамилия, имя и отчество каждого автора с указанием ученой степени и ученого звания, служебные и домашние номера телефонов, домашние адреса с указанием почтового индекса, адрес электронной почты (в 2-х экземплярах).

4. Рецензия.

5. Научные учреждения, высшие учебные заведения, промышленные предприятия и каждый автор научной статьи, имеющий ученую степень доктора или кандидата наук, представляют ксерокопию или скан-версию квитанции **о годовой подписке** на «Химический журнал Казахстана». (Подписной индекс в каталоге АО «КазПочта» или в дополнении к нему – 75 241). Без этого документа статьи не принимаются.

Материалы, не соответствующие указанным требованиям, возвращаются на доработку.

Решение о публикации статьи принимает редакционная коллегия Журнала.

Электронная версия представляется на электронном носителе либо отправляется по электронной почте: (ics_rk@mail.ru, lena.yanevskaya47@mail.ru).

Датой принятия к печати считается дата поступления версии, удовлетворяющей всем требованиям Журнала. Очередность публикации устанавливается по дате принятия статьи к печати.

Редакционная коллегия Журнала